This is to certify that the
thesis entitled

PETROLOGY AND GEOCHEMISTRY OF EL HATO SILICIC
IGNIMBRITE, EL VALLE VOLCANO, PANAMA

presented by

PAULO J. HIDALGO

has been accepted towards fulfillment
of the requirements for the

M.S degree in Geological Sciences

Major Professor's Signature

12-07-07

Date

PETROLOGY AND GEOCHEMISTRY OF EL HATO SILICIC IGNIMBRITE, EL VALLE VOLCANO, PANAMA

By

Paulo J. Hidalgo

A THESIS

Submitted to

Michigan State University

in partial fulfillment of the requirements

for the degree of

MASTER OF SCIENCE

Department of Geological Sciences

2007

ABSTRACT

PETROLOGY AND GEOCHEMISTRY OF EL HATO SILICIC IGNIMBRITE, EL VALLE VOLCANO, PANAMA

By

Paulo J. Hidalgo

El Valle volcano in Panama, results from the eastward subduction of the Nazca plate underneath the Panama Block. It was dominated by andesitic volcanism during the Miocene (~10-5 Ma) and silicic (dacitic) volcanism during the Quaternary.

Chemically, the products of El Valle volcano Quaternary volcanism have pronounced depletions in the in HREE, low Y, high Sr, high Sr/Y, low K_2O/Na_2O that are best explained by partial melting of a low K garnet-bearing source (e.g. eclogite). This contrasts with the silicic deposits from Costa Rica and Nicaragua that have high K_2O/Na_2O (and relatively high REEs) characteristic of an evolved source with medium to high-K as starting composition (Vogel et al., 2006),

Partial melting accompanying dehydration of the El Valle volcano Quaternary eclogitic source magmas at the base of thickened crust (e.g. Caribbean Large Igneous Province, CLIP), would produce compositionally appropriate TTG (Tonalite-Trondhjemite-Granodiorite) like granitoids in equilibrium with eclogite residues. This model is a direct way of producing high silica magmas in subduction environments without involving fractionation or more complicated processes.

A MI MADRE SIEMPRE VALIENTE Y ESTOICA ANTE LA ADVERSIDAD

ACKNOWLEDGMENTS

I will like to thank my advisor Dr. Tom Vogel for his advice and for his guidance throughout my master's studies and for always making sure that I will get the most out my program. I will also like to thank Lina Patino and Bill Cambray for their advice and patient revisions. Special gratitude to Lepolt Linkimer and Ryan Currier for being an important friends and colleagues who played an important role during my studies deliberating with me about geology and even more important giving me moral support. Collaboration during the laboratory work given by Pavel Izbekov, Dave Szymanski and Paul Layer was invaluable. Finally, I will like to thank all my friends in Michigan State University for their support and greatly appreciated company.

TABLE OF CONTENTS

LIST OF TABLES

LIST OF FIGURES

I. INTRODUCTION

El Valle volcano in Panama, results from the eastward subduction of the Nazca plate underneath the Panama Block (Figure 1). In this respect El Valle is different from volcanoes in the northwestern segment of the Central American volcanic front (from Costa Rica to Guatemala), that are derived from the subduction of the Cocos plate.

Silicic volcanism (SiO_2 >65%) associated with Cocos subduction has been well documented (Williams and McBirney, 1969; Rose et al., 1999; Hannah et al., 2002; Rogers, 2003; Viray, 2003; Vogel et al., 2004; and Vogel et al., 2006a; Vogel, 2007), but there have been no detailed studies of silicic volcanism in Panama.

In El Valle volcano two periods of volcanic activity can be defined: from 10 Ma to 5 Ma volcanic arc andesites were emplaced with similar characteristics to the present day lavas of the Central America Volcanic Front. After ~5 Ma of quiescence (in the Quaternary), the volcanic activity on El Valle Volcano resumed with the eruption of dacitic lava flows and dacitic El Hato pyroclastic flow. El Hato ignimbrite is perhaps one of the largest Quaternary pyroclastic flows in region. The recent eruptive products of El Valle contain little chemical variation with respect to both major- and trace-elements.

The silicic Quaternary volcanism of El Valle can be added to other Central American silicic deposits in the debate of producing high silica magmas in volcanic arcs. The occurrence of silicic magmas on volcanic arcs without continental crust has puzzled researchers for a long time and the silicic volcanism at El Valle volcano and other Costa

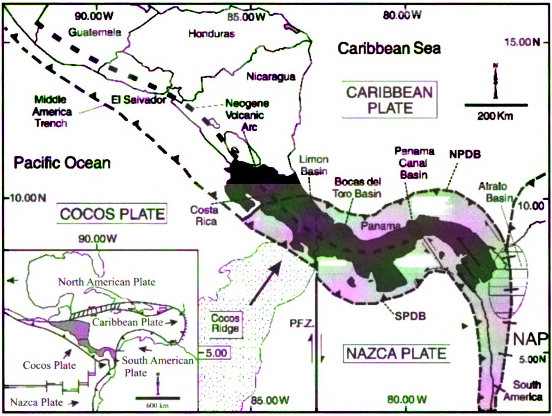

Figure 1. Tectonic features of the study area. Part of Southern Central America (dark grey Shade) is included in the Panama microplate (pale grey shade). Dash lines with teeth mark represent zones of convergence; zippered line is Panama - Colombia suture. Very heavy dashed line marks location of Neogene volcanic arc. Fine arrows are Paleogene Faults; thick arrows are late Neogene faults. Principal Neogene sedimentary basins located by striped ovals. Spotted pattern defines the Cocos Ridge. Arrows on the inset indicate directions of relative plate motions of the plates. PFZ=Panama fracture zone, SPDB=South Panama deformed belt, NPDB= North Panama deformed belt, NAP= North Andes Plate (modified from Coates et al., 2005).

Rican silicic volcanic deposits are part of this puzzle. Silicic magmas were not thought to be common in areas that lacked continental crust. However, in recent years a number of workers have described abundant silicic volcanic rocks in a number of oceanic arcs (Tamura and Tatsumi, 2002; Leat et al., 2003; Smith et al., 2003; Vogel et al., 2004, and Vogel et al., 2006a; Vogel 2006b). Recent models for the origin of silicic magmas in these settings have been proposed (Tamura and Tatsumi, 2002; Smith et al., 2003; Vogel et al., 2004, Hirotani and Ban, 2006 and Vogel et al., 2006b) and involve partial melting or extreme crystal fractionation (liquid extraction) of previously emplaced, subduction-related magmas (Tamura and Tatsumi, 2002; Smith et al., 2003; Grove et al., 2003; Vogel et al., 2004; Hirotani and Ban, 2006 and, Vogel et al., 2006).

In this study I evaluate models by Rapp et al. (1991), Sen and Dunn (1994), Rapp and Watson (1995), Pertermann (2003) Rapp et al. (2003) that have resulted in rocks that are compatible with the characteristics of the silicic deposits of El Valle volcano. By direct experimental evidence these authors showed that partial melting of eclogite produced granitoid liquids with major- and trace-element compositions equivalent to Archaean TTG (Tonalite-Trondjhemite-Granodiorite) rocks. The Archean TTG complexes have similar chemical properties to the adakitic magmas from the Quaternary volcanism in Panama.

The goals of this project are to document the nature of the silicic volcanism in El Valle volcano and compare it to silicic deposits associated with the subduction of the Cocos plate. In addition, geochemical, mineralogical and geochronological data are used to evaluate models that have been proposed for the origin of silicic magmas in magmatic arcs that do not contain evolved continental crust.

II. TECTONIC SETTING

The tectonic region that encompasses the Panama Block, Nazca plate and the North Andes plate is one of the most complex active tectonic areas of the western hemisphere (Figure 1). In this chapter a brief description of the tectonic setting and tectonic history is presented.

2.1 Tectonic Context

The southeastern most part of Central America (southern Costa Rica and Panama, Figure 1 in dark shade) is sandwiched between the E-W-trending North Panama deformed belt (NPDB) and the South Panama deformed belt (SPDB) (Figure 1), both of them seismically active. This region is known as the Panama block (Figure 1 in pale grey shade) and it is in moving northward relative to the Caribbean plate and eastward relative to the South American plate (Kellogg et al., 1985).

The North Andes Plate (NAP) a small plate south of the Panama block, is converging with Central America, confirmed by a slab of subducting Caribbean lithosphere (West of Colombia) that dips 17° towards the southeast down to a depth of 275 km (van der Hilst and Mann, 1994). Bird (2003) has suggested that the subducted slab implies that tectonically the Panama block does not extend north and/or southeast (towards South America) of the North Panama deformed belt. The collisional boundary between the Panama block and the North Andes Plate is near the Panama-Colombia border, and has been described extensively by Mann and Kolarsky (1995).

The northern boundary of the Panama block is characterized by subduction of Caribbean Plate, where one of the prominent features is the frontal thrust of the North

Panama deformed belt (Kellogg and Vega, 1995; Mann and Kolarsky, 1995). It has been interpreted that the deformed belt crosses Costa Rica on a westward trend to meet the Middle America Trench in a Caribbean Plate-Cocos Plate-Panama Block triple junction.

The Southern Panama deformed belt is defined by the southern limit of the Panama block. The SPDB is complex; it changes character eastward from oblique subduction (between 83°W–80.5°W) of the Nazca plate (V=1.2-1.8 cm/yr, Jarrard, 1986) to a sinistral strike-slip component fault (from 80°W to 78.8°W, Westbrook et al., 1995). The thrust front including the Cocos-Nazca-Panama Block triple-junction at the Panama Fracture Zone (PFZ) has been mapped in detail by Moore and Sender (1995). Deformation and stress produced by the interaction of the SPDB and NPPB is accommodated by the active array of faults in the Rio Flores and Azuero-Sona areas (Kolarsky and Mann, 1995).

Longsdale and Klitgord (1978) interpreted that subduction in the southern limit of the Panama Block stopped at about 9 Ma. However, the recent volcanic deposits dated in this study (~56 ka), recent seismicity reported by local institutes, well developed Bouguer anomalies indicating a prominent trench, and the significant sediment deformation of young sediments in the accretionary wedge offshore western Panama have been interpreted as evidence of active subduction of the Nazca Plate under the Panama Block (Moore et al. 1985; Heil, 1988).

2.2 Tectonic History

2.2.1 Origin of Cocos and Nazca Plates

Spreading of the Cocos-Nazca spreading centers (CNS-1, CNS-2 and CNS-3) have produced the plateau part of the Cocos plate and part of the Nazca plate. In addition, spreading in the East Pacific Rise (EPR) has also contributed to part of the Nazca plate (Meschede et al., 1998).

East of the Panama Fracture Zone (PFZ), several inactive spreading centers have been identified (Hardy, 1991; Lonsdale and Klitgord, 1978, Lonsdale, 2005). All of the oceanic crust east of the PFZ came from these inactive spreading centers, excluding the Galapagos hot spot-derived Malpelo Ridge. Isochrons give the ages for the subducting plate, some of them are as old as ~23 Ma immediately east of the Coiba Fracture Zone (CFZ) and south of the Panama Block–Nazca plate boundary (Barckhausen et al., 2001) (Figure 2). East of the Coiba ridge (Figure 2) there is a fossil spreading center (sometimes referred to as 80°W fracture zone). East of this spreading center the age of the subducted lithosphere is considerably younger (~13 Ma) and is associated to spreading in the Sandra Rift (SR) discussed later in this chapter.

The offset portion of the northern CNS-1/ EPR boundary east of the CFZ has not been identified. Because of the presence of older CNS-1 crust, the initial breakup of the Cocos and Nazca plates must have started in the east and the propagated to the west. It is uncertain how old this breakup occurred, because no limit between EPR-derived crust

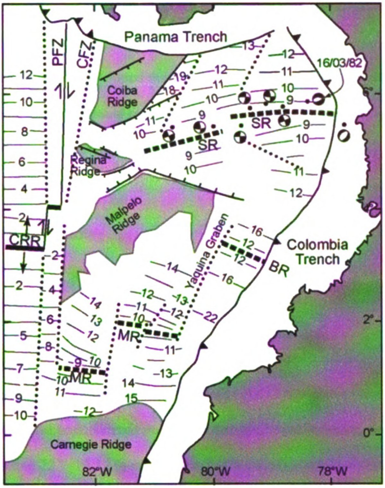

Figure 2. Pattern of crustal isochrons (Hardy 1991; Lonsdale 2005) and plate boundaries in the Panama Basin (modified from Lonsdale 2005). Earthquakes (black dots) and fault plane solution are from the Harvard University archive of centroid-moment tensor solutions, taken from Marcaillou et al. (2006). Plain lines are active spreading axis and transform faults: Costa Rica Rift (CRR) and Panama Fracture Zone (PFZ). Dashed and dotted lines are fossil spreading axis and transform faults: Buenaventura Rift (BR), Malpelo Rift (MR), Coiba Fracture Zone (CFZ) and Yaquina Graben. Possible spreading activity along Sandra Rift (SR) is indicated in heavy dash lines.

and CNS-1-derived crust has been identified east of the Panama Fracture Zone. MacMillan (2004) suggests that this boundary probably lies very close to the modern Caribbean–Nazca plate boundary, either just offshore, or it was recently subducted (see

Appendix A which presents a series of slides with a paleogeographic restoration model of the Cocos and Nazca Plates from 12 Ma to present).

Silver et al. (1998) suggested that the Farallon plate broke into the Cocos and Nazca plates as a result of Global rearrangement of plate boundaries during the Oligocene. This is consistent with Meschede et al. (1998) dates for the oldest magnetic anomalies on CNS-1 (Figure 2).

2.2.2 Cocos-Nazca Spreading

Wilson and Hey, (1995); Barckhausen et al. (2001) have described the magnetic anomaly pattern offshore southern Central America as complex. It includes several propagators and ridge jumps. Barckhausen et al. (2001) describe a number of ridge jumps and changes in ridge orientation between the Nazca and Cocos plates since 23 Ma. The naming agreement for crust derived from these three different spreading centers is CNS-1 (northeast-trending 22.7–19.5 Ma anomalies), CNS- 2 (east–northeast-trending 19.5–14.5 Ma anomalies), and CNS-3 (east–west-trending 14.5–0 Ma anomalies).

According to Meschede et al. (1998) the periods of activity of the spreading centers can be simplified as follow:

"Spreading Center CNS-1 remained active until 19.5 Ma when the orientation of the spreading axis changed direction from northwest – southeast to east northeast – west southwest. The second spreading system (CNS-2) was abandoned at 14.7 Ma, when the presently active east-west–oriented CNS-3 started its activity." (p. 212)

2.2.3 Panama Block – Cocos - Nazca Triple point

The triple junction between the Caribbean, Cocos, and Nazca plates is positioned just south of the Burica peninsula. At ~50 and ~100 km to the east of the PFZ there are two fracture zones, Balboa and Coiba. The subduction of these migrating fractures zones have produced upper plate deformation in the accretionary wedge of southwestern Panama, including major slumps, thrust faults, and reorientation of the plate boundary (Moore and Sender, 1995). These three fracture zones are all probably related to the Nazca–Cocos plate boundary, however, their histories with respect to one other are unknown. Based on tentative identification of magnetic anomalies, Lonsdale and Klitgord (1978) noted that due to the presence of the Coiba Ridge, it seems that the Coiba fracture zone was the active plate boundary prior to ~2 Ma.

2.2.4 Sandra Rift

Bathymetric and seismic profiles by Batiza (1986) supported the identification of the Sandra rift fossil spreading center (figure 2). Its eastern part has the axial rift valley typical of many abandoned risecrests and the western part has a high volcanic ridge. The risecrest is still marked by a band of seismicity with several recent earthquakes large enough to yield centroid moment tensor (CMT) fault plane solutions (i.e., mb>5.3). The association of seismicity with an east–west band of rough topography has provoked the suggestion that this is a nascent spreading center beginning to detach a "North Nazca" microplate from the Nazca Plate (DeBoer, 1988). Lonsdale (2005) interpreted based on magnetic data that modern seismicity along the Sandra Rift as evidence of residual or reactivated tectonism along an imperfect Late Miocene plate suture.

Recent magnetic re-interpretation suggests that the spreading ceased along the Malpelo Rift shortly after 9 Ma but continued along the Sandra Rift, maybe until 8.5 Ma (Lonsdale, 2005). This interpretation is consistent with the Sandra Rift being a Cocos-Nazca spreading axis that propagated westward from at least 12 Ma to ~9 Ma overlapping the concurrently spreading eastern segment of Malpelo Rift where spreading slowed after 12 Ma. Since this period, the Sandra Rift has possibly been rejuvenated at times by tension resulting from slab pull forces acting in different directions due to the curvature of the Colombian trench (Hardy, 1991).

Some authors proposed that a partial spreading reactivation along the Sandra Rift may have partially caused a reactivation of a slow northeast-directed subduction beneath Panama, possibly since 3–5 Ma (de Boer et al. 1988; Silver et al. 1990). Several normal-faulting focal mechanisms along the Sandra Rift (as the March 16, 1982 event) are consistent with a ''not-quite-abandoned'' spreading axis. Alternatively, other authors pointed out an E-W trending sinistral shear zone, coincident with the Sandra Rift and active since at least 1 my (Adamek et al., 1988; Hey 1977; Lonsdale and Klitgord, 1978; Sallares and Charvis, 2003).

III. STRATIGRAPHY OF EL VALLE VOLCANO

El Valle volcano lies at the easternmost extent of the Central American volcanic front, in Panama. (Figure 3, Coordinates 8°35'0"N and 80°10'0"W). It is situated 80 km SW of Panama city, and consists of a broad stratovolcano with a 30 km^2 caldera on its summit where the town of El Valle is located.

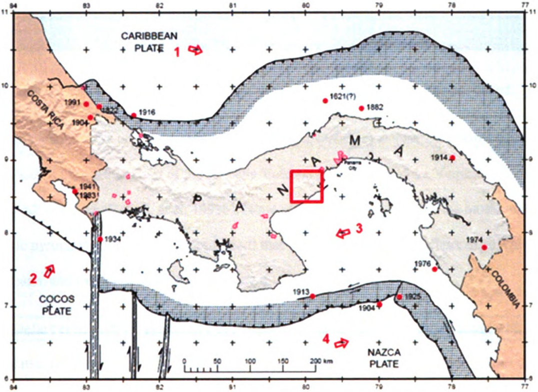

Figure 3. Location map of El Valle Volcano (red box). Plate boundaries and major historical earthquakes are shown (red dots) . Map modified from USGS, *Quaternary Faults and Folds of Panama and its Offshore Regions.*

The caldera is bounded by steep, 200-300 m high walls overlooking a flat floor, which contain lake deposits. Cerro Pajita, Cerro Gaital, and Cerro Caracoral are made up of dacitic lava dome complexes that were constructed along an E-W-trending lineament in the northern limit of the caldera and form the high point (1185 meters, Cerro Gaital) of the volcano (Figure 4).

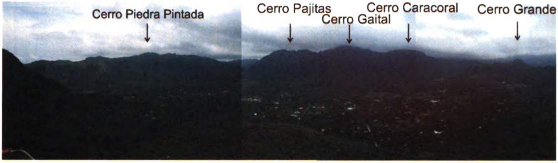

Figure 4. El Valle caldera features (taken from the south flank). Cerro Pajitas, Gaital, Piedra Pintada, Caracoral and Grande.

In Panama there are few detailed geologic maps. Defant et al. (1991a) studied silicic deposits in the northern part of the El Valle Volcano caldera, and on La Yeguada volcanic complex (Defant, et al. 1991b). None of these studies addresses the most recent silicic pyroclastic flow (El Hato formation) that occurs on the southern flank of El Valle Volcano, and extends 35 km south towards the Pacific coast.

Defant et al. (1991a) produced a geological map of the El Valle caldera along with K-Ar dates. In the present study I provide Ar^{39}/Ar^{40} dates, along with field observations to better constrain the stratigraphic and age relations at el Valle volcano. El Valle volcano consists of rugged terrain, dense vegetation and steep river channels; an outcrop map is presented in figure 5. A stratigraphic column is presented in figure 6 and a brief description of the geology of the El Valle volcano is summarized below.

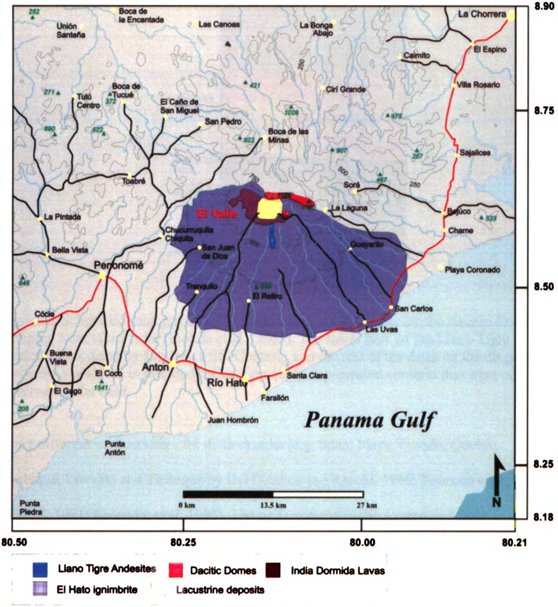

Figure 5. Outcrop map of El Valle Volcano and surrounding areas.

3.1 Regional Basement

The regional basement in western Panama is composed of oceanic assemblages that are part of Caribbean Large Igneous Province (CLIP) and crust of the Galapagos hot spot track. The assemblages are referred to as the Azuero-Soná Complex. It has been mapped

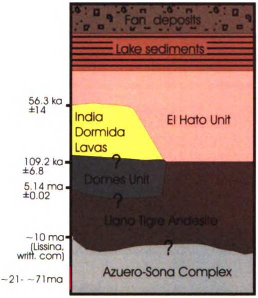

Figure 6. Schematic stratigraphy of El Valle volcano area. Dates for the Azuero-Sona complex were taken from Hoernle et al. (2002). The lower part of the Llano Tigre Andesite was dated by Lissina (writt. Comm)_ and the rest of the dates on the diagram come from analyses in this study. Question marks represented contacts that were no observed in the field.

using different nomenclature for distinct units (e.g. Soná, Playa Venado, Quebro, Tiribique, Lovaina and Tiribique by Del Giudice and Recchi, 1969; Tournon et al., 1989; DGRM, 1991; Kolarsky et al, 1995). The units outcrop in the Azuero and Soná peninsulas, and various islands of the Chiriquí and Montijo gulfs, (e.g. Coiba, Cébaco, Montuosa, Ladrones, Parida, Boca Brava and Contreras islands).

Lithologically, the Azuero-Soná Complex consists of massive, columnar and pillow basalts with interbedded radiolarites. Schistose amphibolites (Tournon et al., 1989) are exposed as slivers along the Azuero-Soná fault zone (Kolarsky et al., 1995). Additionally, metatuffs with pronounced shear foliation and tectonic mélanges were found by Tournon et al. (1989).

The Ar^{39}/Ar^{40} radioisotopic dates (Hoernle et al., 2002) of lava flows and pillow basalts range from 21 Ma to 71 Ma. The 21-66 Ma basalts of Azuero, Soná and Coiba are interpreted as accreted pieces of the subducted Galápagos hotspot track, while the 71.3 ± 2.1 Ma basalt of Soná peninsula is thought to represent the Caribbean Igneous Province (Hoernle et al., 2002).

3.2 Andesites Llano Tigre (Neogene)

Andesites characterized over a 5 m.y. magmatic activity interval, dated by Ar^{39}/Ar^{40} at the base of the sequence (Figures 5 and 6) by Lissina (written communication) at 10 Ma at stratigraphically higher localities, and at the top of the sequence in this study at 5.14 ± 0.02 Ma (Results Chapter 5).

The andesites have medium to coarse (3.5 mm- 0.5 mm) euhedral to subeuhedral crystals of plagioclase and augite in a very fine ground mass of microcrystalline plagioclase laths and augite (for petrographic details of this an other units refer to Appendix C). This unit underlies the el Hato Unit and the India Dormida Lavas on the south flank of the caldera.

3.3 Silicic volcanism (Quaternary)

Lava Domes unit and India Dormida dacitic Lavas unit

After a ~5 Ma of interval without any recorded volcanism, the dacitic lava Domes that form the peaks on the north flank of the caldera (Gaital, Caracoral and Pajitas)

(Figure 4); were erupted (109.2 ± 6.8 ka; see geochronological results). The silicic volcanism continued represented by the dacitic lava flows of the India Dorminda Lava unit at least until 56.3 ± 13.9 ka with the eruption of lava flows in Cerro India Dormida, Guacamaya and Cerro Iguana (84.5 ± 20.3 ka). Typical mineralogy of the Domes and India Dormida units consists of plagioclase, hornblende, quartz and biotite. No contacts were observed with other geological units.

El Hato Ash flow

El Hato dacitic ignimbrite (younger than 56.3 ± 13.9 ka) overlies the India Dormida dacitic lavas near La Cruz (Figure 6). This unit is an extensive silicic ignimbrite sheet (approximately 300 km^2), which resulted in a caldera collapse event creating a 30 km^2 depression. The thickness of this unit is variable but it can be more than a hundred meters (Figure 7). Detailed geochemical data is presented in the results section of the present study (Chapter 5). Typically, the mineralogy includes large (up to 3.5 mm) plagioclase, augite and quartz with small amounts of oxides (Appendix C).

3.4 Sedimentary deposits

After the caldera collapsed, more than 90 m of lake sediments were deposited (Bush and Colinvaux, 1990). The lake may have drained through a breach in the southwest caldera wall, where the main drain of the modern superficial waters is located. Bush and Colinvaux (1990) dated lacustrine sediments in el Valle volcano caldera that range from

Figure 7. The tan material outcropping in the side of that mountain is the Hato ash flow. The outcrop is more than 100 meters in height.

31,850 ka ± 1800 to 2370 ka ±150. This agrees with volcanic stratigraphy and events proposed earlier in this chapter.

Finally, near the Pacific coast river deposits rich in pumice fragments and ash from el Hato unit are found in the flanks of el Valle volcano filling the flat areas. This process continues today.

IV. METHODS

4.1 Pumice and lava sample collection

Images in this thesis are presented in color. The collection of over 100 pumice fragments and over 50 lava samples on an area of 300 km^2 were taken from the el Valle volcano. An attempt was made to sample the entire distribution of the silicic deposits. At a given outcrop, the sampling scheme was to take a wide variety of samples based on physical characteristics of the samples. For the ash-flow tuff, the samples were pumice fragments and sampling was designed to sample the variation in pumice-fragment size, vessiculation, color, and phenocrysts. For the lavas, sampling was designed to sample any variations in color or mineralogy. Samples were collected from road cuts and quarries, and natural outcrops (Figure 5). When possible, samples were taken from the same localities identified by Defant et al. (1991).

4.2 Bulk geochemical analyses

Over 100 samples were selected for bulk geochemical analyses of major- and trace-elements. Of all samples collected, only those that were unweathered were selected for analysis, weathered samples were identified by either thin section or hand sample observation. Both X-ray fluorescence (XRF) and Laser Ablation Inductively Coupled Plasma Mass Spectrometry (LA-ICP-MS) analyses at Michigan State are made on fused glass disks. The procedure followed the outline described by Hannah et al. (2002) for the preparation of low-dilution fusion glass disks (LDF).

The fused disks were analyzed using a Bruker Pioneer S4 X-Ray fluorescent spectrograph. XRF element analyses were reduced using Bruker Spectra Plus software®, which uses fundamental parameters (Criss, 1980).

For LA-ICP-MS trace element analyses, a Cetac+ LSX200 laser ablation system coupled with a Micromass Platform ICP-MS was used. The Cetac® LSX-200+ is a Nd:YAG laser with a frequency quadrupled to an UV wavelength of 266nm. The analyses were done using continuous ablation (line scan) for approximately three minutes. Strontium, determined by XRF, was used as an internal standard to correct for variations in ablated sample volume and instrument response. Trace element data reduction was done using MassLynx® software. Prior to any calculations, the background signal from the argon plasma was subtracted from each of the standards and samples. Element concentrations in the samples were calculated based on a linear regression method using BHVO, W-2, JB-1, JB-2, JB-3, JA-2, JA-3, BIR, QLO-1, and RGM-1 standards. Only standards with calculated values within 15% of the preferred standard values were used in the final calibration line for samples.

4.3 Individual phase chemistry

Eight pumice samples, one dacite sample and one andesite sample were selected for electron microprobe (EPMA) analyses at the University of Alaska Fairbanks. These samples represented both the bulk geochemical and physical variations observed in the eruptive products of El Valle volcano.

The major element compositions of minerals (from both the lavas and the pumice) and glass (from the pumice) were analyzed using a Cameca SX-50 Electron Microprobe at the University of Alaska Fairbanks, equipped with four wavelength-dispersive spectrometers and one energy-dispersive spectrometer. The procedure followed the depicted in Browne et al. (2006).

Quantitative analysis of glasses was performed using 15 kV accelerating voltage, 10 nA beam current, and a defocused beam (10 μm diameter). In order to minimize Na migration, the count rate of Na was scanned through time and corrected using a built-in procedure (Devine et al., 1995). The composition of minerals was determined using similar analytical conditions, but with a focused beam.

Elements were acquired using analyzing crystals LIF for Fe, PET for Ca and Ka; and TAP for Na, Al, and Si. For plagioclases the standards were Anorthite, USNM 137041 for Ca, OR10 CT for Fe, K, and TALBITE for Na, Al, Si. The standards for the glass analyses were Basaltic Glass (BG-2), USNM 113498/1 VG-A99 for Ca, Ti and Fe, Mn; Rhyolitic Glass, USNM 72854 VG-568 for Na, and Al; OR10 CT for K, MgO for Mg; and (TALBITE) for Si.

4.4 $^{40}Ar/^{39}Ar$ step heat analyses

Seven samples, handpicked for datable mineral phases (feldspars and groundmass) were submitted to the Geochronology laboratory at the University of Alaska Fairbanks (UAF) for $^{40}Ar/^{39}Ar$ analysis. The monitor mineral TCR-2 with an age of 27.87 Ma (Lanphere and Dalrymple, 2000) was used to monitor neutron flux and calculate the irradiation parameter, J, for all samples. The samples and standards were wrapped in aluminum foil and loaded into aluminum cans of 2.5 cm diameter and 6 cm height. All samples were irradiated in position 5c of the uranium enriched research reactor of McMaster University in Hamilton, Ontario, Canada for 0.75 megawatt-hours.

Upon their return from the reactor, the samples and monitors were loaded into 2 mm diameter holes in a copper tray that was then loaded in an ultra-high vacuum extraction line. The monitors were fused, and samples heated, using a 6-watt argon-ion laser following the technique described in York et al. (1981), Layer et al. (1987) and Layer (2000). Argon purification was achieved using a liquid nitrogen cold trap and a SAES Zr-Al getter at 400°C. The samples were analyzed in a VG-3600 mass spectrometer at the Geophysical Institute, University of Alaska Fairbanks. The argon isotopes measured were corrected for system blank and mass discrimination, as well as calcium, potassium and chlorine interference reactions following procedures outlined in McDougall and Harrison (1999). System blanks generally were $2x10^{-16}$ mol ^{40}Ar and $2x10^{-18}$ mol ^{36}Ar, which are 10 to 50 times smaller than fraction volumes. Mass discrimination was monitored by running both calibrated air shots and a zero-age glass sample. These measurements were made on a weekly to monthly basis to check for changes in mass discrimination.

V. RESULTS

5.1 Geochemistry of bulk Pumice and bulk Lava samples

Average compositions and standard deviations for major- and trace-elements are provided in Tables 1, 2 and 3; the complete geochemical analyses are presented in Appendix B. Samples with totals lower than 96% are excluded from the discussion because it was assumed that these samples were altered. In the figures all the major elements have been normalized to 100%.

5.1.1 Major Elements

The LeBas et al. (1986) chemical classification of samples from el Valle volcano is shown in Figure 8. In this diagram it can be seen that the samples are either andesites or dacites with no transitional compositions and all plot in the calc-alkaline field (Figure 9). The andesites are Neogene lava flows (5-10 Ma) and the dacites are either pyroclasts or lava flows from the Quaternary (<100 ka).

The major- and trace-element data is presented in variation diagrams in Figures 10 and 11, respectively. Samples from the dacite (Quaternary group) have very little chemical variation. The largest variations are observed in Al_2O_3, Na_2O and Fe_2O_3 that are compatible and K_2O that is incompatible. Within the Quaternary dacites, the India Dormida unit has higher Al_2O_3 and Fe_2O_3 content than most of El Hato pumices and lava samples from the Domes unit. In addition, K_2O content is higher on the Domes unit and lower on the India Dormida unit. It is remarkable that El Hato pumices overlap the entire major element variation that occurs within the Quaternary dacites.

Table 1: Average major and trace element composition and standard deviations for El Hato pumices. Major element oxides (wt.%) and trace elements (ppm).

	Mean	Standard Deviation
XRF Analyses		
SiO2	66.78	2.08
TiO2	0.23	0.05
Al2O3	16.78	0.70
Fe2O3	2.64	0.55
MnO	0.07	0.01
MgO	1.02	0.32
CaO	4.08	0.42
Na2O	4.17	0.34
K2O	1.38	0.18
P2O5	0.09	0.03
Ni	20.23	3.44
Cu	27.15	20.52
Zn	39.68	3.55
Rb	15.47	1.33
Zr	73.85	7.59
Sr	714.09	50.93
Laser ablation ICP-MS		
Y	5.38	1.25
Nb	2.32	0.49
Ba	556.45	36.80
La	7.92	1.14
Ce	16.57	2.15
Pr	1.84	0.28
Nd	7.18	1.11
Sm	1.50	0.23
Eu	0.55	0.08
Gd	1.43	0.21
Tb	0.23	0.04
Dy	0.95	0.19
Ho	0.17	0.06
Er	0.35	0.21
Yb	0.54	0.16
Lu	0.05	0.03
Hf	1.77	0.18
Ta	0.14	0.06
Pb	4.71	0.66
Th	1.61	0.54
U	1.09	0.36

Table 2. Average and standard deviations for major and trace element analyses for the dacitic lavas and dacitic domes units. Major element oxides (wt.%) and Trace elements (ppm).

	Mean	Standard Deviation
XRF Analyses		
SiO2	68.16	0.75
TiO2	0.26	0.02
Al2O3	17.44	0.39
Fe2O3	3.08	0.41
MnO	0.07	0.01
MgO	1.14	0.23
CaO	4.10	0.24
Na2O	4.29	0.23
K2O	1.35	0.16
P2O5	0.10	0.03
Ni	20.37	0.81
Cu	28.63	12.24
Zn	40.58	4.00
Rb	14.11	1.12
Zr	77.64	7.31
Sr	704.89	45.41
Laser ablation ICP-MS		
Y	5.13	0.82
Nb	2.53	0.36
Ba	585.22	53.38
La	8.45	1.03
Ce	17.23	2.39
Pr	1.89	0.35
Nd	7.19	1.01
Sm	1.48	0.32
Eu	0.59	0.15
Gd	1.39	0.26
Tb	0.23	0.06
Dy	0.92	0.19
Ho	0.17	0.06
Er	0.33	0.14
Yb	0.53	0.14
Lu	0.05	0.05
Hf	1.74	0.32
Ta	0.14	0.08
Pb	4.72	1.00
Th	1.88	0.67
U	1.28	0.61

Table 3. Average and standard deviations for major and trace element analyses for the Llano Tigre Lavas. Major element oxides (wt.%) and trace elements (ppm).

	Mean	Standard Deviation
XRF Analyses		
SiO2	58.22	0.33
TiO2	1.29	0.20
Al2O3	14.92	0.34
Fe2O3	6.39	0.09
MnO	0.11	0.01
MgO	4.45	0.16
CaO	9.44	0.22
Na2O	3.22	0.02
K2O	1.13	0.05
P2O5	0.83	0.07
Ni	55.67	4.50
Cu	102.33	34.45
Zn	69.33	3.30
Rb	15.33	1.25
Zr	182.45	78.42
Sr	812.00	134.48
Laser ablation ICP-MS analyses		
Y	23.61	6.64
Nb	6.30	0.92
Ba	565.59	49.55
La	31.41	11.05
Ce	75.71	33.42
Pr	10.95	5.22
Nd	47.45	23.39
Sm	8.47	3.89
Eu	2.37	0.94
Gd	6.87	2.84
Tb	0.78	0.25
Dy	3.86	1.04
Ho	0.69	0.17
Er	1.82	0.39
Yb	1.67	0.26
Lu	0.25	0.04
Hf	4.20	1.74
Ta	0.30	0.04
Pb	3.82	1.32
Th	3.76	1.61
U	1.37	0.54

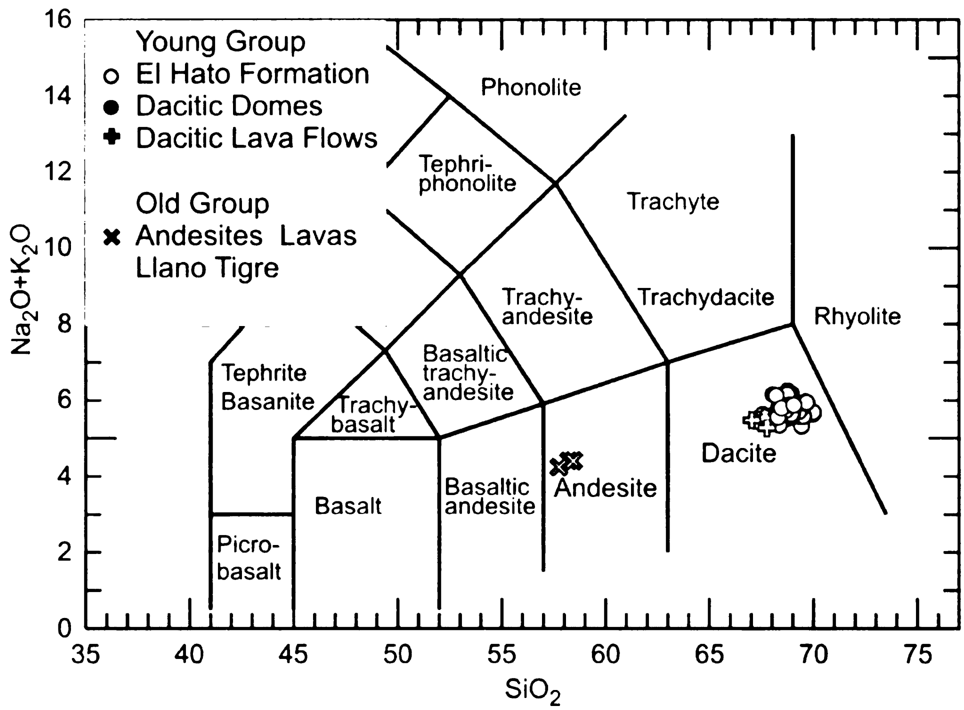

Figure 8. Alkalies versus silica on samples from el Valle volcano, LeBas et al. (1986) classification diagram.

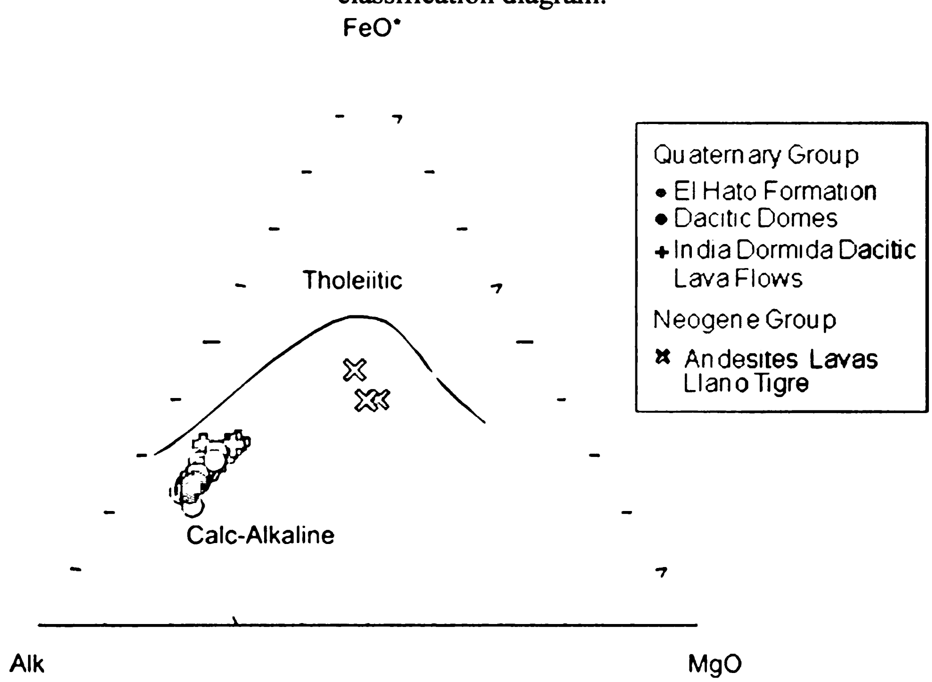

Figure 9. AFM diagram with tholeiitic and calc-alkaline fields.

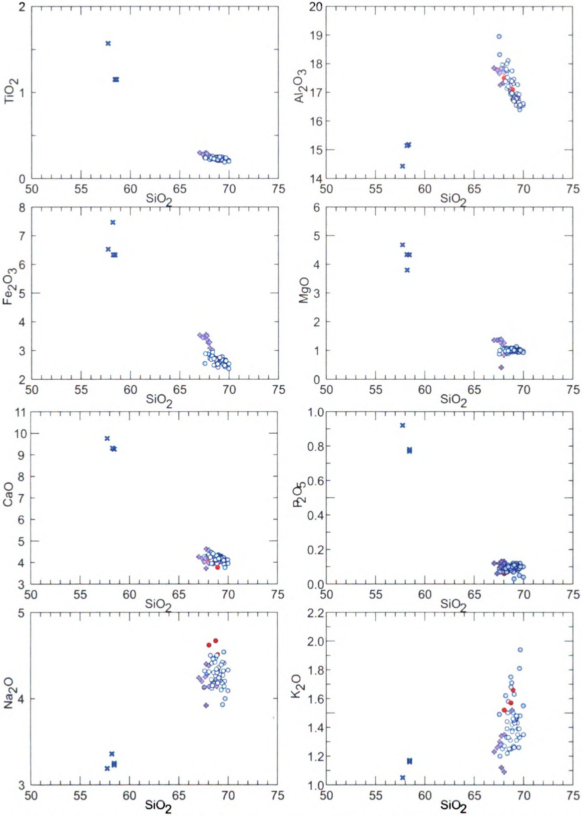

Figure 10. Bulk rock geochemistry – major element variation diagrams shown versus SiO_2. Symbols come from figure 8.

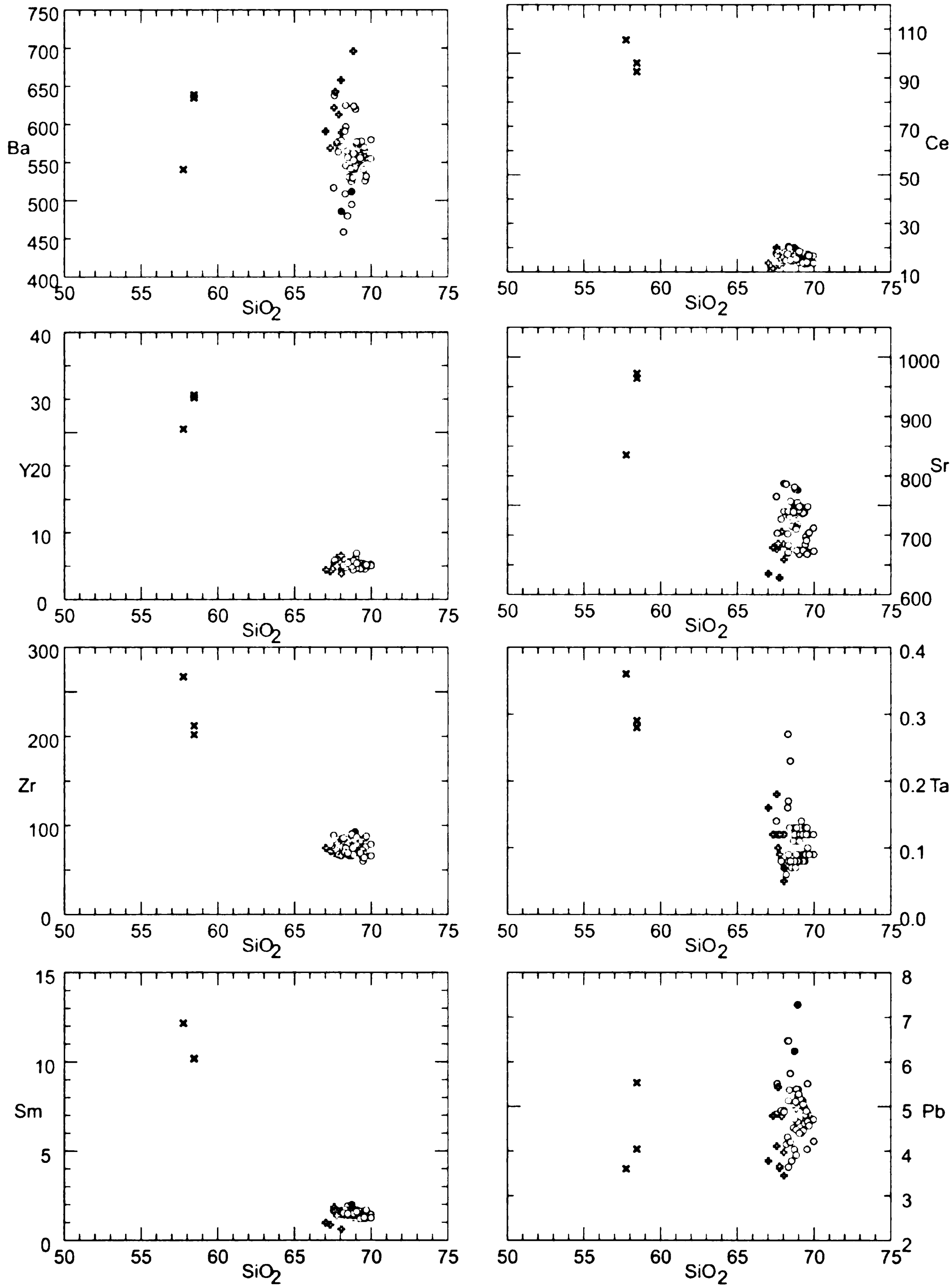

Figure 11. Pumice bulk geochemistry-trace element variation versus SiO_2. Symbols from figure 8.

5.1.2 Trace elements

Trace element variations with respect to SiO_2 are presented in Figure 11. There is little variation with respect to most of the trace elements in the Quaternary dacites except for Sr, Pb, Ta and Ba, which have the typical variability range observed in other Central American ignimbrites (Section 6.3). No systematic correlation is observed in the variation of Sr, Pb and Ta and Ba with other trace elements. The India Dormida dacitic lavas, Lava domes and the El Hato ash flow units contain little geochemical variation within each unit. However, Sr and Pb are higher in the domes and lower in the India Dormida dacitic lavas, while Ta and Ba are higher in the India Dormida unit and lower on the domes unit. As described for the mayor element concentrations, the pumice samples from El Hato unit cover the whole compositional range observed in the dacites. It is worth to note that Sr content in El Valle Quaternary volcanic rocks is high (>600 ppm), which will be address in a later section.

Spider diagrams and rare earth element (REE) diagrams for each of the four units are shown in Figure 12. The REE diagram shows the contrasting geochemical properties between the Neogene group (andesites) and the Quaternary group (dacites). The Neogene group is enriched with respect to the Quaternary group in all the rare earth elements (REE). Both groups on the spider diagrams are enriched in the large ion lithophile elements (LIL) and depleted (the Quaternary group even more) in high field strength elements (HFSE) and phosphorus (only the Quaternary group). The patterns on the spider diagrams are similar to Central America subduction zone magmas observed by others (Carr et al., 1984; Carr et al., 1990; Carr et al., 2003; Patino et al., 2000; Voget et al, 2006a; Vogel et al., 2006b; etc). The REEs for the Quaternary dacite samples are

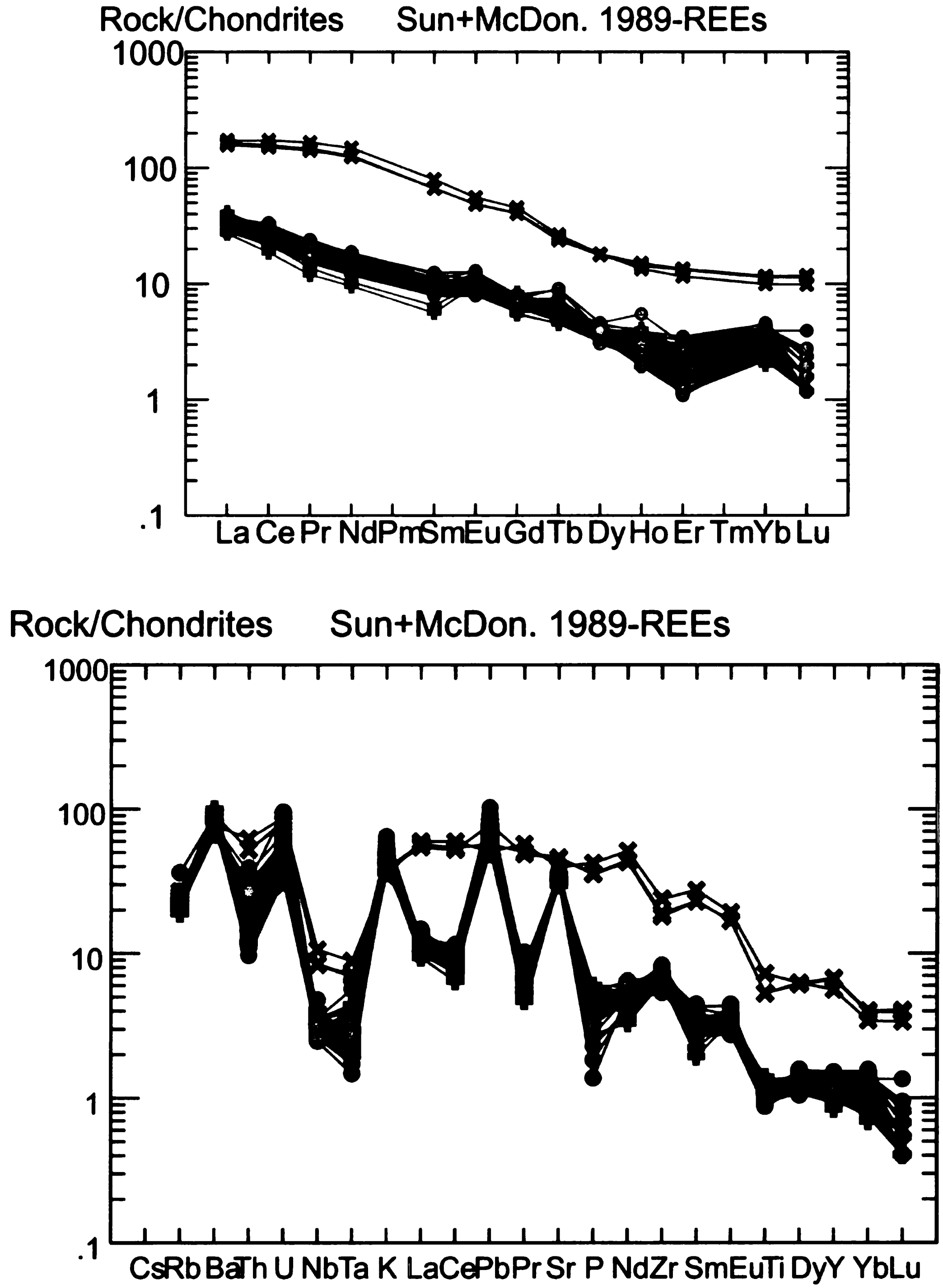

Figure 12. REE and spider diagrams of representative pumice samples of the Quaternary and Neogene group that conform El Valle volcano. Samples normalized to primitive mantle value of Sun and McDonough (1989). Symbols from figure 8.

extremely low in abundance with a slight enrichment of LREE over HREE. Some of the HREEs on the dacites are near delectability limits (the slight Yb anomaly may be an artifact of the low concentration). The REE for the andesite samples are similar to other subduction-related magmas with an enrichment of LREEs over HREEs.

5.2 Petrographic analyses and Mineral Chemistry

Petrographic analyses were performed on forty-three thin sections representing pumice samples for El Hato unit, dacitic lava samples from the India Dormida and Domes unit and andesites from the Llano Tigre unit. Complete petrographical analyses for all the units can be found in Appendix C. In addition, representative averages of mineral abundances estimated in modal percent and sizes of mineral phases for each of the units are included in table 4.

In addition, plagioclase chemistry of nine samples representing all of the units is provided in Appendix D (BSE images of the analyzed crystals are presented also in Appendix D). Major element data for the glass in the El Hato ignimbrites are also presented in this section and in Appendix D. Glass and plagioclase analyses are normalized to 100% and given in wt.% oxides.

Table 4. Petrographic summary giving averages of crystal proportions and size of crystals for El Hato, Dacitic Lavas and Llano Tigre andesites.

Unit/Sample	Plagioclase	Amphibole	Biotite	Quartz	Augite	Opaques
	modal %	modal %	modal %	modal %	modal %	modal %
El Hato	8-10	1-2		1-2		<1
Size of phase (mm)	2.0-1.2	0.5-0.3		1.5-1.0		0.5-0.3
Dacitic Lavas						
	17-26	3-6	1-6	2-7		<1-2
Size of phase (mm)	4.5 -0.05	2.50-0.25	0.20-0.10	4.5-0.5		0.3-0.6
Llano Tigre andesite						
	21				6	>1
Size of phase(mm)	3.5-0.5				1.5-1.0	0.5-0.2

5.2.1 Llano Tigre Andesites (Neogene group)

Lava samples from the Llano Tigre Andesites (Neogene group) typically have 20-28% crystallinity and hypocrystalline aphanitic porphyritic texture (figure 13a, b). Primary mineralogy consists of plagioclase, clinopyroxene (augite) and oxides. In plagioclase crystals textures such as discontinuous zoning, sieving on crystals edges, and

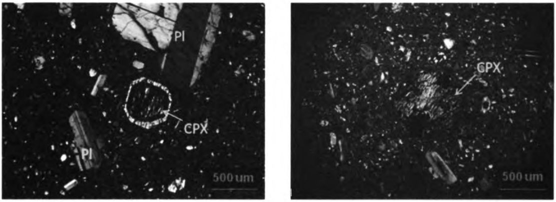

A B

Figure 13 a,b. Photomicrograph (XPL) of andesitic lava samples from the Llano Tigre andesites (Neogene group) with the representative minerals of this unit. Plagioclase (Pl), augite (CPX) and oxides are the most common minerals. A) Altered core of augite crystal with an unaltered rim. B) Completely altered pyroxene.

reaction on some of the rims are common. Most of the pyroxenes are altered and some of them are completely replaced by fine grained alteration products, perhaps smectite or vermiculate (Figure 13a, b).

Typically, plagioclase crystals have anorthite contents that are <50% (figure 14b). Although, in Figure 14a it can be seen that there are two anorthite peaks that reach 55%. The textures described at the beginning of this section (sieve textures and reaction on some of the rims) could be indicative of crystal melt disequilibria, which will be explored further in a later chapter.

5.2.2 Dacitic Domes (Gaital, Caracoral and Pajitas)

Lava samples from the three dacitic domes have 23-30% crystallinity and hypocrystalline texture (Figures 15a, b). Primary mineralogy consists of plagioclase, hornblende, quartz and biotite. Plagioclase crystals display discontinuous zoning, sieve

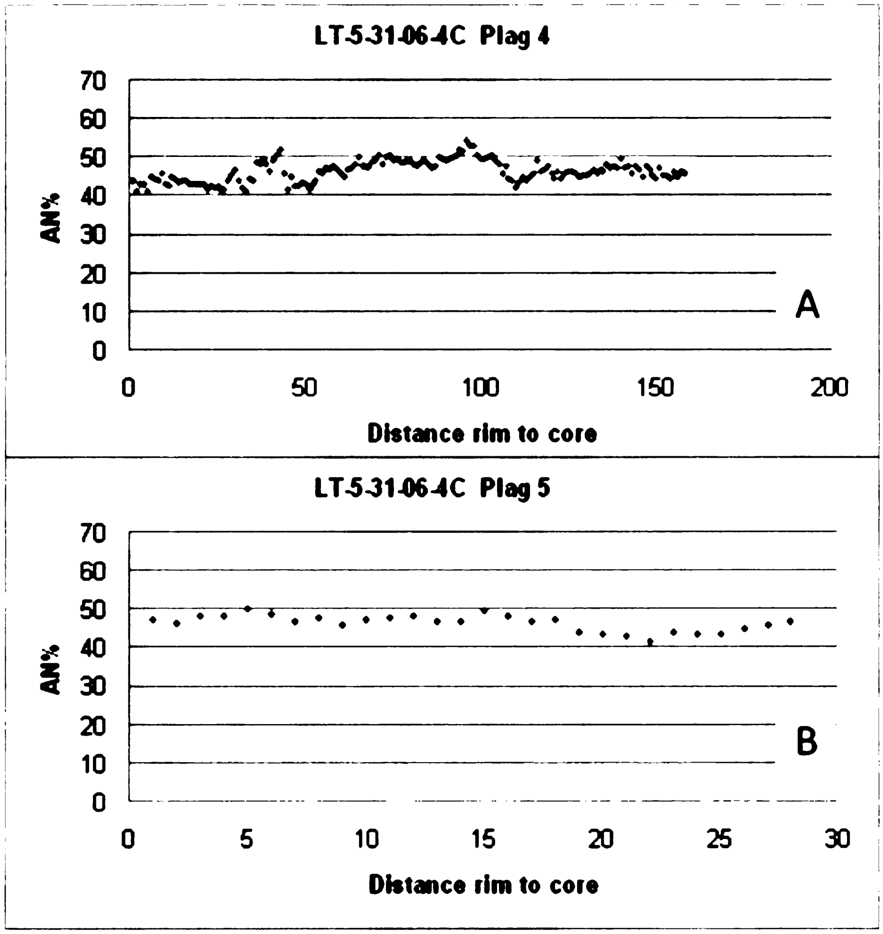

Figure 14. The Llano Tigre andesite (Neogene group) plagioclase analyses from rim to core on individual crystals. Anorthite contents are typically <50% . Although, in it can be seen that there are two anorthite peaks that reach 55%.

textures, and reaction on some of the rims, which are consistent with crystal- melt disequilibrium. In addition, most of the samples contain embayed quartz grains and opacite rims on hornblende (Figure 15a,b). Glomeroporphyritic accumulations of plagioclase, hornblende and oxides can be seen in some of the thin sections analyzed (Figure 15a, b). This last feature is best seen in samples from the easternmost lava dome Cerro Caracoral (Figure 4).

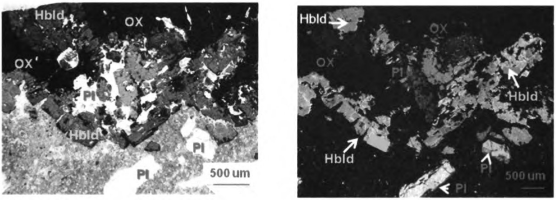

A B

Figure 15 a,b. Photomicrograph (PPL and XPL) of Dacitic domes samples (Quaternary group) with representative minerals of this unit. Plagioclase (Pl), hornblende (Hbld) and oxides (Ox) are the most common minerals. A) Glomeroporfiritic accumulation in PPL B) Glomeroporfiritic accumulation in XPL.

Microprobe analyses on plagioclase crystals are consistent with at least three rims with high anorthite content (Figure 16). In general it can be observed that the cores of the analyzed plagioclases are between An_{45} and An_{50}, then anorthite content declines and increases rapidly again to An_{50} to decline once again, and increase for the last time between An_{45} and An_{53}.

The sieved textures, resorbed plagioclases and embayed quartz crystals in conjunction with the plagioclase compositional variation are consistent with crystals grains in contact with magmas that may have driven them briefly out of equilibrium. In the next chapter this features will be discussed in more detail.

5.2.3 India Dormida dacitic lavas

Lava samples from this unit typically have 28-30% crystals and hypocrystalline texture (Figures 17a, b). Primary mineralogy includes plagioclase, quartz, hornblende and oxides. Crystals are found typically isolated, but some plagioclase and hornblende are

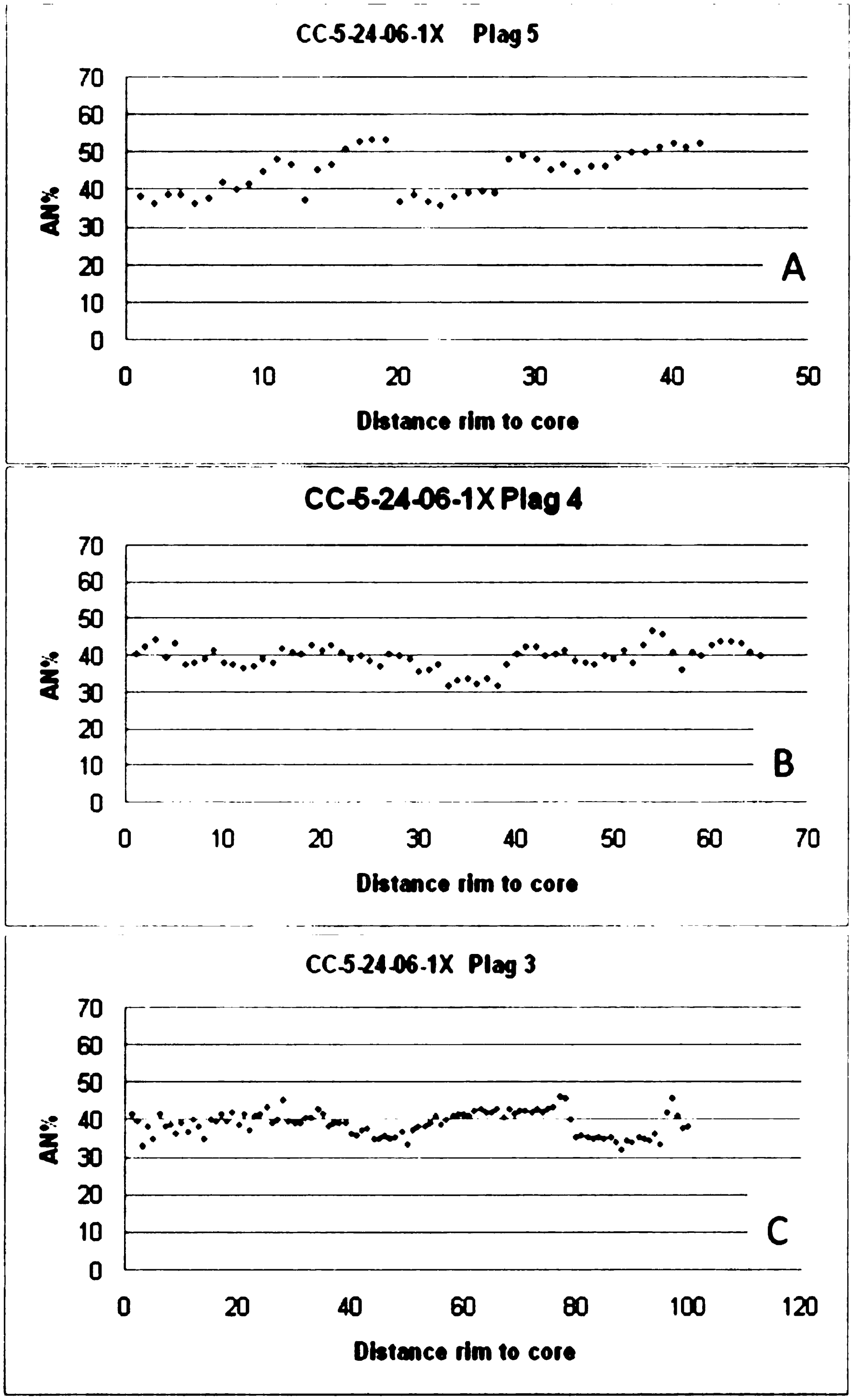

Figure 16. The Lava domes unit (Quaternary group) plagioclase analyses from rim to core on individual crystals. The cores of the analyzed plagioclases are between An_{45} and An_{50}, then anorthite content declines and rapidly peaks again at An_{50} to decline once again, and peak for the last time between An_{45} and An_{53}.

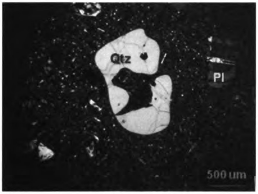

A

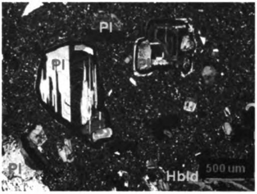

B

Figure 17 a,b. Photomicrograph (XPL) of India Dormida dacitic samples (Quaternary group) . Plagioclase (Pl), hornblende (Hbld) and oxides (Ox) are the most common minerals. A) resorbed and fracture quartz crystal B) Complex zoning in plagioclase.

intergrown along with the scarce Fe-Ti oxides. In the plagioclase crystals features that are consistent with crystal-melt disequilibrium textures such as discontinuous zoning, sieve textures and reaction on some of the rims are characteristic. Other important textures occur in quartz crystals were some of them are broken and are embayed on the edges (Figure 17). The textures previously described in plagioclase and quartz are consistent with disequilibrium between the mineral and the melt and will be discussed in a later section.

Plagioclase analysis from one crystal from this is most unusual compared to plagioclase analyses from other units. It contains cores with An_{70} and rims with anorthite contents as low as 45% (figure 18). These values are abnormal compared to the results found on the other units. A possible explanation for the abnormality is that the analyzed plagioclase crystal may be a xenocryst. The lack of plagioclase analyses in this unit weakens this interpretation which needs to be explored in the future with new analyses.

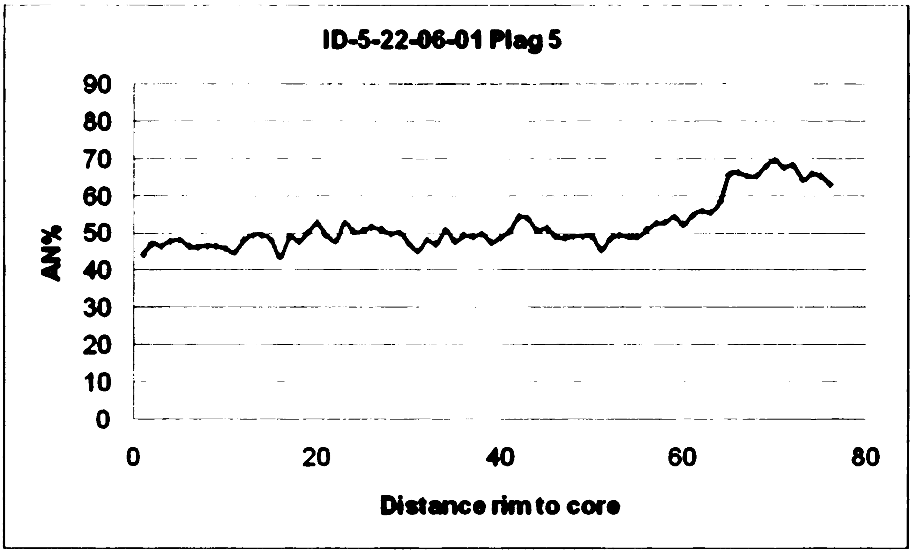

Figure 18. The India Dormida dacitic lava (Quaternary group) plagioclase analyses from rim to core on individual crystals. Normal zoning is observed. Cores are usually around 70% An and rims are 48% An.

5.2.4 El Hato ash flow

Pumices from El Hato unit are hypocrystalline with degrees of crystallinity typically between 10-14% (Figure 19a, b). Most samples display a glassy groundmass, but a small portion has some plagioclase microlites and crystallites. Primary mineralogy consists of plagioclase, quartz, hornblende and trace amounts of oxides. In plagioclase crystals, complex zoning patterns (Figure 19b) and resorbtion textures are common. A few of the samples have glomeroporphyritic clots of several or all of the primary minerals (figure 19a). The significance for petrological processes of the textures observed in this section will be address in a later section.

The variation in plagioclase composition in El Hato unit were produced by at least two events that increased rapidly the anorthite content in transects from rim to core. One

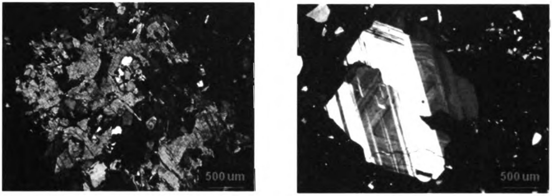

A B

Figure 19 a,b. Photomicrograph (XPL) of El Hato unit samples (Quaternary group). Plagioclase, hornblende and trace of oxides are the most common minerals. A) Glomeroporfiritic accumulation of plagioclase and hornblende B) Complex zoning in plagioclase

crystal has cores with An_{60} and rims of An_{35}-An_{45} (figure 20a, d), and another group of plagioclases have nearly constant composition of An_{40}, with some peaks that approach An_{50} (figures 16, 18, 20).

Glass chemistry for the pumice samples from El Hato is presented in Appendix D and Figure 21. A total of six thin sections were selected for glass analyses, no distinct glass populations were identified (Figure 21). This is consistent with the homogeneity found in the whole rock analyses presented at the beginning of this chapter.

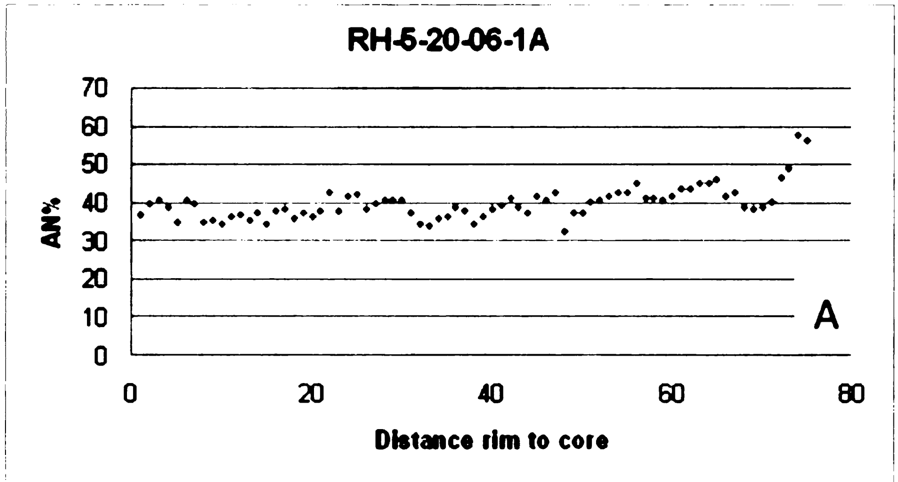

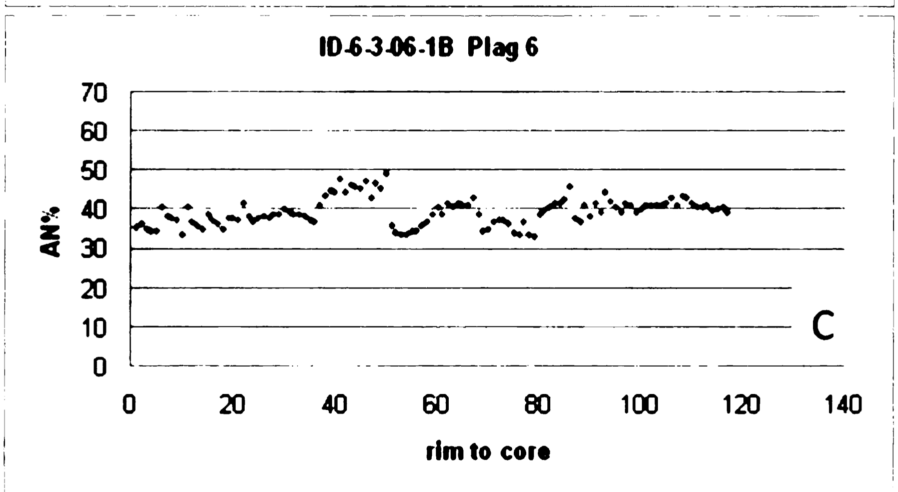

Continuation of figure 20

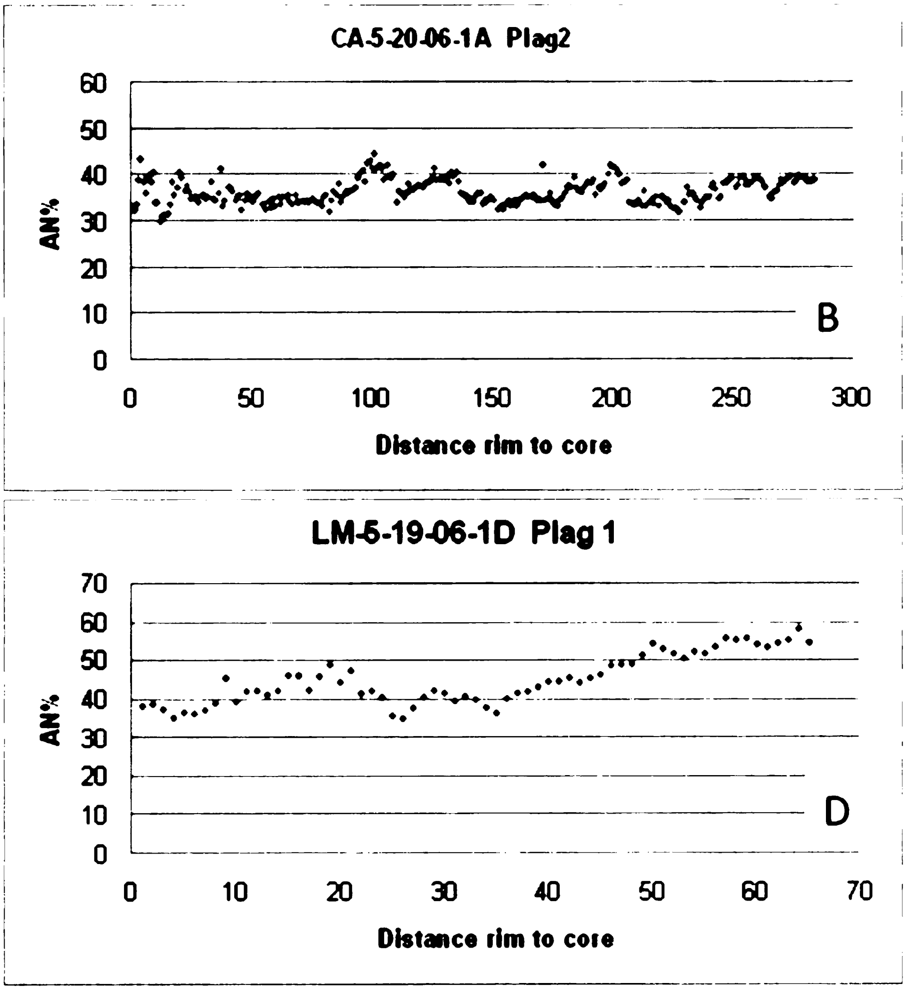

Figure 20. The El Hato (Quaternary group) Plagioclase, analyses from rim to core on individual crystals on representative geographical localities. El Hato unit resulted in two populations of plagioclase according to the variations of anorthite content in transects from rim to core. One population has cores with An_{60} and rims with An_{35}-An_{45}. The other group typically has cores of An_{40}.

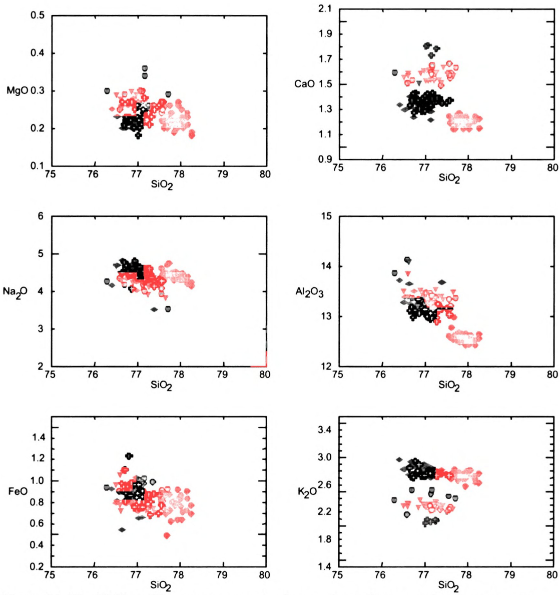

Figure 21. The El Hato (Quaternary group) glass analyses from pumice fragments on representative geographical localities. Major element variation diagrams showing the geochemical array of glass from individual pumice. There is no correlation with silica content for most of the major elements except for the negative Al_2O_3 vrs SiO_2. The different symbols used reflect individual thin section analyses.

5.4 $^{40}Ar/^{39}Ar$ Geochronology

5.4.1 Whole rock analyses

The detailed $^{40}Ar/^{39}Ar$ analyses are given in Appendix E, and a summary of the results is provided in Table 5; all ages are quoted to the ± 1-sigma level and calculated using the constants of Steiger and Jaeger (1977). Only the Llano Tigre andesites, India Dormida and Domes units were processed using whole rock samples, while age calculations on El Hato unit were done using single plagioclase crystals.

The integrated age produce by whole rock analyses, is the age given by the total gas measured and is equivalent to a potassium-argon (K-Ar) age. For the whole rock samples (Table 5), the spectrum provides a plateau age if three or more consecutive gas fractions represent at least 50% of the total gas release and are within two standard deviations of each other (Mean Square Weighted Deviation less than ~2.5). If possible, multiple plateaus have been combined by calculating the error-weighted mean of their steps.

The isochron age is proportional to the X-intercept of the best-fit regression of the data on an isotope correlation diagram; the Y-intercept is the inverse of the initial $^{40}Ar/^{39}Ar$. The isochron ages were chosen as the preferred ages when possible, and are shown (along with composite plateaus) (Figure 22 and 23).

Geologically meaningful plateau (Figures 22 and 23) and isochron ages (Figures 24 and 25) were obtained from all samples. High Ca/K fractions were excluded, as these were likely due to the degassing of plagioclase phenocrysts. Isochron analyses from three samples indicate the presence of slight amounts of excess argon. Thus, all isochron ages \

Table 5 Summary of whole rock analyses. Irradiation parameter, J, calculated using an age of 27.87 Ma for standard TCR-2 (after Lanphere and Dalrymple, 2000). Bold print denotes preferred age. In all the cases the composite plateau and the isochron age agree within the error limits.

Sample	Min.	Integrated age (ka)	Plateau age (ka)	Plateau information	Isochron Age (ka)	Isochron Information
Domes Unit CG-5-24-06-03	WR#1	98.8 ± 32.8	89.4 ± 28.8	5 fractions 95% 39Ar release MSWD = 0.4	82.3 ± 46.2	7 fractions 40Ar/36Ari = 303 ± 30 MSWD = 0.4
	WR#2	133.6 ± 6.0	100.3 ± 6.0	3 fractions 53% 39Ar release MSWD = 1.3	89.6 ± 7.8	4 fractions 40Ar/36Ari = 314 ± 10 MSWD = 0.3
	Composite Plateau:		98.4 ± 7.1	**Composite Isochron:**	**109.2 ± 6.8**	**13 fractions 40Ar/36Ari = 306 ± 8 MSWD = 1.7**
India Dormida Lavas ID-5-22-06-04	WR#1	161.1 ± .01	120.0 ± 47.3	5 fractions 94% 39Ar release MSWD = 1.0	-	-
	WR#2	32.4 ± 27.3	33.2 ± 20.7	5 fractions 97% 39Ar release MSWD = 0.2	44.0 ± 23.1	7 fractions 40Ar/36Ari = 292 ± 6 MSWD = 1.2
	WR#3	141.1 ± 10.0	92.0 ± 9.9	3 fractions 70% 39Ar release MSWD = 0.8	66.1 ± 13.6	5 fractions 40Ar/36Ari = 318 ± 7 MSWD = 1.3

Cont. Table 5

	Composite Plateau:		79.9 ± 10.1	**Composite Isochron:**	**56.3 ± 13.9**	**18 fractions** **40Ar/36Ari = 319 ± 7** **MSWD = 1.5**
India Dormida Lavas IG-05-28-06-0	WR#1	46.1 ± 16.8	-	-	-	-
	WR#2	98.5 ± 13.3	104.5 ± 10.4	4 fractions 90% 39Ar release MSWD = 1.4	107.3 ± 23.7	4 fractions 40Ar/36Ari = 292 ± 11 MSWD = 2.0
	WR#3	87.0 ± 47.3	109.3 ± 19.8	3 fractions 80% 39Ar release MSWD = 0.6	65.8 ± 37.2	4 fractions 40Ar/36Ari = 317± 13 MSWD = 2.3
	Composite Plateau:		101.9 ± 9.1	**Composite Isochron:**	**84.5 ± 20.3**	**8 fractions** **40Ar/36Ari = 306± 9** **MSWD = 2.2**
Llano Tigre Andesites LT-5-31-06-4A	WR#1	4862.6 ± 0.0	-	-	-	-
	WR#2	4870.4 ± 23.5	**5138.4 ± 22.8**	**5 fractions** **58% 39Ar release** **MSWD = 2.3**	-	-

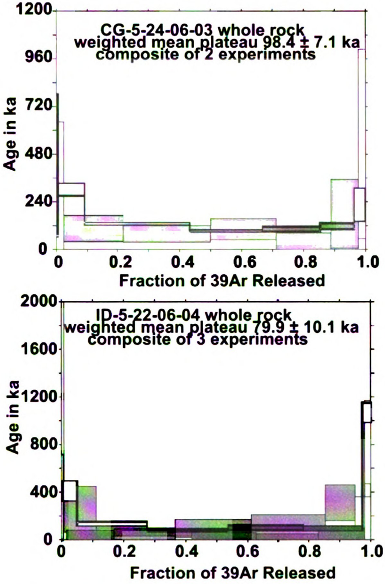

Figure 22. Composite plateau based in 2 experiments for CG-5-24-06-03 (Lava domes, Quaternary group) and 3 experiments for ID-5-22-06-04 (India Dormida dacitic lavas, Quaternary group).

are slightly different from the plateau ages (which might be biased by excess argon), but the plateau and isochron ages are generally within 2-sigma of one another. Because of the prospect of excess argon, the isochron ages may reflect the eruption ages of these samples.

The analyzed Dome unit sample (CG-5-24-06-03) produced a two-run composite plateau age of 98.4 ± 7 ka (Figure 21) and an isochron age of 109 ± 7 ka (Figure 22, Table 5). The initial $^{40}Ar/^{36}Ar$ ratio from the isochron is slightly, but not significantly,

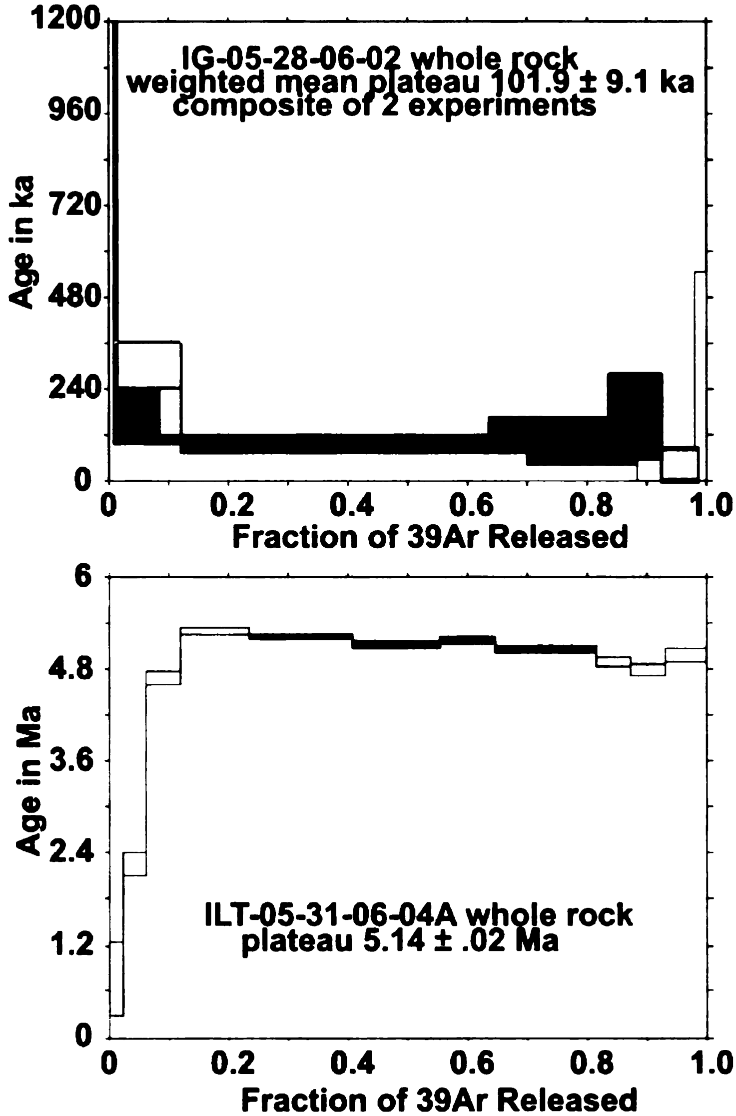

Figure 23. Composite plateau based in 2 experiments for IG-5-28-06-02 (India Dormida dacitic lavas, Quaternary group) and single plateau for LT-05-31-06-04A (Llano Tigre andesitic tic lavas, Neogene group).

different than the atmospheric value at the 2-sigma level. The isochron age is a geologically meaningful age.

The India Dormida unit (sample ID-5-22-06-04) is the only analyzed unit to exhibit significant amounts of excess argon, with a composite isochron yielding a $^{40}Ar/^{36}Ar_i$ of 319 ± 7 ka and an age of 56 ± 14 ka (Figure 22). One of the runs was unaffected by this excess argon and produced a younger age, which in combination with the other runs yielded a composite plateau age of 80 ± 10 ka (Figure 22, Table 5).

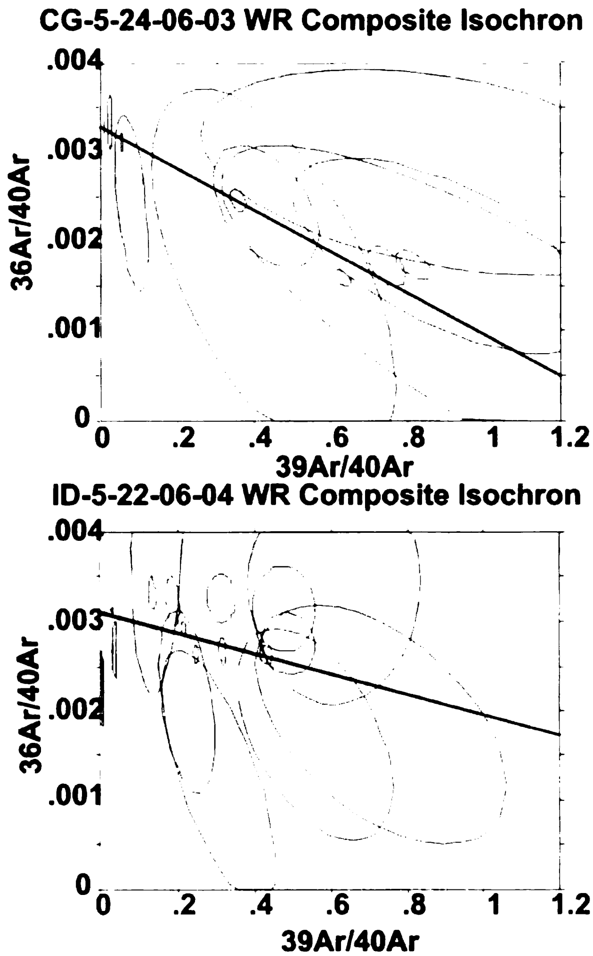

Figure 24. Composite Isochron based in 2 experiments for CG-5-24-06-03 (Lava domes, Quaternary group) and 3 experiments for ID-5-22-06-04 (India Dormida dacitic lavas, Quaternary group).

Another sample from the same unit but from a different locality (IG-05-28-06) in the first run produced an age that was significantly younger than its other runs, which is interpreted to be due to a high noise level on the mass spectrometer at the time; two subsequent runs produced a well-defined composite plateau at 102 ± 9 ka (Figure 23) and an isochron age of 85 ± 29 ka (table 5) with an initial $^{40}Ar/^{36}Ar$ ratio from the isochron that is slightly, but not significantly, different than the atmospheric value at the 2-sigma level.

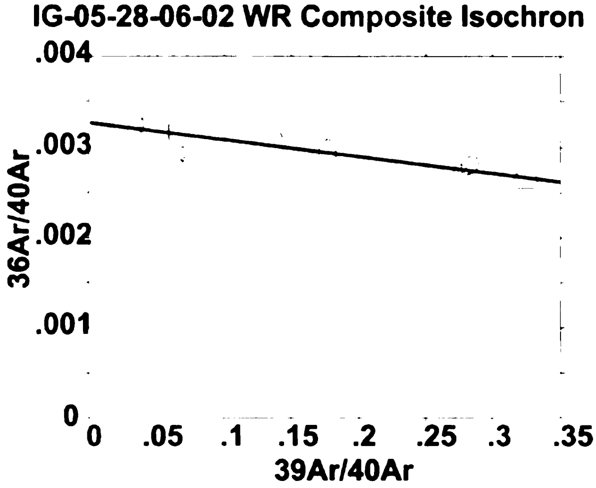

Figure 25. Composite isochron for LT-05-31-06-04A (Llano Tigre andesitic tic lavas, Neogene group).

The spectra from samples from the Llano Tigre Andesites (LT-05-31-06-04A) appear disturbed, yet the second run produced a plateau of 5.14 ± 0.02 Ma (Figure 23, Table 5). Further modeling could be conducted on this sample to extract an age of argon loss. Nonetheless, this age is considered to be geologically meaningful.

5.4.2 Plagioclase analyses

Single plagioclase analyses were picked from El Hato unit for $^{40}Ar/^{39}Ar$ dating. The picked crystals were confirmed to be plagioclases based on a Ca/K ratio > 1. $^{40}Ar/^{39}Ar$ analysis of the grains proceeded as single-fraction total fusions (Table 6), where a weighted mean age is calculated for each sample by weighting each analysis by the inverse of its variance. No plateau ages were calculated, as a plateau requires multiple heating steps, nor were isochron ages (due to the low potassium content and consequent non-radiogenic argon release of the plagioclase).

Table 6. Summary of plagioclase analyses from El Hato Unit. Irradiation parameter, J, calculated using an age of 27.87 Ma for standard TCR-2 (after Lanphere and Dalrymple, 2000). No Geologically meaningful ages were produced.

Sample	Min.	Integrated Age (ka)	Weighted Mean age (ka)	Weighted Mean Information
AT-06-02-06-02A	Pl	928.8 ± 196.7	941 ± 340	Probability = 0.2 0 of 10 Rejected
ID-5-22-06-04	Pl	2744.2 ± 522.5	2699 ± 950	Probability = 0.6 0 of 7 Rejected
LG-06-04-06-1B	Pl	708.4 ± 175.9	533 ± 330	Probability = 0.6 2 of 13 Rejected
LM-05-19-06-1D	Pl	644.2 ± 118.4	498 ± 220	Probability = 0.09 1 of 14 Rejected

The weighted mean ages of the plagioclase analyses are all much older than the whole rock ages from the same sample (Table 6). The scatter of the data was too great to compute an isochron, but is possible that the plagioclases are highly contaminated by excess argon and are not yielding geologically meaningful age information.

The dates calculated in this study can be summarized as followed: Domes Unit 109 ± 7 ka, India Dormida lavas 80 ± 10 ka to 56 ± 14 ka and Llano Tigre Lavas 5.14 ± 0.02 Ma.

VI. DISCUSSION

The goals of this study are to document the nature and source of the silicic volcanism in El Valle volcano and compare it with similar deposits associated with the subduction of the Cocos plate. Another goal is to evaluate models that have been proposed for the origin of silicic magmas in arcs without evolved continental crust.

6.1 Chemical and mineralogical variation of El Valle volcanic products

The volcanic activity in El Valle volcano can be separated both chemically and temporarily in two periods, the first during the Neogene (~10 Ma- ~5 Ma) and the second period represented by dacitic volcanism in the last ~100 Ka (Quaternary group, section 5.4). This section presents a discussion of the chemical and mineralogical variation on these contrasting periods of volcanic activity with special emphasis on the Quaternary silicic volcanism of El Valle volcano.

6.1.1 Neogene Group

The origin of the Neogene volcanism was not one of the objectives of this study. However, our limited sampling provides some constraint on their origin. The andesites that characterized the Neogene period in El Valle volcano have geochemical signatures similar to subduction zone magmas, presenting enrichment in large ion lithophile elements (LILE) relative to light rare earth elements (LREE) and high field strength elements (HFSE).

The geochemical signature of El Valle Neogene andesites is consistent with a process of differentiation from a more mafic magma originated by partial melting of the mantle wedge. This is based on: 1) Geochemical similarity between El Valle andesites and other arc andesites that have been interpreted to be derived from basalt-andesite differentiation (for example: New Hebrides – Gorton 1977; Lesser Antilles - Hawkesworth and Powell, 1980; Devine, 1995; Marianas- Wade et al., 2005). In addition, the El Valle andesites are metaluminous which it has been described as typical of basalt-andesite fractionation suites (Conrad et al., 1988; Drummond and Defant, 1989; and Sen and Dunn, 1994). 2) Magma compositions similar to El Valle andesites have been generated by experiments from potential mafic parental magmas by crystal fractionation (Clark, 1989). 3) The El Valle andesites do not meet the La/Yb criteria proposed by Gill (1981), and Drummond and Defant (1989); as magmas derived from direct partial melting of the subducted lithosphere (La/Yb>20, Yb<1 and Y<15).

6.1.2 El Hato unit and Quaternary volcanics

Chemical Characteristics

Similar to the Neogene andesitic volcanism, the Quaternary volcanic products in El Valle volcano have geochemical signatures similar to subduction zone magmas, although they are extremely depleted in heavy rare earth elements (HREE) (Figure 12), which will be discussed on a later on this chapter.

The dacitic volcanism produced during the Quaternary is characterized by little chemical variation (Figures 8, 10, 11, 12). The largest variations are observed in Al_2O_3,

Na_2O, Fe_2O_3, K_2O, Sr, Ba, Ta and Pb. These variations in the Quaternary dacites can be explained by processes in the magma chamber that can result in small amounts of crystal accumulation (Table 4 and appendix C). Plagioclase composition and content will control the variation of Al_2O_3, Na_2O, Sr and Pb, biotite and amphibole content will control Ba and K_2O respectively and the oxides the Fe_2O_3 and Ta.

Within the Quaternary dacites, the India Dormida unit has higher Al_2O_3 and Fe_2O_3 content than most of El Hato pumices and lava samples from the Domes unit, which is consistent with their relatively high plagioclase and oxide content. In addition, K_2O concentration is larger in the most amphibole rich unit (Domes unit), and lower on the India Dormida unit, which contains lower proportion of amphibole. Trace element variations among samples follow the behavior described for the major elements, where the variation is in function of the abundance of distinct crystal phases.

Despite the uniform geochemical character of the Quaternary volcanism, plagioclase chemistry and disequilibrium textures (e. g. resorbtion, sieve textures) are consistent with at least two events that increased the anorthite content in transects from rim to core (Figures 18 through 20). This could be explained by at least two periods in which a more mafic magma was injected into the system. In glass analyses from El Hato unit, there is no evidence that supported any mixing event occurrence (Appendix D and Figure 21). After the injection of the mafic magma, there was enough time to completely homogenize the dacitic magma body.

Source of Quaternary volcanism: Slab derived melts

It has been proposed that basalt originates in the mantle wedge to feed arc volcanism (for example see Gill, 1981; Peacock 1991; Hildreth et al., 2004; and Price et al., 2005). It is widely accepted that andesites, the most common type of lavas found in island arcs, are derived from parental basalts. This is confirmed by the common occurrence of calcic plagioclase and magnesian olivines on arc andesites (Izbekov et al., 2004).

A slab component has also been described in subduction related magmas, and is associated with sediment input (including detrital volcanic material produced by subduction erosion) and has been described by Morris (1991); Plank and Langmuir (1993); and Patino et al. (2000).

Recently, it has also been proposed that melting of the down-going slab can play an important role in magma generation in some modern-day arc environments (e.g. Kay, 1978; Marsh, 1979; Defant and Drummond, 1990, and Drummond and Defant, 1990). This interpretation of slab melts as magma source in some volcanic arc environments, comes from the trace element and rare earth element (REE) patterns of andesitic to dacitic volcanics in several subduction zones in which young, hot, oceanic crust (< 5 Ma) is being subducted (e.g. Cook Island on the Austral Volcanic Zone in Chile Kay et al., 1993; and the recent volcanism in Mt St. Helens, United States; Defant and Drummond,1993).

Geochemically slab derived melts have been characterized by specific signatures such as, high Sr, high Sr/Y, low K/La, low $^{87}Sr/^{86}Sr$, low FeO/MgO, high Na_2O, and high Al_2O_3, for a complete discussion see Drummond and Defant (1990); Stern et al. (1984);

Defant et al. (1991a) and Defant et al. 1991b) (Table 7). These authors have described that slab derived melts are similar in composition (in particular in their trace element and REE characteristics) to Archaean high-Al trondhjemites, tonalites and granitoids (TTG belts) (Drummond and Defant, 1990). It has been suggested that these may have form by partial melting of oceanic basalt (e.g. Drummond and Defant, 1990; Martin, 1986).

Table 7: Summary of geochemical characteristics of slab derived magmas (for a complete discussion Drummond and Defant, 1990; Stern et al., 1984; Defant et al., 1991a; and Defant et al., 1991b).

Slab Melts characteristics	Implications
Low HREE	Garnet in the source region.
Low Y	Y has a high Kd in hornblende, garnet, and clinopyroxene.
High Sr	Possible melting of plagioclase. Sr has low Kd for hornblende, garnet, or clinopyroxene.
High Sr/Y	These ratios are quite different from the patterns seen in andesites and rhyolites produced by fractional crystallization.
Low to moderate K/Rb (not observed at all sites)	Hornblende in source fractionates K over Rb.
Low HFSE (Nb, Ta)	Suggests Ti-phase or hornblende in source.
Erratic or lack of Eu anomaly	Suggests that either minor plagioclase is left in the residue or that the source was depleted in Eu. High Na_2O and Al_2O_3 argue against plagioclase in the source region.
High La/Yb	Enrichment of LREE compared to HREE.
Low K/La, low Rb/La, low Ba/La, Low $^{87}Sr/^{86}Sr$, low $^{206}Pb/^{204}Pb$, High $\varepsilon(Nd)$	N-MORB signature. No significant component of continental crust, subducted sediments.
High LILE (K, Sr)	Small melt fraction of N-MORB basalt or crustal contamination.

The Quaternary dacites of el Valle volcano have most of the characteristics of melts produced from melting of eclogite (Table 7), which are extreme depletion of HREEs, high Sr, high Sr/Y, Low Nb and Ta, lack of Eu anomaly (Figure 11), high La/Yb ratio, and low Yb and Y, High LILE.

A chondrite normalized La/Yb versus Yb is presented in Figure 26 showing two fields that have been superimposed: an Archean field consisting of trondhjemite-tonalite-dacite (TTD) samples supposed to be produced by partial melting of the subducted lithosphere; and a post-Archean field generated by plotting TTD related samples generated by differentiation of mafic magmas derived from the partial melting of the mantle wedge (Jahn et al., 1981; Martin, 1986). integrated in Figure 26 are partial melting curves that model the source of the Archean field from the partial melting of a MORB-like source (in this case, Archean tholeiite). The Archean tholeiite is within the MORB field and represents partial melting of Archean subducted crust. The partial melting curves on the diagram were produced by Martin (1986) and represent models of the partial melting of Archean tholeiites having a composition similar to: eclogite, garnet free amphibolites and amphibolites with 10 and 25 percent garnet.

During the subduction process, MORB is transformed into amphibolites that with increasing pressure and temperature dehydrate to garnet eclogite (Peacock, 1993). In the melting process, garnet and/or amphibole (depending on the case) are left behind as residual phases that results in low concentrations of Yb (and other HREEs that have high distribution coefficients in garnet) and Y in partial melts (TTD complexes). The Quaternary dacites from El Valle fall within the Archean field with very low $(La/Yb)_{CN}$ ratios along the eclogite partial melting curve. The geochemical characteristics

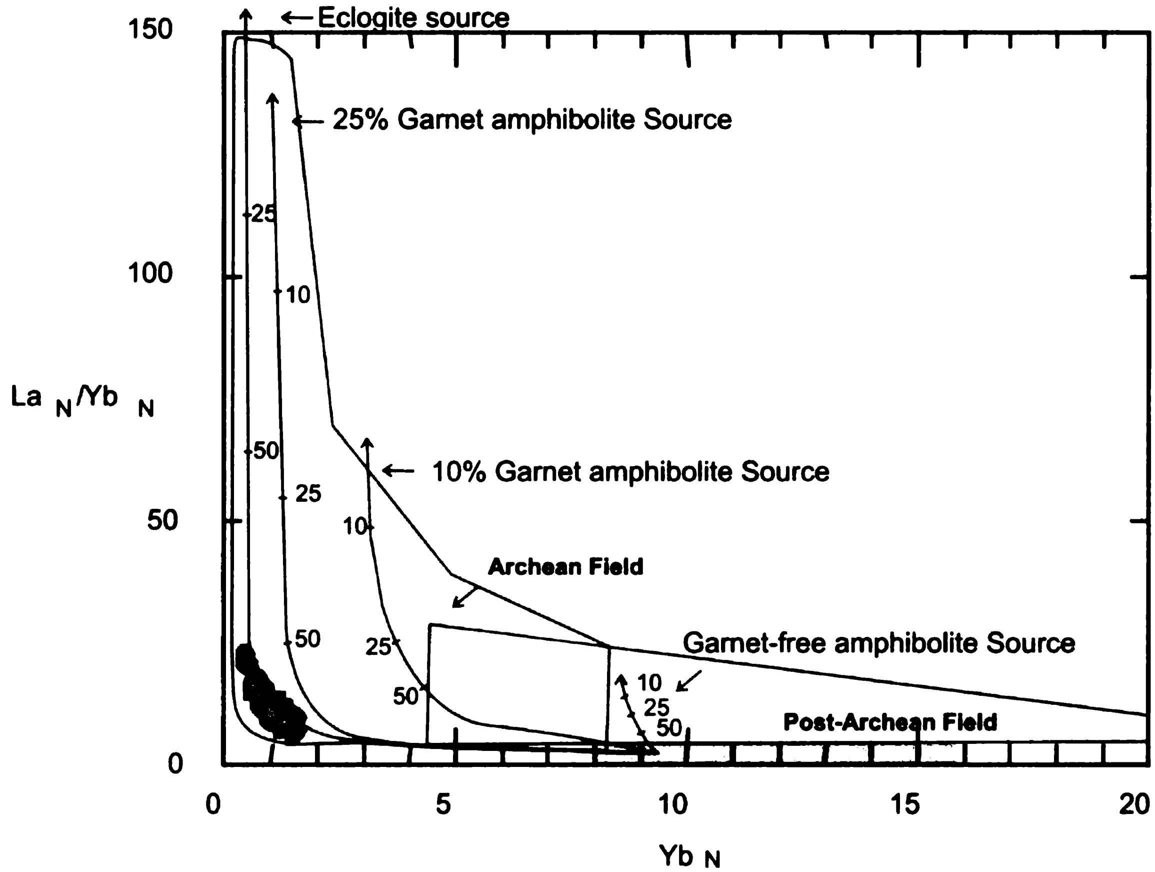

Figure 26. Chondrite normalized (values Sun and McDonough, 1989) La/Yb vs. Yb diagram. The superimposed Archean and post-Archean fields are after Jahn et al. (1981). The partial melting curves on the diagram are from Martin (1986) and represent models of the partial melting of Archean tholeiites. The values among the partial melting curves represent the percentage of partial melting. The gray area represents the range in MORB compositions (the Archean tholeiite falls within this field and represents the partial melting of Archean subducted crust). The dacites form El Valle fall within the Archean field. Same symbols as in figure 8.

enumerated for the Quaternary dacites of El Valle volcano are consistent with <75% melting of an eclogite source (Figure 26) that produced the extreme depletion observed in the HREEs, with garnet remaining in the restite. No geochemical variation observed in the Quaternary dacites are consistent with fractionation of hornblende ± other mineral phases (Figures 8 through 11). In that manner, the subducting lithosphere may be a source for the Quaternary dacites.

Further evidence of eclogite melting as a source for the El Valle dacites comes from Sr/Y versus Y diagram (Figure 27). The general model presented in the diagram has been discussed in detail by Defant and Drummond (1989). Figure 27 presents the field from Archean TTD complexes, the field for the andesite –dacite – rhyolite (ADR) Quaternary samples from island arcs, and El Valle dacites data. The ADR data fall along a differentiation path (Y becomes enriched with differentiation) believed to be the result of combinations of crystal fractionation, mixing, and/or assimilation of magmas derived from basaltic parents that originated from partial melting of the mantle wedge (Defant and Nielsen, 1989). The dacites from El Valle have low Y values typical of the Archean trondhjemites and high Sr/Y. In addition, several melting curves derived from the partial melting of depleted MORB (point 4) and altered MORB (point 5) leaving an amphiolite and an eclogite restite (Hole et al., 1984) are included in Figure 27. Restites are described in the figure caption. The curves go through Archean TTD data, and under the proper circumstances (variations in MORB compositions, degrees of partial melting, and/or mineral partition coefficients), are consistent with the dacite group originated by the partial melting of eclogite possibly derived from subducted MORB, leaving a eclogitic restite.

I have suggested that the Quaternary dacites of El Valle volcano have been derived from the subducted lithosphere. It is important to review other ways to achieve HREEs depletion, high Sr/Y and low Y in subduction environments. One way is by amphibole and clinopyroxene dominated crystal fractionation. In that way, the fractionation process drives the magma compositions to higher Sr/Y and lower Y values if starting with an andesite like composition as parent for the dacites. The problem with such process is

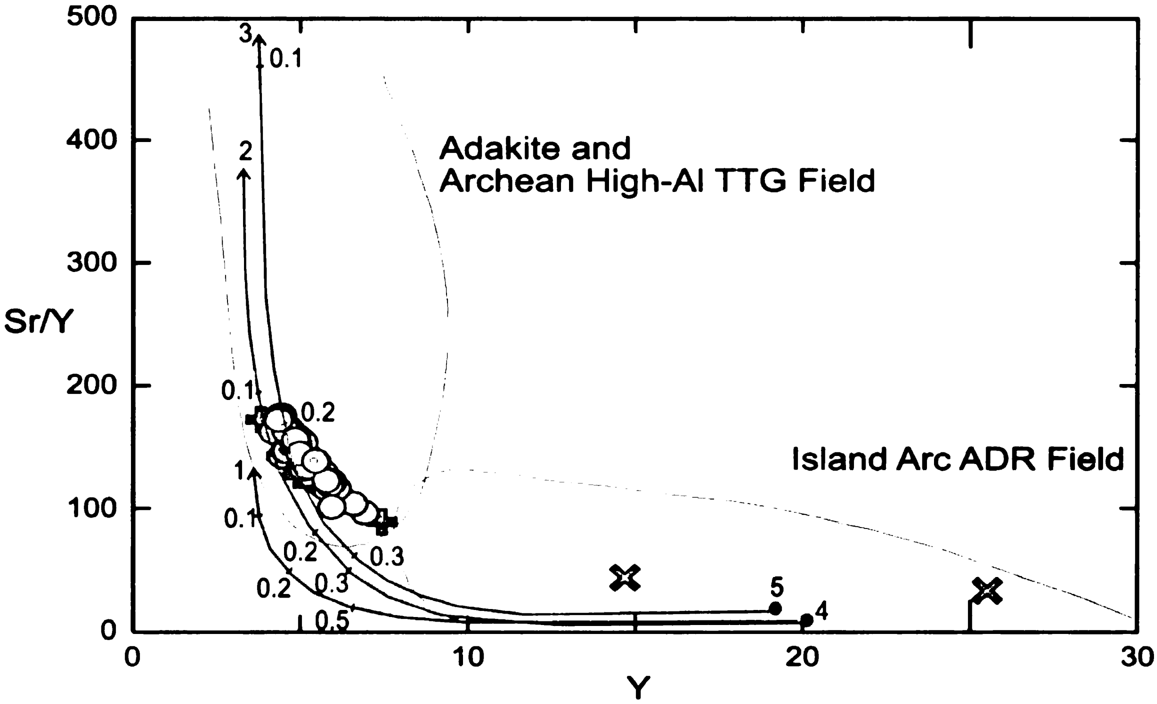

Figure 27. Plot of Sr/Y vs. Y. Three curves derived from partial melting of a depleted MORB (point 4) or altered MORB (point 5) (partial melting curves from Hole et al., 1984) leaving an amphibolite and eclogite restite are superimposed on the diagram. Curve 1 residual solid=35% CPX, 30% Am, and 35% GT; curve 2 residual solid = 10% am, 45% GT, and 45% CPX and curve 3 residual solid = 50% GT and 50% CPX. Sams symbols as in figure 8.

that clinopyroxene has not been found in any of the dacites and to replicate the extreme HREE depletion observed in the data, an unacceptable large percentage of amphibole fractionation is required - which is not consistent with the amount of amphibole that occurs in the samples. Furthermore, there would have to be a large amount of crystal fractionation without eruption of intermediate products, which is not present.

Other ways to produce similar magmas have been described in continental arcs where the crust is thick enough for garnet stability (P > 1.2–1.5 GPa, Peacock et al., 1994), and the lower crust has the appropriate mafic composition (Atherton and Petford, 1993). These melts are referred to as continental arc root-derived adakites (Stevenson et al., 2005), and have also been described by Xu et al. (2005) and Guo et al., (2006) as a process that accompanies delamination of the lower crust. The standard explanation is that as the continental crust thickened, the lower mafic section reached the pressure and temperature conditions favorable to the formation of eclogite (40- and 80-km deep and between 700 and 800 °C). The eclogitic materials is denser than the mantle rocks and breaks away from the crust and sinks i.e. delaminate (Kay and Kay, 1993), resulting in a thinner crust. Although there is no crustal thickness data for Panama, it is unlikely that the crust has reached the thickness necessary for the garnet to be stable. Basement rocks that outcrop near the Pacific Coast (Caribbean Large Igneous Province, CLIP), close to the actual volcanic front, are not consistent with a thick continental crust.

The mineralogy, concentrations of key trace elements, and depleted HREE patterns of the dacites is consistent with partial melting of an eclogite source with garnet in the restite (Figures 23, 24). However, the age of the Nazca plate (23 ± 5 Ma, Barckhausen et al., 2001 near the Coiba Ridge and ~14 km east of same ridge, Figure 2) is too older (and therefore colder) than is necessary to produce partial melting of the subducted lithosphere (Peacock, et al. 1994). Usually, plates older than 5 Ma are too cold to be melted as modeled by Peacock et al. (1994). However, the Nazca plate is characterized by very high heat flow (which is more typical for oceanic plates younger than 5 Ma), averaging 0.14 W/m^2 in the Panama Basin (Jarrard, 1986 and Bowin, 1976).

The source of the high heat flow in the Panama basin may be related to the Sandra Rift system described in chapter 2 and presented in figure 2. The association of seismicity with an east–west band of rough topography has prompted the suggestion that this is a nascent spreading center beginning to detach a "North Nazca" microplate from the Nazca

Plate (Lonsdale, 2005). Reinterpretation of the magnetic data by Lonsdale (2005) is consistent with spreading ceasing along the Malpelo Rift shortly after 9 Ma but continued along the Sandra Rift. This interpretation is consistent with the Sandra Rift being a Cocos-Nazca spreading axis that propagated westward from at least 12 Ma to ~9 Ma overlapping the concurrently spreading eastern segment of Malpelo Rift where spreading slowed after 12 my. Since this period, the Sandra Rift has possibly been rejuvenated at times by tension resulting from slab pull forces acting in different directions due to the curvature of the Colombian trench (Hardy, 1991)

Some authors proposed that a spreading reactivation along the Sandra Rift may has partially caused a reactivation of a slow northeast-directed subduction beneath Panama, possibly since 3–5 Ma (de Boer et al., 1988; Silver et al., 1990). Moreover, spreading along the Sandra Rift has been proposed by Mutter and Mutter (1993) as the responsible for crustal thinning process in the Malpelo Ridge region, as indicated by the relative variations in thickness of the upper and lower crusts. To the southeast, the ridge thinning is mostly accommodated by layer 3 thinning from 18 to 6 km, whereas layer 2 thins only from 4 to 3 km. To the northwest, from the ridge summit to the 12 km thick oceanic crust north of the ridge, thinning of layer 2 is larger than thinning of layer 3. No detailed crustal thinning studies have been done on the whole extension of the Sandra Rift, but if thinning of the crust in the Malpelo Ridge region was caused by Sandra Rift spreading, then crustal thinning may be a regional feature in the Panama basin. When a cold lithospheric plate is being rifted (crustal thinning processes) upraising of the asthenosphere occurs and shearing and fracturing in the cold plate facilitate a positive contribution to the surface heat flux. The magnitude of the heat contribution depends on the distribution of shear stresses, strain rates and characteristics of the boundaries (Sass et al., 1974).

If spreading is occurring along the Sandra Rift, then this may be the cause for the anomalous hot oceanic lithosphere in the Panama basin. A warm subducting plate has increased buoyancy (accompanied by a decrease in subduction angle, favoring melting Gutscher et al., 2000), low seismicity, and may result in partial melting of the slab. Most of these conditions have been described for the Panama basin area (van Andel et al., 1971; de Boer et al., 1991; Von Herzen and Anderson, 1972; Case, 1974; Bowin, 1976, and Collins et al., 1989). Analogous conditions have been described for other regions that have magmas interpreted to be derived from slab melts (Kay, 1978; Stern et al., 1984; de Boer et al., 1991; Martin, 1999; Gutscher et al., 2000; Ramos et al., 2004; Samsonov et al., 2005; Hidalgo et al., 2007).

Another alternative to produce melts with adakitic-like characteristics has been proposed by Proteau and Scaillet (2003). They propose H_2O rich conditions in the mantle wedge joined with high pressure fractionation of oxidized primitive basalt that crystallized amphibole and garnet upon cooling; could generate the extreme REE depletions observed in adakitic magmas. Constraints on temperature and pressure conditions for the El Valle Quaternary magmatic products are needed to test this model in the Panama portion of the arc.

6.2 Silicic Volcanism (origin)

During the Quaternary, silicic magmas have been the only product of El Valle volcano. The occurrence of silicic volcanism in different tectonic settings have been described by several authors (e.g. Cameron et al., 1980, de Silva and Wolff, 1995; Eichelberger et al., 2000) and a diversity of processes have been described for their origin.

When a thick continental crust is involved models for the origin of these magmas in subduction zones are prolific. Processes such as partial melting of continental crust (White and Chappell, 1983; Vielzeuf and Holloway, 1988) or assimilation of crustal rocks and fractionation of the resulting magma (DePaolo, 1981; Hildreth and Moorbath, 1988) have been proposed.

A more complicated problem to resolve is the occurrence of silicic magmas in volcanic arcs without continental crust. Silicic magmas were not thought to be common in these areas due to the absence of continental crust. However, several authors (Hannah et al., 2002; Tamura and Tatsumi, 2002; Leat et al., 2003; Smith et al., 2003; Vogel et al., 2004) have described such type of magmas making them more common than once thought. In this section I will give a brief review of models for that have been proposed for the origin of silicic magmas in volcanic arc settings and then I will described a model that is consistent with the results found in El Valle Quaternary volcanics.

Tamura and Tatsumi (2002) proposed a model to explain the origin of silicic melts in arc settings based on petrologic and geochemical evidence. The process involved an upper mantle derived intermediate melt (hydrous magnesian andesite composition) that ascends and stalls and crystallizes as it reaches buoyant equilibrium. Dehydration melting of the stalled andesitic magma could produce partial melts with high silica contents. Another way to produce high silica magmas is the extraction of the silicic interstitial liquid from a medium to high-K_2O basaltic melt that undergoes high degrees of fractional crystallization or partial melting of a crystalline to medium to high-K_2O basalt (Sisson et al., 2005).

The starting rock composition in the Sisson et al. (2005) experiments involved partial melting of amphibole rich calc-alkaline sources. In a scenario with amphibole being incorporated in the melt, the resulting magma composition will not be consistent with the depletions observed in the MREE or HREE in the dacites of El Valle. Furthermore, the initial compositions used by Sisson, et al. (2005) were mafic and to achieve such compositions from an eclogite source (source for El Valle Dacite, previous section on this chapter), almost 100 % melting is required (Rapp and Watson, 1995). Aside from the difficulties of achieving 100% degree of melting, the process will result in no HREE depleted liquids as the ones observed in El Valle.

The homogeneous geochemical composition of the Quaternary products of El Valle volcano and the lack of any trends that may represent a liquid line of descend from andesitic composition magma; is inconsistent with fractional crystallization. Fractional crystallization yields continuity in the compositions of generated liquids which is not a characteristic in El Valle Quaternary volcanism. Moreover, as it was described by Eichelberger et al. (2006), the separation of crystals from the melt in which they grew will be impeded by increasing melt viscosity with increasing SiO_2 content.

The chemical characteristics of the El Valle Quaternary volcanism cannot be explained by the models described above. However, the origin of the silicic, HREE depleted magmas of El Valle volcano is consistent with models of Rapp et al. (1991), Sen and Dunn (1994), Rapp and Watson (1995), Pertermann (2003) Rapp et al. (2003) Rapp et al. (2003). Rapp et al. (2003) showed that partial melting of an eclogite rock produces granitoid liquids with major- and trace-element compositions equivalent to Archaean TTG, including the low Nb/Ta and high Zr/Sm ratios of 'average' Archaean TTG (Foley et al., 2002), but from a source with initially sub-chondritic Nb/Ta. The major-element compositions of the great majority of Archaean TTG are characterized by SiO_2 contents of 65–73 wt% and Mg-numbers of 0.30–0.50; which are similar compositions to the El Valle Dacite.

Remelting or residual melt extraction from stalled, crystallized (or partially crystallized) plutons (Tamura and Tatsumi, 2002; Bachmann and Bergantz, 2004) derived from melting of eclogite (and other more mafic sources, consistent with disequilibrium textures in Quaternary volcanics) may have been important in the generation of the Quaternary dacites of El Valle, but are not necessary. Certainly, the thickened CLIP crust represented in Panama by the Azuero- Sona Complex, would have been an excellent thermal insulator (Tamura et al., 2003) inhibiting the diffusion of heat and not contributing any material to new batch of melt.

Partial melting accompanying dehydration of these generally eclogitic source magmas transferred in to the base of a thickened crust (e.g. CLIP), would produce compositionally appropriate TTG like granitoids in equilibrium with eclogite residues. Silicic magmas with HREE depletions similar to El Valle magmas can be produced in this manner.

6.3 Comparison of El Hato with other silicic ignimbrites Central America

Several large volume silicic pyroclastic flows have been described in the Central American Volcanic Front by different authors, for example Gillot et al. (1994), Villegas (1997); Rose et al. (1999) and Vogel et al. (2004). This section will assess a brief geochemical comparison of selected silicic ignimbrites from Costa Rica (Sandillal, Alto Palomo and Tiribi) and Nicaragua (Apoyo, Coyol, Las Sierras, Las Maderas and Monte Galan) with el Hato unit from El Valle volcano.

The silicic volcanic products from El Valle volcano are compositionally homogeneous compared to the silicic ignimbrites of the Nicaragua and Costa Rica. The Cocos Plate subduction related ignimbrites display chemical variation from basalt-basaltic andesites to rhyolites (Figure 29). In El Valle Volcano, dacite is the only composition erupted during the Quaternary. During this period of time, volcanism has been characterized by silicic ignimbrites and lava units that show little variation in major elements (Figure 10) and trace elements (Figure 31). The el Valle silicic volcanism is compositionally distinct with HREE depletion (figure 12), low Y (Figures 11 and 12), high Sr, high Sr/Y (Figures 30), low HFSE, low FeO/MgO and low K_2O/Na_2O ratios (Figure 28). These data are unique to El Valle Volcano silicic ignimbrites and differentiates them from the silicic ignimbrites of Costa Rica and Nicaragua.

These differences indicate a distinct source for the silicic magmas from the Panama portion of the arc compared to silicic magmas from Nicaragua and Costa Rica. The K_2O/Na_2O ratio and relatively high REEs in most ignimbrites associated with the Cocos plate subduction requires an evolved source with medium to high-K concentration as starting compositions (Vogel et al., 2006). The composition of El Valle Volcano deposits, with HREE depletion requires a lower K, garnet-bearing source (e.g. eclogite).

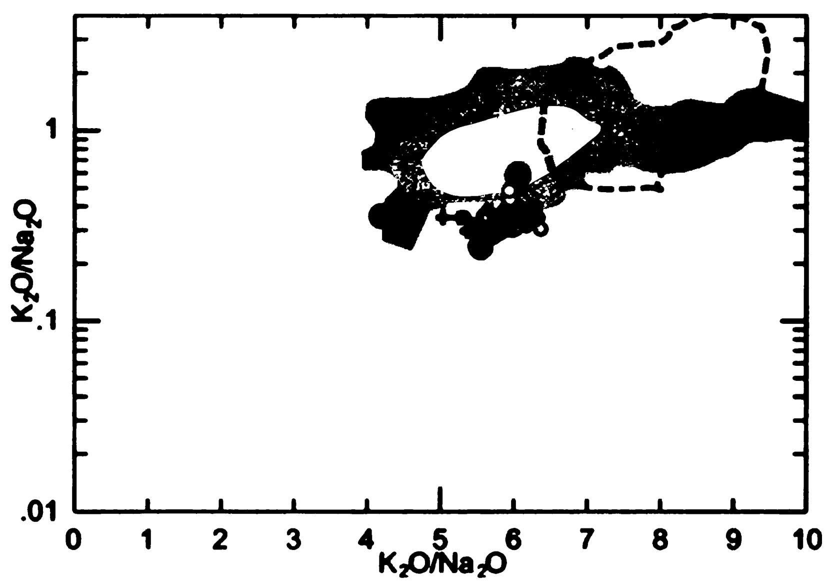

Figure 28. K_2O/Na_2O versus K_2O+Na_2O for the Costa Rican and Nicaraguan pumice fragments (shaded area) and the silicic pumice fragments and associated deposits of El Valle Volcano. El Hato formation (blue dots), Dacitic lava flows unit (purple crosses) and the Dacitic domes unit (red dots). Blue dash line defines a real of experimental liquids under various conditions and amounts of melt produced by Sisson et al. (2005) experiments. (Black dots are the starting compositions of those experiments).

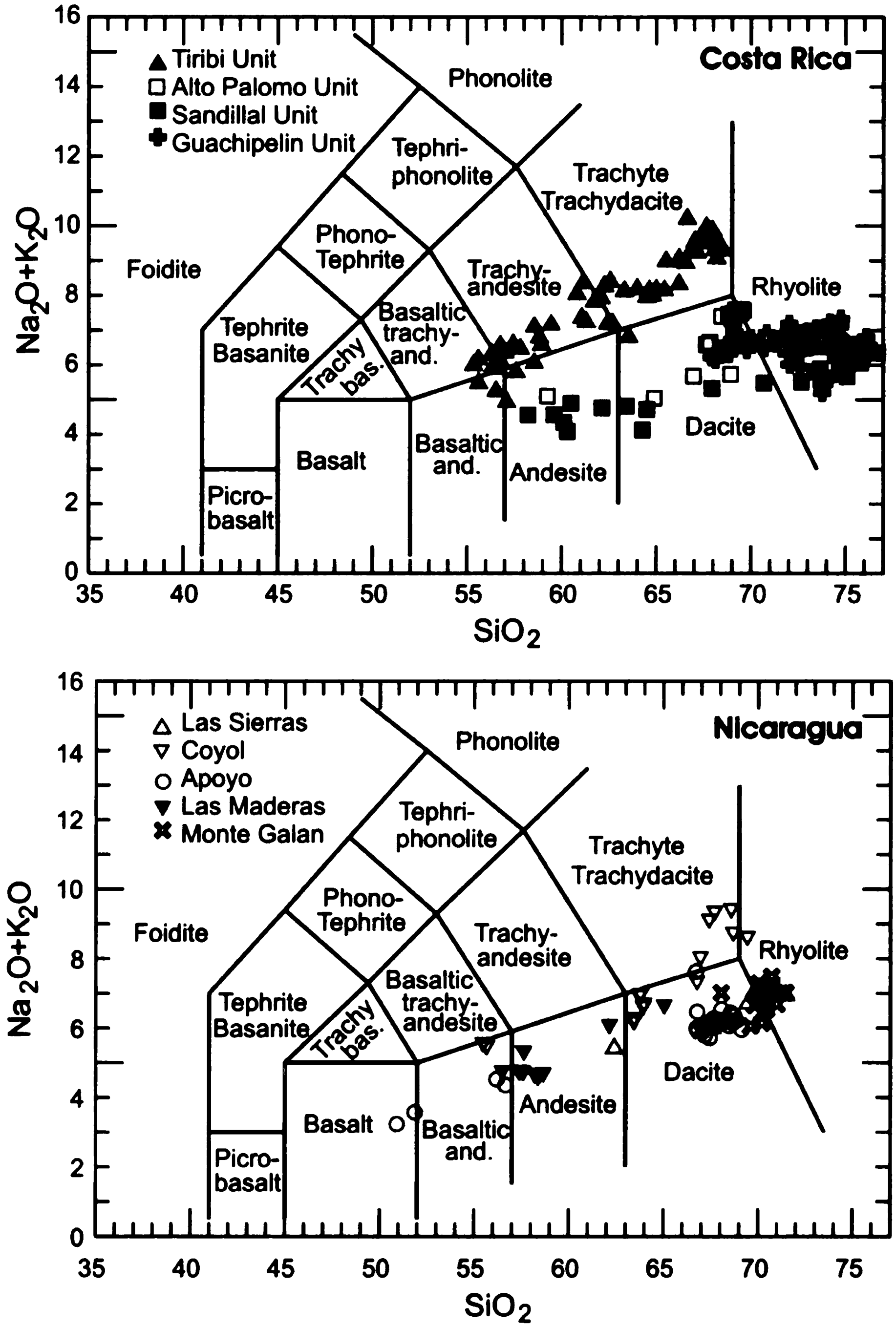

Figure 29. Alkali–silica classification diagram (LeBas et al., 1986) for pumice (pyroclastic) fragments (flows) and associated deposits from from Costa Rica and Nicaragua. Compare with figure 8 from El Valle volcano.

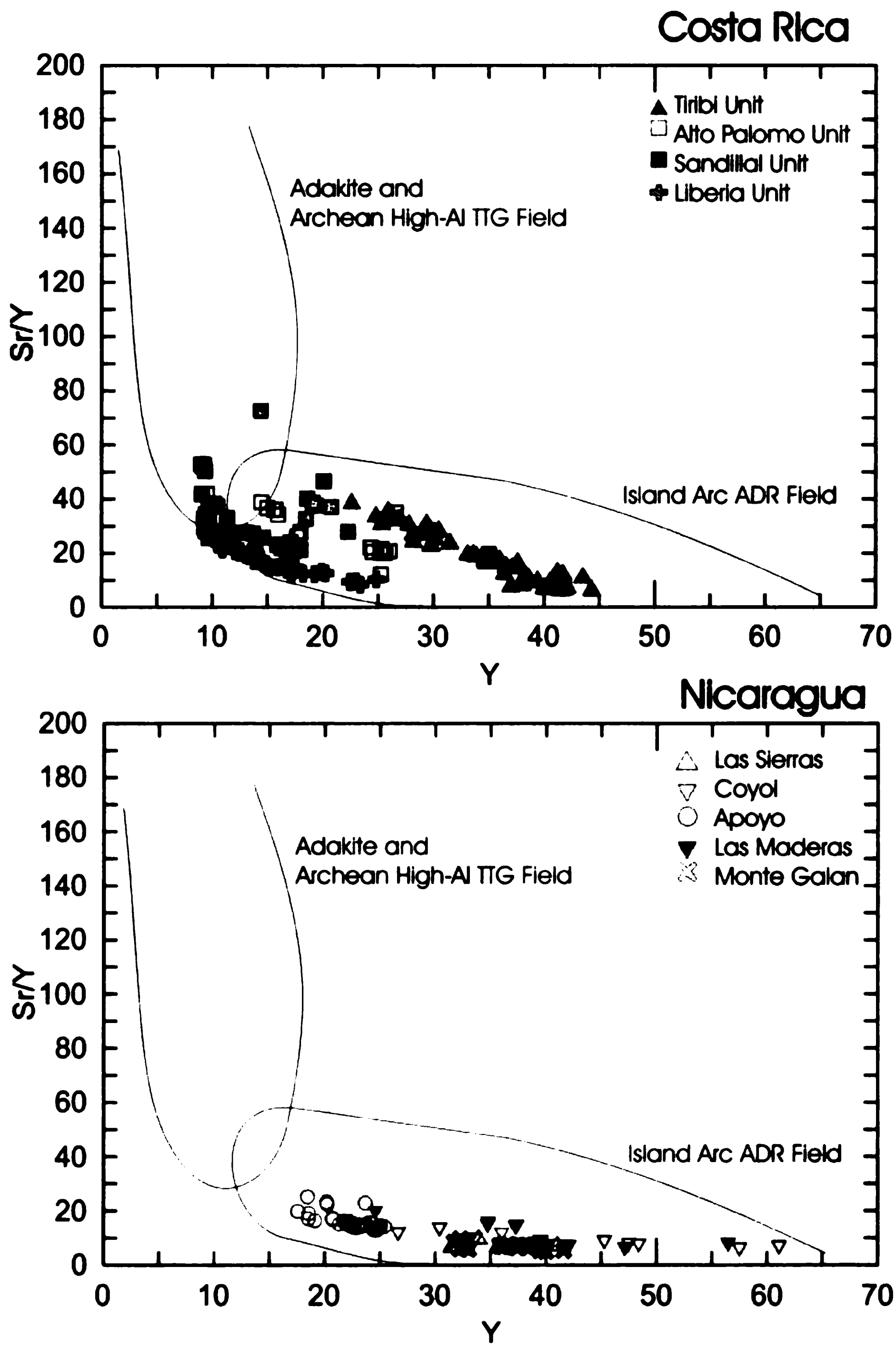

Figure 30. Sr/Y vs. Y Costa Rican and Nicaraguan ignimbrites. Adakite and Archean high Al-TDD and Island-arc ADR fields (Nielsen, 1988) have been superimposed.

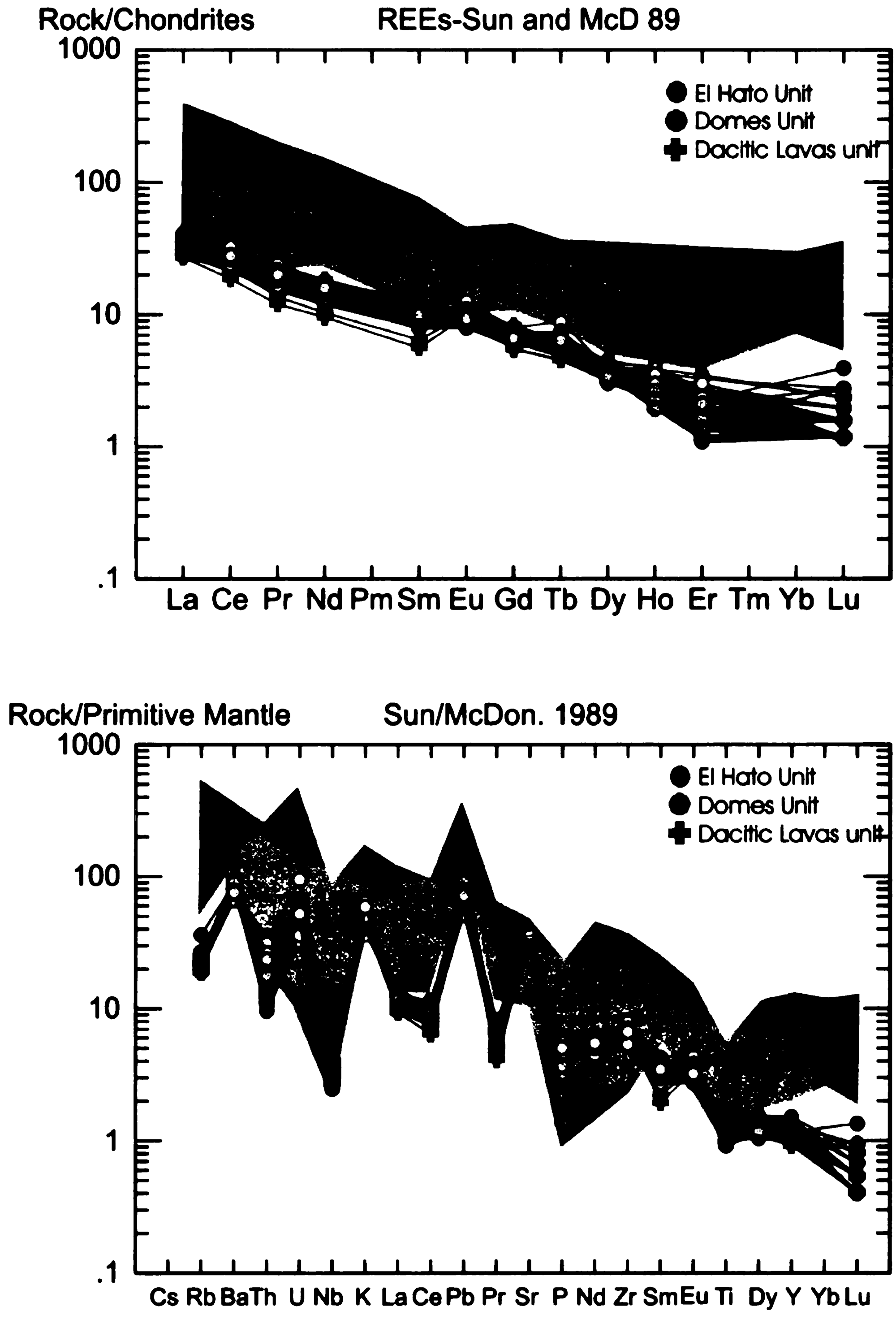

Figure 31. Chondrite-normalized spider diagrams for el Valle volcano Ignimbrites and associated deposits. Shade area represents compositional range for ignimbrites from Costa Rica and Nicaragua.

VII. CONCLUSIONS

The new $^{40}Ar/^{39}Ar$ geochronological analyses of the volcanism of El Valle volcano presented in this study unraveled one of the most recent periods of volcanic activity (younger than ~56 ka) in the Central American Volcanic Front and modified previous K/Ar age determinations by Defant et al. (1991a). Moreover, the new age determinations allowed for the categorization of the El Hato pyroclastic flow as one of the largest eruptions during the Quaternary period in the region.

The geochemical homogeneity found in El Valle volcano Quaternary volcanism is unique in the studied silicic ignimbrites of the Central America volcanic front. The depletion of HREE, low Y, high Sr, high Sr/Y, low K_2O/Na_2O ratios are unseen in the well-studied deposits in Costa Rica and Nicaragua. This results in a different interpretation for the source of the Quaternary dacites in El Valle with respect to the rest on the Central American Volcanic Front. The composition of El Valle Quaternary deposits best characterized by the HREE depletion and a low K_2O/Na_2O, are best explained by a low K garnet-bearing source (e.g. eclogite melts), while the high K_2O/Na_2O (and relatively high REEs) characteristic of most ignimbrites associated with the Cocos plate subduction are consistent with an evolved source with medium to high-K as starting composition (Vogel et al., 2006).

Another distinct feature of El Valle Quaternary volcanism from the other silicic Central American ignimbrites is the model for their origin. The model that I am proposing for the origin of the silicic volcanism in El Valle volcano was introduced by Rapp et al. (2003), and involves partial melting accompanying dehydration of eclogite-like source materials (or rocks derived from eclogite sources). This process will produce compositionally appropriate TTG-like granitoids in equilibrium with eclogite residues. This model is a direct way of producing high silica magmas in subduction environments without involving fractionation processes. Moreover, Rapp et al. (2003) model is a straightforward interpretation to explain the occurrence of silicic volcanism in regions that lack developed continental crust and slab melts are possible in the garnet stability field.

The age of the Nazca plate in the Panama basin would, at first glance be evidence against any partial melting processes of the subducted lithosphere. However, the Nazca plate near the Panamenian trench is characterized by very high heat flow anomaly (Jarrard, 1986 and Bowin, 1976) that heats part of the oceanic crust in the basin. The most likely source for the thermal rejuvenation of the Panama basin is the possible spreading (or rifting) along the Sandra Rift. Spreading or rifting (crustal thinning processes) can result in a positive contribution to the surface heat flux, the magnitude of which depends on upwelling of the asthenosphere during rifting, as well as the distribution of shear stresses, strain rates and characteristics of the boundaries. A warm subducting plate has increased buoyancy (accompanied by a decrease in subduction angle, favoring melting Gutscher et al., 2000) and encourages partial melting of the slab.

APPENDIX

APPENDIX A

A.1 PLATE TECTONIC RECONSTRUCTION OF THE NAZCA AND COCOS PLATES WITH RESPECT TO THE STATIC CARIBBEAN PLATE. STAR IN THE LOWER LEFT IS THE GALAPAGOS HOT SPOT. LIGHT ARROWS INDICATE MOTION OF TECTONIC FEATURES WITH RESPECT TO MIDDLE AMERICA TRENCH. HEAVY ARROWS GIVE PRESENT PLATE MOTIONS.

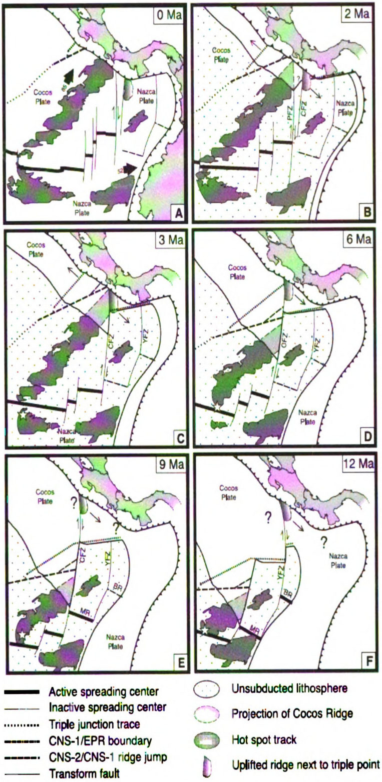
0 Ma
Cocos Plate
Nazca Plate
A
2 Ma
Cocos Plate
PFZ
CFZ
Nazca Plate
B
3 Ma
Cocos Plate
CFZ
YFZ
Nazca Plate
C
6 Ma
Cocos Plate
CFZ
YFZ
Nazca Plate
D
9 Ma
Cocos Plate
CFZ
YFZ
BR
MR
Nazca Plate
E
12 Ma
Cocos Plate
YFZ
BR
MR
Nazca Plate
F
Active spreading center
Inactive spreading center
Triple junction trace
CNS-1/EPR boundary
CNS-2/CNS-1 ridge jump
Transform fault
Unsubducted lithosphere
Projection of Cocos Ridge
Hot spot track
Uplifted ridge next to triple point

APPENDIX B

B.1 MAJOR AND TRACE ELEMENT ANALYSES

Pumice Sample bulk geochemical data (El Hato unit)
Major element oxides (wt%) trace elements (ppm).

Sample	AT-06-02-06-1A	AT-06-02-06-2B	CA-05-20-06-01	CA-05-20-06-1A	CA-05-20-06-2A
Location					
Latitude	8.5510	8.5637	8.5343	8.5343	8.5168
Longitudee	80.2379	80.2140	80.0416	80.0416	80.0381
XRF Analyses					
SiO2	65.81	65.22	65.17	68.67	65.19
TiO2	0.23	0.22	0.23	0.22	0.22
Al2O3	16.32	16.86	18.28	17.09	17.24
Fe2O3	2.56	2.87	2.46	2.50	2.37
MnO	0.07	0.07	0.05	0.06	0.05
MgO	1.04	1.04	0.85	0.96	0.85
CaO	3.88	3.87	3.91	4.13	3.74
Na2O	4.09	3.95	3.98	4.70	3.98
K2O	1.68	1.27	1.44	1.58	1.50
P2O5	0.08	0.10	0.09	0.09	0.08
Total	95.76	95.47	96.46	96.14	95.22
Ni	20.00	20.00	20.00	20.00	20.00
Cu	12.00	20.00	29.00	22.00	26.00
Zn	38.00	45.00	42.00	37.00	36.00
Rb	15.00	16.00	14.00	15.00	15.00
Zr	88.11	81.00	88.52	78.00	80.00
Sr	748.00	670.00	765.00	769.00	736.00
Laser ablation ICP-MS analyses					
Y	5.10	5.66	4.81	4.81	5.28
Nb	1.80	2.83	2.43	2.43	2.55
Ba	525.19	509.00	517.00	574.68	480.00
La	7.85	7.30	7.94	7.94	8.39
Ce	17.51	16.53	17.76	17.76	18.25
Pr	1.90	2.04	1.96	1.96	2.28
Nd	7.55	6.76	7.72	7.72	8.52
Sm	1.63	1.65	1.66	1.66	1.91
Eu	0.57	0.75	0.57	0.57	0.73
Gd	1.54	1.53	1.44	1.44	1.65
Tb	0.21	0.34	0.24	0.24	0.33
Dy	0.93	1.17	0.90	0.90	1.01
Ho	0.18	0.31	0.15	0.15	0.22
Er	0.43	0.50	0.24	0.24	0.37
Yb	0.62	0.78	0.46	0.46	0.67
Lu	0.04	0.21	0.03	0.03	0.10
Hf	2.07	1.92	2.22	2.22	2.01
Ta	0.13	0.27	0.14	0.14	0.23
Pb	4.04	6.47	4.83	4.83	5.74
Th	2.19	1.65	2.58	2.58	2.66
U	1.27	2.84	1.25	1.25	2.00

cont. (El Hato)

Sample	CA-05-20-06-2C	CA-5-19-06-1B	CY-06-02-06-4A	CY-06-02-06-4B	CY-06-02-06-4C
Location					
Latitude	8.5168	8.5343	8.5608	8.5608	8.5608
Longitude	80.0381	80.0416	80.1568	80.1568	80.1568
XRF Analyses					
SiO2	69.18	68.89	66.15	66.61	65.81
TiO2	0.23	0.23	0.22	0.23	0.23
Al2O3	17.52	16.88	16.00	15.69	15.99
Fe2O3	2.32	2.68	2.48	2.55	2.61
MnO	0.05	0.06	0.06	0.06	0.07
MgO	0.88	1.00	0.98	0.99	1.03
CaO	3.77	4.21	4.11	3.97	4.05
Na2O	4.21	4.47	4.01	4.02	4.13
K2O	1.75	1.49	1.39	1.42	1.43
P2O5	0.08	0.09	0.11	0.11	0.11
Total	95.7	97.06	95.51	95.65	95.46
Ni	22.00	20.00	21.00	20.00	20.00
Cu	18.00	16.00	39.00	27.00	15.00
Zn	41.00	37.00	40.00	39.00	39.00
Rb	17.00	14.00	15.00	15.00	15.00
Zr	85.00	75.00	77.84	75.89	75.99
Sr	737.00	781.00	736.00	703.00	718.00
Laser ablation ICP-MS analyses					
Y		5.00	4.76	4.68	4.84
Nb		2.34	2.24	2.26	2.27
Ba		476.28	552.06	555.67	561.59
La		7.23	8.41	8.24	8.56
Ce		15.88	17.31	17.19	17.83
Pr		1.73	1.89	1.91	1.96
Nd		6.81	7.19	7.16	7.49
Sm		1.41	1.40	1.49	1.49
Eu		0.54	0.54	0.52	0.56
Gd		1.32	1.36	1.34	1.37
Tb		0.20	0.23	0.24	0.23
Dy		0.89	0.90	0.88	0.84
Ho		0.14	0.12	0.14	0.14
Er		0.16	0.19	0.20	0.22
Yb		0.25	0.39	0.44	0.41
Lu		0.04	0.03	0.03	0.03
Hf		1.98	1.81	1.84	1.75
Ta		0.10	0.09	0.12	0.09
Pb		3.86	5.14	4.82	5.23
Th		2.12	2.10	1.95	1.99
U		1.76	1.21	1.15	1.39

cont. (El Hato)

Sample	EE-05-20-06-02	GT-05-30-06-02C	GT-05-30-06-03	GT-05-30-06-1B	GT-05-30-06-1C
Location					
Latitude	8.4859	8.5508	8.5549	8.5438	8.5438
Longitude	80.0208	80.0157	80.0185	80.0068	80.0068
XRF Analyses					
SiO2	69.52	66.49	65.61	65.84	69.16
TiO2	0.24	0.21	0.23	0.21	0.22
Al2O3	16.54	16.68	17.36	16.64	17.17
Fe2O3	2.57	2.57	2.78	2.60	2.51
MnO	0.06	0.07	0.07	0.07	0.06
MgO	1.02	0.96	1.03	0.96	1.05
CaO	4.04	3.91	4.16	4.11	4.11
Na2O	4.11	4.19	4.16	4.08	4.24
K2O	1.82	1.22	1.21	1.20	1.39
P2O5	0.09	0.07	0.07	0.09	0.09
Total	96.38	96.37	96.68	95.8	96.2
Ni	20.00	20.00	20.00	19.00	19.00
Cu	31.00	24.00	29.00	14.00	31.00
Zn	39.00	40.00	39.00	37.00	38.00
Rb	16.00	16.00	16.00	15.00	18.00
Zr	80.00	68.72	66.60	65.69	73.00
Sr	749.00	675.00	727.00	714.00	681.00
Laser ablation ICP-MS analyses					
Y	4.60	6.29	5.73	4.96	5.45
Nb	2.36	2.51	2.20	2.29	2.45
Ba	520.61	619.70	564.40	541.43	579.41
La	7.60	7.26	7.60	7.02	7.41
Ce	16.78	16.24	15.97	15.28	16.20
Pr	1.86	1.76	1.87	1.64	1.76
Nd	7.25	6.78	7.48	6.34	6.80
Sm	1.39	1.59	1.61	1.46	1.49
Eu	0.53	0.57	0.56	0.55	0.54
Gd	1.34	1.48	1.50	1.29	1.36
Tb	0.24	0.27	0.25	0.23	0.24
Dy	0.86	1.07	1.00	0.92	0.95
Ho	0.13	0.19	0.17	0.16	0.16
Er	0.21	0.50	0.27	0.23	0.39
Yb	0.34	0.68	0.53	0.51	0.53
Lu	0.04	0.04	0.04	0.04	0.03
Hf	1.88	1.66	1.59	1.56	1.55
Ta	0.22	0.12	0.08	0.12	0.12
Pb	4.38	5.38	4.91	5.05	4.88
Th	2.30	1.14	1.15	1.09	1.05
U	1.75	0.97	0.77	1.16	0.93

cont. (El Hato)

Sample	GT-05-30-06-1D	GT-05-30-06-1E	GT-05-30-06-2D	GT-05-30-06-4A	GT-05-30-06-1C
Location					
Latitude	8.5438	8.5438	8.5508	8.5679	8.5679
Longitude	80.0068	80.0068	80.0157	80.0294	80.0294
XRF Analyses					
SiO2	65.83	66.25	64.98	66.10	65.47
TiO2	0.22	0.20	0.23	0.20	0.21
Al2O3	16.77	16.05	17.61	16.72	17.15
Fe2O3	2.62	2.44	2.78	2.47	2.62
MnO	0.07	0.06	0.07	0.07	0.07
MgO	0.97	0.96	0.96	0.93	1.00
CaO	4.13	3.93	4.11	3.84	4.21
Na2O	4.13	4.07	4.15	4.17	4.15
K2O	1.20	1.33	1.15	1.21	1.22
P2O5	0.09	0.09	0.07	0.03	0.09
Total	96.03	95.38	96.11	95.74	96.19
Ni	20.00	19.00	19.00	19.00	20.00
Cu	21.00	19.00	32.00	16.00	11.00
Zn	39.00	36.00	41.00	38.00	41.00
Rb	14.00	17.00	16.00	15.00	14.00
Zr	66.24	60.33	73.52	70.50	65.90
Sr	715.00	697.00	703.00	668.00	740.00
Laser ablation ICP-MS analyses					
Y	5.47	4.76	5.87	6.92	5.45
Nb	1.93	2.12	2.44	2.06	2.45
Ba	531.09	558.50	638.35	573.83	579.41
La	7.21	7.33	7.82	7.47	7.41
Ce	14.37	15.28	17.03	13.99	16.20
Pr	1.63	1.67	1.86	1.69	1.76
Nd	6.61	6.46	6.84	7.10	6.80
Sm	1.39	1.36	1.60	1.71	1.49
Eu	0.71	0.49	0.64	0.56	0.54
Gd	1.49	1.31	1.50	1.65	1.36
Tb	0.21	0.23	0.28	0.24	0.24
Dy	0.98	0.89	1.03	1.15	0.95
Ho	0.18	0.12	0.20	0.22	0.16
Er	0.37	0.23	0.25	0.58	0.39
Yb	0.55	0.46	0.55	0.76	0.53
Lu	0.04	0.03	0.07	0.06	0.03
Hf	1.58	1.52	1.71	1.65	1.55
Ta	0.07	0.09	0.12	0.11	0.12
Pb	3.78	4.71	5.51	5.04	4.88
Th	1.11	1.13	1.03	1.05	1.05
U	0.78	0.78	0.97	0.94	0.93

cont. (El Hato)

Sample	GT-05-30-06-02	GT-05-30-06-1A	GT-05-30-06-1B	GT-05-30-06-1D	GT-05-30-06-1E
Location					
Latitude	8.5438	8.5679	8.5438	8.5438	8.5438
Longitude	80.0068	80.0294	80.0068	80.0068	80.0068
XRF Analyses					
SiO2	68.99	69.16	68.73	65.83	69.46
TiO2	0.22	0.22	0.22	0.22	0.21
Al2O3	17.31	17.17	17.37	16.77	16.83
Fe2O3	2.67	2.51	2.71	2.62	2.56
MnO	0.07	0.06	0.07	0.07	0.06
MgO	1.00	1.05	1.00	0.97	1.01
CaO	4.06	4.11	4.29	4.13	4.12
Na2O	4.35	4.24	4.26	4.13	4.27
K2O	1.27	1.39	1.25	1.20	1.39
P2O5	0.07	0.09	0.09	0.09	0.09
Total	96.37	96.2	95.8	96.03	95.38
Ni	20.00	19.00	19.00	20.00	19.00
Cu	24.00	31.00	14.00	21.00	19.00
Zn	40.00	38.00	37.00	39.00	36.00
Rb	16.00	18.00	15.00	14.00	17.00
Zr	73.00	73.00	67.00	65.00	63.00
Sr	675.00	681.00	714.00	715.00	697.00
Laser ablation ICP-MS analyses					
Y	5.58	5.52		5.47	4.76
Nb	2.95	3.03		1.93	2.12
Ba	635.95	592.95		531.09	558.50
La	7.41	7.37		7.21	7.33
Ce	16.96	16.35		14.37	15.28
Pr	1.88	1.81		1.63	1.67
Nd	7.35	6.91		6.61	6.46
Sm	1.49	1.40		1.39	1.36
Eu	0.54	0.54		0.71	0.49
Gd	1.41	1.30		1.49	1.31
Tb	0.21	0.22		0.21	0.23
Dy	0.94	0.94		0.98	0.89
Ho	0.16	0.47		0.18	0.12
Er	0.31	1.51		0.37	0.23
Yb	0.50	1.05		0.55	0.46
Lu	0.05	0.16		0.04	0.03
Hf	1.67	1.64		1.58	1.52
Ta	0.25	0.27		0.07	0.09
Pb	4.86	5.34		3.78	4.71
Th	1.10	1.45		1.11	1.13
U	1.33	2.21		0.78	0.78

cont. (El Hato)

Sample	GT-05-30-06-2B	GT-05-30-06-2H	GT-05-30-06-4B	HG-05-30-06-1A	HG-05-30-06-1B
Location					
Latitude	8.5508	8.5508	8.5679	8.5904	8.5076
Longitude	80.0157	80.0157	80.0294	80.1066	79.9528
XRF Analyses					
SiO2	68.63	67.61	68.67	66.00	65.76
TiO2	0.22	0.24	0.20	0.20	0.20
Al2O3	17.75	18.32	18.52	16.13	16.61
Fe2O3	2.63	2.89	2.52	2.41	2.42
MnO	0.07	0.07	0.06	0.07	0.06
MgO	0.96	1.00	0.89	0.92	0.92
CaO	4.06	4.28	3.84	3.96	4.05
Na2O	4.35	4.32	4.02	3.98	4.03
K2O	1.28	1.20	1.24	1.36	1.36
P2O5	0.05	0.07	0.04	0.10	0.10
Total	96.28	96.11	95.69	95.13	95.51
Ni	19.00	19.00	20.00	19.00	20.00
Cu	18.00	32.00	32.00	17.00	28.00
Zn	39.00	41.00	37.00	38.00	37.00
Rb	16.00	16.00	15.00	17.00	15.00
Zr	70.00	68.00	67.00	70.31	72.49
Sr	686.00	703.00	661.00	738.00	712.00
Laser ablation ICP-MS analyses					
Y	5.04		7.43	5.36	5.06
Nb	2.56		2.89	2.03	1.95
Ba	627.18		621.20	577.80	562.42
La	6.87		7.13	7.87	7.44
Ce	15.22		16.39	15.05	15.00
Pr	1.56		1.81	1.68	1.64
Nd	5.95		7.04	6.70	6.69
Sm	1.17		1.59	1.40	1.39
Eu	0.50		0.59	0.51	0.50
Gd	1.13		1.58	1.43	1.39
Tb	0.18		0.25	0.20	0.20
Dy	0.83		1.26	0.90	0.88
Ho	0.14		0.21	0.17	0.17
Er	0.39		0.64	0.26	0.34
Yb	0.48		0.71	0.49	0.60
Lu	0.08		0.10	0.03	0.04
Hf	1.69		1.75	1.67	1.75
Ta	0.22		0.26	0.12	0.11
Pb	5.18		5.28	4.98	3.91
Th	1.13		1.25	1.25	1.28
U	1.02		1.03	0.87	0.85

cont. (El Hato)

Sample	HG-05-30-06-1D	HG-05-30-06-1E	HG-05-30-06-1C	HG-05-30-06-1D	HG-05-31-06-1F
Location					
Latitude	8.5076	8.5076	8.5076	8.5076	8.5076
Longitude	79.9528	79.9528	79.9528	79.9528	79.9528
XRF Analyses					
SiO2	66.40	65.32	68.64	66.40	65.34
TiO2	0.21	0.22	0.22	0.21	0.21
Al2O3	16.52	17.20	17.46	16.52	17.12
Fe2O3	2.52	2.64	2.74	2.52	2.52
MnO	0.07	0.08	0.07	0.07	0.07
MgO	0.90	0.92	1.04	0.90	0.93
CaO	3.84	4.01	4.28	3.84	3.88
Na2O	3.76	3.94	4.11	3.76	3.82
K2O	1.33	1.17	1.34	1.33	1.34
P2O5	0.08	0.07	0.10	0.08	0.08
Total	95.63	95.57	95.41	95.63	95.31
Ni	21.00	20.00	20.00	21.00	20.00
Cu	22.00	21.00	15.00	22.00	26.00
Zn	40.00	40.00	38.00	40.00	39.00
Rb	15.00	15.00	15.00	15.00	15.00
Zr	71.85	74.40	72.00	72.00	73.00
Sr	684.00	683.00	711.00	684.00	704.00
Laser ablation ICP-MS analyses					
Y	5.39	5.32	6.10	5.39	
Nb	1.90	2.11	2.91	1.90	
Ba	569.33	596.65	570.90	569.33	
La	7.69	7.93	7.89	7.69	
Ce	15.74	20.50	16.29	15.74	
Pr	1.68	1.76	1.74	1.68	
Nd	6.76	6.58	6.89	6.76	
Sm	1.45	1.36	1.39	1.45	
Eu	0.47	0.50	0.50	0.47	
Gd	1.40	1.32	1.40	1.40	
Tb	0.21	0.24	0.22	0.21	
Dy	0.92	0.92	0.99	0.92	
Ho	0.17	0.15	0.17	0.17	
Er	0.38	0.30	0.29	0.38	
Yb	0.64	0.60	0.39	0.64	
Lu	0.03	0.04	0.05	0.03	
Hf	1.74	1.72	1.82	1.74	
Ta	0.13	0.09	0.12	0.13	
Pb	4.82	6.47	3.69	4.82	
Th	1.39	1.09	1.40	1.39	
U	0.89	0.79	0.85	0.89	

cont. (El Hato)

Sample	ID-06-03-06-1B	ID-06-03-06-1A	LC-06-06-06-01	LC-06-06-06-03C	LC-06-06-06-2B
Location					
Latitude	8.6127	8.5966	8.5890	8.5934	8.5869
Longitude	80.1513	80.1534	80.1260	80.1674	80.1868
XRF Analyses					
SiO2	66.81	69.62	66.51	66.65	66.33
TiO2	0.20	0.22	0.22	0.19	0.24
Al2O3	15.80	16.75	16.20	16.22	16.01
Fe2O3	2.26	2.56	2.53	2.33	2.61
MnO	0.06	0.07	0.06	0.07	0.06
MgO	0.94	0.98	0.98	0.91	0.99
CaO	3.93	4.05	4.14	3.88	4.10
Na2O	3.91	4.19	4.12	4.22	4.04
K2O	1.48	1.53	1.38	1.27	1.40
P2O5	0.10	0.02	0.10	0.05	0.10
Total	95.49	94.66	96.24	95.79	95.88
Ni	20.00	20.00	20.00	19.00	20.00
Cu	27.00	17.00	34.00	22.00	22.00
Zn	37.00	39.00	39.00	38.00	40.00
Rb	16.00	15.00	15.00	15.00	15.00
Zr	78.70	76.00	78.18	65.39	83.42
Sr	712.00	729.00	748.00	671.00	747.00
Laser ablation ICP-MS analyses					
Y	5.24		5.27	4.54	5.03
Nb	2.13		2.00	1.99	2.20
Ba	554.88		549.49	565.62	555.31
La	8.76		8.58	6.72	8.63
Ce	16.66		16.71	13.48	17.20
Pr	1.86		1.84	1.45	1.92
Nd	7.36		7.47	5.56	7.36
Sm	1.45		1.51	1.22	1.52
Eu	0.52		0.53	0.47	0.54
Gd	1.44		1.47	1.17	1.42
Tb	0.20		0.21	0.22	0.20
Dy	0.90		0.93	0.81	0.89
Ho	0.17		0.17	0.14	0.17
Er	0.40		0.41	0.22	0.40
Yb	0.61		0.63	0.49	0.61
Lu	0.04		0.04	0.03	0.04
Hf	1.87		1.90	1.55	1.93
Ta	0.12		0.12	0.10	0.14
Pb	4.71		5.17	5.51	4.41
Th	2.20		2.03	0.96	2.12
U	1.06		1.00	0.75	1.13

cont. (El Hato)

Sample	LC-06-06-06-2C	LC-06-06-06-3B	LC-06-06-06-4A	LC-06-06-06-4B	LC-06-06-06-2D
Location					
Latitude	8.5934	8.5934	8.5869	8.0101	8.0101
Longitude	80.1674	80.1674	80.1868	80.2019	80.2019
XRF Analyses					
SiO2	66.28	68.60	67.07	65.04	69.24
TiO2	0.24	0.20	0.19	0.23	0.25
Al2O3	15.83	16.28	16.16	16.66	16.62
Fe2O3	2.67	2.49	2.45	2.64	2.75
MnO	0.07	0.07	0.07	0.06	0.07
MgO	1.09	0.91	0.98	1.00	1.12
CaO	4.03	3.87	4.08	3.96	4.20
Na2O	3.92	4.24	4.17	3.95	4.14
K2O	1.42	1.32	1.22	1.43	1.49
P2O5	0.11	0.04	0.09	0.10	0.11
Total	95.66	98.02	96.48	95.07	95.89
Ni	20.00	20.00	19.00	22.00	20.00
Cu	24.00	18.00	35.00	32.00	19.00
Zn	41.00	39.00	39.00	42.00	40.00
Rb	16.00	16.00	14.00	15.00	16.00
Zr	83.30	66.46	68.41	78.27	80.00
Sr	738.00	673.00	691.00	731.00	709.00
Laser ablation ICP-MS analyses					
Y	5.39	5.05	5.02	4.95	4.76
Nb	2.09	1.99	2.04	2.40	2.75
Ba	558.70	580.47	541.47	564.55	565.88
La	8.82	7.02	6.82	8.60	8.02
Ce	17.82	13.65	14.80	20.01	18.13
Pr	2.00	1.49	1.67	2.00	1.96
Nd	7.91	5.98	6.12	7.74	7.36
Sm	1.63	1.26	1.40	1.65	1.33
Eu	0.56	0.48	0.58	0.56	0.54
Gd	1.58	1.28	1.23	1.50	1.30
Tb	0.22	0.18	0.25	0.25	0.20
Dy	0.97	0.83	0.92	0.93	0.88
Ho	0.19	0.16	0.17	0.15	0.15
Er	0.41	0.27	0.35	0.27	0.28
Yb	0.61	0.53	0.62	0.55	0.42
Lu	0.03	0.03	0.07	0.03	0.05
Hf	2.00	1.65	1.63	1.84	1.76
Ta	0.12	0.09	0.12	0.13	0.22
Pb	4.46	4.22	4.90	5.37	4.65
Th	2.25	1.04	0.92	2.24	2.02
U	1.08	0.80	0.85	1.11	1.34

cont (El Hato)

Sample	LG-06-06-06-03	LG-06-04-06-1A	LG-06-04-06-1AR	LG-06-04-06-1C	LM-05-19-06-1C
Location					
	8.5674	8.5674	8.5674	8.5674	8.5674
Latitude	79.9625	79.9625	79.9625	79.9625	79.9625
Longitude					
XRF Analyses					
	69.46	66.46	66.48	64.67	65.83
SiO2	0.20	0.20	0.21	0.18	0.25
TiO2	17.06	16.09	16.10	15.48	17.11
Al2O3	2.47	2.40	2.56	2.31	2.83
Fe2O3	0.07	0.07	0.07	0.07	0.06
MnO	0.94	0.97	0.94	0.88	0.90
MgO	4.06	3.96	4.02	3.80	3.81
CaO	4.34	4.23	4.21	4.22	4.06
Na2O	1.34	1.29	1.26	1.29	1.39
K2O	0.05	0.09	0.10	0.09	0.09
P2O5	95.42	95.76	95.95	92.99	96.33
Total	19.00	20.00	19.00	20.00	20.00
Ni	27.00	46.00	46.00	10.00	133.00
Cu	40.00	40.00	39.00	37.00	40.00
Zn	15.00	16.00	15.00	16.00	23.00
Rb	67.00	64.73	69.15	64.36	75.11
Zr	675.00	674.00	674.00	668.00	671.00
Sr					
Laser ablation ICP-MS analyses					
		5.40	4.59	5.24	5.78
Y		2.14	1.93	2.27	2.42
Nb		554.20	556.48	570.36	624.64
Ba		7.05	6.63	7.08	8.48
La		13.36	13.76	14.10	16.93
Ce		1.51	1.48	1.57	1.89
Pr		6.05	5.91	6.12	7.39
Nd		1.30	1.20	1.28	1.61
Sm		0.49	0.46	0.47	0.55
Eu		1.36	1.20	1.37	1.54
Gd		0.19	0.22	0.19	0.21
Tb		0.89	0.77	0.87	0.99
Dy		0.17	0.13	0.17	0.20
Ho		0.25	0.19	0.42	0.48
Er		0.46	0.46	0.65	0.69
Yb		0.03	0.03	0.04	0.05
Lu		1.60	1.58	1.62	1.79
Hf		0.08	0.08	0.13	0.17
Ta		4.62	5.05	4.04	3.64
Pb		0.98	0.82	1.04	1.57
Th		0.74	0.68	0.82	0.97
U					

cont. (El Hato)

Sample	LM-05-19-06-1D	LT-05-31-06-03C	LT-05-31-06-2C	LT-05-31-06-3B	LT-5-31-06-1
Location					
Latitude	8.5607	8.5607	8.5780	8.5838	8.5780
Longitude	80.0630	80.0630	80.1185	80.1245	80.1185
XRF Analyses					
SiO2	66.37	66.42	66.43	65.48	56.94
TiO2	0.20	0.23	0.24	0.22	0.66
Al2O3	17.11	16.11	16.32	16.42	17.26
Fe2O3	2.33	2.63	2.62	2.66	7.31
MnO	0.07	0.07	0.07	0.07	0.11
MgO	0.92	1.03	0.99	1.03	3.72
CaO	3.81	4.19	4.15	4.27	7.20
Na2O	4.14	4.05	4.03	4.23	3.29
K2O	1.33	1.40	1.41	1.33	1.02
P2O5	0.09	0.11	0.11	0.10	0.29
Total	96.37	96.24	96.37	95.81	97.8
Ni	19.00	21.00	20.00	20.00	50.00
Cu	37.00	22.00	13.00	17.00	136.00
Zn	38.00	41.00	44.00	39.00	65.00
Rb	17.00	15.00	14.00	14.00	15.00
Zr	74.44	79.20	84.28	74.20	78.00
Sr	674.00	742.00	755.00	740.00	637.00
Laser ablation ICP-MS analyses					
Y	5.09	4.67	5.50	4.79	14.69
Nb	2.40	2.11	2.02	1.99	5.41
Ba	624.33	546.33	543.52	545.62	521.19
La	7.76	8.25	8.91	7.73	15.93
Ce	16.84	17.37	17.63	16.40	29.05
Pr	1.79	1.89	1.93	1.77	3.69
Nd	6.92	7.38	7.61	6.82	15.02
Sm	1.42	1.54	1.62	1.47	3.09
Eu	0.49	0.53	0.55	0.52	1.05
Gd	1.35	1.37	1.50	1.34	2.89
Tb	0.23	0.23	0.20	0.23	0.43
Dy	0.95	0.86	0.93	0.85	2.39
Ho	0.15	0.13	0.18	0.13	0.46
Er	0.23	0.19	0.28	0.18	1.30
Yb	0.57	0.44	0.51	0.44	1.34
Lu	0.03	0.03	0.03	0.03	0.19
Hf	1.81	1.77	1.95	1.71	1.84
Ta	0.13	0.08	0.08	0.08	0.26
Pb	5.39	5.28	4.66	5.13	2.33
Th	1.39	1.84	2.25	1.53	1.54
U	0.94	1.01	1.07	0.97	0.61

cont. (El Hato)

Sample	LT-05-31-06-2A	LT-05-31-06-3A	LT-05-31-06-2B	LU-05-20-06-1A	LU-05-20-06-1B
Location					
Latitude	8.5838	8.5780	8.5838	8.4611	8.4611
Longitude	80.1245	80.1185	80.1245	80.0065	80.0065
XRF Analyses					
SiO2	69.14	66.90	69.57	67.02	66.25
TiO2	0.24	0.25	0.23	0.23	0.23
Al2O3	17.10	18.10	16.59	15.90	16.36
Fe2O3	2.61	3.06	2.54	2.52	2.54
MnO	0.06	0.05	0.07	0.06	0.06
MgO	1.01	1.05	1.03	0.98	0.95
CaO	4.15	5.34	4.29	3.77	3.96
Na2O	4.04	3.96	4.16	3.99	4.18
K2O	1.55	1.28	1.42	1.74	1.65
P2O5	0.10	0.01	0.10	0.09	0.10
Total	95.58	95.38	95.85	96.3	96.28
Ni	20.00	21.00	20.00	20.00	20.00
Cu	25.00	25.00	27.00	13.00	10.00
Zn	39.00	40.00	38.00	38.00	37.00
Rb	15.00	12.00	16.00	17.00	14.00
Zr	86.00	67.00	74.00	86.06	75.16
Sr	748.00	976.00	727.00	748.00	777.00
Laser ablation ICP-MS analyses					
Y	4.85	4.60	5.96	5.14	4.43
Nb	2.62	2.57	2.48	1.94	2.06
Ba	570.61	563.34	491.99	525.72	529.67
La	8.43	7.85	8.96	8.43	8.15
Ce	20.00	17.68	12.99	16.68	17.02
Pr	2.18	1.92	1.89	1.94	1.91
Nd	8.04	7.18	7.44	7.72	7.44
Sm	1.48	1.38	1.50	1.65	1.54
Eu	0.57	0.54	0.59	0.53	0.54
Gd	1.35	1.27	1.43	1.51	1.37
Tb	0.21	0.19	0.21	0.21	0.24
Dy	0.87	0.83	0.96	0.90	0.87
Ho	0.14	0.14	0.17	0.18	0.11
Er	0.25	0.22	0.25	0.32	0.19
Yb	0.42	0.38	0.38	0.58	0.37
Lu	0.05	0.04	0.04	0.03	0.03
Hf	1.92	1.66	1.52	2.05	1.73
Ta	0.23	0.21	0.11	0.10	0.07
Pb	5.28	4.64	3.45	4.66	5.11
Th	2.50	1.89	1.04	2.28	2.00
U	1.51	1.27	0.71	1.23	1.10

cont. (El Hato)

Sample	LU-05-20-06-1C	MS-06-01-06-1A	MS-06-01-06-1B	MS-06-01-06-1C	RH-06-02-06-1B
Location					
Latitude	8.4611	8.4611	8.6201	8.6201	8.4914
Longitude	80.0065	80.0065	80.1022	80.1022	80.1838
XRF Analyses					
SiO2	66.39	66.31	69.68	68.93	66.71
TiO2	0.23	0.23	0.24	0.23	0.21
Al2O3	15.78	16.33	16.27	17.04	16.75
Fe2O3	2.52	2.58	2.58	2.47	2.60
MnO	0.06	0.06	0.06	0.06	0.07
MgO	0.96	0.96	1.02	0.98	0.96
CaO	3.58	3.98	3.94	4.05	4.19
Na2O	3.81	4.31	4.39	4.48	4.29
K2O	1.85	1.62	1.71	1.67	1.27
P2O5	0.10	0.08	0.10	0.09	0.09
Total	95.28	96.46	96.72	95.74	97.14
Ni	19.00	20.00	20.00	19.00	20.00
Cu	21.00	13.00	28.00	11.00	14.00
Zn	38.00	40.00	39.00	36.00	38.00
Rb	16.00	15.00	16.00	15.00	16.00
Zr	88.27	89.62	80.00	82.00	66.79
Sr	704.00	781.00	747.00	751.00	739.00
Laser ablation ICP-MS analyses					
Y	5.17	4.95	4.57	4.36	5.70
Nb	1.91	1.96	2.64	2.51	1.86
Ba	532.22	494.60	530.92	506.94	542.27
La	8.64	7.84	8.12	7.37	7.59
Ce	16.74	16.22	17.84	16.98	14.72
Pr	1.93	1.81	1.93	1.74	1.74
Nd	7.85	7.35	7.43	6.62	7.02
Sm	1.69	1.59	1.41	1.34	1.44
Eu	0.52	0.53	0.55	0.51	0.53
Gd	1.59	1.47	1.33	1.22	1.50
Tb	0.22	0.21	0.20	0.20	0.21
Dy	0.94	0.92	0.82	0.80	0.96
Ho	0.17	0.17	0.14	0.13	0.19
Er	0.27	0.32	0.24	0.19	0.47
Yb	0.46	0.56	0.35	0.33	0.67
Lu	0.03	0.03	0.05	0.04	0.03
Hf	2.09	2.15	1.88	1.88	1.60
Ta	0.09	0.08	0.20	0.20	0.11
Pb	4.57	4.72	5.58	4.46	4.52
Th	2.41	2.32	2.14	2.17	1.14
U	1.18	1.17	1.40	1.26	0.80

Cont. (El Hato)

Sample	RH-06-02-06-1C	RH-06-02-06-3A	RH-06-02-06-03C	RH-06-02-06-1A	RH-06-02-06-2B(IMP)
Location					
Latitude	8.4914	8.4914	8.5193	8.4914	8.4927
Longitude	80.1838	80.1838	80.1788	80.1838	80.1846
XRF Analyses					
SiO2	64.21	65.67	69.01	68.12	65.95
TiO2	0.22	0.23	0.23	0.23	0.22
Al2O3	16.75	16.74	17.09	17.77	16.56
Fe2O3	2.63	2.59	2.57	2.79	2.70
MnO	0.07	0.06	0.06	0.07	0.07
MgO	0.98	0.94	1.00	1.01	1.02
CaO	3.88	4.08	4.00	4.24	4.09
Na2O	3.97	4.33	4.35	4.40	4.13
K2O	1.25	1.56	1.59	1.30	1.31
P2O5	0.07	0.09	0.10	0.08	0.10
Total	94.03	96.29	96.8	96.42	96.15
Ni	20.00	20.00	19.00	22.00	20.00
Cu	15.00	17.00	16.00	17.00	28.00
Zn	47.00	43.00	39.00	39.00	41.00
Rb	16.00	13.00	15.00	16.00	15.00
Zr	70.05	85.83	81.00	69.00	68.00
Sr	702.00	786.00	744.00	700.00	728.00
Laser ablation ICP-MS analyses					
Y	5.88	5.11	4.91	5.23	
Nb	2.15	1.76	2.44	2.68	
Ba	591.21	459.38	517.20	576.49	
La	8.86	7.52	7.58	7.81	
Ce	17.41	14.76	17.58	16.45	
Pr	2.13	1.64	1.89	1.99	
Nd	8.42	6.85	7.18	7.40	
Sm	1.71	1.52	1.47	1.40	
Eu	0.57	0.53	0.56	0.60	
Gd	1.66	1.45	1.39	1.34	
Tb	0.23	0.20	0.22	0.22	
Dy	1.03	0.91	0.91	0.92	
Ho	0.21	0.15	0.16	0.16	
Er	0.54	0.22	0.32	0.44	
Yb	0.71	0.42	0.41	0.51	
Lu	0.07	0.03	0.06	0.08	
Hf	1.75	1.97	1.83	1.61	
Ta	0.16	0.06	0.21	0.21	
Pb	4.31	4.15	4.08	4.26	
Th	1.37	2.07	2.13	1.21	
U	0.95	1.09	1.47	0.89	

cont. (El Hato)

Sample	RH-06-02-06-2C	RH-06-02-06-3B	RM-05-29-06-1A(IMP)	RM-05-29-06-1B	RM-05-29-06-1H(IMP)
Location					
Latitude	8.4927	8.5193	8.4914	8.4914	8.4914
Longitude	80.1846	80.1788	80.1838	80.1838	80.1838
XRF Analyses					
SiO2	68.39	68.69	59.32	68.58	64.00
TiO2	0.21	0.23	0.20	0.22	0.23
Al2O3	19.20	17.19	15.62	17.21	17.56
Fe2O3	2.45	2.50	2.67	2.88	2.94
MnO	0.06	0.06	0.07	0.08	0.08
MgO	0.91	1.00	1.48	1.04	1.12
CaO	3.65	4.06	3.63	4.23	4.22
Na2O	3.72	4.48	6.56	4.55	4.34
K2O	1.34	1.69	1.03	1.10	1.03
P2O5	0.06	0.10	0.08	0.10	0.09
Total	94.78	96.47	90.66	95.72	95.61
Ni	19.00	20.00	20.00	19.00	20.00
Cu	42.00	41.00	41.00	87.00	33.00
Zn	38.00	40.00	41.00	42.00	46.00
Rb	16.00	14.00	15.00	16.00	15.00
Zr	78.00	80.00	56.00	60.00	69.00
Sr	639.00	759.00	556.00	600.00	625.00
Laser ablation ICP-MS analyses					
Y		4.86		5.94	
Nb		2.37		2.93	
Ba		521.03		569.92	
La		7.59		7.62	
Ce		17.46		16.71	
Pr		1.87		1.82	
Nd		7.32		7.08	
Sm		1.41		1.40	
Eu		0.55		0.55	
Gd		1.35		1.35	
Tb		0.21		0.23	
Dy		0.88		1.00	
Ho		0.15		0.19	
Er		0.30		0.48	
Yb		0.46		0.61	
Lu		0.06		0.10	
Hf		1.88		1.42	
Ta		0.20		0.24	
Pb		4.26		4.01	
Th		2.10		0.92	
U		1.18		0.93	

cont. (El Hato)

Sample	SR-06-06-06-1C	SR-06-06-06-1A	SR-06-06-06-1B	ZT-05-26-06-1A
Location				
Latitude	8.4605	8.4605	8.4605	8.4605
Longitude	80.2241	80.2241	80.2241	80.2241
XRF Analyses				
SiO2	69.16	66.03	66.12	66.28
TiO2	0.21	0.21	0.22	0.24
Al2O3	16.89	16.28	16.62	16.02
Fe2O3	2.53	2.43	2.63	2.65
MnO	0.07	0.07	0.07	0.07
MgO	0.97	1.03	0.96	0.97
CaO	4.23	4.13	4.26	4.01
Na2O	4.44	4.32	4.31	4.07
K2O	1.41	1.31	1.28	1.56
P2O5	0.09	0.10	0.10	0.11
Total	96.55	95.91	96.57	95.98
Ni	19.00	19.00	20.00	20.00
Cu	25.00	22.00	17.00	26.00
Zn	40.00	37.00	40.00	41.00
Rb	17.00	16.00	15.00	16.00
Zr	63.00	66.81	69.10	86.72
Sr	722.00	710.00	757.00	748.00
Laser ablation ICP-MS analyses				
Y	4.99	5.78	5.46	5.40
Nb	2.84	1.87	1.87	2.23
Ba	590.82	552.54	556.64	576.86
La	7.64	7.92	7.72	9.14
Ce	17.02	15.35	14.99	18.45
Pr	1.84	1.75	1.74	2.04
Nd	6.68	7.10	6.94	7.96
Sm	1.34	1.50	1.48	1.60
Eu	0.54	0.53	0.51	0.54
Gd	1.29	1.47	1.45	1.55
Tb	0.22	0.21	0.21	0.21
Dy	0.86	0.98	0.99	1.01
Ho	0.16	0.19	0.18	0.17
Er	0.35	0.45	0.34	0.30
Yb	0.53	0.63	0.51	0.53
Lu	0.07	0.04	0.04	0.03
Hf	1.68	1.63	1.66	2.09
Ta	0.26	0.09	0.08	0.11
Pb	4.67	4.48	4.20	4.40
Th	1.20	1.25	1.19	2.29
U	1.09	0.82	0.81	1.11

Lava Sample bulk geochemical data.
Major element oxides (wt%) trace elements (ppm).

Sample	CG-05-28-06-01	CG-05-28-06-02	GY-05-19-06-03	ID-05-22-06-03
Formation	Dacitic Lavas	Dacitic Lavas	Dacitic Lavas	Dacitic Lavas
Location				
Latitude	8.5919	8.5919	8.5904	8.6127
Longitude	80.1142	80.1142	80.1066	80.1513
XRF Analyses				
SiO2	67.89	67.59	68.03	68.85
TiO2	0.27	0.29	0.26	0.24
Al2O3	17.32	17.65	17.33	17.01
Fe2O3	3.27	3.46	3.29	2.72
MnO	0.08	0.08	0.08	0.06
MgO	1.21	1.37	0.84	1.05
CaO	4.27	4.02	4.57	4.30
Na2O	4.28	4.13	4.38	4.14
K2O	1.28	1.30	1.09	1.52
P2O5	0.11	0.12	0.13	0.10
Total				
Ni	21.00	22.00	20.00	20.00
Cu	31.00	62.00	32.00	26.00
Zn	42.00	45.00	37.00	39.00
Rb	14.00	12.00	15.00	15.00
Zr	69.76	68.65	67.00	73.00
Sr	706.00	676.00	661.00	704.00
Laser ablation ICP-MS analyses				
Y	5.63	5.44	7.43	
Nb	2.42	2.53	2.89	
Ba	613.37	621.89	621.20	
La	8.67	8.89	7.13	
Ce	16.59	20.05	16.39	
Pr	1.81	2.23	1.81	
Nd	7.25	8.65	7.04	
Sm	1.51	1.86	1.59	
Eu	0.54	0.63	0.59	
Gd	1.48	1.71	1.58	
Tb	0.21	0.24	0.25	
Dy	0.99	1.03	1.26	
Ho	0.19	0.20	0.21	
Er	0.27	0.55	0.64	
Yb	0.53	0.71	0.71	
Lu	0.04	0.06	0.10	
Hf	1.73	1.61	1.75	
Ta	0.08	0.18	0.26	
Pb	4.78	4.11	5.28	
Th	1.44	1.57	1.25	
U	0.94	1.19	1.03	

Table 2 cont.

Sample	IG-5-28-06-01	IG-05-22-06-03	IG-05-22-06-02	IG-05-22-06-04
Formation	Dacitic Lavas	Dacitic Lavas	Dacitic Lavas	Dacitic Lavas
Location				
Latitude	8.5894	8.5881	8.5881	8.5870
Longitude	80.1434	80.1356	80.1356	80.1324
XRF Analyses				
SiO2	69.58	67.67	67.54	67.76
TiO2	0.23	0.30	0.28	0.29
Al2O3	17.01	17.26	18.16	17.84
Fe2O3	2.70	3.56	3.50	3.51
MnO	0.07	0.09	0.08	0.08
MgO	1.11	1.29	1.36	1.39
CaO	3.96	4.20	3.77	3.73
Na2O	3.96	4.25	3.91	3.92
K2O	1.25	1.28	1.27	1.34
P2O5	0.12	0.10	0.12	0.13
Total				
Ni	21.00	19.00	20.00	21.00
Cu	42.00	33.00	25.00	34.00
Zn	45.00	39.00	44.00	52.00
Rb	13.00	14.00	14.00	13.00
Zr	73.00	76.00	73.39	77.00
Sr	698.00	660.00	686.00	635.00
Laser ablation ICP-MS analyses				
Y	5.30	5.28	5.10	4.45
Nb	2.69	2.72	2.64	2.50
Ba	602.80	630.60	643.45	591.32
La	8.72	10.28	9.42	7.62
Ce	19.01	21.95	18.72	13.74
Pr	2.05	2.35	1.98	1.30
Nd	8.17	8.42	7.46	4.83
Sm	1.79	1.61	1.62	0.99
Eu	0.59	0.60	0.59	0.58
Gd	1.55	1.45	1.39	1.14
Tb	0.26	0.23	0.24	0.17
Dy	1.01	0.96	0.96	0.80
Ho	0.16	0.17	0.15	0.16
Er	0.26	0.45	0.23	0.31
Yb	0.45	0.60	0.50	0.59
Lu	0.03	0.06	0.03	0.04
Hf	1.65	1.59	1.66	1.74
Ta	0.09	0.23	0.10	0.16
Pb	5.07	4.32	5.43	3.78
Th	1.52	1.44	1.39	1.55
U	1.02	1.67	0.88	1.06

Table 2 Cont.

Sample	IG-05-28-06-02	CG-05-24-06-03	CG-05-24-06-3B	CG-05-24-06-04
Formation	Dacitic Lavas	Dacitic Domes	Dacitic Domes	Dacitic Domes
Location				
Latitude	8.5870	8.6244	8.6244	8.6245
Longitude	80.1324	80.1193	80.1193	80.1235
XRF Analyses				
SiO2	67.03	68.94	68.06	68.56
TiO2	0.30	0.25	0.25	0.24
Al2O3	17.85	17.10	17.50	17.42
Fe2O3	3.54	2.60	2.72	2.45
MnO	0.08	0.06	0.06	0.05
MgO	1.36	1.04	1.07	1.06
CaO	4.26	3.77	4.13	3.99
Na2O	4.24	4.51	4.62	4.61
K2O	1.23	1.66	1.52	1.56
P2O5	0.12	0.07	0.06	0.06
Total				
Ni	21.00	21.00	21.00	20.00
Cu	45.00	20.00	16.00	19.00
Zn	42.00	38.00	37.00	34.00
Rb	14.00	14.00	13.00	15.00
Zr	79.71	92.85	84.70	81.00
Sr	628.00	776.00	787.00	767.00
Laser ablation ICP-MS analyses				
Y	4.94	4.69	4.47	4.36
Nb	2.36	2.14	1.88	2.67
Ba	576.60	541.24	486.05	509.03
La	6.89	9.11	8.15	7.51
Ce	12.95	18.77	16.85	15.96
Pr	1.44	1.96	1.76	1.69
Nd	5.67	7.38	6.89	6.82
Sm	1.36	1.56	1.43	1.41
Eu	0.56	0.57	0.56	0.61
Gd	1.30	1.49	1.41	1.28
Tb	0.20	0.21	0.19	0.21
Dy	0.92	0.88	0.86	0.80
Ho	0.18	0.16	0.14	0.08
Er	0.33	0.25	0.22	0.14
Yb	0.57	0.46	0.39	0.24
Lu	0.04	0.03	0.03	0.03
Hf	1.83	2.12	1.92	2.06
Ta	0.12	0.12	0.07	0.13
Pb	3.66	7.28	4.91	3.92
Th	1.68	3.07	2.45	2.84
U	1.12	1.42	1.17	1.75

Table 2 cont.

Sample	CP-05-28-06-01	CP-05-28-06-02	GD-06-03-06-1	LT-5-31-06-4A
Formation	Dacitic Domes	Dacitic Domes	Dacitic Domes	Llano Tigre
Location				
Latitude	8.6210	8.6210	8.6014	8.5839
Longitude	80.1384	80.1384	80.1009	80.1227
XRF Analyses				
SiO2	69.19	68.74	67.77	58.45
TiO2	0.24	0.25	0.28	1.15
Al2O3	16.73	16.96	17.80	15.18
Fe2O3	2.54	2.63	3.39	6.33
MnO	0.06	0.06	0.08	0.11
MgO	1.03	1.05	0.41	4.33
CaO	3.98	3.97	4.62	9.26
Na2O	4.60	4.67	4.40	3.25
K2O	1.55	1.57	1.12	1.16
P2O5	0.09	0.10	0.13	0.77
Total				
Ni	21.00	21.00	20.00	50.00
Cu	13.00	13.00	31.00	136.00
Zn	38.00	39.00	44.00	65.00
Rb	14.00	15.00	12.00	15.00
Zr	90.00	91.00	69.87	78.00
Sr	745.00	747.00	682.00	637.00
Laser ablation ICP-MS analyses				
Y		5.16	6.24	14.69
Nb		3.42	2.28	5.41
Ba		512.00	574.00	521.19
La		10.18	8.42	15.93
Ce		20.09	16.04	29.05
Pr		2.83	1.79	3.69
Nd		8.79	7.16	15.02
Sm		2.00	1.63	3.09
Eu		1.06	0.58	1.05
Gd		1.66	1.54	2.89
Tb		0.42	0.22	0.43
Dy		1.08	1.05	2.39
Ho		0.35	0.21	0.46
Er		0.47	0.41	1.30
Yb		0.78	0.65	1.34
Lu		0.24	0.05	0.19
Hf		2.23	1.60	1.84
Ta		0.39	0.09	0.26
Pb		6.24	3.62	2.33
Th		3.35	1.01	1.54
U		3.38	0.68	0.61

Table 2 cont.

Sample	LT-5-31-06-4B	LT-5-31-06-4C	LT-05-31-06-1C
Formation	Llano Tigre	Llano Tigre	Llano Tigre
Location			
Latitude	8.5650	8.5650	8.5650
Longitude	80.1209	80.1209	80.1209
XRF Analyses			
SiO2	57.75	58.45	68.34
TiO2	1.57	1.15	0.23
Al2O3	14.43	15.14	17.14
Fe2O3	6.53	6.33	2.78
MnO	0.12	0.10	0.07
MgO	4.68	4.34	1.08
CaO	9.76	9.31	4.46
Na2O	3.19	3.23	4.41
K2O	1.05	1.17	1.39
P2O5	0.92	0.78	0.10
Total			
Ni	56.00	61.00	57.00
Cu	116.00	55.00	109.00
Zn	73.00	70.00	73.00
Rb	17.00	14.00	16.00
Zr	202.38	266.96	211.72
Sr	964.00	835.00	972.00
Laser ablation ICP-MS analyses			
Y	30.61	25.52	30.20
Nb	5.92	7.56	6.00
Ba	634.74	540.83	638.77
La	37.32	40.99	39.02
Ce	92.50	105.57	96.09
Pr	13.40	15.76	13.92
Nd	57.99	69.34	59.54
Sm	10.17	12.16	10.20
Eu	2.83	3.22	2.81
Gd	8.39	9.32	8.28
Tb	0.93	0.99	0.89
Dy	4.58	4.60	4.49
Ho	0.85	0.76	0.81
Er	2.23	1.92	2.18
Yb	1.98	1.69	1.94
Lu	0.30	0.25	0.29
Hf	4.80	5.97	4.89
Ta	0.28	0.36	0.29
Pb	5.53	3.60	4.04
Th	4.44	5.30	4.41
U	1.66	1.83	1.72

APPENDIX C

C.1 PETROGRAPHIC ANALYSES

Petrographic summary

Unit/Sample	Plagioclase	Amph.	Biotite	Quartz	Augite	Opaque
El Hato	modal %	modal %	modal %	modal %	modal %	modal %
CY-06-02-06-04A	11	2		1		<1
GT-05-30-06-02A	11	1		2		<1
LC-06-06-06-04A	13	2		2		<1
LG-06-04-06-01A	11	2		1		<1
AT-06-02-06-02A	12	1		2		<1
HG-5-30-06-01C	10	2		2		<1
LM-05-19-06-01C	11	2		1		<1
RH-06-02-06-3B	12	2		2		<1
GT-05-30-06-03	12	1		2		<1
MS-06-01-06-1B	11	1		2		<1
LM-05-19-06-1D	13	1		1		<1
GT-05-30-06-01A	14	1		1		<1
CA-05-19-06-01A	10	2		2		<1
SR-06-6-06-1A	12	2		1		<1
LT-05-31-06-02A	13	1		1		<1
ID-06-03-06-01B	11	1		2		<1
LC-06-6-06-01	14	1		1		<1
RH-06-02-06-02B	12	1		2		<1
LC-06-6-06-02A	10	2		1		<1
RH-6-2-06-1A	11	2		2		<1
LU-5-20-06-01C	12	1		2		<1
LC-06-06-06-03A	13	1		2		<1
GT-05-30-06-04B	13	2		1		<1
LT-05-31-06-03A	12	1		1		<1
Size (mm)	2.0-1.2	0.5-0.3		1.5-1.0		0.5-0.3

Cont.

Unit/Sample	Plagioclase	Amphibole	Biotite	Quartz	Augite	Opaques
Dacitic Lavas	modal %	modal %	modal %	modal %	modal %	modal %
CP-5-28-06-01	17	6		5		2
CG-05-28-06-01	26	4	2	2		<1
CG-5-24-06-01	19	4		5		2
GD-06-03-06-01	28	4		7		<1
CP-05-28-06-02	17	4	2	5		2
CG-5-24-06-03	25	4	2	2		2
CG-5-24-06-04	26	3	2	2		2
CG-5-24-06-02	27	4	2	5		<1
CC-05-24-06-01X	27	3	6	2		2
IG-5-28-06-02	21	3	1	4		<1
IG-05-22-06-03	26	2	2	5		<1
ID-05-22-06-04	23	2	2	4		<1
IG-5-22-06-02	19	3	1	4		<1
ID-05-22-06-05	21	2	2	4		<1
PP-05-27-06-01	23	4		7		<1
IG-5-28-06-01	21	3	1	4		<1
IG-05-22-06-01	21	3	1	4		<1
GY-5-19-06-03	19	3	1	6		<1
Size (mm)	4.5 -0.05	2.50-0.25	0.20-0.10	4.5-0.5		0.3-0.6
Llano Tigre andesite						
LT-05-31-06-04C	21				6	>1
Size (mm)	3.5-0.5				1.5-1.0	0.5-0.2

C1. PETROGRAPHIC DESCRIPTIONS

LLANO TIGRE ANDESITES

(Pictures of augite crystals, corroded plagioclase, magnetite alteraded to iron oxyhydroxides)

1. INTRODUCTION:

This thin section report for sample LT-5-31-06-04c, identified as an andesitic flow.

2. MINERALOGY:

Primary. Coarse to medium (3.5 mm- 0.5 mm) euhedral to subhedral crystals, Plagioclase and Augite in a very fine ground mass of microcrystalline plagioclase laths and augite microcristals. Most plagioclase phenocrysts are fractured and euhedral to subhedral crystals that range from 3.5 mm to microcrystalline. Zoning and selective corrosion of rims can be seen. Augite is euhedral and up to 1.5 mm and present altered crystals. Oxides are scarce small (0.3 mm) and some of them are completely altered to iron oxydroxides.

Secondary. Most grains on the thin section appear very fresh except for augite.

3. ESTIMATED MODAL PERCENTAGES

Phenocrysts	**28 %**	
Plagioclase	21 %	
Augite	6 %	
Oxides	1 %	
Groundmass		**72 %**
Plagioclase		
Augite		
oxides		

4. OVERALL AND SPECIAL TEXTURES:

Intersertal Hypocrystalline Aphanitic porphyritic texture. Discontinuous zoning, sieve textures, and reaction on some of the rims are common in plagioclase. Alteration can be observed in the some of the pyroxenes, where some of them are completely replaced by smectite or vermiculate. Probably, only the most calcic rich rims of the pyroxenes are affected.

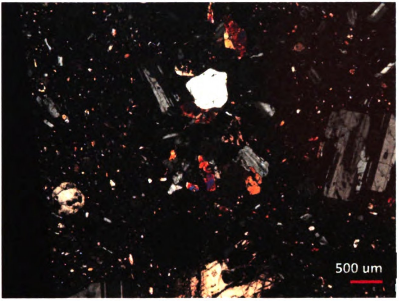

Accumulation of plagioclase (corroded), augite and oxides.

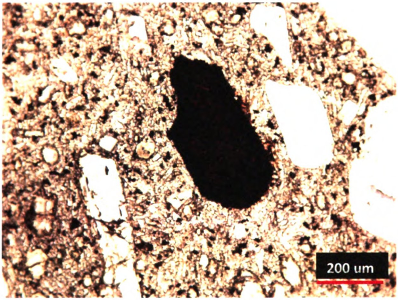

Alteration of magnetite to oxyhydroxide.

DACITIC DOMES (GAITAL, CARACORAL, PAJITAS, TORTUGA, GRANDE)

(pictures of plagioclase corrosion, opacite rims, desorbed hornblende crystals, and glomeroporphyritic accumulations)

1. INTRODUCTION:

This description is a product of the petrographical analysis of samples CG-5-24-06-02, CG-05-28-06-01, GD-06-03-06-01, CP-05-28-06-01, CG-5-24-06-04, CC-05-24-06-02, CG-05-24-06-01,CG-05-24-06-0, Cp-05-28-06-02, CC-05-24-06-01X.

2. MINERALOGY:

Primary. The main characteristics are the coarse to medium (4.5 mm- 0.5 mm) euhedral to subhedral crystals of Quartz, Plagioclase and Hornblende in a very fine ground mass of microcrystalline plagioclase laths, hornblende, Biotite and small and altered portions of glass. Most plagioclase phenocrysts are fractured and are euhedral to subhedral with sizes that range from 4.5 mm to microcrystalline. Most of them display zoning, where in some of the rims are corroded as if they reacted with the liquid. Quartz phenocrysts are generally large (4.5 mm to 0.5 mm) and fractured and embayment is common. Hornblende is present in euhedral to subhedral crystals. Sizes are from 2.5 mm – 0.25 mm. Post-eruptional oxidation and hydration has resulted in opacite rims, some of them covering whole crystals. Biotite crystals are usually euhedral and small (0.10-0.20 mm). Some biotite crystals seem to have grown on rims around hornblende. Oxides are related mostly to hornblende but scarce and single and small (0.3 mm) crystals can occur.

3. ESTIMATED MODAL PERCENTAGES

Phenocrysts	***23-30 %***
Plagioclase	17-28 %
Quartz	2-7 %
Hornblende	6-3 %
Biotite	0-2 %
Oxides	<1-2 %

Groundmass **70-77 %**

Plagioclase

Amphibole

Glass

4. OVERALL AND SPECIAL TEXTURES:

Hypocrystalline Aphanitic porphyritic texture. Discontinuous zoning, sieve textures, and reaction on some of the rims are common in plagioclase. Embayed quartz crystals opacite rims and glomeroporfiritic texture are observed. The textures on plagioclase suggests disequilibrium between the mineral and the melt.

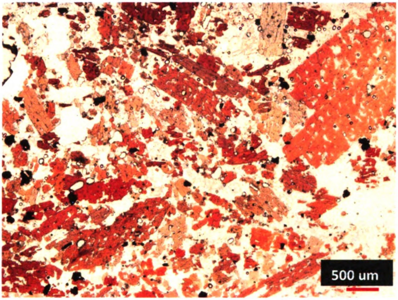

Hornblende, Biotite, quartz and oxide Glomeroporfiritic accumulations (PPL)

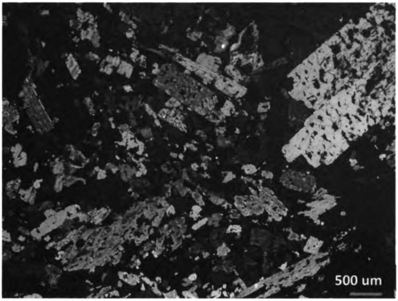

Hornblende, Biotite, quartz and oxide Glomeroporfiritic accumulations (PPL)

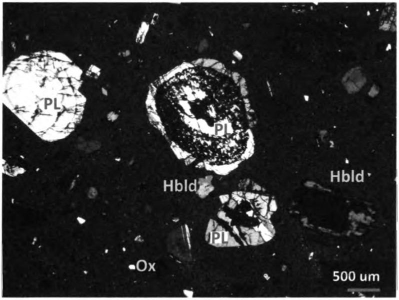

Corroded plagioclase and hornblende (XPL)

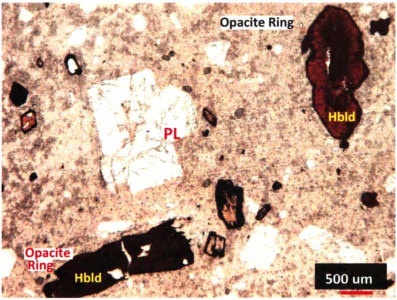

Opacite rims around hornblende (PPL)

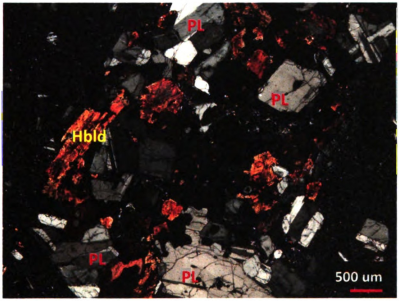

Accumulation of plagioclase and hornblende (XPL)

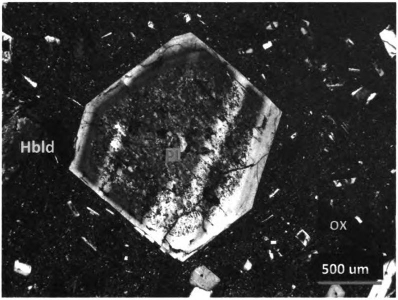

Corroded Plagioclase crystal (XPL)

DACITIC LAVAS INDIA DORMIDA

1. INTRODUCTION:

This thin section report for samples IG-05-28-06-02, IG-05-22-06-02, IG-5-22-06-03,ID-05-22-06-04, IG-05-22-06-05, PP-05-27-06-01, IG-05-28-06-01, IG-05-22-06-01 and GY-05-19-06-03 identified as a dacitic lava flows in cerro India Dormida, cerro Iguana, cerro Guacamaya, cerro Piedra Pintanda.

2. MINERALOGY:

Primary. Phenocrysts are coarse to medium (4.5 mm- 0.5 mm) euhedral to subhedral crystals of Quartz, Plagioclase and Hornblende in a very fine ground mass of microcrystalline plagioclase laths, hornblende, biotite and rarely glass. Most plagioclase phenocrysts are fractured and shapes are euhedral to subhedral with sizes that range from 4.0 mm to microcrystalline. Most of them display zoning with corrosion in some of the rims, as if they reacted with the liquid. Quartz phenocrysts are generally 3.5 mm to 0.5 mm and fractured. Embayment on the edges on quartz crystals are common. Hornblende is present in euhedral to subhedral crystals. Sizes are from 2.50 mm – 0.2 mm. Biotite crystals are usually euhedral (1.5 mm -0.20 mm) and some do not present opacite rims.

Some biotite crystals seem to have grown on rims around hornblende. Oxides are related mostly to hornblende, but scarce and single small (0.3 mm) crystals can occur.

3. ESTIMATED MODAL PERCENTAGES

Phenocrysts	***28-30*** **%**
Plagioclase	19-26 %
Quartz	4-7 %
Hornblende	4-2 %
Biotite	0-2 %
Oxides	< 1 %
Groundmass	**70-72 %**
Plagioclase	
Amphibole/Biotite	
Glass	

4. OVERALL AND SPECIAL TEXTURES:

Hypocrystalline Aphanitic porphyritic texture. Discontinuous zoning, sieve textures, reaction on some of the rims are common in plagioclase. Broke and embayed shaped corners in quartz crystals are seen.

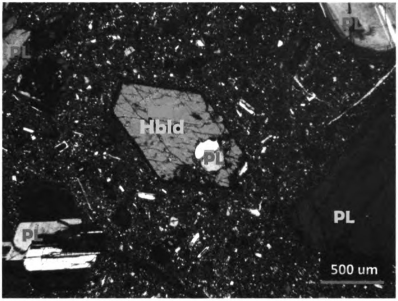

Opacite rims around an hornblende with poikilitic plagioclase.

EL HATO DACITIC FLOW

The El Hato pumice fragments are light gray to white in color, Hypocrystalline with a degress of crystallinity 14-18%. The matrix is dominated by light glass with a few microlites.

1. INTRODUCTION:

This petrographic description was produced by analyzing 25 different thin sections for el Hato unit in different localities over an approximate 300 km^2 area.

2. MINERALOGY:

Primary. The phenocrysts are coarse to medium (2 mm- 1.2 mm) euhedral to subhedral. Mineralogy is composed of Quartz, Plagioclase and Hornblende. Most plagioclase phenocrysts are fractured and/or broken euhedral to subhedral crystals that range from 2.0 mm to microcrystalline. Most of them display complex zoning, were in some phenocrysts some of the rims are corroded. Quartz phenocrysts are generally 1.5 mm to 1.0 mm and fractured. Embayment on the edges on quartz crystals are common. Hornblende is present in euhedral to subhedral crystals. Sizes are from 0.50 mm – 0.30 mm. Oxides are related mostly to hornblende, but scarce and single small (0.3 mm) crystals can occur.

3. ESTIMATED MODAL PERCENTAGES

Phenocrysts	***14-17*** **%**
Plagioclase	11-14 %
Quartz	1-2 %
Hornblende	1-2 %
Oxides	< 1 %
Groundmass	**83-86 %**
Plagioclase	
Amphibole	
Glass	

4. OVERALL AND SPECIAL TEXTURES:

Phenocrysts are tipically found isolated, but some plagioclase and hornblende are intergrown along with the Fe-Ti oxides. Discontinuous zoning, sieve textures, reaction on some of the rims are common in plagioclase. Broke and embayed shaped corners in quartz crystals are seen.

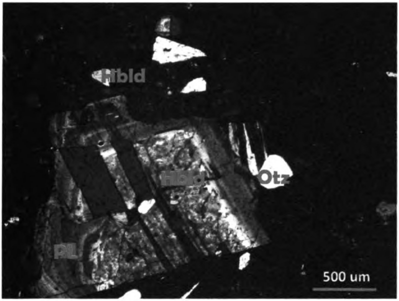

Corroded plagioclase crystal

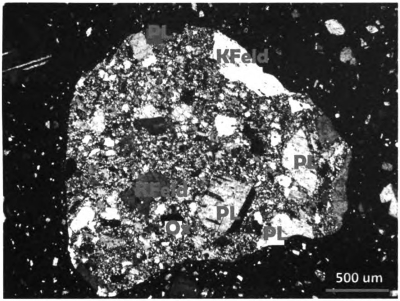

Lithic fragment probably from the wall of the magma chamber

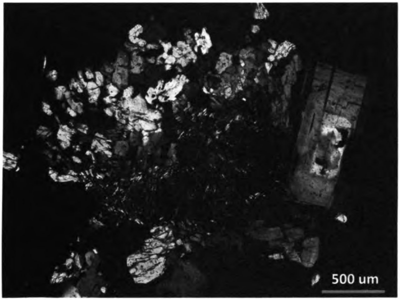

Accumulation of hornblende crystals and plagioclase

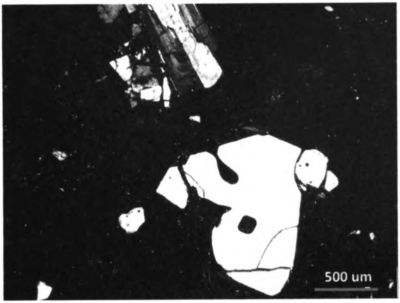

Resorbed quartz crystal

APPENDIX D

D.1 BSE IMAGES INDIVIDUAL PHASE GEOCHEMISTRYAND INDIVIDUAL PHASE GEOCHEMISTRY FOR PLAGIOCLASE AND GLASS

CA-05-20-06-1A Plag 4 (El Hato)

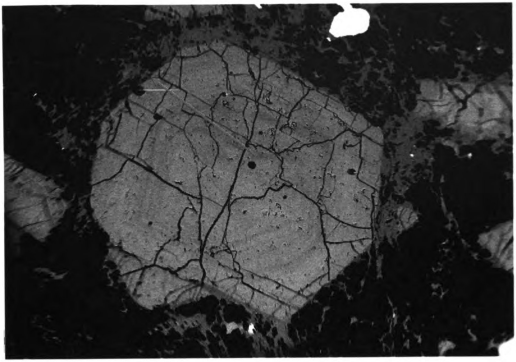

CA-05-20-06-1A Plag 3 (El Hato)

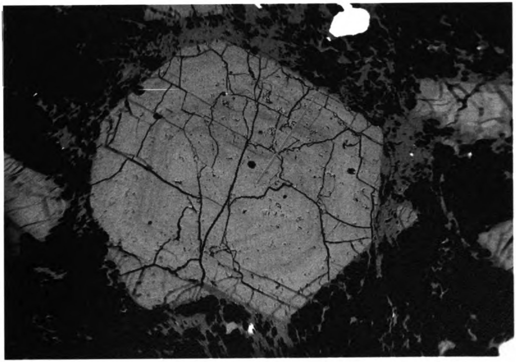

CA-05-20-06-1A Plag 2 (El Hato)

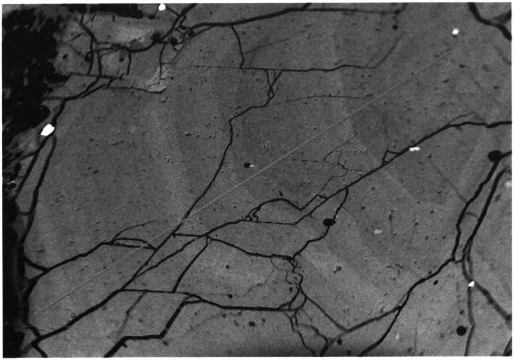

CA-05-20-06-1A Plag 1 (El Hato)

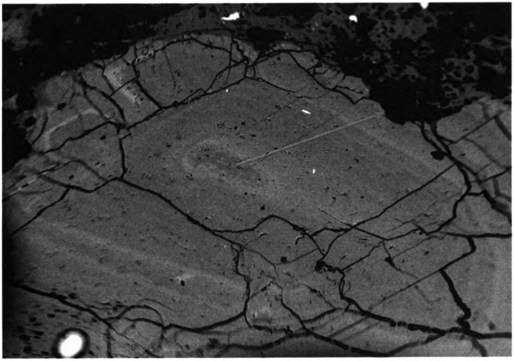

RH-6-2-06-1A Core to Rim (El Hato)

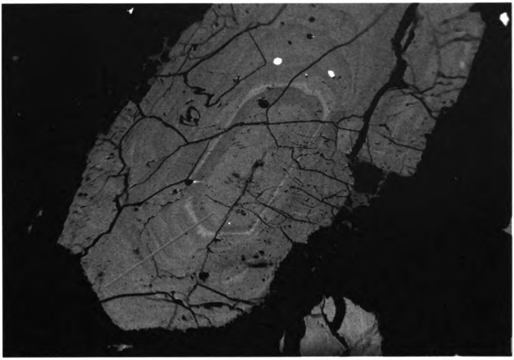

SR-6-6-06-1A-Plag-3 Core to Rim (El Hato)

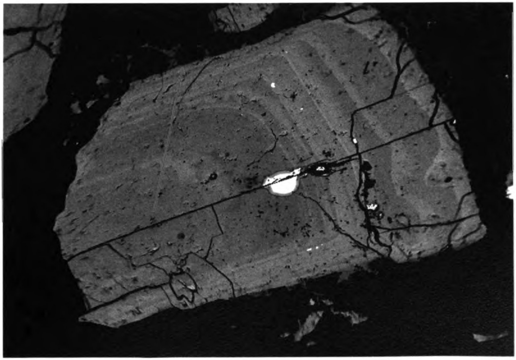

SR-6-6-06-1A-Plag-2 Core to Rim (El Hato)

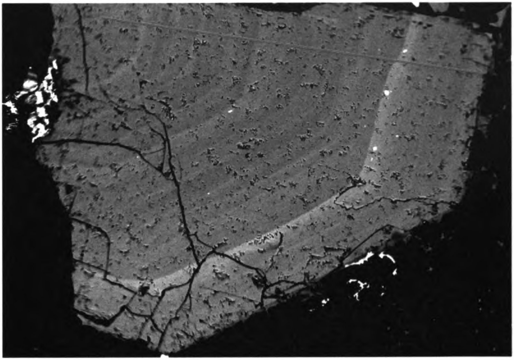

SR-6-6-06-1A-Plag-1 Core to Rim (El Hato)

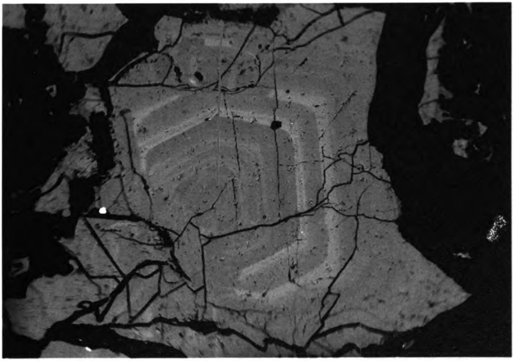

LM-5-19-06-1D Plag-1 Core to Rim (EL Hato)

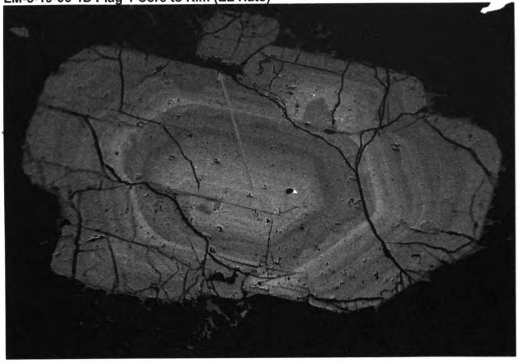

LM-5-19-06-1D Plag-2 Core to Rim (El Hato)

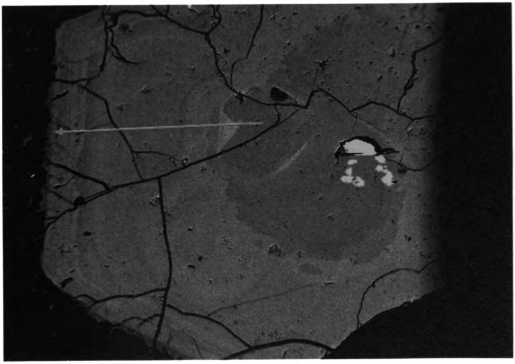

LM-5-19-06-1D Plag-3 Core to Rim (El Hato)

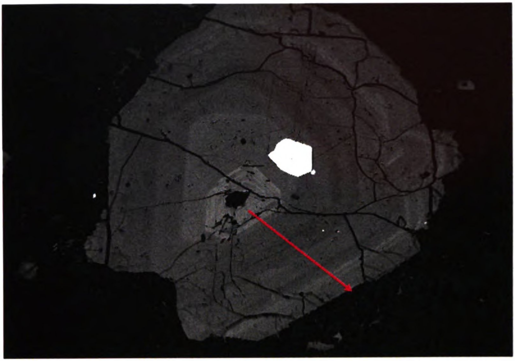

CC-5-24-06-1X Plag-5 Core to Rim (Dacitic Domes)

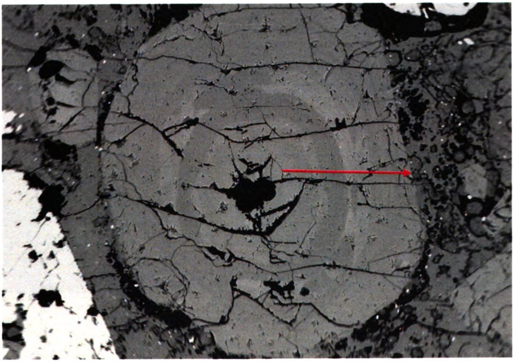

CC-5-24-06-1X Plag-4 Core to Rim (Dacitic Domes)

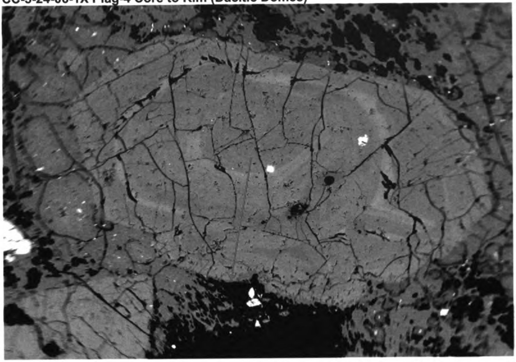

CC-5-24-06-1X Plag-3 Core to Rim (Dacitic Domes)

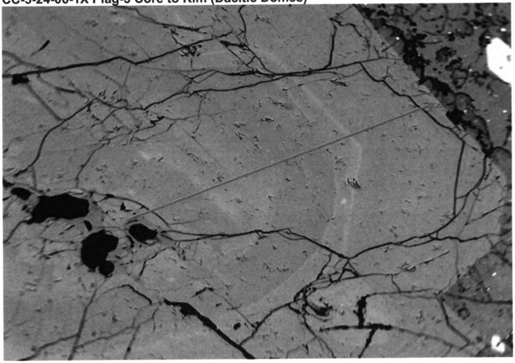

ID-6-3-06-1B Plag-6 Core to Rim (El Hato)

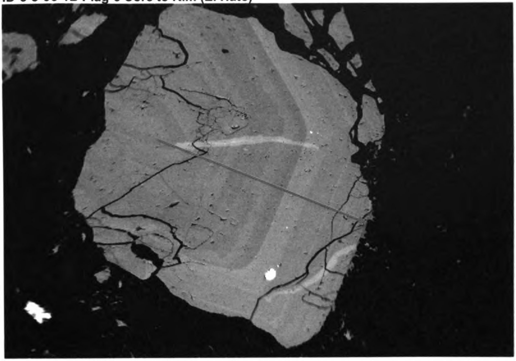

ID-6-3-06-1B Plag-3 Core to Rim (El Hato)

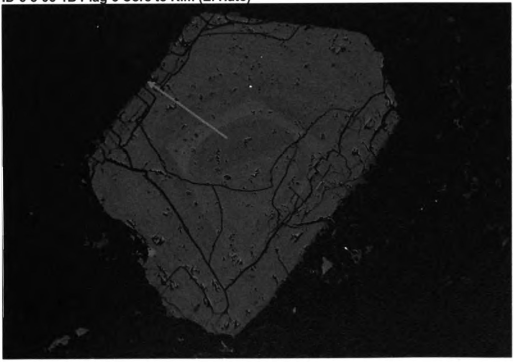

ID-6-3-06-1B Plag-2 Core to Rim (El Hato)

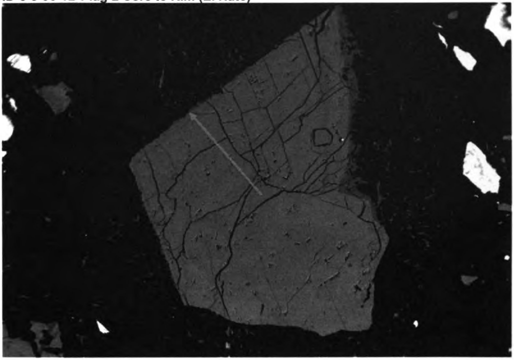

ID-6-3-06-1B Plag-1 Core to Rim (El Hato)

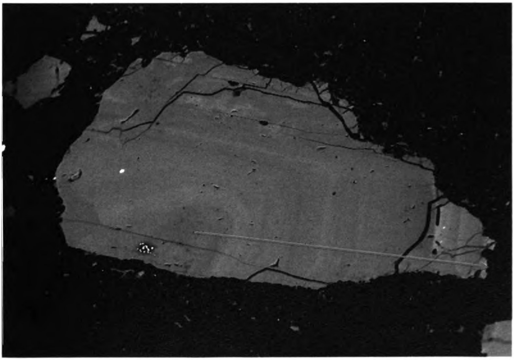

ID-5-22-06-01 Plag-5 Core to Rim (India Dormida Dacite Lava)

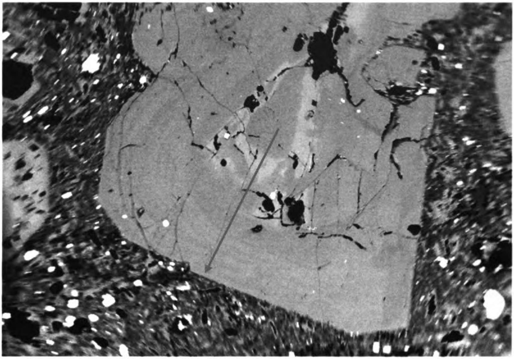

LT-5-31-06-4C Plag-4 Core to Rim (Llano Tigre Andesite)

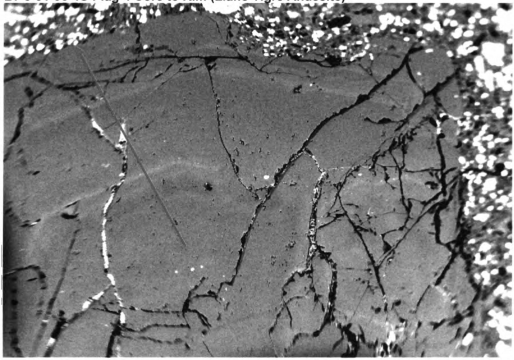

LT-5-31-06-4C Plag-5 Core to Rim (Llano Tigre andesite)

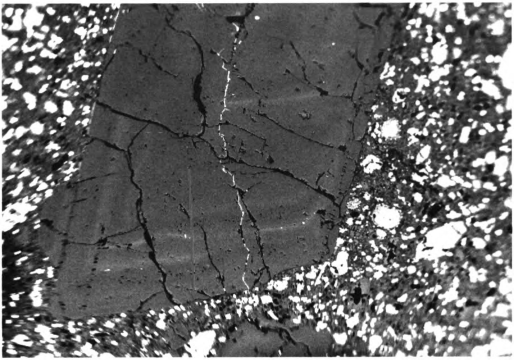

APPENDIX E

E1. DATA FROM INDIVIDUAL PHASE GEOCHEMISTRY

Sample RH-06-02-06-1A Random
Glass points

Sample	1	2	3	4	5	6	7
Na2O	3.85	4.40	4.30	4.11	4.14	4.04	4.14
MgO	0.23	0.23	0.21	0.26	0.25	0.23	0.24
Al2O3	12.58	12.65	12.87	12.78	12.81	13.13	12.80
SiO2	73.13	74.42	74.68	75.07	75.18	71.18	75.58
K2O	2.10	2.23	2.22	2.20	2.18	2.01	2.19
CaO	1.56	1.59	1.49	1.53	1.45	1.41	1.51
TiO2	0.15	0.00	0.23	0.00	0.15	0.10	0.00
FeO	0.67	0.93	0.73	0.79	0.96	0.83	0.88
MnO	0.02	0.01	0.01	0.00	0.04	0.00	0.09
Totals	94.30	96.46	96.73	96.74	97.16	92.94	97.42

Samople LM-05-19-06-1D Random
Glass points

Sample	1	2	3	4	5	6	7
Na2O	4.41	4.21	3.96	4.60	3.71	3.93	3.98
MgO	0.23	0.26	0.24	0.30	0.25	0.22	0.22
Al2O3	13.02	12.98	12.98	12.97	13.07	12.79	12.66
SiO2	75.87	74.96	70.58	75.18	75.21	73.71	73.47
K2O	2.21	2.16	2.14	2.23	2.18	2.24	2.18
CaO	1.57	1.49	1.39	1.47	1.52	1.52	1.56
TiO2	0.00	0.23	0.15	0.28	0.15	0.26	0.10
FeO	0.93	0.88	0.67	0.78	0.73	0.73	0.67
MnO	0.13	0.01	0.00	0.00	0.02	0.00	0.04
Totals	98.37	97.18	92.11	97.81	96.86	95.40	94.88

Sample	8	9	10	11	12	13	14
Na2O	4.23	4.43	3.80	4.22	4.10	4.20	4.35
MgO	0.23	0.26	0.25	0.29	0.25	0.25	0.27
Al2O3	12.60	13.01	13.14	13.02	12.92	12.88	13.45
SiO2	72.04	75.92	74.97	74.84	75.36	74.24	74.33
K2O	2.20	2.20	2.29	2.25	2.25	2.18	2.22
CaO	1.49	1.56	1.55	1.56	1.50	1.46	1.52
TiO2	0.15	0.13	0.18	0.05	0.13	0.00	0.13
FeO	0.99	0.73	0.84	0.94	0.84	0.72	0.76
MnO	0.10	0.04	0.03	0.04	0.11	0.00	0.01
Totals	94.04	98.27	97.04	97.23	97.46	95.93	97.04

Sample	15	16	17	18	19	20	21
Na2O	4.28	4.12	4.15	4.60	4.53	4.33	4.28
MgO	0.25	0.25	0.25	0.28	0.27	0.21	0.28
Al2O3	12.88	13.18	12.99	13.27	12.90	12.92	13.01
SiO2	74.63	74.89	74.26	75.11	75.35	74.90	75.60
K2O	2.22	2.33	2.20	2.26	2.27	2.26	2.26
CaO	1.48	1.55	1.56	1.53	1.49	1.49	1.59
TiO2	0.15	0.08	0.08	0.05	0.00	0.18	0.13
FeO	0.93	0.89	0.87	0.95	0.71	0.89	0.90
MnO	0.07	0.13	0.06	0.11	0.09	0.01	0.01
Totals	96.91	97.40	96.41	98.17	97.60	97.19	98.07

Sample LM-05-19-06-1C
Random Glass points

Sample	1	2	3	4	5	6	7	8	9
Na2O	3.52	3.87	3.32	3.03	3.93	3.20	3.79	3.44	3.54
MgO	0.24	0.28	0.23	0.25	0.23	0.34	0.32	0.25	0.30
Al2O3	11.78	12.45	10.65	11.44	13.03	11.14	12.73	11.18	11.10
SiO2	69.58	71.33	61.09	66.54	75.01	60.67	73.25	61.52	64.58
K2O	2.18	2.12	2.01	2.05	2.40	1.80	2.40	1.92	1.87
CaO	1.41	1.47	1.22	1.40	1.54	1.50	1.56	1.28	1.38
TiO2	0.28	0.05	0.18	0.10	0.26	0.00	0.05	0.28	0.05
FeO	0.70	0.92	0.88	0.79	0.86	1.13	0.79	0.76	0.86
MnO	0.02	0.00	0.07	0.04	0.00	0.06	0.04	0.00	0.01
Totals	89.71	92.50	79.64	85.63	97.25	79.83	94.92	80.62	83.69

Sample RH-06-02-06-3B
Random Glass Points

Sample	1	2
Na2O	4.17	4.34
MgO	0.23	0.19
Al2O3	12.58	12.88
SiO2	73.79	74.05
K2O	2.67	2.78
CaO	1.23	1.19
TiO2	0.18	0.08
FeO	0.74	0.94
MnO	0.08	0.07
Totals	95.66	96.50

Sample RH-06-02-06-3B Random
Glass points

Sample	1	2	3	4	5	6	7	8	9
Na2O	4.07	4.35	4.34	4.43	4.48	4.38	4.51	4.54	4.34
MgO	0.21	0.24	0.21	0.26	0.22	0.21	0.22	0.22	0.20
Al2O3	12.68	12.66	12.63	12.75	12.67	12.77	12.89	12.89	12.80
SiO2	72.11	74.11	74.40	75.22	74.18	75.41	73.76	74.30	74.21
K2O	2.70	2.75	2.64	2.76	2.71	2.72	2.72	2.74	2.67
CaO	1.20	1.30	1.34	1.32	1.27	1.19	1.24	1.26	1.29
TiO2	0.24	0.00	0.03	0.16	0.08	0.21	0.24	0.34	0.21
FeO	0.73	0.83	0.99	0.96	0.74	0.86	0.78	0.76	0.77
MnO	0.03	0.04	0.08	0.00	0.05	0.02	0.00	0.05	0.07
Totals	93.96	96.27	96.64	97.86	96.39	97.76	96.36	97.10	96.57

Sample	10	11	12	13	14	15	16	17	18
Na2O	4.32	3.40	2.41	4.34	4.41	3.77	4.02	3.98	4.16
MgO	0.21	0.22	0.22	0.19	0.25	0.23	0.18	0.21	0.24
Al2O3	12.75	13.22	12.68	12.70	12.59	12.45	11.77	12.33	12.66
SiO2	74.55	74.82	75.32	73.67	73.29	69.42	68.97	70.35	71.16
K2O	2.67	2.72	2.70	2.74	2.81	2.69	2.63	2.61	2.55
CaO	1.31	1.29	1.36	1.29	1.24	1.21	1.23	1.19	1.22
TiO2	0.03	0.13	0.13	0.16	0.08	0.11	0.13	0.00	0.03
FeO	0.97	0.84	0.85	0.76	0.79	0.83	0.98	0.67	0.82
MnO	0.09	0.03	0.00	0.00	0.00	0.14	0.00	0.00	0.02
Totals	96.89	96.66	95.67	95.85	95.46	90.85	89.91	91.34	92.86

Sample	19	20	21	22	23	24	25	26	27
Na2O	3.88	4.36	4.41	3.98	4.17	3.92	4.07	4.34	4.10
MgO	0.24	0.20	0.23	0.24	0.26	0.23	0.19	0.26	0.20
Al2O3	12.95	12.55	12.70	11.97	12.76	12.16	12.94	12.74	12.46
SiO2	74.50	72.99	74.22	70.05	73.46	70.82	74.09	74.11	72.19
K2O	2.81	2.71	2.59	2.63	2.61	2.62	2.67	2.70	2.60
CaO	1.27	1.28	1.27	1.16	1.26	1.23	1.34	1.29	1.26
TiO2	0.21	0.00	0.00	0.24	0.08	0.21	0.03	0.08	0.24
FeO	0.86	0.84	0.75	0.75	0.86	0.60	0.90	0.88	0.61
MnO	0.04	0.05	0.05	0.03	0.04	0.04	0.01	0.05	0.05
Totals	96.76	94.97	96.21	91.04	95.51	91.83	96.23	96.44	93.71

Sample	28	29	30	31
Na2O	4.65	4.00	4.12	4.24
MgO	0.20	0.18	0.22	0.22
Al2O3	12.81	12.46	12.90	12.78
SiO2	74.11	72.24	74.64	75.01
K2O	2.76	2.70	2.69	2.78
CaO	1.36	1.24	1.33	1.25
TiO2	0.18	0.26	0.13	0.08
FeO	0.52	0.66	0.88	0.92
MnO	0.08	0.04	0.02	0.00
Totals	96.68	93.78	96.94	97.28

Sample CA-05-19-06-1A Random Glass points

Sample	1	2	3	4	5	6	7	8	9
Na2O	4.00	4.32	4.27	4.33	4.37	4.16	4.23	4.51	4.17
MgO	0.18	0.23	0.25	0.22	0.19	0.18	0.21	0.19	0.24
Al2O3	12.23	12.28	12.24	12.04	12.07	12.23	11.97	12.12	12.12
SiO2	75.75	75.55	75.21	75.44	75.24	75.30	75.38	74.57	75.78
K2O	2.67	2.58	2.66	2.72	2.60	2.67	2.54	2.71	2.64
CaO	1.18	1.19	1.14	1.14	1.10	1.20	1.18	1.10	1.17
TiO2	0.00	0.21	0.08	0.13	0.29	0.08	0.13	0.31	0.13
FeO	0.74	0.70	0.84	0.62	0.74	0.78	0.80	0.47	0.70
MnO	0.04	0.07	0.04	0.02	0.02	0.11	0.00	0.00	0.03
Totals	96.79	97.14	96.73	96.66	96.61	96.72	96.43	95.98	96.97

Sample	10	11	12	13	14	15	16	17	18
Na2O	4.36	4.32	4.24	4.21	4.31	4.24	4.57	4.30	4.24
MgO	0.21	0.26	0.21	0.19	0.25	0.23	0.20	0.19	0.23
Al2O3	12.26	12.07	12.14	12.20	12.28	12.65	12.09	12.45	12.34
SiO2	76.13	75.74	75.76	75.88	75.62	75.75	75.10	75.64	75.74
K2O	2.66	2.70	2.51	2.65	2.61	2.68	2.66	2.62	2.72
CaO	1.16	1.19	1.20	1.19	1.19	1.18	1.21	1.17	1.23
TiO2	0.00	0.10	0.24	0.29	0.13	0.08	0.08	0.24	0.26
FeO	0.74	0.79	0.89	0.77	0.62	0.67	0.71	0.86	0.60
MnO	0.04	0.00	0.00	0.00	0.00	0.04	0.00	0.00	0.00
Totals	97.56	97.17	97.20	97.39	97.01	97.52	96.63	97.47	97.36

Sample	19	20	21	22	23	24	25	26	27	28
Na2O	4.13	4.09	4.34	4.46	4.20	4.37	4.20	4.25	4.43	4.18
MgO	0.17	0.22	0.21	0.22	0.24	0.21	0.21	0.22	0.22	0.20
Al2O3	12.20	12.18	12.30	12.18	12.13	12.17	12.12	12.08	12.28	12.22
SiO2	76.08	75.98	75.78	75.02	75.76	75.38	75.95	75.83	76.57	75.63
K2O	2.56	2.61	2.67	2.63	2.70	2.69	2.72	2.71	2.72	2.72
CaO	1.11	1.21	1.17	1.20	1.11	1.11	1.15	1.11	1.20	1.17
TiO2	0.29	0.05	0.34	0.10	0.03	0.31	0.21	0.16	0.18	0.08
FeO	0.67	0.87	0.87	0.79	0.80	0.83	0.82	0.83	0.79	0.69
MnO	0.00	0.00	0.00	0.11	0.11	0.00	0.02	0.00	0.02	0.00
Totals	97.21	97.21	97.68	96.72	97.08	97.07	97.39	97.18	98.42	96.88

Sample LC-06-6-06-4A Random Glass points

Sample	1	2	3	4	5	6
Na2O	4.02	4.09	4.42	4.20	4.13	4.09
MgO	0.25	0.28	0.26	0.21	0.25	0.25
Al2O3	12.44	12.49	12.73	12.32	12.80	12.56
SiO2	73.26	72.63	75.33	71.71	73.97	71.91
K2O	2.09	1.97	2.02	1.90	2.00	1.89
CaO	1.50	1.70	1.74	1.60	1.70	1.68
TiO2	0.10	0.13	0.10	0.13	0.13	0.10
FeO	0.81	0.94	0.85	0.79	0.71	0.89
MnO	0.03	0.02	0.04	0.10	0.06	0.00
Totals	94.50	94.25	97.50	92.96	95.76	93.38

Sample MS-60106-1B Random Glass points

Sample	1	2	3	4	5	6	7	8	9
Na2O	4.36	4.25	4.53	3.94	4.13	4.43	4.15	4.54	4.40
MgO	0.20	0.22	0.23	0.24	0.23	0.18	0.25	0.22	0.21
Al2O3	12.54	12.57	12.77	12.52	12.51	12.57	12.65	12.71	12.64
SiO2	74.50	73.84	74.79	73.72	74.16	73.59	74.56	74.89	74.92
K2O	2.71	2.66	2.68	2.63	2.65	2.60	2.64	2.64	2.68
CaO	1.29	1.33	1.33	1.28	1.37	1.25	1.30	1.36	1.33
TiO2	0.16	0.08	0.31	0.03	0.13	0.00	0.00	0.13	0.08
FeO	0.88	1.18	0.79	0.84	0.83	0.84	0.66	0.75	0.93
MnO	0.00	0.01	0.04	0.07	0.08	0.08	0.00	0.02	0.07
Totals	96.65	96.13	97.47	95.27	96.10	95.54	96.21	97.27	97.27

Sample	10	11	12	13	14	15	16	17	18
Na2O	4.13	4.39	4.29	4.46	4.33	4.53	4.36	4.32	4.61
MgO	0.26	0.22	0.22	0.23	0.23	0.19	0.20	0.26	0.24
Al2O3	12.64	12.56	12.79	12.55	12.74	12.68	12.98	12.44	12.65
SiO2	75.23	74.85	74.69	74.70	75.43	75.22	75.10	73.10	73.95
K2O	2.64	2.70	2.63	2.70	2.75	2.69	2.65	2.80	2.62
CaO	1.33	1.35	1.32	1.28	1.36	1.38	1.25	1.36	1.32
TiO2	0.00	0.10	0.03	0.08	0.00	0.13	0.16	0.00	0.00
FeO	0.75	0.87	0.66	0.82	0.81	0.73	0.94	0.89	0.72
MnO	0.00	0.00	0.00	0.02	0.02	0.07	0.00	0.05	0.00
Totals	96.98	97.04	96.63	96.85	97.67	97.62	97.64	95.21	96.11

Sample	19	20	21	22	23	24	25	26	27
Na2O	4.29	4.30	4.44	4.23	4.59	4.50	3.89	4.34	4.52
MgO	0.23	0.22	0.27	0.22	0.20	0.21	0.26	0.24	0.23
Al2O3	12.35	12.86	12.57	12.77	12.70	12.71	12.51	12.55	12.67
SiO2	73.63	74.08	74.83	75.32	74.02	75.14	73.73	74.15	74.16
K2O	2.65	2.70	2.67	2.69	2.61	2.68	2.77	2.65	2.61
CaO	1.29	1.32	1.34	1.35	1.32	1.39	1.25	1.28	1.22
TiO2	0.05	0.08	0.00	0.00	0.13	0.13	0.47	0.16	0.31
FeO	0.80	0.83	0.78	0.78	0.87	1.08	0.94	0.72	0.85
MnO	0.01	0.02	0.08	0.04	0.07	0.11	0.09	0.05	0.06
Totals	95.30	96.41	96.98	97.40	96.52	97.94	95.91	96.14	96.64

Sample	28	29	30
Na2O	4.44	4.21	4.32
MgO	0.20	0.25	0.26
Al2O3	12.46	12.65	12.65
SiO2	74.74	74.21	73.99
K2O	2.64	2.63	2.74
CaO	1.34	1.23	1.28
TiO2	0.00	0.31	0.29
FeO	0.84	0.81	0.94
MnO	0.05	0.08	0.07
Totals	96.72	96.38	96.54

CA-5-20-06-1A Plag-4 Rim to Core
(El Hato)

Sample	1	2	3	4	5	6	7	8	9
FeO	0.19	0.23	0.23	0.27	0.32	0.30	0.28	0.29	0.26
CaO	7.78	7.64	7.81	7.75	7.71	7.61	7.40	7.00	7.50
K2O	0.29	0.29	0.28	0.27	0.23	0.30	0.25	0.30	0.30
Na2O	7.37	7.32	7.32	7.03	7.00	7.31	6.92	7.47	7.64
Al2O3	26.12	26.45	26.53	26.08	26.02	26.25	26.11	25.99	26.33
SiO2	58.62	58.36	58.22	58.59	58.11	58.34	58.61	58.71	58.91
Totals	100.38	100.30	100.39	100.00	99.39	100.11	99.57	99.77	100.94

Sample	10	11	12	13	14	15	16	17	18
FeO	0.26	0.26	0.23	0.27	0.24	0.25	0.32	0.26	0.18
CaO	7.92	8.54	8.19	8.41	8.24	8.76	7.95	8.04	8.62
K2O	0.26	0.23	0.19	0.22	0.28	0.22	0.24	0.25	0.23
Na2O	7.14	6.79	7.62	6.77	6.68	6.76	6.85	6.82	6.82
Al2O3	26.53	27.03	25.87	27.42	27.01	26.92	26.50	26.97	27.02
SiO2	57.99	57.54	55.84	56.85	57.83	57.01	58.33	57.79	56.61
Totals	100.09	100.39	97.96	99.95	100.28	99.93	100.18	100.14	99.49

Sample	19	20	21	22	23	24	25	26	27
FeO	0.23	0.25	0.22	0.23	0.15	0.18	0.27	0.27	0.12
CaO	8.13	7.69	7.97	6.90	7.66	7.28	7.30	7.11	7.21
K2O	0.26	0.29	0.26	0.29	0.23	0.28	0.39	0.27	0.23
Na2O	7.23	6.93	6.91	7.79	6.96	7.49	7.41	7.46	6.67
Al2O3	26.00	26.36	26.71	25.76	26.48	26.34	25.85	26.09	25.76
SiO2	56.92	58.08	57.70	59.78	59.25	58.89	58.60	59.18	59.02
Totals	98.77	99.60	99.79	100.74	100.73	100.46	99.82	100.39	99.01

Sample	28	29	30	31	32	33	34	35	36
FeO	0.27	0.21	0.22	0.16	0.12	0.18	0.08	0.24	0.23
CaO	7.67	8.05	7.80	7.97	7.95	8.39	7.59	7.80	8.07
K2O	0.27	0.25	0.28	0.27	0.31	0.24	0.27	0.23	0.27
Na2O	7.02	6.80	7.02	6.90	6.93	6.64	7.36	7.21	6.47
Al2O3	26.64	26.87	26.31	26.71	27.10	27.08	26.50	26.10	24.48
SiO2	58.65	57.78	58.57	57.98	58.53	57.45	58.84	58.19	52.36
Totals	100.52	99.96	100.21	99.99	100.94	99.98	100.64	99.77	91.89

Sample	37	38	39	40	41	42	43	44	45
FeO	0.20	0.92	0.24	0.21	0.20	0.26	0.19	0.16	0.25
CaO	7.34	6.97	7.84	7.61	8.48	8.44	8.38	7.94	8.22
K2O	0.29	0.23	0.26	0.29	0.28	0.24	0.23	0.25	0.24
Na2O	6.92	5.74	7.01	7.53	6.81	6.72	6.66	7.26	6.81
Al2O3	26.64	31.88	26.71	26.14	27.39	27.17	26.72	26.46	26.48
SiO2	59.54	52.16	57.90	58.76	57.09	56.62	57.30	58.04	57.91
Totals	100.93	97.90	99.97	100.54	100.25	99.44	99.48	100.12	99.91

Sample	46	47	48	49	50	51	52	53	54
FeO	0.17	0.16	0.16	0.13	0.09	0.23	0.20	0.12	0.09
CaO	8.29	8.66	8.76	8.40	7.77	7.85	8.06	8.90	8.40
K2O	0.21	0.21	0.23	0.25	0.25	0.27	0.20	0.25	0.20
Na2O	6.87	6.90	6.20	6.79	7.12	7.94	7.96	6.72	6.63
Al2O3	27.44	27.39	27.38	26.97	26.59	25.25	25.76	27.12	27.77
SiO2	57.46	57.33	56.50	57.11	58.04	55.66	56.38	57.03	57.50
Totals	100.44	100.64	99.23	99.65	99.86	97.19	98.56	100.15	100.59

Sample	55	56	57	58	59	60	61	62	63
FeO	0.09	0.15	0.07	0.12	0.14	0.14	0.00	0.09	0.20
CaO	9.03	8.91	8.88	8.83	9.00	9.07	0.00	8.95	8.80
K2O	0.22	0.20	0.20	0.19	0.22	0.20	0.00	0.18	0.20
Na2O	6.68	6.40	6.73	6.54	6.70	6.48	0.00	7.39	6.76
Al2O3	27.39	27.20	27.61	27.97	27.26	27.57	0.00	26.70	28.25
SiO2	56.78	56.05	56.59	56.34	57.23	56.25	0.00	55.19	57.13
Totals	100.18	98.91	100.08	99.98	100.55	99.72	0.00	98.51	101.34

Sample	64	65	66	67	68	69	70	71	72
FeO	0.13	0.11	0.07	0.17	0.14	0.22	0.12	0.10	0.23
CaO	8.79	8.94	9.22	8.92	8.98	9.13	9.09	9.07	8.92
K2O	0.23	0.24	0.23	0.20	0.19	0.19	0.21	0.24	0.19
Na2O	5.64	6.48	5.92	6.33	6.78	6.73	6.35	6.78	6.80
Al2O3	27.13	27.14	27.66	27.18	27.21	27.36	27.56	27.42	27.61
SiO2	57.07	56.88	55.70	56.24	56.33	56.90	56.11	56.64	56.63
Totals	99.00	99.79	98.80	99.05	99.63	100.53	99.45	100.26	100.38

Sample	73	74	75	76	77	78	79	80	81
FeO	0.19	0.07	0.03	0.11	0.00	0.22	0.09	0.21	0.14
CaO	8.79	8.97	9.04	9.11	0.00	8.42	8.87	8.88	8.90
K2O	0.22	0.20	0.19	0.19	0.00	0.18	0.16	0.17	0.25
Na2O	6.30	6.72	6.39	7.31	0.00	6.00	6.40	6.32	6.63
Al2O3	27.13	27.52	27.62	26.91	0.00	26.77	27.57	27.15	27.51
SiO2	56.64	56.91	56.31	56.10	0.00	55.53	57.51	56.92	56.50
Totals	99.27	100.38	99.59	99.73	0.00	97.11	100.59	99.66	99.93

Sample	82	83	84	85	86	87	88	89	90
FeO	0.13	0.16	0.15	0.15	0.16	0.13	0.15	0.09	0.11
CaO	7.70	7.70	8.46	8.58	8.66	7.75	8.10	8.03	8.15
K2O	0.24	0.26	0.19	0.27	0.21	0.26	0.25	0.20	0.24
Na2O	7.44	7.02	6.90	6.96	6.69	7.35	7.04	7.25	7.01
Al2O3	26.42	26.10	27.15	27.06	27.27	26.56	26.74	26.65	26.90

SiO2	58.77	58.64	57.24	57.07	57.22	58.09	58.00	57.56	57.85
Totals	100.71	99.87	100.08	100.09	100.22	100.13	100.28	99.79	100.27

Sample	91	92	93	94	95	96	97	98	99
FeO	0.17	0.18	0.14	0.13	0.11	0.15	0.12	0.18	0.10
CaO	8.25	8.48	8.68	8.94	9.43	10.15	9.49	7.59	7.73
K2O	0.20	0.21	0.19	0.18	0.19	0.18	0.19	0.23	0.24
Na2O	6.87	7.01	7.20	6.48	6.21	5.88	6.17	7.38	7.37
Al2O3	27.07	27.02	27.24	28.03	28.17	28.35	27.85	26.20	26.34
SiO2	56.91	57.33	56.58	55.85	56.09	55.59	56.04	59.19	58.43
Totals	99.47	100.23	100.03	99.62	100.20	100.29	99.87	100.79	100.21

Sample	100	101	102	103	104	105	106	107	108
FeO	0.15	0.11	0.15	0.13	0.06	0.15	0.19	0.17	0.07
CaO	7.78	7.03	6.91	6.95	6.98	7.15	7.90	8.64	8.69
K2O	0.26	0.26	0.24	0.22	0.23	0.29	0.20	0.20	0.20
Na2O	7.34	7.07	7.70	7.32	7.28	7.69	6.30	6.03	5.26
Al2O3	26.37	25.92	25.97	25.61	25.79	26.24	28.43	27.45	15.61
SiO2	58.48	59.42	58.46	55.00	58.76	59.15	61.40	56.99	29.90
Totals	100.38	99.81	99.43	95.23	99.10	100.68	104.42	99.48	59.73

Sample	109	110	111	112	113	114	115	116	117
FeO	0.07	0.18	0.17	0.16	0.17	0.21	0.05	0.14	0.07
CaO	8.60	8.24	8.60	9.31	8.99	8.48	8.28	7.79	7.92
K2O	0.19	0.24	0.30	0.18	0.18	0.22	0.20	0.21	0.25
Na2O	6.56	7.17	7.04	6.44	6.57	6.87	6.82	7.20	7.14
Al2O3	27.07	26.91	26.89	27.56	27.53	26.50	26.84	26.90	26.86
SiO2	56.01	57.26	57.14	56.23	56.61	57.64	56.77	58.07	58.73
Totals	98.51	100.01	100.14	99.87	100.07	99.92	98.94	100.31	100.96

Sample	118	119	120	121	122	123	124	125	126
FeO	0.05	0.23	0.08	0.05	0.13	0.07	0.16	0.16	0.19
CaO	7.96	8.70	9.37	9.94	9.89	9.05	8.28	8.12	8.01
K2O	0.25	0.19	0.21	0.16	0.18	0.18	0.21	0.26	0.24
Na2O	7.41	6.54	5.93	5.99	5.79	6.45	6.77	7.08	7.21
Al2O3	26.40	27.40	28.15	28.35	28.82	27.58	26.90	26.70	26.65
SiO2	58.53	56.98	55.23	54.76	55.12	56.30	56.80	57.37	58.47
Totals	100.60	100.04	98.97	99.25	99.94	99.63	99.13	99.68	100.77

CA-5-20-06-1A Plag-2 Rim to Core (El Hato)

Sample	1	2	3	4	5	6	7

FeO	0.11	0.21	0.35	0.09	0.20	0.19	0.22
CaO	6.90	7.26	8.27	4.61	8.99	10.20	7.94
K2O	0.28	0.26	0.25	0.22	0.21	0.14	0.24
Na2O	7.65	7.67	6.99	4.07	6.33	6.07	6.74
Al2O3	25.68	25.68	26.28	16.14	27.51	27.34	26.97
SiO2	59.58	59.02	57.36	36.91	56.12	53.67	57.65
Totals	100.19	100.09	99.49	62.02	99.36	97.61	99.76

Sample	10	11	12	13	14	15	16
FeO	0.19	0.17	0.19	0.16	0.28	0.11	0.09
CaO	8.12	8.13	8.46	7.33	7.12	6.60	6.48
K2O	0.24	0.24	0.25	0.26	0.24	0.35	0.30
Na2O	6.63	7.00	6.64	7.60	7.45	8.16	7.60
Al2O3	26.93	26.74	26.55	26.36	25.88	25.09	25.14
SiO2	57.64	57.37	57.67	58.84	59.04	60.32	59.36
Totals	99.75	99.66	99.76	100.55	100.01	100.63	98.97

Sample	19	20	21	22	23	24	25
FeO	0.13	0.01	0.15	0.13	0.17	0.04	0.23
CaO	7.29	8.36	7.64	8.04	8.58	8.37	7.58
K2O	0.26	0.27	0.27	0.23	0.22	0.30	0.26
Na2O	7.73	7.10	7.38	7.24	6.81	6.94	7.11
Al2O3	25.96	26.92	25.76	26.98	27.35	27.06	26.67
SiO2	58.22	57.68	58.30	58.13	57.63	57.67	58.01
Totals	99.59	100.33	99.51	100.75	100.76	100.38	99.86

Sample	28	29	30	31	32	33	34
FeO	0.15	0.24	0.11	0.15	0.16	0.14	0.13
CaO	7.61	7.79	7.59	7.20	7.55	7.57	7.48
K2O	0.26	0.24	0.29	0.27	0.26	0.29	0.25
Na2O	7.56	7.63	7.38	7.53	7.25	7.35	7.50
Al2O3	26.25	26.69	26.36	25.90	26.06	25.76	25.74
SiO2	58.29	58.42	58.91	58.82	58.80	57.71	58.90
Totals	100.13	101.01	100.63	99.88	100.06	98.83	99.99

Sample	37	38	39	40	41	42	43
FeO	0.15	0.12	0.28	0.14	0.03	0.19	0.07
CaO	7.98	7.51	7.41	7.70	7.84	8.71	7.04
K2O	0.23	0.27	0.27	0.30	0.22	0.21	0.28
Na2O	6.87	7.53	7.58	7.30	7.21	6.61	7.57
Al2O3	26.00	26.06	25.93	26.38	25.78	26.94	25.90
SiO2	58.20	58.51	58.71	58.81	56.54	57.77	59.27
Totals	99.45	100.00	100.17	100.63	97.61	100.43	100.13

Sample	46	47	48	49	50	51	52
FeO	0.13	0.17	0.02	0.11	0.17	0.15	0.19
CaO	7.83	7.62	7.47	7.51	7.65	7.04	7.35

K2O	0.25	0.24	0.29	0.26	0.19	0.20	0.30
Na2O	7.03	7.13	7.54	7.38	7.43	7.90	7.38
Al2O3	26.78	26.25	26.43	25.76	26.41	26.48	26.64
SiO2	58.01	58.30	58.92	58.51	58.51	59.26	60.20
Totals	100.03	99.70	100.68	99.54	100.36	101.03	102.05

Sample	55	56	57	58	59	60	61
FeO	0.20	0.10	0.07	0.15	0.14	0.11	0.15
CaO	7.30	7.22	7.57	7.46	7.64	7.55	7.14
K2O	0.26	0.26	0.20	0.26	0.24	0.24	0.28
Na2O	7.10	7.50	7.68	7.35	7.34	7.19	7.57
Al2O3	26.41	26.34	26.41	25.09	26.59	26.50	25.79
SiO2	60.08	58.36	59.18	56.81	59.35	58.06	59.54
Totals	101.34	99.78	101.10	97.13	101.30	99.65	100.47

Sample	64	65	66	67	68	69	70
FeO	0.18	0.08	0.05	0.17	0.08	0.16	0.16
CaO	7.34	7.10	7.11	7.27	7.46	7.35	7.57
K2O	0.28	0.26	0.26	0.27	0.23	0.25	0.27
Na2O	7.45	7.73	7.05	7.79	7.30	7.75	7.41
Al2O3	25.79	26.22	26.35	26.30	25.84	25.96	25.97
SiO2	58.57	59.88	59.37	58.82	58.37	58.98	58.99
Totals	99.62	101.28	100.19	100.60	99.27	100.46	100.36

Sample	73	74	75	76	77	78	79
FeO	0.18	0.23	0.16	0.08	0.17	0.18	0.17
CaO	7.49	7.31	7.54	7.13	7.37	7.25	7.25
K2O	0.24	0.25	0.25	0.24	0.26	0.21	0.26
Na2O	7.79	7.77	7.25	7.36	7.63	7.47	7.58
Al2O3	26.37	26.07	25.91	25.50	26.07	26.03	25.95
SiO2	58.44	58.07	58.77	58.95	58.99	58.72	58.49
Totals	100.50	99.69	99.88	99.27	100.50	99.86	99.71

Sample	82	83	84	85	86	87	88
FeO	0.17	0.13	0.13	0.01	0.16	0.23	0.15
CaO	7.37	7.28	7.13	7.24	7.22	7.71	7.37
K2O	0.21	0.27	0.25	0.18	0.22	0.19	0.24
Na2O	7.41	7.48	7.46	7.55	7.87	7.70	7.13
Al2O3	25.77	25.48	25.99	25.76	25.85	26.06	26.54
SiO2	58.39	59.27	58.58	59.24	58.58	57.77	59.34
Totals	99.31	99.90	99.53	99.98	99.90	99.66	100.78

Sample	91	92	93	94	95	96	97
FeO	0.06	0.06	0.22	0.11	0.19	0.19	0.10
CaO	7.53	7.50	7.89	7.30	7.44	7.89	7.73
K2O	0.27	0.23	0.24	0.25	0.24	0.23	0.23
Na2O	7.01	7.32	6.92	7.54	7.33	7.38	7.35
Al2O3	26.23	25.92	26.30	26.11	26.04	26.63	26.33
SiO2	58.65	58.40	57.64	58.74	58.52	57.99	58.56
Totals	99.75	99.43	99.21	100.05	99.76	100.32	100.29

Sample	100	101	102	103	104	105	106
FeO	0.15	0.11	0.10	0.14	0.10	0.19	0.07
CaO	8.09	8.39	8.53	8.72	8.45	8.30	8.75
K2O	0.22	0.21	0.18	0.20	0.16	0.19	0.17
Na2O	7.35	7.00	6.90	6.81	7.26	6.26	6.23
Al2O3	26.71	26.74	27.02	26.75	26.69	26.35	26.95
SiO2	58.21	57.51	57.01	57.35	57.19	55.68	56.14
Totals	100.73	99.96	99.74	99.97	99.84	96.97	98.32

Sample	109	110	111	112	113	114	115
FeO	0.14	0.07	0.14	0.20	0.14	0.09	0.17
CaO	8.67	9.53	8.95	8.89	8.63	8.35	9.04
K2O	0.13	0.16	0.14	0.19	0.18	0.26	0.20
Na2O	6.62	6.38	6.93	6.55	6.64	7.03	6.67
Al2O3	27.75	28.15	27.70	27.42	27.46	26.83	27.23
SiO2	56.75	55.86	57.20	56.69	57.57	56.92	56.76
Totals	100.06	100.15	101.06	99.94	100.61	99.49	100.07

Sample	118	119	120	121	122	123	124
FeO	0.02	0.11	0.22	0.20	0.19	0.18	0.11
CaO	8.51	7.24	7.42	7.65	7.61	7.58	7.79
K2O	0.22	0.22	0.23	0.21	0.25	0.22	0.19
Na2O	6.88	7.53	6.99	7.25	7.43	7.20	6.83
Al2O3	26.64	25.86	25.99	26.23	26.22	26.07	26.27
SiO2	57.00	59.05	58.70	58.29	58.45	57.99	57.96
Totals	99.27	100.01	99.54	99.84	100.16	99.25	99.14

Sample	127	128	129	130	131	132	133
FeO	0.17	0.14	0.19	0.10	0.05	0.12	0.02
CaO	7.89	7.88	8.00	7.88	8.15	8.08	1.11
K2O	0.21	0.16	0.21	0.19	0.17	0.26	0.02
Na2O	7.13	7.06	7.11	7.18	7.14	6.99	0.22
Al2O3	26.56	26.73	26.63	26.42	26.43	26.52	3.68
SiO2	57.82	57.87	57.59	58.30	58.02	57.49	8.26
Totals	99.79	99.84	99.75	100.07	99.96	99.45	13.30

Sample	136	137	138	139	140	141	142
FeO	0.11	0.13	0.16	0.19	0.23	0.12	0.23
CaO	8.54	8.40	8.36	8.23	8.45	8.39	8.25
K2O	0.23	0.14	0.21	0.21	0.22	0.23	0.25
Na2O	6.51	7.11	7.06	6.83	7.15	6.81	7.16
Al2O3	27.56	26.89	27.32	27.27	26.69	27.17	26.81
SiO2	56.85	56.98	56.77	57.45	57.37	57.50	56.98
Totals	99.81	99.67	99.89	100.18	100.10	100.21	99.67

Sample	145	146	147	148	149	150	151
FeO	0.18	0.17	0.15	0.12	0.17	0.17	0.14
CaO	8.37	8.49	8.09	7.79	7.51	7.59	7.55

K2O	0.21	0.21	0.22	0.18	0.21	0.24	0.16
Na2O	6.13	6.67	6.96	7.38	7.31	7.51	7.56
Al2O3	26.47	27.26	26.53	26.54	26.29	26.36	26.09
SiO2	56.07	56.91	57.69	57.75	58.31	58.80	59.11
Totals	97.42	99.70	99.64	99.76	99.81	100.68	100.61

Sample	154	155	156	157	158	159	160
FeO	0.17	0.10	0.11	0.16	0.12	0.04	0.10
CaO	7.44	7.58	7.46	7.22	7.43	7.27	7.42
K2O	0.23	0.23	0.23	0.17	0.22	0.20	0.25
Na2O	7.33	7.17	7.11	7.66	7.54	7.58	7.28
Al2O3	25.76	25.56	26.59	26.42	26.12	26.52	26.30
SiO2	58.25	58.56	58.27	57.90	57.96	58.41	58.37
Totals	99.17	99.20	99.79	99.52	99.40	100.03	99.72

Sample	163	164	165	166	167	168	169
FeO	0.14	0.19	0.25	0.24	0.12	0.16	0.10
CaO	6.91	6.97	7.08	6.92	7.25	7.32	6.99
K2O	0.18	0.22	0.20	0.22	0.26	0.27	0.25
Na2O	7.82	7.65	7.69	7.78	7.55	7.52	7.59
Al2O3	25.85	25.91	25.40	25.93	26.02	26.15	26.03
SiO2	59.43	59.21	59.00	59.16	58.96	58.83	58.68
Totals	100.32	100.15	99.62	100.25	100.15	100.25	99.64

Sample	172	173	174	175	176	177	178
FeO	0.18	0.20	0.21	0.18	0.14	0.21	0.12
CaO	7.16	7.07	7.24	7.37	7.49	7.56	7.35
K2O	0.23	0.26	0.20	0.25	0.28	0.19	0.27
Na2O	7.27	7.67	7.44	7.46	7.40	7.35	7.27
Al2O3	26.63	26.47	25.72	25.59	26.42	26.00	25.75
SiO2	60.96	58.93	58.28	58.35	58.39	57.53	58.23
Totals	102.43	100.59	99.09	99.20	100.11	98.82	99.00

Sample	181	182	183	184	185	186	187
FeO	0.10	0.16	0.13	0.16	0.01	0.13	0.18
CaO	7.49	7.40	7.59	6.90	7.40	7.36	7.64
K2O	0.25	0.20	0.22	0.20	0.27	0.22	0.23
Na2O	7.38	7.57	7.80	5.03	7.50	7.43	7.31
Al2O3	26.60	25.98	25.59	27.25	26.33	26.90	26.08
SiO2	58.24	58.86	58.25	61.35	59.00	58.91	58.94
Totals	100.06	100.17	99.58	100.89	100.51	100.95	100.39

Sample	190	191	192	193	194	195	196
FeO	0.19	0.20	0.08	0.09	0.11	0.19	0.08
CaO	7.12	7.01	7.64	7.71	7.81	7.85	8.00
K2O	0.26	0.22	0.25	0.24	0.23	0.23	0.14
Na2O	7.60	7.22	7.60	7.32	7.03	7.35	7.11
Al2O3	25.93	25.90	26.52	26.31	26.66	26.97	26.62
SiO2	58.82	59.23	58.38	58.49	58.58	59.09	58.30
Totals	99.93	99.78	100.48	100.15	100.42	101.69	100.26

Sample	199	200	201	202	203	204	205
FeO	0.21	0.24	0.11	0.17	0.11	0.13	0.14
CaO	7.94	7.81	7.76	7.99	8.14	8.26	8.14
K2O	0.18	0.26	0.23	0.25	0.16	0.19	0.19
Na2O	7.21	7.24	7.39	7.24	7.21	7.56	6.82
Al2O3	26.43	26.31	26.40	26.65	25.83	24.32	27.46
SiO2	57.54	57.65	57.80	57.39	55.63	51.71	59.36
Totals	99.52	99.51	99.70	99.69	97.09	92.17	102.11

Sample	208	209	210	211	212	213	214
FeO	0.14	0.20	0.11	0.08	0.12	0.19	0.33
CaO	8.03	8.22	7.85	7.83	8.06	8.10	8.03
K2O	0.20	0.18	0.24	0.18	0.21	0.22	0.23
Na2O	7.05	6.94	7.54	7.05	7.43	7.34	7.01
Al2O3	26.57	26.84	26.27	26.52	26.80	26.61	26.69
SiO2	57.05	57.70	57.88	58.01	57.32	57.83	57.60
Totals	99.03	100.08	99.88	99.68	99.95	100.29	99.88

Sample	217	218	219	220	221	222	223
FeO	0.10	0.10	0.21	0.18	0.09	0.25	0.10
CaO	8.59	8.82	8.71	8.36	7.87	8.38	8.22
K2O	0.18	0.20	0.11	0.20	0.24	0.19	0.13
Na2O	6.50	6.76	7.00	6.75	6.83	7.18	7.00
Al2O3	26.97	27.03	27.09	27.16	26.40	26.72	26.67
SiO2	56.88	57.21	56.88	57.43	57.79	56.57	56.93
Totals	99.21	100.12	100.00	100.08	99.22	99.30	99.05

Sample	226	227	228	229	230	231	232
FeO	0.14	0.10	0.16	0.14	0.18	0.12	0.10
CaO	7.02	7.24	7.04	6.98	7.06	7.10	7.30
K2O	0.23	0.26	0.25	0.27	0.26	0.25	0.26
Na2O	7.48	7.69	7.49	7.04	7.60	6.65	7.87
Al2O3	25.79	25.66	25.88	25.87	25.87	26.40	25.64
SiO2	58.42	58.37	58.80	59.02	59.27	60.79	59.20
Totals	99.09	99.32	99.64	99.30	100.26	101.31	100.37

Sample	235	236	237	238	239	240	241
FeO	0.15	0.10	0.19	0.18	0.15	0.19	0.20
CaO	7.12	7.22	7.29	7.16	7.30	7.38	7.53
K2O	0.23	0.22	0.23	0.24	0.24	0.21	0.22
Na2O	7.32	7.60	7.19	7.70	7.25	7.27	7.82
Al2O3	25.93	25.81	25.57	25.97	26.13	26.06	25.87
SiO2	58.63	58.55	59.35	58.38	59.30	58.78	58.69
Totals	99.38	99.51	99.82	99.64	100.37	99.89	100.33

Sample	244	245	246	247	248	249	250
FeO	0.20	0.09	0.13	0.10	0.18	0.16	0.16
CaO	7.01	6.73	6.70	6.85	7.19	7.27	7.72

K2O	0.28	0.23	0.24	0.19	0.23	0.26	0.19
Na2O	7.68	7.41	7.61	7.86	7.53	7.49	6.99
Al2O3	25.89	25.55	25.23	25.35	25.98	26.09	26.08
SiO2	59.97	59.46	60.33	59.41	59.29	59.23	58.27
Totals	101.04	99.48	100.25	99.75	100.40	100.51	99.42

Sample	253	254	255	256	257	258	259
FeO	0.12	0.17	0.15	0.15	0.14	0.17	0.09
CaO	7.78	7.38	6.74	7.28	7.42	7.50	7.26
K2O	0.27	0.19	0.26	0.19	0.25	0.22	0.22
Na2O	7.59	7.52	7.38	7.63	7.58	7.37	7.20
Al2O3	26.39	25.98	25.52	25.75	26.11	26.09	25.93
SiO2	58.17	59.16	59.87	58.61	58.25	58.24	58.07
Totals	100.32	100.40	99.92	99.62	99.74	99.59	98.76

Sample	262	263	264	265	266	267	268
FeO	0.13	0.15	0.04	0.05	0.25	0.09	0.21
CaO	7.94	7.28	7.64	8.20	8.16	7.95	8.22
K2O	0.25	0.22	0.19	0.19	0.22	0.18	0.27
Na2O	7.26	7.31	7.54	7.22	7.17	6.71	6.85
Al2O3	26.90	25.87	26.14	26.58	26.75	26.35	26.43
SiO2	58.16	58.58	57.93	57.85	57.39	57.45	57.20
Totals	100.63	99.40	99.48	100.08	99.93	98.74	99.19

Sample	271	272	273	274	275	276	277
FeO	0.11	0.18	0.08	0.19	0.16	0.18	0.05
CaO	8.05	8.01	8.39	8.37	8.05	8.16	8.12
K2O	0.22	0.19	0.18	0.20	0.16	0.20	0.25
Na2O	7.15	6.70	6.72	6.81	7.14	6.99	7.19
Al2O3	26.70	27.21	26.54	27.02	26.82	26.45	27.03
SiO2	57.86	57.88	56.27	56.88	57.47	57.85	57.86
Totals	100.09	100.18	98.18	99.48	99.80	99.84	100.50

Sample	280	281	282	283	284	285	286
FeO	0.12	0.13	0.17	0.19	0.13	0.21	0.10
CaO	8.54	8.20	8.20	7.91	8.17	7.62	7.55
K2O	0.18	0.21	0.22	0.23	0.21	0.20	0.27
Na2O	7.12	6.94	7.03	7.10	7.45	7.61	7.54
Al2O3	26.72	27.17	26.80	26.73	26.71	26.18	26.08
SiO2	57.53	57.69	57.75	57.67	58.38	58.44	59.06
Totals	100.22	100.34	100.18	99.83	101.05	100.25	100.60

Sample	289	290	291	292	293	294	295
FeO	0.15	0.23	0.13	0.16	0.16	0.12	0.14
CaO	7.81	8.20	8.11	8.17	8.12	8.36	8.08
K2O	0.23	0.25	0.19	0.19	0.23	0.20	0.23
Na2O	6.94	6.92	7.11	6.93	6.76	6.79	7.06
Al2O3	26.64	26.45	26.90	26.66	27.00	26.73	26.93
SiO2	58.24	58.03	57.55	57.76	57.48	56.75	56.10
Totals	100.02	100.08	99.98	99.87	99.75	98.95	98.54

Sample	298	299	300	301	302	303	304
FeO	0.13	0.04	0.11	0.13	0.18	0.15	0.16
CaO	8.73	8.33	8.38	8.17	8.07	8.22	8.14
K2O	0.21	0.21	0.22	0.20	0.23	0.18	0.23
Na2O	7.10	6.96	6.89	7.00	6.92	6.98	6.83
Al2O3	27.34	26.75	26.79	26.49	26.94	26.78	26.90
SiO2	57.32	56.91	57.21	57.86	57.62	57.75	57.45
Totals	100.83	99.20	99.60	99.85	99.97	100.06	99.72

CA-5-20-06-1A Plag-1 Rim to Core (El Hato)

Sample	1	2	3	4	5	6	7
FeO	0.19	0.12	0.27	0.13	0.08	0.15	0.15
CaO	8.09	8.12	6.76	6.86	7.01	7.02	7.51
K2O	0.22	0.25	0.27	0.28	0.27	0.26	0.27
Na2O	7.27	6.82	7.79	7.64	7.79	7.71	7.35
Al2O3	26.98	26.30	25.36	25.44	25.59	25.92	25.93
SiO2	57.40	57.88	59.09	59.02	59.88	59.69	58.81
Totals	100.14	99.48	99.55	99.37	100.62	100.75	100.02

Sample	8	9	10	11	12	13	14
FeO	0.22	0.10	0.23	0.18	0.12	0.16	0.11
CaO	7.61	7.46	7.67	7.75	7.93	8.01	8.12
K2O	0.29	0.26	0.24	0.17	0.22	0.24	0.19
Na2O	7.33	7.25	6.88	7.08	6.96	7.17	7.14
Al2O3	25.98	26.03	26.81	26.23	26.13	26.40	27.03
SiO2	58.72	58.14	59.87	57.78	58.01	57.67	58.14
Totals	100.16	99.24	101.70	99.18	99.38	99.65	100.75

Sample	15	16	17	18	19	20	21
FeO	0.12	0.04	0.09	0.15	0.20	0.22	0.18
CaO	8.32	8.45	8.37	8.75	8.48	8.61	8.65
K2O	0.20	0.22	0.20	0.17	0.20	0.19	0.22
Na2O	6.75	6.97	6.80	6.63	6.69	6.87	6.45
Al2O3	26.76	26.97	26.85	27.16	26.92	27.60	27.45
SiO2	57.80	56.89	57.25	57.17	57.05	57.39	56.43
Totals	99.96	99.54	99.55	100.03	99.55	100.87	99.37

Sample	22	23	24	25	26	27	28
FeO	0.14	0.16	0.24	0.22	0.09	0.08	0.22
CaO	9.42	8.95	8.91	7.68	7.82	7.76	7.96
K2O	0.15	0.21	0.24	0.22	0.21	0.27	0.25
Na2O	6.06	7.34	6.66	7.12	7.44	7.47	7.22
Al2O3	28.07	26.38	27.40	25.01	26.08	26.41	26.27
SiO2	56.70	54.76	56.91	55.72	58.18	57.44	58.27
Totals	100.54	97.80	100.37	95.98	99.82	99.44	100.20

Sample	29	30	31	32	33	34	35
FeO	0.22	0.16	0.05	0.26	0.22	0.18	0.19
CaO	8.06	7.58	8.11	8.16	8.30	7.41	7.77
K2O	0.23	0.25	0.20	0.19	0.16	0.27	0.26
Na2O	6.98	7.30	7.17	7.07	6.95	7.04	7.16
Al2O3	26.89	26.23	26.43	26.90	27.12	26.04	26.35
SiO2	57.74	58.42	58.46	58.65	57.74	58.42	58.20
Totals	100.12	99.94	100.42	101.24	100.49	99.37	99.95

Sample	36	37	38	39	40	41	42
FeO	0.15	0.08	0.15	0.13	0.10	0.13	0.18
CaO	8.06	7.53	7.64	7.62	7.65	7.84	8.06
K2O	0.27	0.26	0.26	0.26	0.27	0.18	0.19
Na2O	7.41	7.09	7.04	6.89	7.21	7.22	6.78
Al2O3	26.69	26.22	26.78	27.05	25.96	26.63	25.96
SiO2	59.51	59.04	59.00	59.80	58.39	58.74	55.48
Totals	102.08	100.22	100.88	101.75	99.58	100.74	96.65

Sample	43	44	45	46	47	48	49
FeO	0.11	0.11	0.14	0.06	0.16	0.20	0.15
CaO	7.79	7.54	7.40	7.43	7.65	7.53	7.51
K2O	0.23	0.22	0.17	0.21	0.27	0.28	0.26
Na2O	7.26	7.17	7.57	7.42	7.35	7.27	7.32
Al2O3	26.47	25.90	25.78	26.10	26.03	25.82	26.24
SiO2	57.94	58.59	59.21	58.60	58.57	58.92	59.57
Totals	99.81	99.53	100.27	99.82	100.04	100.03	101.05

Sample	50	51	52	53	54	55	56
FeO	0.17	0.03	0.20	0.08	0.15	0.07	0.19
CaO	7.50	7.85	8.31	7.95	7.56	7.74	7.30
K2O	0.26	0.24	0.16	0.25	0.22	0.21	0.23
Na2O	6.85	7.57	6.91	6.81	7.26	7.41	7.32
Al2O3	26.60	25.92	26.24	26.30	26.26	26.70	26.39
SiO2	58.85	57.22	57.78	58.03	58.26	58.29	58.33
Totals	100.24	98.82	99.59	99.41	99.71	100.42	99.76

Sample	57	58	59	60	61	62	63
FeO	0.23	0.20	0.09	0.11	0.14	0.18	0.18
CaO	7.56	7.61	7.65	7.89	7.83	8.27	8.38
K2O	0.19	0.19	0.21	0.17	0.21	0.22	0.22
Na2O	7.29	7.14	7.19	7.46	7.22	6.93	7.18
Al2O3	26.44	26.14	25.97	26.31	26.29	26.11	26.99
SiO2	59.13	59.04	58.23	58.51	57.85	57.60	57.10
Totals	100.84	100.33	99.34	100.45	99.55	99.30	100.03

Sample	64	65	66	67	68	69	70
FeO	0.09	0.14	0.16	0.15	0.12	0.11	0.11
CaO	8.27	8.36	8.59	8.62	8.13	8.03	8.20
K2O	0.22	0.20	0.20	0.21	0.18	0.22	0.18
Na2O	6.63	7.11	6.74	7.10	7.18	6.81	6.75
Al2O3	26.93	27.46	27.62	26.72	26.96	26.79	26.85
SiO2	57.22	58.31	57.62	57.20	57.64	58.14	57.73
Totals	99.36	101.58	100.94	100.01	100.20	100.10	99.82

Sample	71	72	73	74	75	76	77
FeO	0.25	0.19	0.16	0.16	0.06	0.18	0.23
CaO	8.62	8.62	8.78	8.72	8.76	8.68	9.04
K2O	0.21	0.23	0.16	0.18	0.25	0.20	0.23
Na2O	6.61	6.71	6.41	6.69	6.67	5.81	6.40
Al2O3	27.51	27.46	27.30	27.94	27.40	26.24	27.48
SiO2	57.48	57.61	56.99	57.59	57.11	54.25	56.70
Totals	100.69	100.81	99.81	101.27	100.25	95.37	100.07

Sample	78	79	80	81	82	83	84
FeO	0.20	0.16	0.07	0.17	0.18	0.03	0.17
CaO	8.97	8.72	8.74	8.84	9.18	9.34	9.53
K2O	0.18	0.24	0.18	0.16	0.21	0.15	0.18
Na2O	6.96	6.71	6.61	6.64	6.49	6.40	6.80
Al2O3	27.26	27.02	27.61	27.86	27.45	27.89	27.76
SiO2	56.34	57.14	57.08	56.88	56.65	55.87	56.30
Totals	99.91	99.99	100.29	100.56	100.15	99.68	100.74

Sample	85	86	87	88	89	90	91
FeO	0.15	0.21	0.15	0.17	0.07	0.20	0.19
CaO	9.73	10.28	10.03	9.58	9.56	8.11	7.61
K2O	0.16	0.15	0.13	0.14	0.17	0.23	0.25
Na2O	5.57	5.76	5.95	6.15	6.29	7.32	7.21
Al2O3	28.17	28.58	28.86	28.62	28.01	27.05	27.00
SiO2	55.58	54.67	55.55	55.35	55.84	58.48	58.61
Totals	99.35	99.65	100.68	99.99	99.95	101.39	100.87

Sample	92	93	94	95	96	97
FeO	0.11	0.21	0.10	0.14	0.08	0.18
CaO	7.46	7.67	7.37	7.38	7.30	7.29
K2O	0.25	0.25	0.19	0.19	0.22	0.21
Na2O	7.35	7.13	7.85	7.48	7.42	7.51
Al2O3	26.11	26.37	26.04	26.16	25.96	26.06
SiO2	59.14	58.65	58.88	58.90	58.81	58.55
Totals	100.43	100.28	100.44	100.26	99.79	99.80

RH-6-2-06-1A Rim to Core (El Hato)

Sample	1	2	3	4	5	6	7
FeO	0.19	0.32	0.14	0.22	0.29	0.23	0.13
CaO	7.26	8.30	8.30	8.16	7.23	8.30	8.44
K2O	0.18	0.18	0.20	0.22	0.21	0.19	0.21
Na2O	6.69	6.76	6.47	6.93	7.31	6.60	6.89
Al2O3	26.81	27.37	27.15	26.92	25.83	26.70	26.66
SiO2	59.65	57.54	58.24	58.60	58.38	57.57	58.20
Totals	100.78	100.47	100.50	101.03	99.25	99.59	100.53

Sample	8	9	10	11	12	13	14
FeO	0.12	0.18	0.15	0.24	0.25	0.13	0.11
CaO	7.28	7.60	7.49	7.66	7.71	7.47	7.79
K2O	0.21	0.19	0.22	0.23	0.21	0.25	0.19
Na2O	7.29	7.45	7.65	7.29	7.08	7.27	7.12
Al2O3	26.09	26.54	26.24	25.87	26.43	26.11	26.36
SiO2	58.79	58.81	58.68	58.52	57.68	58.07	58.09
Totals	99.79	100.76	100.43	99.80	99.37	99.30	99.65

Sample	15	16	17	18	19	20	21
FeO	0.19	0.10	0.12	0.13	0.07	0.26	0.25
CaO	7.24	7.99	8.13	7.72	7.95	7.85	8.06
K2O	0.26	0.18	0.23	0.21	0.19	0.18	0.21
Na2O	7.50	7.11	7.10	7.41	7.20	7.39	7.11
Al2O3	25.95	26.40	26.56	26.42	26.91	26.40	26.78
SiO2	58.71	57.80	58.06	57.96	57.95	58.01	57.97
Totals	99.85	99.58	100.20	99.85	100.27	100.09	100.39

Sample	22	23	24	25	26	27	28
FeO	0.18	0.21	0.12	0.09	0.21	0.27	0.19
CaO	9.02	7.67	8.66	8.69	8.03	8.28	8.63
K2O	0.20	0.27	0.20	0.19	0.22	0.18	0.20
Na2O	6.50	6.84	6.50	6.50	6.92	6.74	6.74
Al2O3	27.55	26.60	27.24	27.43	26.81	26.81	27.25
SiO2	56.34	58.06	56.89	56.69	57.31	57.24	57.34
Totals	99.80	99.64	99.62	99.58	99.49	99.53	100.35

Sample	29	30	31	32	33	34	35
FeO	0.07	0.10	0.16	0.24	0.19	0.06	0.18
CaO	8.69	8.74	7.84	7.23	7.18	7.52	7.62
K2O	0.19	0.18	0.17	0.26	0.25	0.21	0.24
Na2O	6.88	6.90	7.18	7.38	7.51	7.35	7.21
Al2O3	27.55	27.34	26.40	25.62	26.16	25.90	26.31
SiO2	57.25	56.61	57.77	58.46	58.77	58.64	58.37
Totals	100.64	99.87	99.53	99.20	100.05	99.67	99.93

Sample	36.00	37	38	39	40	41	42
FeO	0.13	0.24	0.11	0.17	0.12	0.10	0.17
CaO	8.08	7.98	7.46	7.78	7.94	8.52	8.60
K2O	0.19	0.23	0.21	0.23	0.15	0.20	0.17
Na2O	6.95	7.04	7.71	7.32	6.95	7.07	6.59
Al2O3	26.50	26.24	26.55	26.50	26.39	27.10	26.90
SiO2	57.65	57.91	58.85	58.32	57.90	57.53	56.85
Totals	99.50	99.63	100.89	100.32	99.47	100.52	99.28

Sample	43	44	45	46	47	48	49
FeO	0.13	0.07	0.12	0.16	0.12	0.25	0.12
CaO	8.37	8.07	8.95	8.71	9.00	6.74	7.89
K2O	0.19	0.19	0.10	0.18	0.19	0.23	0.23
Na2O	7.15	7.34	6.79	6.84	6.61	7.63	7.12
Al2O3	26.49	26.77	27.52	27.40	27.73	25.67	26.62
SiO2	57.07	57.58	56.47	56.77	56.02	59.57	57.71
Totals	99.39	100.01	99.95	100.06	99.67	100.09	99.69

Sample	50	51	52	53	54	55	56
FeO	0.08	0.12	0.14	0.04	0.17	0.17	0.18
CaO	8.02	8.46	8.70	9.05	8.92	9.32	9.26
K2O	0.28	0.23	0.17	0.18	0.17	0.16	0.19
Na2O	7.23	6.78	6.85	6.82	6.52	6.76	6.14
Al2O3	26.67	26.75	27.45	27.63	27.81	27.72	27.44
SiO2	57.86	56.93	57.31	56.51	56.03	56.43	55.88
Totals	100.15	99.27	100.62	100.23	99.61	100.56	99.10

Sample	57	58	59	60	61	62	63
FeO	0.22	0.09	0.08	0.15	0.18	0.02	0.05
CaO	8.54	8.48	8.72	8.71	9.14	9.26	9.60
K2O	0.21	0.16	0.17	0.20	0.15	0.20	0.16
Na2O	6.56	6.56	6.82	6.56	6.45	6.44	6.40
Al2O3	26.97	26.81	27.10	27.53	27.85	27.81	28.21
SiO2	57.35	57.09	56.77	57.24	55.97	56.43	56.19
Totals	99.86	99.19	99.66	100.37	99.74	100.16	100.61

Sample	64	65	66	67	68	69	70
FeO	0.20	0.19	0.05	0.17	0.08	0.13	0.18

CaO	9.51	9.70	9.05	9.04	8.14	8.15	8.00
K2O	0.20	0.18	0.17	0.16	0.20	0.20	0.20
Na2O	6.25	6.18	6.80	6.55	7.01	7.15	6.84
Al2O3	27.96	28.19	27.21	27.76	26.36	26.51	27.09
SiO2	56.09	55.64	56.97	56.66	57.00	58.38	56.97
Totals	100.21	100.07	100.26	100.34	98.80	100.51	99.29

Sample	71	72	73	74	75	76	77
FeO	0.10	0.09	0.07	0.07	0.18	0.13	0.12
CaO	8.48	9.73	10.09	11.96	11.82	11.22	8.87
K2O	0.16	0.14	0.11	0.08	0.05	0.12	0.18
Na2O	6.89	6.10	5.73	4.83	5.03	5.18	6.41
Al2O3	26.91	27.94	28.96	30.08	29.57	29.39	27.43
SiO2	57.37	54.99	54.63	52.84	53.46	53.76	56.48
Totals	99.92	98.99	99.60	99.86	100.12	99.79	99.49

Sample	78	79	80	81	82	83	84
FeO	0.12	0.08	0.16	0.08	0.11	0.10	0.21
CaO	8.79	8.88	7.86	8.27	8.08	8.68	9.42
K2O	0.18	0.17	0.20	0.14	0.19	0.16	0.18
Na2O	6.72	6.83	7.33	7.00	6.92	7.05	6.10
Al2O3	27.08	27.21	26.46	26.31	26.75	27.06	28.04
SiO2	56.52	57.11	58.14	57.60	57.34	57.17	55.86
Totals	99.40	100.27	100.16	99.40	99.38	100.22	99.82

Sample	85	86	87
FeO	0.19	0.06	0.07
CaO	10.35	9.87	9.44
K2O	0.12	0.17	0.16
Na2O	5.75	6.13	6.27
Al2O3	28.65	28.06	28.62
SiO2	55.29	55.68	55.91
Totals	100.34	99.98	100.48

SR-6-6-06-1A-Plag-3 Rim to Core (El Hato)

Sample	1	2	3	4	5	6	7
FeO	0.21	0.17	0.22	0.19	0.17	0.15	0.15
CaO	7.96	8.22	7.54	8.23	8.86	9.29	8.14
K2O	0.23	0.26	0.18	0.12	0.16	0.18	0.18
Na2O	7.66	6.95	7.31	7.06	6.55	6.36	4.33
Al2O3	26.72	26.84	26.11	27.10	27.33	27.93	28.07
SiO2	57.53	57.37	58.00	58.01	56.94	56.99	58.16
Totals	100.32	99.81	99.35	100.71	100.02	100.90	99.04

Sample	8	9	10	11	12	13	14
FeO	0.12	0.20	0.29	0.19	0.27	0.12	0.17
CaO	5.87	9.85	9.76	9.74	10.36	7.66	7.44
K2O	0.12	0.13	0.15	0.14	0.07	0.21	0.25
Na2O	5.27	7.03	7.06	6.64	5.76	7.25	7.66
Al2O3	14.85	28.48	26.55	28.19	28.37	26.38	26.09
SiO2	33.58	56.61	52.60	55.57	54.06	58.46	58.43
Totals	59.81	102.30	96.41	100.47	98.89	100.09	100.05

Sample	15	16	17	18	19	20	21
FeO	0.05	0.16	0.14	0.16	0.01	0.18	0.20
CaO	7.68	7.54	7.80	7.65	7.70	7.65	8.03
K2O	0.18	0.20	0.17	0.17	0.22	0.20	0.21
Na2O	7.15	7.39	7.69	7.57	7.33	7.14	7.00
Al2O3	26.56	25.88	25.59	26.11	26.70	26.65	26.68
SiO2	59.27	56.66	56.75	58.26	59.11	58.40	58.15
Totals	100.89	97.84	98.15	99.91	101.06	100.21	100.27

Sample	22	23	24	25	26	27	28
FeO	0.14	0.04	0.18	0.11	0.20	0.07	0.18
CaO	7.71	7.55	7.67	7.79	7.67	7.91	7.63
K2O	0.22	0.17	0.23	0.19	0.21	0.17	0.17
Na2O	6.92	7.59	7.50	7.15	7.33	7.39	7.22
Al2O3	26.65	26.73	26.56	26.65	26.68	26.71	26.73
SiO2	58.02	58.61	58.06	58.74	58.75	57.97	58.24
Totals	99.66	100.69	100.21	100.64	100.85	100.22	100.17

Sample	29	30	31	32	33	34	35
FeO	0.14	0.18	0.20	0.02	0.08	0.14	0.18
CaO	7.85	7.91	7.99	7.99	8.11	8.10	7.93
K2O	0.21	0.23	0.19	0.21	0.23	0.22	0.19
Na2O	7.23	7.22	6.84	7.34	6.99	6.86	7.15
Al2O3	26.78	26.51	26.93	26.99	27.06	27.04	26.73
SiO2	58.23	57.92	57.93	58.05	57.92	57.37	57.92
Totals	100.44	99.98	100.08	100.60	100.38	99.73	100.10

Sample	36	37	38	39	40	41	42
FeO	0.05	0.16	0.16	0.15	0.05	0.11	0.15
CaO	8.13	8.23	8.31	8.06	8.04	8.72	9.44
K2O	0.17	0.18	0.18	0.18	0.22	0.18	0.16
Na2O	6.92	6.76	7.00	6.97	7.05	6.61	6.25
Al2O3	26.92	27.50	27.06	26.34	26.65	27.52	27.94
SiO2	57.70	57.25	57.63	57.99	57.85	56.18	56.59
Totals	99.89	100.08	100.33	99.68	99.87	99.31	100.52

Sample	43	44	45	46	47	48	49
FeO	0.12	0.17	0.11	0.19	0.15	0.13	0.27
CaO	9.20	9.58	9.68	9.64	9.92	7.16	7.80
K2O	0.18	0.17	0.13	0.15	0.15	0.22	0.23
Na2O	6.51	6.27	6.07	5.95	6.17	7.63	7.19
Al2O3	28.03	27.96	28.46	27.75	28.41	26.63	26.38
SiO2	56.14	56.02	55.72	55.40	55.09	58.96	58.01
Totals	100.16	100.16	100.17	99.09	99.91	100.72	99.87

Sample	50	51	52	53	54	55	56
FeO	0.12	0.15	0.10	0.18	0.15	0.05	0.16
CaO	7.72	7.63	7.68	7.83	7.76	8.25	8.34
K2O	0.23	0.24	0.20	0.22	0.23	0.19	0.18
Na2O	7.36	7.31	7.29	7.15	7.23	6.91	6.95
Al2O3	25.97	26.17	26.44	26.33	26.75	26.95	26.78
SiO2	58.85	57.93	58.62	58.22	58.56	57.38	58.06
Totals	100.23	99.43	100.32	99.93	100.68	99.73	100.46

Sample	57	58	59	60	61	62	63
FeO	0.11	0.08	0.13	0.14	0.29	0.23	0.12
CaO	8.89	8.82	9.10	9.90	9.92	9.63	9.94
K2O	0.15	0.16	0.21	0.17	0.15	0.11	0.18
Na2O	6.78	6.63	6.69	6.32	6.08	6.02	6.30
Al2O3	27.56	27.50	28.16	28.58	28.67	28.33	28.35
SiO2	57.22	57.26	56.29	55.32	54.65	56.04	54.75
Totals	100.71	100.45	100.58	100.42	99.76	100.37	99.64

Sample	64	65	66	67	68	69	70
FeO	0.12	0.17	0.18	0.11	0.10	0.15	0.16
CaO	9.50	11.05	11.23	8.94	9.14	9.26	9.40
K2O	0.16	0.16	0.15	0.18	0.19	0.17	0.17
Na2O	6.06	5.47	5.58	6.43	6.62	6.44	6.13
Al2O3	28.02	29.45	29.36	27.77	27.62	27.64	28.40
SiO2	55.02	53.36	53.46	56.95	56.36	56.94	56.09
Totals	98.88	99.67	99.95	100.39	100.01	100.60	100.35

Sample	71	72	73	74	75	76	77
FeO	0.11	0.21	0.13	0.20	0.12	0.20	0.25
CaO	9.62	9.79	8.24	8.82	9.72	10.01	9.10
K2O	0.21	0.18	0.15	0.16	0.15	0.13	0.16
Na2O	5.99	6.05	6.52	6.81	6.32	6.19	3.34
Al2O3	27.92	28.28	25.50	27.34	27.72	28.75	29.39
SiO2	55.88	55.24	52.91	56.16	55.79	55.72	58.82
Totals	99.74	99.74	93.44	99.49	99.82	100.99	101.05

Sample	78	79	80	81	82	83	84
FeO	0.20	0.09	0.16	0.17	0.17	0.21	0.19
CaO	9.54	9.87	9.98	9.44	10.15	8.72	7.99
K2O	0.15	0.11	0.14	0.18	0.18	0.15	0.23
Na2O	6.79	6.24	5.98	6.36	6.01	6.92	7.24
Al2O3	25.04	28.03	28.73	27.63	28.82	27.42	26.84
SiO2	49.47	54.15	54.80	55.61	54.11	57.19	57.88
Totals	91.18	98.49	99.79	99.40	99.43	100.61	100.37

Sample	85	86	87	88	89	90	91
FeO	0.26	0.09	0.18	0.14	0.11	0.13	0.18
CaO	9.03	9.92	8.64	8.29	8.56	8.64	8.95
K2O	0.18	0.19	0.18	0.23	0.18	0.17	0.18
Na2O	7.13	6.25	7.19	6.75	6.76	6.56	6.67
Al2O3	27.28	28.35	27.38	27.35	27.33	27.56	28.57
SiO2	56.61	55.70	56.80	57.47	57.37	56.82	58.35
Totals	100.49	100.51	100.38	100.23	100.31	99.88	102.90

Sample	92	93	94	95	96	97	98
FeO	0.21	0.11	0.21	0.13	0.24	0.15	0.11
CaO	7.86	7.86	7.75	8.29	8.72	9.27	8.83
K2O	0.18	0.21	0.23	0.18	0.18	0.14	0.16
Na2O	7.19	7.42	6.92	7.21	6.65	6.74	6.49
Al2O3	26.13	26.02	26.74	27.09	27.13	27.77	27.66
SiO2	57.15	58.07	57.80	57.58	56.49	56.59	56.57
Totals	98.71	99.70	99.65	100.49	99.41	100.68	99.82

Sample	99	100	101	102	103	104	105
FeO	0.10	0.07	0.11	0.22	0.21	0.08	0.13
CaO	7.98	8.44	7.68	7.89	7.99	7.26	7.47
K2O	0.22	0.20	0.19	0.21	0.22	0.21	0.20
Na2O	7.04	6.97	7.09	7.05	7.05	7.25	7.59
Al2O3	26.92	26.95	26.16	26.74	27.04	25.99	26.48
SiO2	57.60	57.17	58.44	57.58	57.77	58.68	58.67
Totals	99.87	99.80	99.66	99.69	100.27	99.47	100.55

Sample	106	107	108	109	110	111	112
FeO	0.19	0.10	0.21	0.19	0.07	0.08	0.07
CaO	7.66	7.81	7.07	6.79	7.01	7.12	7.41
K2O	0.23	0.29	0.24	0.30	0.24	0.30	0.23
Na2O	7.27	7.46	7.66	7.85	7.58	7.55	7.59
Al2O3	26.60	26.09	25.81	25.82	26.04	26.13	26.16
SiO2	58.29	58.34	58.38	59.43	59.12	58.82	58.88
Totals	100.23	100.08	99.36	100.38	100.06	99.99	100.35

Sample	113	114	115	116	117	118	119
FeO	0.15	0.10	0.04	0.01	0.21	0.08	0.18
CaO	7.25	7.31	7.57	4.48	7.67	7.51	8.01

K2O	0.20	0.20	0.21	0.31	0.21	0.23	0.21
Na2O	7.45	7.21	7.33	4.03	7.24	7.21	6.89
Al2O3	26.06	26.21	26.82	16.10	26.82	26.56	27.06
SiO2	59.34	58.50	58.96	73.90	58.66	58.55	57.77
Totals	100.45	99.53	100.93	98.84	100.81	100.13	100.12

Sample	120	121	122	123	124	125	126
FeO	0.12	0.14	0.20	0.22	0.12	0.13	0.09
CaO	7.76	7.68	7.81	7.95	7.94	7.17	6.54
K2O	0.24	0.22	0.19	0.21	0.19	0.23	0.19
Na2O	7.15	7.61	7.29	6.85	6.96	7.48	7.96
Al2O3	26.28	26.19	26.41	27.00	26.63	25.98	25.33
SiO2	58.26	57.96	58.31	57.89	57.46	58.07	59.32
Totals	99.81	99.81	100.20	100.12	99.29	99.07	99.43

Sample	127	128	129	130	131	132	133
FeO	0.19	0.17	0.23	0.09	0.06	0.14	0.09
CaO	7.06	7.36	7.49	5.19	6.00	6.20	6.61
K2O	0.27	0.25	0.23	0.10	0.29	0.27	0.26
Na2O	7.58	7.17	7.53	5.82	7.96	8.11	7.67
Al2O3	25.65	25.89	26.26	36.97	25.05	25.30	25.40
SiO2	58.93	58.97	58.52	40.22	60.51	60.77	59.01
Totals	99.68	99.81	100.26	88.39	99.87	100.79	99.03

Sample	134	135	136	137	138	139	140
FeO	0.06	0.17	0.19	0.17	0.05	0.11	0.09
CaO	6.99	7.82	7.90	8.24	8.00	8.26	8.82
K2O	0.23	0.21	0.20	0.19	0.18	0.24	0.18
Na2O	7.81	7.43	7.10	7.05	7.27	6.96	7.01
Al2O3	25.80	26.46	26.33	26.98	27.02	26.81	27.33
SiO2	58.11	57.60	57.76	57.58	57.83	56.94	56.79
Totals	99.00	99.70	99.47	100.21	100.34	99.32	100.22

Sample	141	142	143	144	145	146	147
FeO	0.14	0.17	0.12	0.10	0.14	0.16	0.22
CaO	8.80	9.18	9.12	8.94	9.22	9.09	8.87
K2O	0.16	0.18	0.16	0.16	0.18	0.15	0.19
Na2O	6.58	6.26	6.52	6.75	6.54	6.48	6.40
Al2O3	27.77	27.82	28.21	27.69	28.27	27.70	28.10
SiO2	56.55	56.03	56.06	56.43	56.60	56.90	57.90
Totals	100.00	99.64	100.20	100.08	100.96	100.49	101.68

Sample	148	149	150	151	152	153	154

FeO	0.15	0.11	0.15	0.29	0.20	0.12	0.22
CaO	8.01	8.01	8.33	8.51	8.36	8.40	7.88
K2O	0.18	0.21	0.19	0.21	0.18	0.13	0.19
Na2O	7.52	6.92	6.79	7.06	6.89	7.13	7.27
Al2O3	26.62	26.76	26.90	27.05	26.90	27.06	26.80
SiO2	57.77	57.98	57.80	57.23	56.93	57.52	57.97
Totals	100.25	99.99	100.15	100.34	99.46	100.36	100.33

Sample	155	156	157	158	159	160	161
FeO	0.12	0.16	0.13	0.22	0.10	0.05	0.07
CaO	7.49	7.48	7.85	7.79	7.62	7.95	7.71
K2O	0.22	0.18	0.26	0.24	0.27	0.19	0.26
Na2O	7.53	7.15	7.04	7.33	7.32	7.42	7.31
Al2O3	26.68	26.67	26.93	26.43	26.44	26.49	26.55
SiO2	58.91	58.52	58.20	57.92	58.96	58.26	57.97
Totals	100.95	100.16	100.39	99.93	100.71	100.36	99.88

Sample	162	163	164	165	166	167	168
FeO	0.08	0.12	0.09	0.14	0.12	0.15	0.08
CaO	7.62	7.94	7.84	7.78	7.66	7.66	7.46
K2O	0.20	0.18	0.21	0.26	0.22	0.23	0.21
Na2O	7.14	7.10	7.28	7.31	7.16	7.28	7.49
Al2O3	26.38	26.32	26.74	26.78	26.18	26.25	26.24
SiO2	57.86	58.71	58.18	58.72	58.14	58.98	58.29
Totals	99.29	100.38	100.34	101.00	99.48	100.55	99.78

Sample	169	170	171	172	173	174	175
FeO	0.19	0.17	0.08	0.16	0.11	0.14	0.02
CaO	7.48	7.47	7.43	7.56	7.68	7.59	7.56
K2O	0.20	0.23	0.23	0.22	0.21	0.21	0.24
Na2O	7.56	7.51	7.51	7.79	7.69	7.16	7.91
Al2O3	26.17	26.49	26.87	26.13	26.25	26.05	26.25
SiO2	58.34	58.57	58.37	58.88	58.60	58.49	58.82
Totals	99.95	100.44	100.49	100.75	100.54	99.64	100.79

Sample	176	177	178	179	180	181	182
FeO	0.11	0.14	0.21	0.17	0.07	0.12	0.18
CaO	7.45	7.49	7.51	7.47	7.48	7.40	7.64
K2O	0.29	0.19	0.19	0.18	0.21	0.20	0.23
Na2O	7.19	7.37	7.58	7.50	8.05	7.73	7.42
Al2O3	26.44	26.44	26.09	26.03	25.31	26.71	26.84
SiO2	58.36	58.12	58.83	58.99	55.94	58.59	58.18
Totals	99.85	99.75	100.41	100.34	97.07	100.74	100.49

Sample	183	184	185	186	187	188	189
FeO	0.18	0.20	0.05	0.22	0.27	0.17	0.15
CaO	7.51	7.70	7.45	7.39	7.55	7.43	7.27
K2O	0.24	0.21	0.19	0.28	0.24	0.21	0.19
Na2O	7.77	7.50	7.58	7.46	7.30	7.45	7.63
Al2O3	26.39	26.43	25.97	26.40	25.94	26.13	25.99
SiO2	58.23	57.91	58.64	58.15	58.93	58.11	59.46
Totals	100.32	99.95	99.89	99.91	100.23	99.50	100.69

Sample	190	191	192	193	194	195	196
FeO	0.19	0.18	0.14	0.07	0.12	0.08	0.17
CaO	7.25	7.05	7.18	6.92	7.00	7.23	7.03
K2O	0.24	0.24	0.21	0.26	0.27	0.25	0.24
Na2O	7.65	8.03	7.65	7.59	7.33	7.88	7.61
Al2O3	26.09	25.50	26.28	25.84	26.02	25.63	25.99
SiO2	59.99	58.49	59.24	59.12	59.03	58.61	59.00
Totals	101.42	99.50	100.69	99.79	99.78	99.67	100.04

Sample	197	198	199	200	201	202	203
FeO	0.11	0.00	0.13	0.17	0.19	0.17	0.11
CaO	6.99	6.84	6.99	7.35	6.94	6.77	6.75
K2O	0.31	0.28	0.23	0.16	0.22	0.25	0.28
Na2O	7.71	7.85	7.73	7.59	7.83	7.82	7.73
Al2O3	25.59	26.11	25.85	26.17	24.98	25.57	25.68
SiO2	59.28	59.56	59.46	59.52	57.10	59.42	58.57
Totals	99.98	100.63	100.40	100.96	97.24	99.99	99.12

Sample	204	205	206	207	208	209	210
FeO	0.21	0.10	0.03	0.11	0.11	0.13	0.18
CaO	6.82	6.78	7.13	7.53	7.53	7.78	7.57
K2O	0.27	0.21	0.24	0.19	0.22	0.20	0.23
Na2O	7.56	7.69	7.29	7.14	7.21	7.16	7.57
Al2O3	25.63	25.10	25.91	26.74	26.27	26.18	26.91
SiO2	59.44	59.54	59.12	59.53	58.83	57.96	59.43
Totals	99.93	99.41	99.72	101.23	100.16	99.41	101.89

Sample	211	212	213	214	215	216	217
FeO	0.13	0.15	0.07	0.18	0.21	0.18	0.09
CaO	7.56	7.58	7.70	7.55	7.58	7.63	7.65
K2O	0.23	0.26	0.23	0.22	0.22	0.26	0.30
Na2O	7.45	7.31	7.17	7.39	7.47	7.37	7.69
Al2O3	26.53	26.11	26.90	25.58	26.10	26.44	26.46
SiO2	58.52	58.65	58.35	56.68	58.61	58.59	58.56
Totals	100.42	100.07	100.42	97.60	100.19	100.46	100.76

Sample	218	219	220
FeO	0.21	0.15	0.10
CaO	7.74	7.63	7.45
K2O	0.26	0.23	0.22

Na2O	7.44	7.27	7.10
Al2O3	26.82	26.40	26.43
SiO2	58.32	58.30	58.43
Totals	100.78	99.99	99.74

SR-6-6-06-1A-Plag-2 Rim to Core (El Hato)

Sample	1	2	3	4	5	6	7
FeO	0.27	0.15	0.27	0.21	0.08	0.13	0.23
CaO	7.42	8.30	8.00	8.24	8.39	7.73	8.04
K2O	0.21	0.17	0.20	0.23	0.18	0.21	0.19
Na2O	7.41	6.72	6.88	6.90	6.50	7.39	7.24
Al2O3	26.25	26.78	27.20	26.56	27.41	27.23	26.81
SiO2	58.77	57.39	57.55	58.02	57.97	57.67	58.34
Totals	100.33	99.50	100.09	100.16	100.53	100.36	100.85

Sample	8	9	10	11	12	13	14
FeO	0.10	0.18	0.16	0.16	0.15	0.00	0.22
CaO	7.07	7.28	7.14	7.33	7.60	7.92	7.97
K2O	0.21	0.19	0.26	0.25	0.20	0.23	0.22
Na2O	7.53	7.80	7.34	7.26	7.59	7.14	7.05
Al2O3	25.99	26.36	26.22	26.06	26.28	26.27	26.92
SiO2	58.56	58.68	59.31	58.12	56.93	58.02	57.37
Totals	99.46	100.49	100.44	99.20	98.74	99.58	99.75

Sample	15	16	17	18	19	20	21
FeO	0.20	0.23	0.19	0.12	0.18	0.16	0.20
CaO	7.41	7.69	7.44	7.99	8.60	7.80	8.07
K2O	0.19	0.24	0.22	0.20	0.18	0.20	0.18
Na2O	7.22	7.39	7.39	7.13	6.79	6.98	6.94
Al2O3	18.57	25.97	26.02	26.53	27.15	26.85	28.21
SiO2	40.90	57.61	58.28	58.11	56.78	57.82	60.91
Totals	74.49	99.13	99.54	100.08	99.67	99.81	104.53

Sample	22	23	24	25	26	27	28
FeO	0.27	0.14	0.15	0.25	0.16	0.20	0.27
CaO	7.99	8.14	8.55	8.21	8.03	7.99	8.50
K2O	0.20	0.24	0.16	0.21	0.22	0.20	0.20
Na2O	7.00	7.11	6.97	7.06	6.97	7.15	6.49
Al2O3	26.46	24.60	26.50	26.97	27.43	27.00	28.16
SiO2	56.30	52.00	56.59	57.66	57.66	57.72	58.53
Totals	98.22	92.22	98.92	100.36	100.47	100.27	102.13

Sample	29	30	31	32	33	34	35
FeO	0.15	0.23	0.15	0.25	0.27	0.26	0.28
CaO	9.00	8.58	10.41	10.89	10.69	11.40	12.34
K2O	0.19	0.21	0.14	0.12	0.11	0.11	0.10
Na2O	5.57	5.96	5.66	5.65	5.32	5.07	4.88
Al2O3	29.26	27.01	28.61	28.97	28.96	22.33	30.67
SiO2	61.46	49.44	54.99	54.02	52.73	40.57	52.18
Totals	105.62	91.43	99.97	99.90	98.09	79.73	100.45

Sample	36	37	38	39	40	41	42
FeO	0.19	0.20	0.15	0.12	0.28	0.17	0.12
CaO	7.96	8.17	8.00	8.26	7.87	8.06	8.17
K2O	0.20	0.22	0.24	0.23	0.26	0.18	0.23
Na2O	6.98	7.13	6.87	6.85	6.79	6.90	6.61
Al2O3	26.65	27.23	26.75	27.15	26.45	26.88	27.27
SiO2	56.92	57.47	57.86	57.21	57.62	57.75	57.92
Totals	98.91	100.42	99.88	99.83	99.27	99.94	100.33

Sample	43	44	45	46	47	48	49
FeO	0.17	0.14	0.10	0.06	0.07	0.20	0.22
CaO	8.44	8.89	7.77	7.62	8.20	8.13	8.89
K2O	0.15	0.22	0.19	0.17	0.21	0.19	0.14
Na2O	7.67	6.90	7.50	7.02	7.07	6.95	6.83
Al2O3	26.26	27.15	26.44	26.74	26.93	26.95	26.92
SiO2	57.11	56.60	58.22	57.67	57.66	57.63	55.82
Totals	99.80	99.90	100.23	99.27	100.14	100.06	98.82

Sample	50	51	52	53	54	55	56
FeO	0.14	0.06	0.14	0.15	0.13	0.20	0.22
CaO	9.12	8.87	7.70	7.96	7.90	8.12	8.76
K2O	0.17	0.20	0.17	0.19	0.18	0.20	0.21
Na2O	7.68	6.67	7.36	7.36	7.00	7.15	6.44
Al2O3	26.51	27.42	26.21	26.50	26.87	26.97	27.28
SiO2	53.52	56.21	58.23	58.17	57.32	57.99	56.61
Totals	97.14	99.45	99.81	100.33	99.40	100.62	99.53

Sample	57	58	59	60	61	62	63
FeO	0.04	0.17	0.10	0.12	0.14	0.18	0.14
CaO	7.78	7.89	7.97	7.91	7.95	9.02	7.69
K2O	0.21	0.20	0.25	0.19	0.24	0.18	0.22
Na2O	7.09	7.56	7.15	7.08	7.25	6.53	7.56
Al2O3	26.38	26.60	27.26	26.81	26.74	28.03	26.73
SiO2	57.41	57.81	58.29	57.26	57.62	56.34	57.89
Totals	98.92	100.23	101.01	99.36	99.93	100.28	100.22

Sample	64	65	66	67	68	69	70
FeO	0.04	0.17	0.19	0.11	0.19	0.11	0.11
CaO	7.60	8.05	7.52	8.15	7.75	7.96	8.10
K2O	0.23	0.24	0.20	0.16	0.21	0.23	0.19
Na2O	7.33	7.71	6.92	7.38	7.43	7.26	7.19
Al2O3	26.87	26.59	26.28	27.16	26.90	26.41	27.05
SiO2	58.45	58.31	58.04	57.20	57.51	58.01	57.31
Totals	100.51	101.07	99.15	100.17	99.99	99.98	99.94

Sample	71	72	73	74	75	76	77
FeO	0.08	0.19	0.09	0.21	0.19	0.26	0.09
CaO	7.72	7.14	7.42	7.47	7.65	7.57	7.71

K2O	0.20	0.16	0.25	0.20	0.19	0.22	0.20
Na2O	7.21	7.48	7.52	7.49	7.42	7.28	7.64
Al2O3	26.82	26.15	26.37	26.60	26.77	26.59	26.37
SiO2	58.62	58.71	58.02	58.43	57.93	58.57	58.41
Totals	100.65	99.84	99.68	100.39	100.15	100.48	100.42

Sample	78	79	80	81	82	83	84
FeO	0.17	0.16	0.14	0.10	0.18	0.17	0.12
CaO	7.73	7.92	8.32	8.51	8.26	8.21	8.27
K2O	0.22	0.18	0.21	0.21	0.20	0.21	0.19
Na2O	7.18	7.14	6.72	6.81	7.30	7.09	6.75
Al2O3	26.67	26.52	27.21	26.99	26.39	26.59	27.02
SiO2	57.82	57.99	57.45	57.77	56.89	57.11	57.04
Totals	99.80	99.91	100.04	100.39	99.22	99.37	99.39

Sample	85	86	87	88	89	90	91
FeO	0.18	0.10	0.23	0.11	0.08	0.21	0.16
CaO	8.78	8.38	8.14	8.69	8.99	8.71	9.01
K2O	0.18	0.17	0.27	0.19	0.20	0.17	0.17
Na2O	6.74	7.34	7.39	6.80	6.82	7.07	6.67
Al2O3	27.36	27.32	26.57	27.55	27.42	27.18	27.53
SiO2	57.15	57.64	57.61	56.55	56.65	56.98	56.71
Totals	100.40	100.95	100.20	99.89	100.16	100.33	100.25

Sample	92	93	94	95	96	97	98
FeO	0.15	0.07	0.14	0.10	0.12	0.14	0.07
CaO	7.99	7.21	7.47	7.63	8.19	7.75	8.08
K2O	0.20	0.22	0.30	0.22	0.17	0.21	0.18
Na2O	7.41	7.59	7.84	7.36	6.88	7.00	6.96
Al2O3	26.51	25.71	26.53	26.41	26.97	26.97	26.73
SiO2	57.82	59.42	58.48	58.65	57.01	59.69	58.82
Totals	100.08	100.21	100.78	100.37	99.33	101.76	100.84

Sample	99	100	101	102	103	104	105
FeO	0.19	0.22	0.15	0.15	0.08	0.06	0.16
CaO	8.49	8.60	8.79	7.83	7.73	8.11	8.08
K2O	0.16	0.20	0.17	0.17	0.20	0.17	0.20
Na2O	6.96	6.94	7.09	6.93	7.29	6.83	7.26
Al2O3	27.64	27.19	27.13	26.45	26.70	26.87	27.03
SiO2	57.05	56.33	56.30	57.72	59.41	57.51	57.79
Totals	100.49	99.48	99.63	99.26	101.41	99.56	100.52

Sample	106	107	108	109	110	111	112
FeO	0.08	0.15	0.14	0.10	0.18	0.04	0.14
CaO	8.04	7.88	8.57	8.21	8.23	7.92	7.74
K2O	0.23	0.18	0.20	0.20	0.21	0.21	0.22
Na2O	6.96	5.69	7.12	6.72	6.92	7.24	7.08
Al2O3	26.48	23.09	26.97	26.92	27.03	26.26	26.34
SiO2	57.65	48.79	56.83	57.37	57.14	58.86	58.36
Totals	99.43	85.77	99.83	99.53	99.71	100.53	99.88

Sample	113	114	115	116	117	118	119
FeO	0.07	0.16	0.17	0.23	0.06	0.24	0.15
CaO	9.12	9.23	7.57	7.65	7.91	8.04	8.44
K2O	0.21	0.22	0.22	0.20	0.22	0.22	0.21
Na2O	6.45	6.74	7.46	7.32	7.35	7.21	6.68
Al2O3	27.74	27.97	26.45	26.64	26.44	26.86	27.42
SiO2	56.58	56.60	57.93	58.12	57.90	57.47	56.84
Totals	100.17	100.92	99.79	100.16	99.87	100.04	99.74

Sample	120	121	122	123	124	125	126
FeO	0.14	0.06	0.15	0.09	0.13	0.13	0.13
CaO	8.46	8.57	8.72	8.94	8.95	8.23	8.03
K2O	0.19	0.19	0.18	0.16	0.17	0.18	0.21
Na2O	6.66	7.20	6.69	6.65	6.59	6.33	7.02
Al2O3	27.17	27.50	27.34	27.28	27.55	26.58	26.92
SiO2	58.00	57.73	57.96	55.49	56.89	55.91	57.70
Totals	100.61	101.25	101.02	98.61	100.28	97.36	100.01

Sample	127	128	129	130	131	132	133
FeO	0.11	0.10	0.16	0.19	0.20	0.00	0.11
CaO	7.72	7.20	8.31	9.04	8.61	8.38	8.98
K2O	0.26	0.21	0.16	0.14	0.25	0.23	0.23
Na2O	7.41	7.73	6.70	6.76	6.57	6.99	6.66
Al2O3	26.43	25.89	26.93	28.00	27.31	27.05	27.26
SiO2	58.67	58.97	58.31	56.68	57.08	57.54	57.00
Totals	100.61	100.10	100.56	100.81	100.03	100.19	100.24

Sample	134	135	136	137	138	139	140
FeO	0.13	0.10	0.21	0.20	0.11	0.05	0.10
CaO	9.52	10.19	10.17	10.22	9.44	8.27	8.48
K2O	0.17	0.12	0.13	0.12	0.16	0.17	0.19
Na2O	6.51	6.22	5.87	5.76	6.18	7.12	7.06
Al2O3	28.65	28.13	28.74	29.16	28.53	27.13	27.54
SiO2	56.97	55.89	55.75	56.35	55.61	57.36	58.72
Totals	101.94	100.66	100.87	101.81	100.04	100.10	102.09

Sample	141	142	143	144	145	146	147
FeO	0.15	0.14	0.24	0.20	0.21	0.21	0.11
CaO	8.98	9.17	9.36	9.02	8.94	8.89	8.90
K2O	0.17	0.15	0.13	0.18	0.15	0.19	0.15
Na2O	6.66	5.93	6.84	6.67	6.61	6.71	6.62
Al2O3	27.25	26.90	23.85	28.14	28.02	27.51	27.81
SiO2	56.85	54.28	47.10	55.82	56.46	56.57	56.94
Totals	100.06	96.57	87.53	100.03	100.38	100.07	100.54

Sample	148	149	150	151	152	153	154
FeO	0.16	0.26	0.17	0.13	0.17	0.15	0.14
CaO	9.00	8.82	8.66	8.95	8.64	8.91	8.63

K2O	0.18	0.19	0.15	0.18	0.17	0.20	0.21
Na2O	6.59	6.65	6.31	7.23	5.00	5.86	6.80
Al2O3	27.65	27.32	27.30	27.03	28.39	21.23	27.50
SiO2	57.38	56.97	56.82	56.89	59.35	42.49	57.74
Totals	100.96	100.21	99.41	100.41	101.72	78.83	101.01

SR-6-6-06-1A-Plag-1 Rim to Core (El Hato)

Sample	1	2	3	4	5	6	7
FeO	0.12	0.17	0.14	0.17	0.13	0.09	0.07
CaO	7.01	7.72	7.88	8.37	7.92	8.12	7.96
K2O	0.26	0.19	0.22	0.22	0.21	0.19	0.22
Na2O	7.59	7.38	7.49	7.16	7.26	6.89	7.58
Al2O3	25.65	26.54	26.49	26.64	26.12	26.97	26.41
SiO2	59.54	58.38	57.89	57.21	57.54	57.90	58.17
Totals	100.17	100.37	100.12	99.76	99.17	100.15	100.41

Sample	8	9	10	11	12	13	14
FeO	0.06	0.15	0.20	0.12	0.09	0.18	0.25
CaO	8.02	7.78	7.85	8.68	9.44	10.67	11.12
K2O	0.18	0.21	0.20	0.18	0.11	0.13	0.08
Na2O	7.35	7.39	7.16	7.00	6.67	5.68	5.49
Al2O3	26.74	26.00	26.89	27.22	27.66	29.65	29.30
SiO2	57.91	57.38	57.83	56.47	56.80	54.77	53.97
Totals	100.26	98.91	100.13	99.67	100.77	101.08	100.20

Sample	15	16	17	18	19	20	21
FeO	0.15	0.14	0.17	0.13	0.04	0.08	0.07
CaO	11.37	11.31	11.81	9.46	8.02	7.26	7.35
K2O	0.11	0.10	0.10	0.15	0.16	0.23	0.24
Na2O	5.27	4.98	5.15	6.26	6.95	7.74	8.05
Al2O3	29.72	30.13	29.99	27.87	26.69	26.04	25.50
SiO2	53.43	53.81	52.87	56.33	57.28	58.89	58.93
Totals	100.05	100.46	100.10	100.20	99.14	100.24	100.15

Sample	22	23	24	25	26	27	28
FeO	0.16	0.17	0.26	0.22	0.12	0.17	0.10
CaO	6.98	7.10	7.37	7.35	7.46	7.48	7.58
K2O	0.30	0.24	0.22	0.21	0.25	0.26	0.18
Na2O	7.40	7.64	7.31	7.31	7.37	7.64	7.59
Al2O3	25.80	25.81	26.14	26.25	26.11	26.09	26.12
SiO2	59.44	58.64	58.37	58.94	58.99	59.16	58.60
Totals	100.08	99.60	99.68	100.28	100.30	100.80	100.17

Sample	29	30	31	32	33	34	35
FeO	0.07	0.16	0.17	0.14	0.22	0.07	0.12
CaO	7.69	7.46	7.44	7.48	7.43	7.43	7.72
K2O	0.21	0.23	0.24	0.19	0.21	0.21	0.20
Na2O	7.53	7.23	7.56	7.69	7.48	7.51	7.63
Al2O3	26.03	26.49	26.43	26.31	26.31	26.37	26.29
SiO2	59.32	59.16	58.44	58.81	58.27	58.42	59.49

Totals	100.85	100.74	100.27	100.63	99.92	100.01	101.45

Sample	36	37	38	39	40	41	42
FeO	0.19	0.09	0.11	0.08	0.22	0.18	0.13
CaO	7.32	7.52	7.30	7.22	7.50	7.21	7.56
K2O	0.24	0.26	0.22	0.22	0.20	0.24	0.21
Na2O	7.43	7.41	7.40	7.19	7.68	7.85	7.44
Al2O3	26.24	25.93	26.43	26.07	25.73	26.32	25.88
SiO2	58.33	58.59	58.86	59.29	58.55	58.19	58.28
Totals	99.74	99.80	100.32	100.07	99.87	100.00	99.50

Sample	43	44	45	46	47	48	49
FeO	0.10	0.06	0.17	0.06	0.19	0.00	0.09
CaO	7.34	7.48	7.60	7.42	7.87	4.00	7.91
K2O	0.28	0.22	0.20	0.23	0.21	0.09	0.21
Na2O	7.44	7.46	7.44	7.50	7.28	3.02	6.79
Al2O3	26.14	26.36	25.67	25.99	27.03	13.14	27.50
SiO2	58.69	58.90	58.97	59.60	58.18	27.46	59.78
Totals	99.99	100.49	100.04	100.81	100.76	47.71	102.27

Sample	50	51	52	53	54	55	56
FeO	0.16	0.22	0.15	0.09	0.16	0.12	0.05
CaO	8.32	8.46	8.87	8.25	8.92	8.93	8.96
K2O	0.20	0.22	0.17	0.18	0.19	0.15	0.18
Na2O	7.06	6.74	6.93	6.90	6.66	6.67	6.79
Al2O3	26.08	27.18	27.46	26.81	27.11	27.38	27.42
SiO2	55.18	56.64	56.29	57.83	57.00	56.46	56.37
Totals	97.01	99.46	99.87	100.06	100.03	99.70	99.77

Sample	57	58	59	60	61	62	63
FeO	0.16	0.05	0.13	0.08	0.09	0.15	0.08
CaO	8.59	8.45	8.91	8.80	8.95	8.90	9.44
K2O	0.19	0.20	0.12	0.21	0.19	0.17	0.16
Na2O	6.85	6.91	6.88	7.03	6.88	6.73	6.55
Al2O3	27.00	27.34	27.67	27.33	27.40	27.75	28.02
SiO2	57.07	57.70	56.22	57.76	56.44	56.34	55.98
Totals	99.87	100.65	99.93	101.21	99.94	100.04	100.24

Sample	64	65	66	67	68	69	70
FeO	0.12	0.25	0.15	0.20	0.17	0.17	0.04
CaO	9.12	10.19	10.46	12.55	11.68	11.23	10.83
K2O	0.15	0.13	0.11	0.10	0.12	0.09	0.12
Na2O	6.43	5.77	5.31	4.42	5.24	5.41	5.77
Al2O3	27.56	28.45	30.12	30.13	29.53	29.32	29.17
SiO2	56.24	55.13	57.50	51.38	53.44	53.75	54.21
Totals	99.62	99.92	103.65	98.78	100.18	99.97	100.14

Sample	71	72	73	74	75	76	77
FeO	0.12	0.08	0.22	0.12	0.20	0.10	0.06

CaO	11.09	11.90	10.40	7.02	7.23	7.80	8.01
K2O	0.11	0.12	0.10	0.22	0.21	0.21	0.17
Na2O	5.63	5.02	5.74	6.77	8.14	7.25	8.06
Al2O3	29.47	29.89	28.64	24.75	26.09	26.81	26.13
SiO2	53.99	52.67	54.86	55.76	58.25	58.05	56.93
Totals	100.42	99.67	99.97	94.64	100.12	100.22	99.35

Sample	78	79	80	81	82	83	84
FeO	0.09	0.11	0.12	0.12	0.10	0.18	0.00
CaO	7.75	7.73	7.86	7.98	8.09	8.11	8.11
K2O	0.23	0.22	0.18	0.21	0.25	0.19	0.19
Na2O	7.03	7.34	7.29	6.89	6.96	7.16	7.17
Al2O3	26.39	26.68	26.51	26.40	26.72	26.88	26.74
SiO2	58.66	58.04	57.62	57.96	57.52	57.14	57.87
Totals	100.16	100.12	99.58	99.57	99.64	99.64	100.09

Sample	85	86	87	88	89	90	91
FeO	0.17	0.15	0.15	0.23	0.17	0.16	0.03
CaO	8.12	8.74	9.11	9.13	9.32	9.45	8.54
K2O	0.19	0.18	0.17	0.18	0.20	0.14	0.18
Na2O	7.56	6.86	6.40	6.38	6.93	5.25	6.71
Al2O3	27.12	27.42	27.89	28.50	24.80	30.84	26.92
SiO2	58.54	57.22	56.56	57.74	49.60	60.04	57.02
Totals	101.70	100.56	100.29	102.15	91.03	105.87	99.39

Sample	92	93	94	95	96	97	98
FeO	0.12	0.09	0.18	0.13	0.24	0.10	0.18
CaO	8.62	9.18	9.33	9.40	9.00	7.85	8.67
K2O	0.20	0.16	0.16	0.16	0.18	0.23	0.19
Na2O	6.84	6.38	6.54	6.34	6.71	7.52	6.78
Al2O3	26.97	27.24	28.23	28.40	28.08	26.99	27.45
SiO2	57.54	56.23	57.74	55.71	56.64	58.58	56.72
Totals	100.30	99.28	102.18	100.15	100.85	101.27	99.99

Sample	99	100	101	102	103	104	105
FeO	0.25	0.14	0.08	0.13	0.11	0.19	0.05
CaO	8.64	8.08	8.31	9.29	9.56	9.30	8.44
K2O	0.21	0.17	0.18	0.15	0.19	0.15	0.17
Na2O	6.84	7.18	7.24	6.57	5.96	6.52	7.08
Al2O3	27.25	26.74	26.66	28.08	28.52	28.03	27.06
SiO2	57.08	57.58	57.46	56.71	56.12	56.28	57.49
Totals	100.27	99.90	99.93	100.92	100.46	100.45	100.29

Sample	106	107	108	109	110	111	112
FeO	0.11	0.16	0.07	0.12	0.09	0.07	0.16
CaO	8.45	9.08	9.56	8.30	9.44	9.02	8.50
K2O	0.19	0.14	0.16	0.09	0.17	0.18	0.20
Na2O	7.17	6.38	6.13	7.09	6.23	6.52	6.80
Al2O3	27.09	27.56	27.82	26.87	27.32	27.73	27.37
SiO2	57.31	56.71	56.75	57.38	55.18	56.66	57.06

Totals	100.31	100.04	100.48	99.84	98.42	100.19	100.08

Sample	113	114	115	116	117	118	119
FeO	0.19	0.16	0.09	0.09	0.12	0.16	0.10
CaO	8.46	8.64	8.49	7.96	7.88	7.77	7.98
K2O	0.21	0.17	0.25	0.22	0.20	0.24	0.19
Na2O	7.06	7.12	6.89	7.40	7.57	7.26	6.77
Al2O3	27.25	26.96	27.04	26.51	26.62	26.76	26.80
SiO2	58.02	57.33	57.51	57.78	58.45	58.43	58.49
Totals	101.19	100.37	100.26	99.97	100.85	100.62	100.34

Sample	120	121	122	123	124	125	126
FeO	0.17	0.17	0.10	0.10	0.22	0.12	0.14
CaO	8.22	8.39	8.61	8.30	8.93	7.89	7.96
K2O	0.21	0.16	0.18	0.14	0.20	0.24	0.22
Na2O	7.04	6.23	5.90	5.77	6.76	7.03	7.28
Al2O3	27.13	27.01	27.59	26.87	26.81	26.75	26.58
SiO2	57.67	57.00	56.85	55.01	56.47	57.72	57.72
Totals	100.45	98.96	99.23	96.18	99.40	99.76	99.90

Sample	127	128	129
FeO	0.10	0.13	0.11
CaO	7.49	7.81	7.83
K2O	0.21	0.22	0.22
Na2O	7.27	7.46	7.29
Al2O3	26.16	27.18	26.78
SiO2	57.71	57.73	57.70
Totals	98.94	100.54	99.93

LM-5-19-06-1D Plag-1 Rim to Core (EL Hato)

Sample	1	2	3	4	5	6	7
FeO	0.21	0.24	0.19	0.10	0.16	0.12	0.20
CaO	8.21	8.29	8.02	7.59	7.72	7.56	7.77
K2O	0.21	0.20	0.16	0.21	0.16	0.18	0.21
Na2O	7.14	7.05	7.25	7.52	7.22	7.16	7.05
Al2O3	26.94	26.68	26.42	26.51	26.31	25.91	26.45
SiO2	57.02	57.41	57.77	58.28	57.61	58.48	58.04
Totals	99.73	99.88	99.82	100.20	99.18	99.41	99.71

Sample	8	9	10	11	12	13	14
FeO	0.12	0.10	0.21	0.25	0.20	0.14	0.15
CaO	8.40	9.79	8.49	8.82	8.98	8.79	9.09
K2O	0.15	0.14	0.15	0.16	0.15	0.19	0.15
Na2O	7.11	6.34	7.06	6.55	6.64	6.77	6.72
Al2O3	26.87	27.94	27.55	27.29	27.97	26.76	27.30
SiO2	58.16	56.13	57.61	56.51	56.74	55.92	55.69
Totals	100.81	100.45	101.06	99.58	100.68	98.57	99.11

Sample	15	16	17	18	19	20	21

FeO	0.15	0.18	0.16	0.20	0.22	0.21	0.16
CaO	9.74	9.86	8.94	9.59	10.20	9.50	10.00
K2O	0.17	0.14	0.20	0.18	0.16	0.13	0.13
Na2O	6.12	6.23	6.55	6.08	5.75	6.44	6.01
Al2O3	28.44	28.37	27.04	27.88	29.05	28.40	28.27
SiO2	55.76	56.23	56.55	54.93	54.55	55.64	55.47
Totals	100.39	101.02	99.44	98.86	99.94	100.32	100.03

Sample	22	23	24	25	26	27	28
FeO	0.10	0.24	0.22	0.16	0.12	0.10	0.17
CaO	8.84	9.10	8.47	7.49	7.52	8.10	8.51
K2O	0.16	0.19	0.17	0.22	0.22	0.21	0.23
Na2O	6.73	6.72	6.71	7.24	7.51	7.19	6.69
Al2O3	27.29	27.83	27.10	26.17	26.03	26.99	26.62
SiO2	56.26	56.75	57.16	58.30	58.87	57.42	57.26
Totals	99.38	100.82	99.83	99.58	100.28	100.02	99.47

Sample	29	30	31	32	33	34	35
FeO	0.12	0.19	0.17	0.09	0.05	0.28	0.22
CaO	8.82	8.87	8.65	8.76	8.37	7.86	8.01
K2O	0.14	0.23	0.15	0.17	0.18	0.21	0.23
Na2O	6.52	6.68	7.15	6.87	6.79	6.83	7.05
Al2O3	26.72	27.53	27.26	27.35	27.27	26.98	26.88
SiO2	57.17	56.20	57.15	56.07	57.42	55.95	57.08
Totals	99.49	99.70	100.52	99.31	100.09	98.12	99.46

Sample	36	37	38	39	40	41	42
FeO	0.18	0.12	0.16	0.18	0.18	0.13	0.14
CaO	7.86	8.49	9.05	9.12	9.24	9.40	9.67
K2O	0.19	0.15	0.21	0.19	0.18	0.15	0.16
Na2O	7.40	6.83	6.83	6.79	6.56	6.33	6.47
Al2O3	26.84	26.92	27.19	27.92	27.85	27.67	28.38
SiO2	56.68	57.00	56.75	56.61	55.94	55.94	55.97
Totals	99.15	99.50	100.18	100.81	99.94	99.62	100.80

Sample	43	44	45	46	47	48	49
FeO	0.15	0.17	0.18	0.14	0.06	0.08	0.19
CaO	9.44	9.46	9.67	9.80	10.00	10.37	10.42
K2O	0.13	0.13	0.15	0.15	0.14	0.12	0.12
Na2O	6.11	6.44	6.26	6.13	5.69	5.87	5.87
Al2O3	28.09	27.84	27.85	27.89	28.37	28.74	28.84
SiO2	55.78	55.94	55.36	55.41	54.56	55.02	54.61
Totals	99.71	99.98	99.47	99.51	98.82	100.19	100.04

Sample	50	51	52	53	54	55	56
FeO	0.15	0.24	0.17	0.17	0.25	0.11	0.13
CaO	10.43	11.46	11.06	10.79	10.58	10.87	11.16
K2O	0.10	0.14	0.10	0.11	0.10	0.13	0.14
Na2O	5.36	5.19	5.33	5.45	5.62	5.37	5.61
Al2O3	29.01	29.30	29.34	29.29	29.47	29.47	29.97

SiO2	54.32	53.18	53.00	54.15	54.07	53.75	54.05
Totals	99.38	99.50	99.00	99.96	100.10	99.70	101.06

Sample	57	58	59	60	61	62	63
FeO	0.18	0.18	0.27	0.05	0.19	0.10	0.22
CaO	11.36	11.81	11.77	11.75	11.48	11.41	11.39
K2O	0.10	0.07	0.13	0.11	0.12	0.10	0.15
Na2O	5.35	5.11	5.14	5.05	5.26	5.41	5.13
Al2O3	29.41	30.00	29.30	30.00	29.84	29.47	29.62
SiO2	53.45	52.45	52.68	52.87	54.00	53.02	53.28
Totals	99.85	99.62	99.29	99.83	100.90	99.51	99.79

Sample	64	65	66
FeO	0.17	0.14	0.00
CaO	11.62	12.06	11.58
K2O	0.14	0.12	0.10
Na2O	5.07	4.69	5.22
Al2O3	30.10	30.74	30.03
SiO2	52.99	52.10	53.74
Totals	100.09	99.85	100.67

LM-5-19-06-1D Plag-2 Rim to Core (El Hato)

Sample	1	2	3	4	5	6	7
FeO	0.24	0.19	0.09	0.19	0.21	0.14	0.17
CaO	7.29	8.05	7.12	7.41	7.02	8.41	7.62
K2O	0.28	0.22	0.20	0.25	0.28	0.17	0.18
Na2O	7.03	7.13	7.37	7.34	7.30	7.02	7.03
Al2O3	26.36	27.15	25.77	26.13	26.13	26.93	26.24
SiO2	58.50	57.75	58.72	58.47	58.84	56.45	58.22
Totals	99.71	100.49	99.27	99.79	99.77	99.11	99.45

Sample	8	9	10	11	12	13	14
FeO	0.19	0.18	0.13	0.25	0.18	0.14	0.19
CaO	8.28	7.89	7.85	9.23	7.24	7.06	7.29
K2O	0.16	0.22	0.21	0.16	0.27	0.26	0.22
Na2O	6.50	6.96	7.19	6.53	7.50	7.59	7.45
Al2O3	26.82	26.87	26.22	27.72	25.84	25.89	25.64
SiO2	56.21	57.41	57.45	55.49	58.56	58.76	58.48
Totals	98.17	99.53	99.05	99.38	99.59	99.71	99.26

Sample	15	16	17	18	19	20	21
FeO	0.13	0.17	0.12	0.16	0.16	0.14	0.11
CaO	7.73	7.92	8.31	8.17	8.58	8.90	8.76
K2O	0.21	0.22	0.16	0.17	0.21	0.15	0.22
Na2O	7.08	7.49	6.90	6.64	6.46	6.53	6.81
Al2O3	26.21	26.42	27.24	27.04	27.08	27.25	27.77
SiO2	57.83	57.68	57.12	57.36	56.93	56.11	56.43
Totals	99.19	99.89	99.85	99.54	99.40	99.08	100.09

Sample	22	23	24	25	26	27	28
FeO	0.22	0.12	0.18	0.21	0.13	0.12	0.13
CaO	8.44	8.96	8.38	8.34	8.49	8.10	8.60
K2O	0.12	0.15	0.22	0.19	0.20	0.17	0.19
Na2O	7.02	6.72	7.03	7.07	6.83	7.40	6.66
Al2O3	27.17	27.65	26.84	27.15	26.61	26.37	27.24
SiO2	57.09	56.56	57.32	56.59	57.00	56.70	56.88
Totals	100.05	100.15	99.97	99.55	99.26	98.87	99.70

Sample	29	30	31	32	33	34	35
FeO	0.19	0.15	0.18	0.14	0.20	0.08	0.24
CaO	8.50	8.47	8.29	8.22	8.55	8.72	8.27
K2O	0.17	0.26	0.18	0.19	0.19	0.15	0.20
Na2O	6.64	6.89	6.79	7.13	6.86	6.94	7.00
Al2O3	27.39	27.15	26.97	26.71	26.96	27.05	27.01
SiO2	57.04	56.32	57.78	56.31	56.73	56.54	56.63
Totals	99.94	99.24	100.18	98.70	99.49	99.48	99.34

Sample	36	37	38	39	40	41	42
FeO	0.14	0.14	0.14	0.02	0.19	0.15	0.18
CaO	8.56	8.65	8.50	8.27	8.49	8.52	8.30
K2O	0.24	0.19	0.18	0.17	0.20	0.20	0.19
Na2O	6.77	6.73	7.04	6.60	6.84	6.92	6.83
Al2O3	27.01	28.28	27.36	27.46	27.24	27.37	27.36
SiO2	56.83	59.29	56.80	57.44	57.14	56.94	57.31
Totals	99.55	103.27	100.03	99.96	100.10	100.10	100.17

Sample	43	44	45	46	47	48	49
FeO	0.09	0.06	0.13	0.21	0.10	0.19	0.13
CaO	8.72	8.09	8.19	8.51	8.28	8.55	8.62
K2O	0.16	0.21	0.21	0.22	0.15	0.19	0.16
Na2O	7.08	7.15	7.22	6.87	6.94	6.82	6.61
Al2O3	26.96	27.14	27.29	26.90	26.89	27.18	27.48
SiO2	57.01	57.21	57.00	56.41	56.85	57.25	56.47
Totals	100.04	99.86	100.04	99.11	99.20	100.17	99.47

Sample	50	51	52	53	54	55	56
FeO	0.17	0.13	0.08	0.14	0.26	0.21	0.15
CaO	8.61	7.93	8.52	9.22	9.46	8.63	8.83
K2O	0.20	0.22	0.14	0.21	0.17	0.14	0.15
Na2O	6.91	6.84	6.80	6.20	6.44	6.88	6.97
Al2O3	27.03	27.19	27.15	27.78	28.02	27.61	27.19
SiO2	56.91	58.01	56.50	56.18	55.40	56.32	56.40
Totals	99.82	100.33	99.19	99.73	99.74	99.79	99.69

Sample	57	58	59	60	61	62	63
FeO	0.11	0.11	0.16	0.21	0.10	0.15	0.16
CaO	8.52	9.06	9.26	9.43	8.64	8.40	8.74
K2O	0.20	0.19	0.17	0.17	0.18	0.15	0.19
Na2O	6.65	6.60	6.65	6.29	6.82	7.23	7.04

Al2O3	28.05	27.66	27.27	27.85	27.30	26.86	27.05
SiO2	56.64	56.39	55.64	56.12	56.29	57.13	56.62
Totals	100.17	100.01	99.15	100.07	99.33	99.93	99.79

Sample	64	65	66	67	68	69	70
FeO	0.14	0.16	0.26	0.11	0.20	0.17	0.15
CaO	8.40	8.64	10.49	10.37	11.33	11.51	11.12
K2O	0.18	0.20	0.10	0.12	0.12	0.10	0.12
Na2O	6.76	6.66	5.84	5.98	5.33	5.20	5.14
Al2O3	26.57	27.05	28.85	28.89	29.49	30.04	30.00
SiO2	57.08	56.33	54.28	54.34	53.72	53.05	54.53
Totals	99.13	99.03	99.82	99.81	100.19	100.07	101.06

Sample	71	72	73	74	75	76	77
FeO	0.15	0.14	0.19	0.17	0.22	0.18	0.15
CaO	11.65	11.45	10.78	8.20	7.65	7.52	7.50
K2O	0.14	0.13	0.17	0.22	0.21	0.22	0.29
Na2O	5.11	5.24	5.31	6.87	7.60	7.46	7.36
Al2O3	30.03	29.97	28.79	26.97	26.30	25.91	26.35
SiO2	52.49	53.34	53.47	57.27	58.19	58.01	58.31
Totals	99.58	100.28	98.71	99.71	100.18	99.29	99.96

LM-5-19-06-1D Plag-3 Rim to Core (El Hato)

Sample	1	2	3	4	5	6	7
FeO	0.13	0.20	0.14	0.04	0.08	0.06	0.17
CaO	7.67	8.38	7.64	8.23	8.52	7.94	8.60
K2O	0.24	0.19	0.18	0.19	0.16	0.20	0.15
Na2O	7.54	7.04	7.42	7.08	7.23	7.18	6.75
Al2O3	26.52	26.83	25.80	27.14	26.88	26.91	27.90
SiO2	57.28	57.59	57.67	57.49	57.37	57.35	56.59
Totals	99.37	100.24	98.85	100.16	100.24	99.63	100.17

Sample	8	9	10	11	12	13	14
FeO	0.07	0.16	0.15	0.18	0.18	0.13	0.10
CaO	8.57	8.13	8.75	9.74	9.58	8.89	9.27
K2O	0.19	0.18	0.16	0.17	0.18	0.16	0.18
Na2O	6.85	7.13	7.03	6.30	6.20	6.83	6.90
Al2O3	27.45	27.17	27.28	28.37	27.78	27.97	27.78
SiO2	57.16	57.09	57.32	55.70	55.82	56.45	56.33
Totals	100.29	99.85	100.69	100.46	99.75	100.42	100.56

Sample	15	16	17	18	19	20	21
FeO	0.21	0.00	0.11	0.10	0.07	0.14	0.08
CaO	10.65	9.16	8.43	8.26	8.53	7.96	7.69
K2O	0.10	0.18	0.18	0.14	0.18	0.21	0.20
Na2O	5.74	6.46	6.69	6.60	7.08	5.99	7.47
Al2O3	29.06	28.03	27.16	26.73	27.35	26.78	26.50
SiO2	54.10	56.27	57.38	57.02	58.01	57.47	58.14
Totals	99.87	100.09	99.95	98.84	101.23	98.55	100.08

Sample	22	23	24	25	26	27	28
FeO	0.17	0.25	0.21	0.19	0.16	0.15	0.17
CaO	7.17	6.69	7.36	7.72	8.89	8.66	8.62
K2O	0.22	0.24	0.28	0.21	0.13	0.14	0.18
Na2O	8.00	7.63	7.55	6.95	6.77	7.07	7.38
Al2O3	26.13	25.46	25.50	26.94	28.04	27.80	26.53
SiO2	59.06	58.90	58.54	58.09	57.55	57.02	55.94
Totals	100.74	99.16	99.44	100.09	101.54	100.83	98.82

Sample	29	30	31	32	33	34	35
FeO	0.23	0.11	0.19	0.18	0.15	0.24	0.14
CaO	8.50	8.14	8.47	8.51	8.53	8.68	9.16
K2O	0.21	0.18	0.20	0.14	0.18	0.18	0.17
Na2O	7.01	7.25	5.85	5.21	6.68	6.72	6.39
Al2O3	27.21	26.84	28.72	27.41	26.34	27.30	27.87
SiO2	57.48	58.40	60.32	56.34	53.62	57.25	55.41
Totals	100.62	100.91	103.75	97.78	95.51	100.38	99.12

Sample	36	37	38	39	40	41	42
FeO	0.14	0.21	0.24	0.04	0.14	0.15	0.15
CaO	8.24	8.31	8.70	8.81	7.72	7.46	8.32
K2O	0.21	0.20	0.19	0.15	0.22	0.17	0.19
Na2O	6.84	6.91	6.83	6.95	7.20	7.37	7.41
Al2O3	26.98	27.25	27.37	27.19	26.74	26.46	26.69
SiO2	57.26	57.50	57.08	56.17	58.61	57.88	57.63
Totals	99.67	100.39	100.41	99.30	100.63	99.50	100.38

Sample	43	44	45	46	47	48	49
FeO	0.21	0.07	0.26	0.12	0.20	0.19	0.13
CaO	8.06	8.41	8.18	8.28	8.57	8.02	7.51
K2O	0.16	0.15	0.19	0.22	0.20	0.20	0.19
Na2O	7.11	6.79	6.88	6.97	7.09	6.91	7.19
Al2O3	26.98	27.08	27.02	26.91	26.98	26.24	25.87
SiO2	57.31	56.86	56.71	57.31	57.42	56.55	58.26
Totals	99.83	99.36	99.24	99.81	100.46	98.11	99.17

Sample	50	51	52	53	54	55	56
FeO	0.23	0.10	0.16	0.11	0.15	0.12	0.20
CaO	7.16	7.40	7.32	7.59	8.22	8.99	8.66
K2O	0.22	0.26	0.27	0.21	0.19	0.18	0.19
Na2O	7.57	8.12	7.19	7.63	7.13	6.58	6.70
Al2O3	25.72	26.12	26.31	25.93	27.17	27.37	27.69
SiO2	58.90	58.22	57.87	57.89	57.38	56.76	56.35
Totals	99.81	100.22	99.12	99.36	100.24	100.01	99.80

Sample	57	58	59	60	61	62	63
FeO	0.09	0.16	0.07	0.19	0.14	0.12	0.10
CaO	9.17	9.03	8.94	8.66	8.73	8.72	8.76
K2O	0.17	0.13	0.16	0.20	0.20	0.20	0.21

Na2O	6.73	7.09	6.55	6.90	6.59	6.67	6.78
Al2O3	27.29	27.24	27.60	27.33	27.33	27.51	27.17
SiO2	56.53	55.70	56.44	56.43	56.61	55.78	56.34
Totals	99.97	99.35	99.76	99.70	99.61	99.00	99.37

Sample	64	65	66	67	68	69	70
FeO	0.14	0.12	0.18	0.07	0.15	0.07	0.17
CaO	8.99	8.61	9.05	9.04	9.40	10.57	10.36
K2O	0.14	0.19	0.20	0.17	0.15	0.13	0.13
Na2O	6.65	6.70	6.81	6.70	6.50	5.91	5.92
Al2O3	27.43	27.27	27.81	27.95	28.04	29.24	28.93
SiO2	56.70	56.09	56.15	57.03	56.26	54.66	54.85
Totals	100.04	98.98	100.19	100.96	100.50	100.57	100.36

Sample	71	72	73	74	75	76	77
FeO	0.18	0.20	0.24	0.10	0.11	0.22	0.16
CaO	9.86	10.42	13.20	14.14	13.76	8.57	13.59
K2O	0.15	0.12	0.09	0.01	0.09	0.04	0.07
Na2O	6.14	5.71	4.35	3.50	3.48	1.56	3.89
Al2O3	28.64	29.22	31.16	31.94	32.24	28.25	31.77
SiO2	54.90	53.84	51.20	50.03	49.54	43.94	50.96
Totals	99.86	99.49	100.24	99.71	99.21	82.59	100.44

Sample	78	79	80	81	82	83	84
FeO	0.28	0.04	0.13	0.19	0.05	0.23	0.08
CaO	13.03	11.20	13.65	11.96	12.48	13.38	13.75
K2O	0.09	0.08	0.08	0.09	0.08	0.09	0.05
Na2O	4.14	5.41	3.85	5.06	4.59	4.00	4.02
Al2O3	30.55	29.51	31.38	30.01	30.72	31.73	32.12
SiO2	49.99	53.42	49.78	52.50	51.79	50.51	51.12
Totals	98.09	99.66	98.87	99.81	99.71	99.95	101.15

CC-5-24-06-1X Plag-5 Rim to Core (Dacitic Domes)

Sample	1	2	3	4	5	6	7
FeO	0.13	0.26	0.25	0.37	0.24	0.19	0.13
CaO	8.41	7.15	7.89	7.30	7.84	8.03	8.63
K2O	0.21	0.25	0.23	0.25	0.27	0.20	0.20
Na2O	6.75	6.41	6.76	8.87	7.25	6.75	6.46
Al2O3	25.89	29.38	26.01	22.13	26.04	26.20	28.28
SiO2	56.75	52.54	59.17	50.74	57.57	57.61	57.81
Totals	98.13	96.00	100.31	89.66	99.21	98.97	101.52

Sample	8	9	10	11	12	13	14
FeO	0.13	0.10	0.28	0.16	0.12	0.20	0.13
CaO	8.83	7.86	8.06	8.45	8.86	8.85	9.82
K2O	0.18	0.24	0.24	0.20	0.19	0.17	0.16
Na2O	7.47	7.36	7.04	6.26	7.16	6.65	6.46
Al2O3	27.57	27.03	26.27	26.92	27.15	27.73	28.50
SiO2	56.88	56.62	57.81	57.04	56.38	55.08	55.27

Totals	101.05	99.21	99.70	99.03	99.86	98.67	100.35

Sample	15	16	17	18	19	20	21
FeO	0.22	0.15	0.16	0.19	0.12	0.11	0.21
CaO	10.22	10.11	8.08	9.40	9.92	10.31	11.16
K2O	0.17	0.17	0.25	0.15	0.19	0.11	0.14
Na2O	5.94	6.14	7.29	6.09	6.04	5.37	5.33
Al2O3	28.51	28.82	26.52	28.52	27.88	30.13	29.41
SiO2	54.37	54.29	57.24	55.26	54.69	54.22	53.14
Totals	99.44	99.68	99.54	99.61	98.85	100.24	99.39

Sample	22	23	24	25	26	27	28
FeO	0.08	0.26	0.10	0.15	0.16	0.05	0.32
CaO	11.56	11.09	7.86	8.13	7.86	7.59	8.07
K2O	0.13	0.13	0.27	0.19	0.18	0.25	0.23
Na2O	5.39	5.16	7.24	6.95	7.26	7.26	6.92
Al2O3	29.92	30.62	27.45	26.50	26.46	25.92	27.12
SiO2	53.23	53.79	57.97	57.14	58.41	57.90	57.25
Totals	100.33	101.05	100.90	99.05	100.33	98.97	99.91

Sample	29	30	31	32	33	34	35
FeO	0.12	0.25	0.18	0.07	0.18	0.24	0.15
CaO	8.39	8.44	8.41	8.40	10.33	10.66	10.01
K2O	0.20	0.21	0.22	0.18	0.13	0.12	0.18
Na2O	6.95	6.92	6.93	7.59	6.04	5.98	5.73
Al2O3	26.18	26.59	27.41	24.67	28.57	28.31	29.65
SiO2	57.01	56.45	57.56	53.01	54.71	55.14	53.53
Totals	98.86	98.86	100.72	93.92	99.95	100.45	99.24

Sample	36	37	38	39	40	41	42
FeO	0.19	0.17	0.25	0.18	0.09	0.08	0.20
CaO	9.62	9.53	10.07	9.81	9.86	9.52	10.33
K2O	0.14	0.21	0.14	0.15	0.16	0.12	0.14
Na2O	6.21	5.84	6.12	6.53	6.17	5.92	5.90
Al2O3	28.17	27.43	28.21	27.50	27.88	28.40	28.64
SiO2	55.38	55.23	55.31	55.98	55.75	55.17	55.04
Totals	99.71	98.42	100.11	100.16	99.92	99.20	100.24

Sample	43	44	45	46	47	48	49
FeO	0.10	0.18	0.24	0.12	0.23	0.24	0.13
CaO	10.75	10.39	10.76	11.28	10.40	10.92	11.26
K2O	0.11	0.11	0.10	0.15	0.13	0.12	0.16
Na2O	5.80	5.54	5.51	5.45	5.46	5.55	5.53
Al2O3	28.66	29.12	28.91	29.08	28.30	29.79	29.47
SiO2	54.59	54.37	54.03	53.46	53.17	54.28	54.16
Totals	100.02	99.70	99.55	99.53	97.70	100.91	100.71

CC-5-24-06-1X Plag-4 Rim to Core (Dacitic Domes)

Sample	1	2	3	4	5	6	7
FeO	0.31	0.33	0.43	0.35	0.36	0.24	0.36
CaO	8.37	8.46	9.14	9.14	8.53	8.02	7.78
K2O	0.25	0.24	0.22	0.23	0.19	0.21	0.26
Na2O	6.63	6.31	6.66	6.16	7.02	5.65	6.88
Al2O3	26.57	26.69	26.96	27.97	27.02	27.35	26.89
SiO2	57.03	56.08	55.87	55.24	56.37	57.24	57.77
Totals	99.16	98.11	99.27	99.10	99.49	98.71	99.94

Sample	8	9	10	11	12	13	14
FeO	0.18	0.23	0.18	0.13	0.13	0.16	0.14
CaO	8.09	8.22	8.80	8.12	8.03	7.83	7.81
K2O	0.22	0.24	0.22	0.22	0.19	0.22	0.21
Na2O	7.03	6.86	6.61	7.09	7.26	7.29	7.11
Al2O3	26.77	26.38	26.87	26.74	26.46	25.68	26.56
SiO2	57.10	56.71	57.09	57.90	57.23	57.56	57.39
Totals	99.39	98.63	99.77	100.20	99.30	98.74	99.23

Sample	15	16	17	18	19	20	21
FeO	0.20	0.09	0.16	0.11	0.16	0.12	0.00
CaO	8.39	7.80	8.41	8.67	9.01	8.63	8.93
K2O	0.22	0.18	0.24	0.19	0.21	0.25	0.20
Na2O	7.04	6.87	6.62	6.48	6.93	6.77	6.35
Al2O3	27.27	26.53	26.59	27.02	27.17	27.03	27.10
SiO2	57.62	57.24	55.70	56.10	56.93	56.67	56.37
Totals	100.73	98.72	97.72	98.57	100.40	99.47	98.94

Sample	22	23	24	25	26	27	28
FeO	0.13	0.14	0.02	0.17	0.08	0.18	0.16
CaO	8.48	9.00	8.63	8.40	8.81	8.38	7.91
K2O	0.18	0.23	0.17	0.25	0.23	0.21	0.23
Na2O	6.50	6.42	6.66	7.03	7.09	7.16	7.15
Al2O3	27.75	28.42	27.39	26.87	26.83	27.80	27.95
SiO2	56.02	56.29	56.53	56.12	56.94	57.16	56.76
Totals	99.07	100.50	99.41	98.84	99.98	100.90	100.17

Sample	29	30	31	32	33	34	35
FeO	0.03	0.11	0.06	0.16	0.07	0.19	0.24
CaO	8.58	8.45	8.37	8.05	6.67	6.42	7.69
K2O	0.27	0.19	0.25	0.21	0.23	0.24	0.25
Na2O	6.79	6.85	6.23	6.80	7.71	8.26	8.04
Al2O3	27.02	26.72	26.68	27.32	24.87	21.67	24.11
SiO2	56.76	56.56	54.32	57.14	58.90	49.83	50.22
Totals	99.45	98.87	95.90	99.68	98.45	86.61	90.55

Sample	36	37	38	39	40	41	42
FeO	0.66	0.22	0.31	0.12	0.11	0.18	0.12

CaO	3.40	7.57	7.78	7.90	6.69	6.90	6.89
K2O	1.71	0.26	0.22	0.25	0.29	0.24	0.24
Na2O	4.70	7.24	7.36	6.96	7.73	7.44	7.34
Al2O3	17.38	26.72	26.84	27.17	25.21	25.45	26.12
SiO2	72.58	57.50	57.03	57.10	59.48	59.31	58.93
Totals	100.43	99.52	99.55	99.49	99.53	99.52	99.62

Sample	43	44	45	46	47	48	49
FeO	0.07	0.24	0.17	0.29	0.03	0.16	0.16
CaO	6.52	7.16	6.76	8.00	8.04	8.38	9.21
K2O	0.19	0.26	0.25	0.21	0.20	0.18	0.14
Na2O	7.39	7.56	7.71	7.08	6.57	6.59	6.74
Al2O3	26.04	25.87	26.70	27.18	26.25	27.06	28.14
SiO2	59.00	58.67	58.86	57.87	55.96	56.32	55.82
Totals	99.22	99.77	100.46	100.63	97.05	98.69	100.21

Sample	50	51	52	53	54	55	56
FeO	0.08	0.19	0.19	0.15	0.10	0.06	0.11
CaO	8.06	8.58	8.41	8.64	9.05	9.93	8.18
K2O	0.19	0.18	0.12	0.16	0.12	0.16	0.17
Na2O	5.76	6.22	6.89	6.84	6.87	6.27	7.06
Al2O3	26.26	27.49	27.49	27.53	27.68	24.31	27.39
SiO2	56.02	56.82	56.54	55.96	55.00	49.12	57.22
Totals	96.37	99.48	99.66	99.28	98.82	89.85	100.12

Sample	57	58	59	60	61	62	63
FeO	0.13	0.20	0.17	0.24	0.12	0.23	0.12
CaO	8.40	8.06	8.99	8.19	8.73	8.07	9.04
K2O	0.23	0.22	0.19	0.14	0.15	0.21	0.11
Na2O	7.40	7.26	7.30	6.91	6.63	7.11	6.47
Al2O3	27.37	27.22	26.69	27.78	27.88	27.59	27.24
SiO2	57.75	56.89	55.78	56.61	56.41	56.98	55.87
Totals	101.27	99.84	99.12	99.86	99.92	100.19	98.86

Sample	64	65	66	67	68	69	70
FeO	0.07	0.08	0.16	0.16	0.26	0.07	0.13
CaO	9.78	9.45	9.19	8.55	7.78	8.60	10.90
K2O	0.13	0.17	0.16	0.23	0.26	0.14	0.10
Na2O	5.96	5.97	6.12	6.63	7.30	6.72	5.48
Al2O3	29.35	27.96	27.79	27.69	27.20	27.20	28.91
SiO2	53.91	55.34	54.67	56.88	57.31	57.23	53.50
Totals	99.20	98.97	98.09	100.13	100.10	99.96	99.02

Sample	71	72	73	74	75	76	77
FeO	0.10	0.06	0.15	0.28	0.15	0.23	0.18
CaO	8.45	9.01	9.62	8.89	9.20	8.47	8.57
K2O	0.12	0.17	0.17	0.15	0.17	0.17	0.18
Na2O	6.92	6.50	6.67	6.10	6.41	6.10	5.80
Al2O3	27.15	27.73	27.71	28.00	28.44	25.52	29.93
SiO2	56.53	56.15	55.66	55.34	55.57	50.26	60.10

Totals	99.27	99.63	99.98	98.75	99.94	90.74	104.75

CC-5-24-06-1X Plag-3 Rim to Core (Dacitic Domes)

Sample	1	2	3	4	5	6	7
FeO	0.26	0.16	0.14	0.11	0.15	0.26	0.47
CaO	9.03	8.40	6.95	8.06	7.45	8.76	4.27
K2O	0.22	0.22	0.26	0.30	0.23	0.20	0.14
Na2O	6.78	6.81	7.58	6.90	7.42	6.63	2.88
Al2O3	28.00	26.92	25.29	26.60	26.03	26.38	23.77
SiO2	56.38	56.68	59.18	57.76	58.04	57.73	38.45
Totals	100.66	99.20	99.41	99.73	99.32	99.95	69.99

Sample	8	9	10	11	12	13	14
FeO	0.12	0.20	0.28	0.19	0.27	0.21	0.13
CaO	7.67	7.91	8.06	7.98	7.62	8.10	7.79
K2O	0.25	0.18	0.24	0.22	0.24	0.17	0.22
Na2O	6.61	6.45	6.85	6.77	7.21	6.81	7.20
Al2O3	26.61	24.33	26.81	26.09	26.33	27.16	26.67
SiO2	58.83	53.45	58.77	56.57	57.55	57.42	58.11
Totals	100.09	92.52	101.01	97.83	99.21	99.88	100.12

Sample	15	16	17	18	19	20	21
FeO	0.12	0.16	0.11	0.12	0.15	0.18	0.25
CaO	7.77	8.64	8.15	7.50	7.54	8.39	8.26
K2O	0.23	0.25	0.23	0.21	0.18	0.22	0.21
Na2O	6.88	6.94	7.04	7.50	7.13	6.71	6.70
Al2O3	26.16	26.41	26.61	27.06	25.80	27.12	27.22
SiO2	56.96	56.63	56.50	57.97	57.01	57.25	56.90
Totals	98.12	99.04	98.63	100.36	97.81	99.86	99.53

Sample	22	23	24	25	26	27	28
FeO	0.13	0.25	0.16	0.15	0.15	0.14	0.17
CaO	8.86	8.61	8.33	8.73	8.32	8.36	8.16
K2O	0.20	0.19	0.20	0.21	0.20	0.22	0.23
Na2O	6.67	6.80	6.85	6.51	7.06	6.34	7.38
Al2O3	27.03	26.34	27.18	27.28	27.46	27.86	25.98
SiO2	57.25	56.20	56.96	57.08	57.66	57.68	56.62
Totals	100.15	98.40	99.68	99.96	100.85	100.59	98.53

Sample	29	30	31	32	33	34	35
FeO	0.19	0.13	0.24	0.12	0.15	0.12	0.07
CaO	8.86	9.05	9.20	8.21	8.19	8.42	8.27
K2O	0.20	0.17	0.19	0.23	0.20	0.13	0.19
Na2O	6.88	6.89	6.46	6.80	6.85	6.82	6.84
Al2O3	27.75	27.47	27.51	26.25	26.26	26.79	26.41
SiO2	56.50	56.77	55.89	56.99	56.71	57.47	56.71
Totals	100.37	100.49	99.48	98.60	98.35	99.75	98.49

Sample	36	37	38	39	40	41	42
FeO	0.13	0.14	0.07	0.17	0.15	0.12	0.23
CaO	11.17	9.43	8.36	7.90	8.47	8.32	8.73
K2O	0.15	0.17	0.21	0.20	0.20	0.15	0.14
Na2O	5.53	6.15	6.83	6.54	7.02	7.00	6.96
Al2O3	28.52	28.74	26.43	27.03	27.24	27.05	27.46
SiO2	54.18	55.41	56.76	56.53	56.83	56.33	57.44
Totals	99.69	100.02	98.66	98.37	99.91	98.96	100.97

Sample	43	44	45	46	47	48	49
FeO	0.16	0.23	0.19	0.18	0.27	0.17	0.16
CaO	8.49	9.22	8.85	8.19	8.33	8.44	8.26
K2O	0.17	0.19	0.22	0.18	0.18	0.16	0.13
Na2O	6.74	6.58	6.64	7.08	6.99	6.71	6.94
Al2O3	27.44	28.47	27.26	27.17	27.92	27.92	27.87
SiO2	56.48	56.17	56.40	56.80	57.15	58.22	56.00
Totals	99.47	100.86	99.56	99.60	100.84	101.62	99.36

Sample	50	51	52	53	54	55	56
FeO	0.13	0.25	0.07	0.04	0.11	0.10	0.19
CaO	8.59	7.68	7.72	8.11	7.94	7.81	7.50
K2O	0.21	0.22	0.25	0.19	0.18	0.19	0.18
Na2O	7.14	7.22	7.38	7.33	7.10	6.93	7.37
Al2O3	27.07	26.02	26.13	26.83	26.55	26.03	25.08
SiO2	56.86	57.21	57.80	57.57	57.88	57.26	57.66
Totals	99.99	98.60	99.34	100.07	99.77	98.32	97.98

Sample	57	58	59	60	61	62	63
FeO	0.14	0.13	0.19	0.16	0.10	0.15	0.31
CaO	7.59	7.59	7.36	7.45	7.26	7.29	7.05
K2O	0.20	0.24	0.22	0.23	0.19	0.24	0.22
Na2O	7.63	7.56	7.11	7.44	7.07	6.66	7.58
Al2O3	26.48	26.25	25.80	26.54	26.50	26.66	26.25
SiO2	58.44	58.46	59.10	57.62	57.97	58.13	58.25
Totals	100.49	100.23	99.77	99.43	99.09	99.12	99.66

Sample	64	65	66	67	68	69	70
FeO	0.08	0.12	0.06	0.08	0.18	0.15	0.32
CaO	7.03	7.47	8.15	7.95	7.99	7.98	8.55
K2O	0.24	0.23	0.22	0.23	0.22	0.21	0.16
Na2O	7.93	7.15	7.31	6.90	6.94	6.64	6.65
Al2O3	25.11	25.79	26.55	27.19	26.87	27.18	28.05
SiO2	56.53	57.29	57.94	56.93	56.83	56.96	57.07
Totals	96.92	98.05	100.23	99.27	99.03	99.11	100.80

Sample	71	72	73	74	75	76	77
FeO	0.16	0.13	0.14	0.06	0.11	0.05	0.19
CaO	8.27	8.26	8.72	8.39	8.92	8.97	8.69
K2O	0.26	0.19	0.17	0.15	0.20	0.20	0.20
Na2O	6.97	6.70	6.80	6.51	6.80	6.72	6.75

Al2O3	27.34	27.16	27.08	25.80	27.34	27.34	27.98
SiO2	57.29	57.71	56.03	53.28	56.28	56.04	56.49
Totals	100.29	100.16	98.94	94.17	99.64	99.33	100.31

Sample	78	79	80	81	82	83	84
FeO	0.13	0.19	0.23	0.19	0.09	0.20	0.12
CaO	8.92	9.13	9.29	8.74	8.88	9.30	8.70
K2O	0.18	0.17	0.19	0.16	0.17	0.17	0.20
Na2O	6.51	6.74	6.65	6.51	6.66	6.68	6.85
Al2O3	27.86	27.19	27.38	27.89	27.83	27.57	27.80
SiO2	56.36	54.67	55.96	55.99	56.31	55.93	56.91
Totals	99.95	98.09	99.70	99.47	99.94	99.84	100.57

Sample	85	86	87	88	89	90	91
FeO	0.15	0.05	0.09	0.14	0.17	0.10	0.21
CaO	9.19	9.01	9.14	9.01	8.90	8.93	8.53
K2O	0.21	0.17	0.21	0.19	0.20	0.21	0.17
Na2O	6.61	6.81	6.65	6.62	6.65	6.39	6.40
Al2O3	28.46	27.76	27.88	27.24	27.83	27.34	27.60
SiO2	56.40	56.43	56.26	56.63	56.15	56.13	55.70
Totals	101.03	100.23	100.23	99.83	99.90	99.11	98.62

Sample	92	93	94	95	96	97	98
FeO	0.09	0.20	0.22	0.18	0.08	0.21	0.15
CaO	9.18	9.16	10.09	9.79	8.58	7.82	7.37
K2O	0.16	0.18	0.16	0.14	0.19	0.17	0.24
Na2O	6.56	6.39	6.33	6.23	6.95	6.88	7.17
Al2O3	27.62	27.34	28.56	28.03	27.68	26.59	26.00
SiO2	56.06	55.61	56.12	54.98	56.33	56.68	58.40
Totals	99.68	98.87	101.48	99.35	99.82	98.35	99.33

Sample	99	100	101	102	103	104	105
FeO	0.20	0.19	0.10	0.15	0.00	0.10	0.01
CaO	7.46	7.42	7.30	7.18	7.41	7.38	6.91
K2O	0.23	0.19	0.20	0.21	0.32	0.25	0.23
Na2O	7.14	7.34	7.39	7.01	7.42	7.23	7.22
Al2O3	25.86	26.03	26.05	26.02	25.59	26.55	26.15
SiO2	57.87	58.13	58.16	59.38	57.99	58.39	58.93
Totals	98.75	99.30	99.20	99.94	98.73	99.90	99.46

Sample	106	107	108	109	110	111	112
FeO	0.22	0.19	0.08	0.15	0.20	0.07	0.22
CaO	6.98	7.72	7.20	7.30	7.40	7.43	7.34
K2O	0.21	0.25	0.26	0.28	0.25	0.26	0.23
Na2O	7.92	7.38	7.31	7.61	7.30	7.41	7.56
Al2O3	25.72	24.81	25.65	26.54	25.81	26.76	26.08
SiO2	58.58	58.06	58.04	58.37	58.23	57.67	58.76
Totals	99.63	98.42	98.55	100.25	99.19	99.60	100.19

Sample	113	114	115	116	117	118	119
FeO	0.14	0.11	0.15	0.17	0.17	0.31	0.23
CaO	7.65	7.14	8.80	9.48	9.81	8.92	7.78
K2O	0.25	0.27	0.19	0.21	0.25	0.22	0.23
Na2O	7.20	7.63	6.53	6.32	6.25	6.89	6.90
Al2O3	25.66	25.04	27.16	28.82	28.38	26.48	26.96
SiO2	58.02	59.07	56.33	57.11	55.77	56.68	57.56
Totals	98.93	99.25	99.16	102.11	100.65	99.50	99.65

ID-6-3-06-1B Plag-6 Rim to Core (El Hato)

Sample	1	2	3	4	5	6	7
FeO	0.24	0.14	0.10	0.19	0.15	0.17	0.12
CaO	7.79	7.80	7.85	7.47	7.50	8.57	8.42
K2O	0.23	0.26	0.24	0.19	0.22	0.18	0.19
Na2O	7.59	7.26	7.78	7.62	7.60	6.77	7.30
Al2O3	26.79	25.76	25.15	26.32	26.18	27.23	26.56
SiO2	57.79	58.34	57.44	58.59	59.06	57.03	57.93
Totals	100.43	99.57	98.56	100.37	100.69	99.95	100.54

Sample	8	9	10	11	12	13	14
FeO	0.18	0.09	0.10	0.10	0.20	0.19	0.09
CaO	8.19	8.02	7.09	8.83	7.82	7.31	7.77
K2O	0.21	0.22	0.22	0.19	0.21	0.22	0.19
Na2O	7.22	7.21	7.45	6.89	7.25	6.95	7.75
Al2O3	26.44	26.82	26.38	26.65	26.97	26.72	26.91
SiO2	57.92	57.32	58.23	57.34	57.93	59.37	57.23
Totals	100.16	99.67	99.47	100.00	100.37	100.76	99.95

Sample	15	16	17	18	19	20	21
FeO	0.12	0.02	0.18	0.17	0.14	0.15	0.08
CaO	8.28	8.14	7.69	7.80	8.11	8.38	8.18
K2O	0.20	0.20	0.25	0.25	0.22	0.17	0.24
Na2O	6.99	7.40	7.22	7.71	7.10	7.46	7.39
Al2O3	26.15	25.92	25.68	26.71	26.09	26.32	26.03
SiO2	57.79	57.73	57.86	58.46	58.08	57.86	57.40
Totals	99.53	99.41	98.88	101.11	99.75	100.34	99.31

Sample	22	23	24	25	26	27	28
FeO	0.26	0.20	0.28	0.23	0.20	0.27	0.17
CaO	8.74	8.21	7.81	8.15	8.18	8.38	8.42
K2O	0.15	0.18	0.16	0.20	0.20	0.18	0.16
Na2O	6.57	7.12	7.24	7.22	7.08	7.40	7.19
Al2O3	27.19	27.48	27.05	25.79	26.87	26.09	26.69
SiO2	56.56	56.93	57.76	57.38	57.15	57.42	58.01
Totals	99.47	100.12	100.30	98.97	99.68	99.75	100.64

Sample	29	30	31	32	33	34	35
FeO	0.15	0.18	0.14	0.19	0.12	0.05	0.14
CaO	8.20	8.52	8.30	8.18	8.24	8.49	7.96
K2O	0.21	0.20	0.21	0.20	0.20	0.21	0.22

Na2O	6.95	6.88	6.94	7.00	7.05	7.29	7.12
Al2O3	26.25	26.48	27.09	26.35	27.34	27.74	26.59
SiO2	57.54	56.86	57.66	56.80	57.58	57.59	57.20
Totals	99.30	99.12	100.34	98.73	100.54	101.36	99.22

Sample	36	37	38	39	40	41	42
FeO	0.07	0.17	0.16	0.30	0.14	0.09	0.19
CaO	7.96	8.79	8.97	9.38	9.66	10.24	9.40
K2O	0.17	0.18	0.15	0.14	0.15	0.13	0.13
Na2O	7.28	6.71	6.32	6.26	6.49	6.06	6.34
Al2O3	27.01	27.25	27.33	28.08	28.11	27.41	27.91
SiO2	58.04	57.55	56.08	56.10	55.79	55.52	55.97
Totals	100.53	100.65	99.01	100.26	100.33	99.46	99.93

Sample	43	44	45	46	47	48	49
FeO	0.28	0.05	0.09	0.18	0.11	0.17	0.06
CaO	10.33	9.30	9.93	9.45	10.22	9.27	9.80
K2O	0.19	0.13	0.20	0.12	0.18	0.24	0.10
Na2O	6.36	5.87	6.30	6.13	6.12	6.57	6.05
Al2O3	28.34	27.49	28.22	28.53	28.28	27.74	28.54
SiO2	55.59	55.33	56.00	56.20	55.28	56.32	55.41
Totals	101.10	98.18	100.75	100.60	100.19	100.31	99.96

Sample	50	51	52	53	54	55	56
FeO	0.11	0.16	0.09	0.10	0.25	0.13	0.18
CaO	9.86	10.55	7.52	7.28	7.27	6.73	7.27
K2O	0.14	0.12	0.27	0.22	0.23	0.29	0.26
Na2O	6.35	5.89	7.23	7.65	7.71	7.38	7.72
Al2O3	27.65	28.38	26.40	25.18	26.00	26.32	26.06
SiO2	55.69	54.16	58.86	59.03	58.83	61.12	59.37
Totals	99.80	99.26	100.37	99.45	100.29	101.96	100.86

Sample	57	58	59	60	61	62	63
FeO	0.21	0.12	0.07	0.19	0.22	0.17	0.15
CaO	7.19	7.24	7.78	7.80	8.62	8.64	8.24
K2O	0.22	0.24	0.22	0.18	0.18	0.15	0.19
Na2O	7.33	7.37	7.50	7.25	7.27	6.80	7.00
Al2O3	25.87	25.67	26.70	26.79	26.71	26.79	27.08
SiO2	59.13	58.88	59.19	58.34	57.06	57.10	57.36
Totals	99.96	99.53	101.46	100.55	100.07	99.64	100.02

Sample	64	65	66	67	68	69	70
FeO	0.13	0.22	0.15	0.22	0.15	0.10	0.08
CaO	8.50	8.70	8.77	8.74	8.77	9.14	9.08
K2O	0.16	0.14	0.19	0.18	0.20	0.23	0.20
Na2O	6.21	6.62	6.85	6.54	6.81	7.00	6.50
Al2O3	26.59	27.64	27.28	27.17	27.58	27.38	27.39
SiO2	56.70	56.79	56.28	57.33	57.01	56.65	57.40
Totals	98.29	100.10	99.52	100.18	100.53	100.49	100.66

Sample	71	72	73	74	75	76	77
FeO	0.11	0.09	0.13	0.08	0.13	0.10	0.11
CaO	8.43	7.42	7.57	8.06	8.05	7.73	8.02
K2O	0.21	0.25	0.27	0.25	0.23	0.22	0.24
Na2O	7.09	7.58	7.48	7.35	7.41	7.22	7.18
Al2O3	27.48	25.84	26.00	26.54	27.31	26.25	26.63
SiO2	57.56	58.31	58.72	58.18	58.89	57.59	58.65
Totals	100.87	99.48	100.17	100.45	102.01	99.11	100.84

Sample	78	79	80	81	82	83	84
FeO	0.11	0.25	0.20	0.07	0.16	0.12	0.07
CaO	8.00	7.59	7.13	7.36	7.15	7.56	7.52
K2O	0.23	0.19	0.20	0.22	0.22	0.24	0.22
Na2O	7.15	7.11	7.48	7.41	7.56	7.50	7.18
Al2O3	25.75	26.33	25.91	24.89	25.41	25.58	25.50
SiO2	57.65	57.51	59.06	58.52	58.04	59.03	58.00
Totals	98.88	98.98	99.98	98.46	98.55	100.03	98.50

Sample	85	86	87	88	89	90	91
FeO	0.21	0.13	0.18	0.11	0.14	0.09	0.11
CaO	7.77	7.16	6.98	6.86	8.59	8.38	8.75
K2O	0.25	0.24	0.26	0.17	0.26	0.20	0.18
Na2O	7.06	7.59	7.71	7.51	7.23	6.84	6.87
Al2O3	26.30	25.88	25.52	26.14	26.44	27.05	27.59
SiO2	58.79	59.15	58.67	59.12	57.66	56.58	56.39
Totals	100.37	100.14	99.32	99.92	100.33	99.14	99.90

Sample	92	93	94	95	96	97	98
FeO	0.32	0.11	0.15	0.23	0.14	0.23	0.16
CaO	8.66	8.72	9.19	9.86	8.08	8.04	9.18
K2O	0.19	0.18	0.17	0.13	0.22	0.19	0.18
Na2O	6.47	6.64	6.64	6.23	7.13	7.39	7.13
Al2O3	27.06	27.27	28.08	27.90	25.85	26.72	27.64
SiO2	56.26	56.78	56.79	55.52	57.55	58.07	56.70
Totals	98.96	99.70	101.02	99.87	98.96	100.65	100.99

Sample	99	100	101	102	103	104	105
FeO	0.18	0.30	0.10	0.18	0.11	0.14	0.18
CaO	8.08	8.73	8.34	9.46	9.26	8.78	8.35
K2O	0.22	0.18	0.19	0.12	0.18	0.12	0.19
Na2O	6.96	6.64	6.89	6.45	6.87	6.93	6.98
Al2O3	26.41	27.02	26.43	27.49	28.11	27.03	26.61
SiO2	57.42	56.97	56.79	55.79	55.90	57.04	56.96
Totals	99.27	99.84	98.73	99.47	100.44	100.03	99.28

Sample	106	107	108	109	110	111	112
FeO	0.11	0.17	0.08	0.05	0.11	0.12	0.06
CaO	8.96	8.44	8.10	8.64	8.77	8.26	8.90
K2O	0.18	0.18	0.20	0.20	0.21	0.48	0.21

Na2O	6.77	6.48	6.78	6.85	6.78	7.11	6.81
Al2O3	27.13	27.10	27.41	26.89	26.31	26.85	26.62
SiO2	56.83	56.52	57.48	56.96	56.62	55.53	56.77
Totals	99.98	98.89	100.05	99.59	98.81	98.34	99.36

Sample	113	114	115	116	117	118	119
FeO	0.18	0.08	0.13	0.12	0.08	0.16	0.20
CaO	9.03	8.84	8.69	9.14	9.33	8.68	7.86
K2O	0.23	0.15	0.16	0.17	0.22	0.15	0.21
Na2O	6.92	6.84	6.96	6.91	6.69	6.70	6.45
Al2O3	26.96	27.34	26.82	27.15	27.17	26.10	24.68
SiO2	56.68	56.26	56.48	56.02	55.98	56.80	51.92
Totals	100.00	99.51	99.23	99.52	99.47	98.59	91.31

Sample	120	121	122	123	124	125	126
FeO	0.02	0.19	0.21	0.07	0.17	0.24	0.15
CaO	6.52	8.97	9.00	8.69	8.72	8.72	8.69
K2O	0.13	0.14	0.16	0.16	0.17	0.18	0.19
Na2O	5.44	6.31	6.44	6.58	6.79	6.82	6.69
Al2O3	20.62	27.60	26.73	26.31	26.70	26.85	26.65
SiO2	43.70	55.55	56.35	56.93	56.54	56.98	56.85
Totals	76.44	98.77	98.89	98.75	99.11	99.78	99.22

Sample	127	128	129	130	131	132
FeO	0.20	0.12	0.22	0.15	0.20	0.14
CaO	8.65	8.52	8.63	8.39	8.56	8.55
K2O	0.17	0.18	0.18	0.16	0.15	0.18
Na2O	6.78	6.25	7.05	6.79	6.77	7.07
Al2O3	27.38	28.28	27.26	27.76	26.69	26.74
SiO2	59.17	59.26	57.06	57.48	56.60	57.11
Totals	102.35	102.61	100.40	100.73	98.98	99.80

ID-6-3-06-1B Plag-3 Rim to Core (El Hato)

Sample	1	2	3	4	5	6	7
FeO	0.29	0.35	0.28	0.22	0.20	0.27	0.08
CaO	7.12	7.74	8.49	8.10	8.10	8.78	8.16
K2O	0.27	0.24	0.20	0.23	0.23	0.24	0.17
Na2O	7.39	7.36	7.17	7.25	7.31	6.74	6.96
Al2O3	25.67	26.17	26.74	26.33	24.10	27.59	28.15
SiO2	58.99	58.19	57.43	58.61	53.03	57.06	57.67
Totals	99.73	100.05	100.31	100.74	92.96	100.67	101.20

Sample	8	9	10	11	12	13	14
FeO	0.13	0.21	0.14	0.12	0.14	0.17	0.07
CaO	8.20	8.24	8.53	8.04	8.87	7.63	7.86
K2O	0.20	0.18	0.15	0.17	0.20	0.19	0.20
Na2O	7.27	7.22	6.62	7.18	7.00	7.26	7.28
Al2O3	26.29	27.40	27.16	26.44	26.92	26.09	25.83
SiO2	57.94	57.23	56.16	57.29	57.33	58.47	58.93
Totals	100.02	100.48	98.76	99.24	100.46	99.80	100.17

Sample	15	16	17	18	19	20	21
FeO	0.36	0.19	0.17	0.12	0.16	0.13	0.19
CaO	7.77	8.40	8.22	7.61	7.48	7.99	9.02
K2O	0.23	0.23	0.20	0.19	0.15	0.23	0.21
Na2O	7.22	6.96	7.26	5.26	6.42	7.33	6.91
Al2O3	26.43	26.65	26.33	19.39	25.74	26.55	28.09
SiO2	57.79	56.77	57.68	41.71	57.32	57.62	56.58
Totals	99.79	99.20	99.86	74.28	97.27	99.85	101.01

Sample	22	23	24	25	26	27	28
FeO	0.13	1.04	0.44	0.27	0.16	0.20	0.06
CaO	8.98	1.38	7.32	9.75	9.15	7.33	7.65
K2O	0.13	1.04	0.41	0.15	0.15	0.20	0.20
Na2O	6.62	1.58	5.53	6.04	6.27	7.52	7.50
Al2O3	27.69	12.68	25.08	28.49	27.69	25.91	26.22
SiO2	56.16	70.18	61.59	55.77	56.18	58.98	58.84
Totals	99.71	87.90	100.38	100.47	99.61	100.14	100.48

Sample	29	30	31	32	33	34	35
FeO	0.13	0.20	0.19	0.11	0.11	0.17	0.09
CaO	7.43	7.10	7.58	7.72	7.48	7.65	7.89
K2O	0.21	0.27	0.23	0.24	0.23	0.24	0.20
Na2O	7.08	7.34	7.46	8.04	7.44	7.44	7.29
Al2O3	26.12	26.81	26.80	24.98	26.53	26.57	25.65
SiO2	58.25	59.01	58.57	55.95	58.09	58.85	58.91
Totals	99.22	100.73	100.83	97.04	99.87	100.91	100.03

Sample	36	37	38	39	40	41	42
FeO	0.14	0.15	0.17	0.10	0.08	0.07	0.18
CaO	7.58	7.46	7.23	7.35	8.12	8.14	8.33
K2O	0.21	0.27	0.25	0.22	0.23	0.15	0.16
Na2O	7.56	7.51	7.64	7.52	7.01	6.89	6.76
Al2O3	25.68	25.76	25.52	25.76	26.25	26.42	27.58
SiO2	58.62	58.97	58.97	59.50	57.65	57.27	57.51
Totals	99.79	100.12	99.79	100.46	99.36	98.93	100.53

Sample	43	44	45	46	47
FeO	0.17	0.12	0.11	0.28	0.24
CaO	8.26	8.47	8.57	8.40	8.81
K2O	0.18	0.24	0.20	0.16	0.16
Na2O	6.89	6.76	6.67	7.34	7.26
Al2O3	27.54	26.51	27.77	25.94	27.27
SiO2	57.06	56.73	56.80	52.98	57.42
Totals	100.10	98.84	100.12	95.09	101.16

ID-6-3-06-1B Plag-2 Rim to Core (El Hato)

Sample	1	2	3	4	5	6	7
FeO	0.80	0.19	0.15	0.18	0.20	0.22	0.07
CaO	1.51	7.95	8.45	7.88	7.31	8.40	8.23
K2O	1.75	0.21	0.22	0.18	0.25	0.20	0.23
Na2O	3.00	6.99	6.88	7.17	7.23	6.78	7.06
Al2O3	13.31	25.37	27.02	26.08	26.58	26.45	26.81
SiO2	75.37	57.80	57.12	57.66	58.28	55.12	57.94
Totals	95.75	98.51	99.83	99.14	99.84	97.17	100.35

Sample	8	9	10	11	12	13	14
FeO	0.14	0.01	0.09	0.21	0.13	0.09	0.28
CaO	8.75	7.79	7.93	7.81	8.21	8.26	8.31
K2O	0.26	0.18	0.18	0.16	0.18	0.24	0.23
Na2O	6.89	6.78	7.48	7.13	7.11	7.06	6.89
Al2O3	26.89	26.86	26.55	26.74	26.98	26.65	27.25
SiO2	57.52	57.60	57.43	58.22	56.97	57.88	57.70
Totals	100.45	99.22	99.66	100.27	99.58	100.17	100.65

Sample	15	16	17	18	19	20	21
FeO	0.18	0.20	0.05	0.27	0.09	0.11	0.13
CaO	8.02	7.83	8.08	8.03	7.71	7.84	7.87
K2O	0.24	0.22	0.17	0.23	0.23	0.18	0.22
Na2O	7.04	7.04	7.32	7.15	7.29	7.37	7.36
Al2O3	26.60	26.79	26.87	25.75	26.64	26.53	26.13
SiO2	58.60	57.48	58.12	58.38	57.65	57.93	58.84
Totals	100.67	99.57	100.61	99.80	99.61	99.95	100.56

Sample	22	23	24	25	26	27	28
FeO	0.15	0.03	0.10	0.20	0.07	0.10	0.14
CaO	6.43	7.98	8.50	8.04	7.76	8.26	7.48
K2O	0.21	0.19	0.19	0.22	0.25	0.21	0.18
Na2O	5.72	6.79	7.26	7.39	7.29	7.17	7.41
Al2O3	21.80	26.79	27.08	26.03	26.51	26.94	26.33
SiO2	50.73	57.16	57.12	58.63	58.43	57.96	58.45
Totals	85.03	98.95	100.26	100.50	100.32	100.63	99.99

Sample	29	30	31	32	33	34	35
FeO	0.11	0.12	0.21	0.07	0.11	0.05	0.00
CaO	7.74	7.24	8.12	8.56	8.14	8.10	7.92
K2O	0.26	0.18	0.20	0.21	0.18	0.18	0.18
Na2O	7.68	4.67	7.05	6.65	6.78	7.18	7.33
Al2O3	25.91	25.08	27.73	27.84	27.00	26.45	26.65
SiO2	58.12	55.82	58.73	57.50	58.07	57.31	58.75
Totals	99.83	93.10	102.05	100.83	100.28	99.26	100.85

Sample	36	37	38	39	40	41	42
FeO	0.14	0.29	0.25	0.11	0.13	0.21	0.24
CaO	8.00	7.42	7.32	7.55	7.80	7.51	8.46

K2O	0.20	0.24	0.23	0.19	0.22	0.24	0.19
Na2O	7.51	7.42	7.27	7.32	7.30	7.44	7.05
Al2O3	26.92	25.81	26.33	25.96	26.80	26.91	26.71
SiO2	59.20	57.94	57.89	58.50	58.28	58.52	57.37
Totals	101.96	99.12	99.29	99.63	100.52	100.82	100.02

Sample	43	44	45	46	47	48	49
FeO	0.25	0.16	0.16	0.14	0.26	0.10	0.13
CaO	8.52	7.53	8.15	8.19	8.40	7.87	7.38
K2O	0.19	0.22	0.20	0.18	0.21	0.20	0.20
Na2O	7.18	7.14	7.46	6.80	6.81	7.01	7.38
Al2O3	26.79	25.67	25.71	27.12	26.51	26.20	26.50
SiO2	58.05	57.94	58.21	57.63	57.65	58.46	59.03
Totals	100.99	98.66	99.88	100.06	99.84	99.84	100.62

Sample	50	51	52	53	54	55	56
FeO	0.21	0.18	0.18	0.12	0.09	0.14	0.18
CaO	7.31	7.39	8.54	6.29	7.22	7.49	7.92
K2O	0.23	0.22	0.18	0.19	0.21	0.20	0.21
Na2O	7.30	7.52	7.13	5.40	7.35	6.54	7.56
Al2O3	26.46	25.75	26.80	21.78	25.18	25.36	26.27
SiO2	58.87	57.87	57.95	49.08	58.19	56.84	58.29
Totals	100.37	98.92	100.77	82.85	98.25	96.58	100.43

Sample	57	58	59
FeO	0.15	0.14	0.16
CaO	7.82	7.82	8.07
K2O	0.24	0.23	0.18
Na2O	7.40	7.06	7.13
Al2O3	26.39	26.27	26.86
SiO2	58.37	58.25	57.61
Totals	100.35	99.78	100.01

ID-6-3-06-1B Plag-1 Rim to Core (El Hato)

Sample	1	2	3	4	5	6	7
FeO	0.25	0.20	0.07	0.14	0.02	0.13	0.03
CaO	10.65	7.54	8.29	8.48	8.95	9.12	9.18
K2O	0.14	0.21	0.21	0.16	0.20	0.22	0.20
Na2O	5.39	7.64	6.40	6.78	6.80	6.46	6.57
Al2O3	29.01	26.01	25.81	27.02	27.28	27.90	27.83
SiO2	54.68	58.87	54.90	57.05	57.12	56.83	56.85
Totals	100.10	100.46	95.67	99.63	100.37	100.67	100.66

Sample	8	9	10	11	12	13	14
FeO	0.05	0.02	0.05	0.23	0.14	0.11	0.12
CaO	10.78	10.88	8.18	8.92	9.55	10.04	7.79
K2O	0.09	0.11	0.19	0.22	0.13	0.14	0.20
Na2O	5.96	5.74	6.74	6.78	6.82	6.55	7.13
Al2O3	28.74	28.84	26.64	26.85	28.02	28.88	26.03
SiO2	54.18	54.46	57.46	57.66	56.51	56.34	58.20

Totals	99.80	100.06	99.28	100.67	101.17	102.07	99.47

Sample	15	16	17	18	19	20	21
FeO	0.16	0.06	0.12	0.17	0.07	0.10	0.16
CaO	7.45	7.29	7.13	7.65	7.90	7.16	6.99
K2O	0.22	0.19	0.22	0.24	0.18	0.28	0.27
Na2O	7.40	7.48	6.35	6.99	6.99	8.25	7.68
Al2O3	26.57	25.84	24.12	26.45	26.67	25.90	25.44
SiO2	58.17	58.43	54.18	58.62	57.57	59.73	59.13
Totals	99.97	99.30	92.12	100.12	99.38	101.43	99.67

Sample	22	23	24	25	26	27	28
FeO	0.07	0.25	0.10	0.08	0.06	0.08	0.00
CaO	7.83	8.05	8.36	8.10	9.26	8.76	0.46
K2O	0.23	0.20	0.20	0.22	0.16	0.19	0.01
Na2O	7.14	6.89	6.96	6.92	6.56	6.74	0.22
Al2O3	26.48	27.36	27.48	26.87	28.58	27.08	1.59
SiO2	58.55	58.21	58.15	57.74	56.16	57.69	4.63
Totals	100.30	100.95	101.24	99.93	100.78	100.54	6.92

Sample	29	30	31	32	33	34	35
FeO	0.12	0.00	0.07	0.07	0.10	0.22	0.13
CaO	7.93	6.85	7.64	7.16	7.30	7.29	7.23
K2O	0.25	0.21	0.21	0.24	0.27	0.24	0.23
Na2O	7.48	7.86	7.86	7.95	7.46	7.27	7.32
Al2O3	25.97	25.51	26.32	26.03	26.39	26.21	26.01
SiO2	58.20	59.38	59.05	59.31	58.40	58.72	58.38
Totals	99.94	99.81	101.13	100.74	99.92	99.94	99.29

Sample	36	37	38	39	40	41	42
FeO	0.09	0.10	0.07	0.06	0.18	0.28	0.07
CaO	7.19	7.85	7.39	8.44	8.47	8.48	8.29
K2O	0.24	0.18	0.24	0.19	0.18	0.19	0.21
Na2O	7.77	7.36	6.97	7.07	7.23	7.23	6.81
Al2O3	26.17	26.68	25.93	26.81	26.82	26.58	26.67
SiO2	58.85	58.00	58.40	56.91	57.48	57.57	57.54
Totals	100.31	100.17	98.99	99.49	100.36	100.33	99.60

Sample	43	44	45	46	47	48	49
FeO	0.06	0.17	0.11	0.07	0.19	0.01	0.08
CaO	7.85	8.17	8.30	8.69	8.14	7.02	7.95
K2O	0.19	0.22	0.21	0.15	0.19	0.20	0.21
Na2O	7.26	7.28	7.13	6.44	6.95	7.68	7.07
Al2O3	25.85	26.41	26.76	27.21	26.84	26.30	26.92
SiO2	58.10	58.27	57.68	56.45	57.43	59.12	57.97
Totals	99.33	100.52	100.20	99.02	99.75	100.33	100.20

Sample	50	51	52	53	54	55	56
FeO	0.09	0.14	0.18	0.07	0.11	0.17	0.08

CaO	7.68	7.90	8.80	8.43	8.23	8.42	8.52
K2O	0.22	0.18	0.20	0.15	0.23	0.19	0.18
Na2O	7.21	6.81	6.67	6.80	7.03	7.09	6.65
Al2O3	27.10	26.95	27.28	27.33	27.27	27.46	27.34
SiO2	58.38	57.19	57.61	57.95	57.89	57.97	56.73
Totals	100.67	99.18	100.74	100.74	100.76	101.29	99.50

Sample	57	58	59	60	61	62	63
FeO	0.08	0.12	0.15	0.21	0.16	0.12	0.09
CaO	8.85	9.01	9.91	9.09	8.39	8.53	8.26
K2O	0.22	0.19	0.16	0.19	0.22	0.22	0.20
Na2O	6.95	6.55	6.14	6.70	6.75	6.88	6.97
Al2O3	27.14	28.23	28.73	27.32	27.20	27.83	25.84
SiO2	57.18	56.68	56.13	57.19	57.19	57.57	56.42
Totals	100.42	100.78	101.22	100.70	99.91	101.14	97.78

Sample	64	65	66	67	68	69	70
FeO	0.09	0.11	0.20	0.21	0.18	0.20	0.15
CaO	8.89	8.57	7.96	8.28	8.70	8.29	7.67
K2O	0.21	0.23	0.16	0.15	0.14	0.22	0.22
Na2O	6.69	7.17	6.95	6.70	6.74	6.89	7.17
Al2O3	27.50	27.44	26.94	27.16	26.71	26.94	26.57
SiO2	57.37	57.51	57.63	57.25	57.55	58.11	57.75
Totals	100.75	101.04	99.84	99.74	100.01	100.67	99.54

Sample	71	72	73	74	75	76	77
FeO	0.12	0.09	0.19	0.15	0.03	0.12	0.25
CaO	8.13	8.57	8.13	8.46	8.78	8.56	9.14
K2O	0.16	0.19	0.17	0.22	0.25	0.19	0.20
Na2O	6.88	6.79	6.81	7.01	6.99	6.64	6.75
Al2O3	26.15	26.76	27.65	26.31	27.40	27.39	27.93
SiO2	57.73	56.77	57.28	57.54	56.92	56.44	56.66
Totals	99.17	99.16	100.24	99.70	100.36	99.35	100.93

Sample	78	79	80	81	82	83	84
FeO	0.08	0.08	0.14	0.15	0.00	0.14	0.03
CaO	9.51	9.10	9.02	8.52	8.83	9.75	8.81
K2O	0.16	0.19	0.13	0.18	0.20	0.17	0.17
Na2O	6.41	6.63	6.71	6.91	6.67	6.26	6.27
Al2O3	27.89	27.88	27.21	27.03	27.09	27.62	28.09
SiO2	56.30	56.02	56.62	56.59	56.95	55.71	57.08
Totals	100.34	99.90	99.82	99.38	99.74	99.65	100.44

Sample	85	86	87	88	89	90	91
FeO	0.20	0.13	0.09	0.13	0.03	0.23	0.30
CaO	9.38	8.79	8.86	9.20	9.54	9.72	10.10
K2O	0.19	0.20	0.14	0.14	0.14	0.20	0.13
Na2O	6.25	6.59	6.52	6.46	6.71	6.04	5.98
Al2O3	28.01	28.41	28.14	28.44	27.04	28.19	28.80
SiO2	56.63	56.78	56.60	55.27	55.92	55.99	54.61

Totals	100.66	100.90	100.33	99.64	99.38	100.36	99.91

Sample	92	93	94	95	96	97	98
FeO	0.13	0.01	0.11	0.12	0.16	0.12	0.05
CaO	9.60	8.81	8.66	8.03	7.78	7.55	8.25
K2O	0.16	0.20	0.21	0.20	0.24	0.22	0.23
Na2O	6.17	6.93	6.65	6.77	7.23	7.29	7.32
Al2O3	28.13	27.09	27.61	26.30	25.95	27.10	26.46
SiO2	56.68	56.83	57.68	57.01	58.20	57.96	57.94
Totals	100.87	99.86	100.92	98.41	99.56	100.23	100.26

Sample	99	100	101	102	103	104	105
FeO	0.04	0.16	0.29	0.03	0.13	0.03	0.13
CaO	8.44	8.27	8.89	8.44	8.41	7.93	8.11
K2O	0.30	0.20	0.19	0.18	0.24	0.20	0.26
Na2O	7.21	6.87	6.87	6.94	5.25	6.74	6.75
Al2O3	27.56	26.78	27.49	27.29	28.61	25.72	26.79
SiO2	56.81	56.53	57.43	57.49	58.70	57.16	57.07
Totals	100.38	98.82	101.16	100.37	101.33	97.77	99.11

Sample	106	107	108	109	110
FeO	0.08	0.16	0.10	0.13	0.06
CaO	7.99	7.87	7.41	7.69	7.53
K2O	0.25	0.24	0.19	0.23	0.21
Na2O	7.39	7.30	7.15	7.41	7.62
Al2O3	26.63	26.60	27.06	26.91	26.59
SiO2	58.51	57.25	58.27	58.28	58.40
Totals	100.85	99.40	100.19	100.66	100.40

ID-5-22-06-01 Plag-5 Rim to Core (India Dormida Dacite Lava)

Sample	1	2	3	4	5	6	7
FeO	0.75	0.44	0.34	0.54	0.35	0.32	0.43
CaO	8.96	10.15	9.99	10.10	9.74	10.01	10.20
K2O	0.37	0.46	0.45	0.45	0.38	0.31	0.32
Na2O	5.97	6.29	5.87	5.88	5.91	5.80	5.84
Al2O3	27.18	28.80	27.41	28.78	28.74	28.40	27.54
SiO2	55.35	56.09	55.94	55.91	55.77	55.88	56.04
Totals	98.58	102.22	100.01	101.66	100.88	100.73	100.38

Sample	8	9	10	11	12	13	14
FeO	0.38	0.38	0.54	0.30	0.45	0.32	0.23
CaO	9.91	9.96	9.60	9.60	9.53	9.56	10.21
K2O	0.38	0.34	0.35	0.28	0.31	0.24	0.30
Na2O	6.07	6.13	5.86	5.91	5.96	6.31	5.90
Al2O3	27.13	27.81	28.16	27.62	27.77	28.22	27.87
SiO2	55.68	56.20	55.95	55.96	55.88	56.13	55.52
Totals	99.55	100.82	100.46	99.68	99.89	100.78	100.01

Sample	15	16	17	18	19	20	21
FeO	0.42	0.32	0.28	0.28	0.32	0.38	0.36
CaO	10.56	10.38	11.32	10.17	9.47	10.55	10.40
K2O	0.26	0.26	0.19	0.28	0.33	0.27	0.29
Na2O	5.77	5.65	5.44	5.85	6.52	5.84	5.79
Al2O3	28.84	29.04	29.62	28.40	28.08	29.09	28.13
SiO2	55.13	54.81	54.79	56.00	56.47	55.76	55.42
Totals	100.97	100.46	101.64	100.97	101.18	101.89	100.37

Sample	22	23	24	25	26	27	28
FeO	0.49	0.36	0.22	0.21	0.39	0.23	0.29
CaO	10.22	10.87	10.94	10.76	10.20	10.89	11.09
K2O	0.31	0.26	0.21	0.34	0.25	0.27	0.24
Na2O	5.97	5.79	5.31	5.81	5.98	5.50	5.31
Al2O3	28.36	27.72	28.82	27.40	28.32	29.19	28.45
SiO2	54.63	54.81	54.11	55.19	55.23	55.47	55.10
Totals	99.97	99.80	99.60	99.70	100.37	101.56	100.49

Sample	29	30	31	32	33	34	35
FeO	0.36	0.38	0.24	0.21	0.31	0.25	0.69
CaO	10.66	10.97	10.93	10.69	10.42	10.53	10.61
K2O	0.27	0.25	0.22	0.27	0.29	0.24	0.25
Na2O	5.64	5.73	5.51	5.50	5.58	5.62	5.76
Al2O3	28.17	28.79	29.59	28.87	28.31	28.49	28.78
SiO2	54.85	54.45	54.61	54.53	55.51	54.91	55.48
Totals	99.95	100.56	101.10	100.07	100.42	100.03	101.57

Sample	36	37	38	39	40	41	42
FeO	0.36	0.33	0.32	0.34	0.31	0.31	0.49
CaO	9.76	9.45	10.05	9.85	10.57	10.22	10.64
K2O	0.30	0.36	0.32	0.24	0.27	0.30	0.23
Na2O	5.81	6.08	5.76	5.95	5.48	5.99	5.88
Al2O3	28.30	27.15	28.36	28.77	29.16	28.37	27.88
SiO2	55.43	55.94	55.68	55.74	55.44	54.58	55.25
Totals	99.97	99.30	100.50	100.90	101.23	99.77	100.39

Sample	43	44	45	46	47	48	49
FeO	0.41	0.39	0.39	0.31	0.34	0.45	0.36
CaO	10.29	10.26	10.62	9.59	10.09	10.54	11.04
K2O	0.29	0.29	0.26	0.25	0.28	0.31	0.23
Na2O	5.88	5.69	5.73	5.71	5.64	5.50	5.36
Al2O3	29.52	28.66	28.45	28.26	28.57	28.41	30.09
SiO2	55.73	55.15	55.17	55.20	54.92	54.59	54.45
Totals	102.11	100.44	100.62	99.33	99.84	99.79	101.54

Sample	50	51	52	53	54	55	56
FeO	0.59	0.24	0.53	0.22	0.45	0.41	0.27
CaO	11.45	11.09	11.01	10.69	10.68	10.39	10.40
K2O	0.24	0.20	0.24	0.24	0.28	0.24	0.29
Na2O	5.18	5.09	5.72	5.44	5.89	5.89	5.74

Al2O3	29.13	29.26	28.31	28.86	28.31	28.50	28.12
SiO2	53.73	53.69	54.31	54.78	55.53	55.33	55.32
Totals	100.31	99.58	100.13	100.22	101.13	100.74	100.15

Sample	57	58	59	60	61	62	63
FeO	0.49	0.18	0.47	0.51	0.23	0.53	0.31
CaO	10.58	10.14	10.33	9.56	10.47	10.38	10.03
K2O	0.32	0.25	0.27	0.22	0.26	0.29	0.29
Na2O	5.82	5.62	6.06	6.19	5.93	5.67	5.55
Al2O3	27.83	27.84	28.88	27.53	28.66	27.24	29.03
SiO2	54.11	55.12	55.66	55.99	55.20	54.61	55.26
Totals	99.16	99.13	101.66	100.01	100.75	98.72	100.47

Sample	64	65	66	67	68	69	70
FeO	0.37	0.00	0.18	0.37	0.46	0.38	0.42
CaO	10.41	0.61	4.61	10.73	10.69	10.81	11.93
K2O	0.31	0.07	0.15	0.30	0.25	0.24	0.17
Na2O	5.77	10.54	9.94	5.50	5.14	5.14	5.02
Al2O3	28.76	21.28	23.42	29.51	29.21	28.77	29.85
SiO2	55.13	69.08	63.79	54.99	53.93	54.31	54.37
Totals	100.76	101.58	102.09	101.39	99.68	99.65	101.76

Sample	71	72	73	74	75	76	77
FeO	0.46	0.46	0.39	0.34	0.31	0.37	0.53
CaO	11.41	11.76	10.89	11.51	11.87	11.52	11.80
K2O	0.25	0.22	0.16	0.21	0.25	0.21	0.20
Na2O	5.12	5.36	5.38	5.11	4.96	4.93	5.34
Al2O3	29.60	29.89	29.72	29.35	29.41	29.82	30.48
SiO2	53.95	54.37	53.69	54.09	53.36	53.72	53.19
Totals	100.79	102.05	100.23	100.62	100.16	100.57	101.54

Sample	78	79	80	81	82	83	84
FeO	0.46	0.38	0.48	0.33	0.44	0.46	0.32
CaO	12.10	13.69	14.26	12.74	13.61	14.48	14.11
K2O	0.20	0.15	0.14	0.24	0.18	0.14	0.19
Na2O	4.63	3.82	3.91	3.56	3.85	3.91	3.52
Al2O3	30.66	31.52	31.67	32.12	31.74	31.74	32.15
SiO2	52.80	50.99	50.54	52.32	51.14	50.87	50.65
Totals	100.85	100.54	101.01	101.30	100.96	101.60	100.94

Sample	85	86	87	88	89	90	91
FeO	0.52	0.63	0.34	0.43	0.60	0.36	0.30
CaO	14.78	14.71	14.47	14.07	13.88	13.81	13.62
K2O	0.16	0.15	0.10	0.13	0.12	0.13	0.18
Na2O	3.45	3.50	3.76	3.53	3.71	4.12	3.76
Al2O3	32.21	32.42	32.68	32.62	32.42	31.55	30.94
SiO2	50.29	50.33	49.88	50.40	51.13	51.50	51.46
Totals	101.40	101.75	101.23	101.17	101.86	101.48	100.26

Sample	92	93	94	95	96	97	98
FeO	0.31	0.23	0.27	0.49	0.38	0.22	0.17
CaO	13.52	13.20	11.94	11.15	11.36	10.87	10.68
K2O	0.14	0.18	0.20	0.30	0.27	0.24	0.24
Na2O	3.88	4.11	5.16	5.18	5.24	5.52	5.45
Al2O3	31.28	30.84	29.51	30.20	29.61	28.74	29.81
SiO2	51.21	52.51	54.64	54.48	54.89	54.58	54.90
Totals	100.33	101.06	101.72	101.81	101.75	100.17	101.24

Sample	99	100	101	102
FeO	0.32	0.46	0.56	0.21
CaO	10.97	10.97	11.21	10.33
K2O	0.28	0.24	0.27	0.31
Na2O	5.49	5.67	5.53	5.55
Al2O3	28.80	29.43	29.11	28.67
SiO2	55.12	55.33	54.17	55.11
Totals	100.97	102.11	100.84	100.17

LT-5-31-06-4C Plag-4 Rim to Core (Llano Tigre Andesite)

Sample	1	2	3	4	5	6	7
FeO	0.44	0.20	0.32	0.40	0.25	0.42	0.28
CaO	9.38	8.69	9.35	9.06	8.87	9.50	9.18
K2O	0.45	0.41	0.42	0.37	0.39	0.38	0.36
Na2O	6.24	6.50	6.44	6.37	6.70	6.17	6.07
Al2O3	28.13	27.59	27.94	27.22	27.35	27.42	27.19
SiO2	55.20	56.54	56.63	56.29	56.78	55.97	56.08
Totals	99.84	99.93	101.11	99.71	100.34	99.87	99.15

Sample	8	9	10	11	12	13	14
FeO	0.29	0.57	0.34	0.43	0.35	0.31	0.37
CaO	9.33	9.80	9.04	8.80	9.33	9.42	9.09
K2O	0.34	0.36	0.37	0.33	0.37	0.30	0.34
Na2O	6.24	6.09	6.25	6.29	6.03	6.29	6.25
Al2O3	26.99	27.84	27.54	27.73	27.17	27.15	27.58
SiO2	55.84	55.72	55.45	56.29	56.09	56.50	56.83
Totals	99.02	100.38	99.00	99.88	99.34	99.97	100.45

Sample	15	16	17	18	19	20	21
FeO	0.36	0.30	0.46	0.23	0.37	0.33	0.31
CaO	9.21	9.27	9.10	8.87	9.69	8.38	8.47
K2O	0.31	0.37	0.38	0.28	0.33	0.30	0.38
Na2O	6.25	6.29	6.34	6.27	6.81	5.25	5.98
Al2O3	27.22	27.17	27.47	27.12	27.28	27.00	28.12
SiO2	56.57	56.05	56.53	56.26	55.78	55.37	54.00
Totals	99.93	99.46	100.27	99.04	100.25	96.63	97.27

Sample	22	23	24	25	26	27	28
FeO	0.31	0.29	0.31	0.38	0.31	0.30	0.26
CaO	9.39	9.43	8.97	9.02	8.68	9.12	8.74
K2O	0.35	0.36	0.37	0.39	0.38	0.34	0.35

Na2O	6.62	6.61	6.65	6.35	6.34	6.46	6.48
Al2O3	27.56	27.77	27.70	26.43	26.97	27.31	27.72
SiO2	56.21	56.37	56.83	56.12	56.02	56.51	56.18
Totals	100.43	100.83	100.83	98.70	98.71	100.05	99.73

Sample	29	30	31	32	33	34	35
FeO	0.44	0.27	0.39	0.33	0.21	0.38	0.59
CaO	9.08	9.18	9.70	9.77	9.38	9.17	7.08
K2O	0.33	0.28	0.29	0.27	0.32	0.36	0.44
Na2O	6.81	6.25	6.17	5.89	6.38	6.63	5.29
Al2O3	27.27	27.53	27.45	28.17	27.58	27.18	25.93
SiO2	56.50	57.02	55.78	55.74	56.05	57.68	61.48
Totals	100.44	100.54	99.77	100.17	99.92	101.40	100.81

Sample	36	37	38	39	40	41	42
FeO	0.33	0.34	0.39	0.45	0.31	0.33	0.45
CaO	8.75	9.05	9.68	9.34	10.29	10.15	10.59
K2O	0.26	0.37	0.30	0.33	0.26	0.27	0.30
Na2O	3.91	5.93	6.45	6.34	5.77	5.77	5.63
Al2O3	29.49	28.41	28.29	27.37	28.81	28.09	28.19
SiO2	61.31	60.64	55.80	56.34	54.81	54.54	54.45
Totals	104.05	104.72	100.91	100.18	100.26	99.15	99.60

Sample	43	44	45	46	47	48	49
FeO	0.32	0.38	0.42	0.58	0.39	0.25	0.40
CaO	9.77	9.63	10.26	10.77	10.79	9.55	9.07
K2O	0.30	0.29	0.29	0.30	0.22	0.28	0.36
Na2O	5.60	5.97	5.61	5.56	5.32	5.98	6.70
Al2O3	28.22	28.35	28.36	28.26	28.32	28.33	27.91
SiO2	55.68	54.76	54.64	54.75	54.75	55.49	56.86
Totals	99.89	99.38	99.59	100.22	99.79	99.89	101.30

Sample	50	51	52	53	54	55	56
FeO	0.56	0.33	0.24	0.24	0.38	0.36	0.28
CaO	9.42	8.84	8.86	9.10	9.06	8.68	9.22
K2O	0.29	0.35	0.34	0.34	0.29	0.30	0.34
Na2O	6.08	6.36	6.28	6.28	6.43	6.42	6.41
Al2O3	26.82	27.81	27.43	26.84	27.64	26.51	27.35
SiO2	56.61	56.86	56.98	56.80	57.32	56.87	56.91
Totals	99.77	100.54	100.14	99.59	101.11	99.15	100.52

Sample	57	58	59	60	61	62	63
FeO	0.38	0.22	0.23	0.40	0.25	0.19	0.36
CaO	8.95	9.49	9.58	10.04	10.24	10.18	9.62
K2O	0.33	0.29	0.32	0.27	0.28	0.31	0.30
Na2O	6.06	5.84	5.93	5.90	6.20	5.87	5.74
Al2O3	26.76	28.24	28.13	28.18	27.03	28.17	28.08
SiO2	56.26	55.79	56.53	55.69	55.89	55.53	56.11
Totals	98.74	99.87	100.73	100.48	99.88	100.25	100.20

Sample	64	65	66	67	68	69	70
FeO	0.38	0.40	0.33	0.27	0.24	0.22	0.32
CaO	9.52	9.62	9.64	10.05	10.08	10.19	9.79
K2O	0.28	0.30	0.27	0.26	0.29	0.31	0.24
Na2O	6.02	6.26	5.86	5.99	5.75	5.33	5.66
Al2O3	27.57	28.27	28.04	28.46	28.49	27.88	28.37
SiO2	55.46	55.88	55.00	56.06	55.45	55.55	55.89
Totals	99.23	100.72	99.13	101.11	100.30	99.48	100.29

Sample	71	72	73	74	75	76	77
FeO	0.31	0.42	0.32	0.22	0.33	0.25	0.39
CaO	9.55	9.67	6.24	9.63	10.38	10.60	10.81
K2O	0.26	0.24	0.20	0.27	0.30	0.26	0.32
Na2O	5.52	5.71	2.91	6.00	5.78	5.80	5.58
Al2O3	28.03	27.92	19.15	26.45	28.10	28.38	28.49
SiO2	55.29	56.09	42.90	53.16	55.62	54.83	55.06
Totals	98.96	100.06	71.72	95.73	100.52	100.11	100.65

Sample	78	79	80	81	82	83	84
FeO	0.33	0.38	0.22	0.40	0.30	0.38	0.43
CaO	10.41	10.59	10.72	10.32	10.19	9.73	10.10
K2O	0.27	0.24	0.21	0.23	0.24	0.24	0.25
Na2O	5.93	5.58	5.63	5.68	5.53	5.74	5.65
Al2O3	28.78	28.24	28.57	28.43	27.92	28.17	28.32
SiO2	55.18	54.96	54.78	54.69	54.36	53.56	54.40
Totals	100.88	99.99	100.13	99.75	98.53	97.82	99.15

Sample	85	86	87	88	89	90	91
FeO	0.39	0.32	0.22	0.24	0.44	0.26	0.38
CaO	10.16	10.63	10.19	9.53	10.01	10.11	10.43
K2O	0.24	0.22	0.25	0.23	0.26	0.25	0.29
Na2O	5.73	5.87	5.60	5.43	5.82	5.66	5.71
Al2O3	28.57	28.82	28.19	28.12	27.36	28.42	28.39
SiO2	54.14	54.91	54.51	55.24	55.10	55.00	55.02
Totals	99.24	100.77	98.96	98.79	98.99	99.70	100.22

Sample	92	93	94	95	96	97	98
FeO	0.33	0.38	0.26	0.27	0.25	0.27	0.34
CaO	10.14	10.22	10.07	10.37	10.34	10.45	10.34
K2O	0.29	0.28	0.29	0.33	0.28	0.26	0.27
Na2O	5.79	6.00	5.83	5.44	5.53	5.69	5.58
Al2O3	28.75	28.49	28.46	27.57	28.17	28.63	28.79
SiO2	54.88	55.55	55.39	54.78	54.81	55.20	54.80
Totals	100.18	100.92	100.29	98.76	99.39	100.50	100.11

Sample	99	100	101	102	103	104	105
FeO	0.32	0.28	0.26	0.30	0.35	0.28	0.22
CaO	10.50	10.45	10.78	10.74	11.42	12.88	11.03
K2O	0.23	0.26	0.19	0.20	0.22	0.14	0.20

Na2O	5.55	5.47	5.37	5.38	5.15	4.38	5.21
Al2O3	28.99	29.25	28.39	29.42	29.68	30.39	29.42
SiO2	54.53	54.45	54.00	53.44	53.20	52.14	53.78
Totals	100.12	100.14	98.99	99.48	100.02	100.21	99.85

Sample	106	107	108	109	110	111	112
FeO	0.45	0.36	0.27	0.25	0.32	0.26	0.36
CaO	11.10	10.96	10.78	10.62	10.18	10.53	10.56
K2O	0.21	0.25	0.28	0.27	0.19	0.22	0.26
Na2O	5.29	5.73	5.76	5.72	5.45	5.48	5.82
Al2O3	29.13	28.26	28.95	28.36	28.56	28.55	28.44
SiO2	54.42	54.92	54.99	55.13	54.38	54.58	54.37
Totals	100.59	100.47	101.03	100.35	99.07	99.62	99.81

Sample	113	114	115	116	117	118	119
FeO	0.56	0.37	0.35	0.34	0.27	0.24	0.23
CaO	10.40	9.73	9.96	9.56	9.12	9.20	8.99
K2O	0.23	0.27	0.27	0.30	0.30	0.34	0.32
Na2O	5.91	6.13	5.77	5.86	6.06	6.17	6.57
Al2O3	28.55	27.44	28.20	26.83	26.93	27.82	27.50
SiO2	55.13	55.51	55.96	55.57	55.83	56.55	57.50
Totals	100.78	99.46	100.52	98.46	98.52	100.33	101.12

Sample	120	121	122	123	124	125	126
FeO	0.26	0.23	0.31	0.30	0.51	0.29	0.18
CaO	9.46	9.43	9.32	9.45	9.35	10.00	10.21
K2O	0.32	0.35	0.34	0.30	0.25	0.28	0.29
Na2O	6.54	6.50	6.07	6.44	6.17	6.22	5.57
Al2O3	28.08	27.48	26.44	27.50	27.42	27.97	28.16
SiO2	59.99	56.02	56.24	56.03	55.84	56.55	55.58
Totals	104.65	100.01	98.72	100.02	99.55	101.33	99.98

Sample	127	128	129	130	131	132	133
FeO	0.36	0.37	0.26	0.48	0.18	0.37	0.35
CaO	9.51	9.85	9.99	9.77	9.34	10.33	9.06
K2O	0.25	0.29	0.25	0.24	0.31	0.30	0.26
Na2O	5.85	5.94	5.80	6.21	6.23	6.32	6.09
Al2O3	28.43	28.20	27.28	27.37	28.05	27.27	27.96
SiO2	55.23	54.96	55.14	55.44	55.86	55.50	56.57
Totals	99.64	99.61	98.72	99.52	99.97	100.11	100.31

Sample	134	135	136	137	138	139	140
FeO	0.45	0.37	0.26	0.38	0.47	0.38	0.33
CaO	9.27	9.53	9.82	9.75	9.81	9.70	9.62
K2O	0.32	0.31	0.31	0.25	0.31	0.28	0.30
Na2O	5.79	5.81	6.08	6.10	6.44	6.21	6.13
Al2O3	27.82	28.32	26.48	27.88	27.30	27.03	27.21
SiO2	56.13	56.33	55.91	56.12	55.15	56.34	55.88
Totals	99.78	100.67	98.85	100.48	99.47	99.96	99.47

Sample	141	142	143	144	145	146	147
FeO	0.27	0.28	0.43	0.30	0.29	0.26	0.21
CaO	9.84	9.85	9.50	9.88	9.87	10.39	9.91
K2O	0.27	0.27	0.31	0.22	0.30	0.28	0.25
Na2O	6.17	6.00	5.92	6.06	6.07	5.95	5.82
Al2O3	28.29	27.12	27.00	28.31	27.45	27.69	28.30
SiO2	56.43	55.60	56.12	55.57	56.13	55.49	55.81
Totals	101.27	99.12	99.28	100.33	100.11	100.07	100.31

Sample	148	149	150	151	152	153	154
FeO	0.45	0.32	0.27	0.46	0.29	0.39	0.41
CaO	10.00	10.01	10.02	10.26	9.90	9.45	9.72
K2O	0.25	0.30	0.25	0.27	0.22	0.27	0.28
Na2O	5.78	5.90	5.95	5.50	5.93	5.51	6.14
Al2O3	28.08	28.58	28.19	27.67	27.74	27.94	27.35
SiO2	55.01	56.40	56.22	55.60	55.55	56.04	55.41
Totals	99.56	101.51	100.90	99.75	99.62	99.61	99.30

Sample	155	156	157	158	159	160	161
FeO	0.30	0.46	0.40	0.35	0.30	0.50	0.38
CaO	9.71	10.24	9.37	10.46	9.92	9.49	9.73
K2O	0.30	0.26	0.31	0.27	0.22	0.33	0.35
Na2O	5.67	6.18	6.04	6.04	6.03	6.06	6.37
Al2O3	28.49	27.98	27.77	28.47	26.89	27.14	28.22
SiO2	55.49	56.09	55.51	55.26	55.21	55.50	56.26
Totals	99.96	101.22	99.40	100.85	98.57	99.02	101.30

Sample	162	163	164	165	166	167	168
FeO	0.34	0.37	0.37	0.38	0.30	0.37	0.44
CaO	10.22	9.59	9.69	9.60	9.85	9.68	9.68
K2O	0.28	0.30	0.28	0.34	0.32	0.33	0.33
Na2O	6.07	6.13	6.22	6.35	6.09	6.32	5.95
Al2O3	27.19	26.91	27.21	27.14	27.85	27.72	28.55
SiO2	55.97	56.21	56.41	56.77	56.41	56.75	56.06
Totals	100.06	99.52	100.18	100.58	100.82	101.16	101.02

LT-5-31-06-4C Plag-5 Rim to Core (Llano Tigre andesite)

Sample	1	2	3	4	5	6	7
FeO	0.23	0.28	0.37	0.39	0.35	0.44	0.31
CaO	9.97	9.59	10.30	10.46	10.48	10.26	10.13
K2O	0.40	0.31	0.33	0.30	0.29	0.32	0.28
Na2O	5.88	5.91	5.81	5.94	5.56	5.74	5.88
Al2O3	27.70	28.12	27.64	28.62	28.20	28.00	27.38
SiO2	55.72	55.65	55.47	55.11	55.45	55.04	53.30
Totals	99.91	99.88	99.93	100.83	100.33	99.80	97.29

Sample	8	9	10	11	12	13	14
FeO	0.42	0.44	0.47	0.27	0.38	0.28	0.24

CaO	10.13	9.79	10.23	9.37	9.89	9.79	10.03
K2O	0.27	0.25	0.32	0.28	0.26	0.27	0.24
Na2O	6.08	5.65	5.99	5.84	5.90	5.64	5.74
Al2O3	27.46	28.49	29.10	28.10	28.13	28.07	27.98
SiO2	55.32	56.03	55.89	56.16	56.47	56.37	55.93
Totals	99.69	100.65	101.99	100.02	101.02	100.43	100.17

Sample	15	16	17	18	19	20	21
FeO	0.30	0.34	0.44	0.29	0.40	0.28	0.47
CaO	10.09	9.86	10.63	10.16	10.03	9.86	9.68
K2O	0.30	0.22	0.29	0.24	0.27	0.30	0.21
Na2O	6.04	6.05	5.70	5.78	6.04	5.79	6.55
Al2O3	28.20	28.13	27.68	28.33	28.53	27.71	27.04
SiO2	55.44	55.79	55.63	55.23	55.91	56.63	56.53
Totals	100.37	100.40	100.37	100.04	101.16	100.56	100.49

Sample	22	23	24	25	26	27	28
FeO	0.26	0.29	0.36	0.46	0.34	0.20	0.29
CaO	9.20	8.82	8.83	8.72	8.75	9.39	9.02
K2O	0.31	0.32	0.34	0.32	0.30	0.31	0.32
Na2O	6.41	6.24	6.57	6.34	5.96	6.49	6.23
Al2O3	26.19	27.74	27.49	26.72	28.25	27.22	27.06
SiO2	56.72	57.10	56.98	55.61	56.46	56.11	56.18
Totals	99.08	100.51	100.57	98.17	100.06	99.74	99.10

Sample	29	30	31	32
FeO	0.35	0.14	0.28	0.27
CaO	9.71	9.68	9.95	9.95
K2O	0.27	0.26	0.30	0.24
Na2O	6.31	6.03	6.04	4.57
Al2O3	27.80	28.18	27.22	29.08
SiO2	55.71	56.15	55.87	58.43
Totals	100.15	100.44	99.65	102.54

REFERENCES

VIII. REFERENCES

Adamek, S., Frohlich, C. and Pennington, W. D., 1988. Seismicity of the Caribbean-Nazca boundary: constraints on microplate tectonics of the Panama region. J. Geophys. Res. 93, 2053–2075.

Anderson, A. T., Jr., 1984. Probable relations between plagioclase zoning and magma dynamics, Fuego volcano, Guatemala. Am. Mineral. 69, 660-676.

Arculus, R. J., 1994. Aspects of magma genesis in arcs. Lithos 33, 189-208.

Atherton, M. P. and Petford, N., 1993. Generation of sodium-rich magmas from newly underplated basaltic crust. Nature 362, 144–146.

Bachmann, O. and Bergantz, G.W., 2004. On the origin of crystal-poor rhyolites: extracted from batholithic crystal mushes. J. Petrol. 1565–1582.

Barckhausen, U., Ranero, C. R., von Huene, R., Cande, S. C. and Roeser, H. A., 2001. Revised tectonic boundaries in the Cocos Plate off Costa Rica; implications for the segmentation of the convergent margin and for plate tectonic models. J. Geophys. Res. 106, 19207–19220.

Batiza, R., 1986. Failed rifts. In: The Eastern Pacific Ocean and Hawaii (Winterer, E. L., Hussong, D.M. and Decker, R.W. (eds). The Geology of North America (N). The Geological Society of America, Boulder, Colorado.

Beard, J. S. and Lofgren, G. E., 1991. Dehydration melting and water saturated melting of basaltic and andesitic greenstones and amphibolites at 1, 3, and 6.9 kb. J. Petrol. 32, 365–401.

Bird, P., 2004. An updated digital model of plate boundaries. Geochem. Geophys. Geosyst. 4, 1027, doi:10.1029/2001GC000252.

Bowin, C., 1976. Caribbean Gravity Field and Plate Tectonics. Geological Society of America Special Paper, 169. Geological Society of America. Boulder, Colorado, pp. 79.

Browne, B. L., Eichelberger, J. C., Patino, L. C., Vogel, T. A., Dehn, J., Uto, K. and Hoshizumi, H., 2006. Generation of Porphyritic and Equigranular Mafic Enclaves during Magma Recharge Events at Unzen Volcano, Japan. J. of Petrol. 47, 301-328.

Bush, M. B. and Colinvaux, P. A., 1990. A pollen Record of a Complete Glacial Cycle from Lowland Panama. J. Veg. Sci. 1, 105-118.

Clark, L. F., 1989. The geology, geochemistry, and petrogenesis of El Valle volcano, Panama. MS Thesis, University of South Florida, Tampa, Florida. Pp. 150.

Cameron, M., Bagby, W. C. and Cameron, K. L., 1980. Petrogenesis of voluminous mid-Tertiary ignimbrites of the Sierra Madre Occidental, Chihuahua, Mexico. Contrib. Mineral. Petrol. 74, 271–284..

Carr, M. J., Rose, E. F. and Stoiber, R. E., 1982. Central America. In: Thorpe, R. S. (Ed.), Orogenic Andesites. John Wiley, New York, pp. 149–166.

Carr, M. J., Feigenson, M. D. and Bennett, E. A., 1990. Incompatible element and isotopic evidence for tectonic control of source mixing and melt extraction along the Central American arc. Contrib. Mineral. Petrol. 105, 369–380.

Carr, M. J., Feigenson, M. D., Patino, L. C. and Walker, J. A., 2003. Volcanism and geochemistry in Central America: progress and problems. In: Eiler, J. M., (Ed.), Inside the Subduction Factory. AGU Geophysical Monograph, 138, 153–174.

Case, J. E., 1974. Oceanic crust forms basement of eastern Panama. Geol. Soc. Am. Bull. 85, 645-652.

Coates, A. G., McNeill, D. F., Aubry, M-P., Berggren, W. A. and Collins, L. S., 2005. An introduction to the Geology of Bocas del Toro Archipielago, Panama. Caribb. Journal Sci. 41, 374-391.

Collins, J. A.; Purdy, M. G. and Brocher, T. M., 1989. Seismic velocity structure at deep sea drilling project site 504B, Panama basin: Evidence for thin oceanic crust. J. Geophys. Res. 94, 9283-9302.

Conrad, W. K., Nicholls, I. A. and Wall, V. J. 1988. Water-saturated and undersaturated melting of metaluminous and peraluminous crustal compositions at 1 kb: evidence for the origin of silicic magmas in the Taupo volcanic Zone, New Zealand, and other occurrences. J. Petrol 29, 765–803.

Criss, J. W., 1980. Fundamental parameters calculations on a laboratory microcomputer. Advan X-ray Anal 23, 93–97

de Silva, S. L. and Wolff, J. A., 1995. Zoned magma chambers; the influence of magma chamber geometry on sidewall convective fractionation. J. Volcanol. Geotherm. Res. 65, 111–118.

DePaolo, D. J., 1981. Trace element and isotopic effects of combined wallrock assimilation and fractional crystallization. Earth Planet. Sci. Lett. 53, 189–202.

de Boer, J. Z., Defant, M. J., Steward, R. H., Restrepo, J. F., Clark, L. F. and Ramirez, A., 1988. Quaternary calc-alkaline volcanism in Western Panama: regional variation and implication for plate tectonic framework. J South Am. Earth Sci. 1, 275–293.

de Boer, J. Z., Defant, M. J., Stewart, R. H. and Bellon, H., 1991. Evidence for active subduction below western Panama. Geology 19, 649-652.

Defant, M. J. and Nielsen, R. L., 1990. Interpretation of open system petrogenetic processes: phase equilibria constrains on magma evolution. Geochim. Cosmochem. Acta 54, 87-102.

Defant, M. J. and Drummond, M. S. 1990. Derivation of some modern arc magmas by melting of young subducted lithosphere. Nature 347, 662-665.

Defant, M. J; Clark, L. F.; Stewart, R. H.; Drummond, M. S.; de Boer, J. Z.; Maury, R. C.; Bellon, H.; Jackson, T. E. and Restrepo, J. F., 1991a. Andesite and dacite genesis via contrasting processes; the geology and geochemistry of El Valle Volcano, Panama. *J. Petrol.* 12, 1101 - 1142.

Defant, M. J., Richerson, P. M., de Boer, J. Z., Stewart, R. H., Maury, R. C., Bellon, H., Drummond, M. S., Feigenson, M. D. and Jackson, T. E., 1991b. Dacite genesis via both slab melting and differentiation: petrogenesis of La Yeguada volcanic complex, Panama, J. Petrol. 32, 1101-1142.

Defant, M. J. and Drummond, M. S., 1993. Mount St. Helens: potential example of the partial melting of subducted lithosphere in a volcanic arc. Geology 21, 547-550.

DelGiudice, D. and Recchi, G., 1969. Geología del área del proyecto minero de Azuero. Map 5. Scale 1:250,000. Administración de Recursos Minerales. República de Panamá.

Devine, J. D., Gardner, J. E., Brack, H. P., Layne, G. D. and Rutherford, M. J.; 1995. Comparison of microanalytical methods for estimating H_2O contents of silicic volcanic glasses. Am. Mineral. 80, 319–328.

Devine, J. D., 1995. Petrogenesis of the basalt-andesite-dacite association of Grenada, Lesser Antilles island arc, revisited. J. Volcanol. Geother. Res. 69, 1-33.

Drummond, M. S. and Defant, M. J., 1989. A model for trondhemite- tonalite-dacite genesis and crustal growth via slab melting: Archean to modern comparisons. J. Geophys. Res. 95, 21503-21521.

Drummond, M. S. and Defant, M. J., 1990. A model for trondhjemite-tonalite-dacite genesis and crustal growth via slab melting; Archean to modern comparisons. *J. Geophys. Res.* 95, 21,503 -21,521.

Eichelberger, J. C., Chertkoff, D. G., Dreher, S. T. and Nye, C. J., 2000. Magmas in collision: rethinking chemical zonation in silicic magmas. Geology 28, 603–606.

Eichelberger, J. C., Izbekov, P. E. and Browne, B. L., 2006. Bulk chemical trends at arc volcanoes are not liquid lines of descend. Lithos 87, 135-154.

Gillot, P. Y., Chiesa, S. and Alvarado, G. E., 1994. Chronostratigraphy and evolution of the Neogene–Quaternary volcanism in north Costa Rica: the Arenal volcano-structural frame work. Rev. Geol. Am. Central 17, 45–53.

Gill, J. B. and Stork, A. L., 1979. Miocene low-K dacites and trondhjemites of Fiji. In: Barker, K. (Ed.), Trondhjemites, Dacites, and Related Rocks. Elsevier, Amsterdam, pp. 629–649.

Gill, J. B., 1981. Orogenic Andesites and Plate Tectonics. New York, Springer – Verlag, pp. 390.

Ginibre, C., Worner, G., Kronz, A., 2002. Minor and trace element zoning in plagioclase: implications for magma chamber processes at Parinacota volcano, northern Chile. Contrib. Mineral. Petrol. 143, 300-315.

Gorton, M. P., 1977. The geochemistry and origin of Quaternary volcanism in the New Hebrides. Geochim. Cosmochim. Acta 41, 1257-1270.

Guo, F., Fan, W. and Li, C., 2006. Geochemistry of late Mesozoic adakites from Sulu belt eastern China: magma genesis and implications for crustal recycling beneath continental collisional orogens. Geol. Mag. 143, 1-13.

Gutscher, M. A., Maury, R., Eissen, J. P. and Bourdon, E., 2000. Can slab melting be caused by flat subduction?. Geology 28, 535-538

Halama, R., Waight, T. and Markl, G., 2002. Geochemical and isotopic zoning patterns of plagioclase megacrysts in gabbroic dykes from the Gadar province, South Greenland: implications for crystallization processes in anorthositic magmas. Contrib. Mineral. Petrol. 144, 109-127.

Hannah, R. S., Vogel, T. A., Patino, L. C., Alvarado, G. E., Perez, W. and Smith, D. R., 2002. Origin of the silicic volcanic rocks in Central Costa Rica: a study of a chemically variable ash-flow sheet in the Tiribí Tuff. Bull. Volcanol. 64, 117–133.

Hardy, N. C., 1991. Tectonic evolution of the easternmonst Panama Basin: some new data and insights. J. South Am. Earth Sci. 4, 261– 269.

Hawkesworth, C. J. and Powell, M., 1980. Magma Genesis in the Lesser Antilles Island Arc. Earth. Planet. Sci. Lett. 51, pp.297-308.

Heil, D. J., 1988. Response on an accretionary prism to transform ridge collision south of Panama. M.S. Thesis, University of California. Santa Cruz, California pp. 88.

Hey, R.N., 1977. Tectonic evolution of the Cocos-Nazca spreading centre. Geol. Soc. Am. Bull. 88, 1414–1420.

Hildreth, W. and Moorbath, S., 1988. Crustal contributions to arc magmatism in the Andes of central Chile. Contrib. Mineral. Petrol. 98, 455–489.

Hildreth, W. and Fierstein J., 2000. Katmai volcanic cluster and the great eruption of 1912. Geol. Soc. Amer. Bull. 112, 1594-1620.

Hildreth, W., Fierstein, J., Siems, D. F., Budahn, J. R. and Ruiz, J., 2004. Rear-arc vs. arc-front volcanoes in the Katmai reach of the Alaska Peninsula: a critical appraisal of across-arc compositional variation. Contrib. Mineral. Petrol. 147, 243– 275.

Hirotani, S. and Ban, M., 2006. Origin of silicic magma and magma feeding system of the Shirataka volcano, NE Japan. J. Volcanol. Geotherm. Res. 156, 229-251.

Hidalgo, S., Monzier, M., Martin, H., Chazot, G., Eissen, J. P. and Cotton, J., 2007. Adakitic magmas in the Ecuatorian Volcanic Front: Petrogenesis of the Illiniza Volcanic Complex (Ecuador). J. Volcanol. Geotherm. Res. 159, 366-392.

Hoernle, K., van den Bogaard, P., Werner, R., Lissinna, B., Hauff, F., Alvarado and Garbe-Schönberg, D., 2002. Missing history (16-71 Ma) of the Galápagos hotspot: Implicationsfor the tectonic and biological evolution of the Americas. Geol. Soc. Am. Bull. 30, 795-798.

Hole, M. J., Saunders, A.D, Mariner, G. F. and Tarney, J., 1984. Subduction of pelagic sediments: implications for theorigin of Ce-anomalous basalts from the Mariana Islands. J. Petrol. Geol. Soc. Lond. 141,.453-472.

Jahn, B. M., Glikson, A. Y., Peucat, J. J. and Hickman, A. H., 1981. REE geochemistry and isotopic data of Archean silicic volcanics and granitoids from the Pilbara Block, Western Australia: Implications for early crust evolution. Geochim. Cosmochim. Acta. 45, 1633-1652.

Jarrard, R. D., 1986. Relations among subduction parameters. Rev. Geophys. 24, 217-284.

Kay, R. W. 1978. Aleutian magnesian andesites: melts from subducted Pacific ocean crust. *J. Volcanol. Geother. Res.* 4, 117–132.

Kay, R. W. and Kay, S. M., 1993. Delamination and delamination magmatism. Tectonophys. 219, 177–189.

Kay, S. M., Ramos, V. A. and Marquez, M., 1993. Evidence in Cerro Pampa volcanic rocks for slab-melting prior to ridge-trench collision in southern South America. J. Geol. 101, 103-114.

Kellogg, J. N., Ogujiofor, I. J. and Kansakar, D. R., 1985. Cenozoic tectonics of the Panama and North Andes blocks/. Mem. Congr. Latinoam. Geol. 6, 40–59.

Kellogg, J. N., Vega, V., Stallings, T. C. and Aiken, C. L. V. 1995. Tectonic development of Panama, Costa Rica, and the Columbian Andes: Constraints from Global Positioning System geodetic studies and gravity; In: Mann, P. (ed), Geologic and Tectonic Development of the Caribbean Plate Boundary in Southern Central America. Geol. Soc. Am. Spec. Pap. 295, 75–86. Boulder, Colorado.

Kolarsky, R. A., and Mann, P., 1995.Structure and neotectonics of an oblique-subduction margin, southwestern Panama, In: Mann, P. (ed), Geologic and Tectonic Development of the Caribbean Plate Boundary; in: Southern Central America.Geol. Soc. Am. Spec. Pap. 295, 131–158.

Kuritani, T., 1998. Boundary layer crystallization in a basaltic magma chamber: evidence from Rishiri volcano, northern Japan. J. Petrol. 39,1619-1640.

Irvine, T. N. and Baragar, W. R., 1971. A guide to the classification of the common volcanic rocks. Can. J. Earth. Sci. 8, 523- 549.

Izbekov, P. E., Eichelberger, J. C. and Ivanov, B. V., 2004. The 1996 eruption of Karymsky Volcano, Kamchatka: historical record of basaltic replenishment of an andesite reservoir. J. Petrol. 45, 2325–2345.

Lanphere, M. A. and Dalrymple, G. B., 2000. First-principles calibration of ^{38}Ar tracers: Implications for the ages of ^{40}Ar/^{39}Ar fluence monitors, U.S. Geological Survey Professional Paper 1621, 10 p.

Layer, P. W., 2000. Argon-40/argon-39 age of the El'gygytgyn impact event, Chukotka, Russia. Meteor. Planet. Sci. 35, 591-599.

Layer, P. W., Hall, C. M. and York, D., 1987. The derivation of ^{40}Ar/^{39}Ar age spectra of single -grains of hornblende and biotite by laser step heating. Geophys. Res. Lett. 14, 757-760.

Leat, P. T., Smellie, J. L., Millar, I. L. and Larter, R. D., 2003. Magmatism in the South Sandwich Arc. In: Larter, R. D. and Leat, P. T. (Eds.), Intra-Oceanic Subduction

Systems: Tectonic and Magmatic Processes. Geol. Soc. London. London, England, pp. 285–313.

LeBas, M. J., LeMaitre, R. W., Streckeisen, A. and Zanettin, B., 1986. A chemical classification of volcanic rocks based on the total alkali silica diagram. J. Petrol. 27, 745–750.

Lonsdale, P. and Klitgord, K. D., 1978. Structure and tectonic history of the eastern Panama Basin. Geol. Soc. Am. Bull. 89, 981-999.

Lonsdale, P., 2005. Creation of the Cocos and Nazca Plates by fission of the Farallon Plate. Tectonophys. 404, 237–264.

McDougall, I. and Harrison, T. M., 1999, Geochronology and Thermochronology by the $^{40}Ar/^{39}Ar$ method. Oxford University Press, New York, pp. 269.

MacMillan, I., Gans, P. B. and Alvarado, G. E., 2004. Middle Miocene Plate tectonic history o of the southern Central American Volcanic Arc. Tectonophys. 39, 325-348.

Mann, P. and Kolarsky, R. A., 1995. East Panama deformed belt: Structure, age, and neotectonic significance, in Geologic and Tectonic Development of the Caribbean Plate Boundary; In: Mann, P. (ed), Southern Central America. Geol. Soc. Am. Spec. Pap. 295, 111–130. Boulder, Colorado.

Marcaillou, B., Charvis, P. and Collot, J. Y., 2006. Structure of the Malpelo ridge (Colombia) from seismic and gravity modeling. Mar. Geophys. Res. 27, 289-300.

Martin, H. 1986. Effect of steeper Archean geothermal gradient on geochemistry of subduction-zone magmas, Geology 14, 753-756.

Martin, H., 1999. Adakitic magmas: modern analogues of Archaean granitoids. Lithos 46, 411-429.

Marsh, B. D., 1979. Island-arc development: some observations, experiments, and speculations, J. Geol. 87, 687-713.

Meschede, M., Barckhausen, U., and Worm, H. U., 1998. Extinct spreading on the Cocos Ridge. *Terra Nova* 10, 211–216.

Meschede, M. and Barckhausen, U., 2001. The relationship of the Cocos and Carnegie ridges age constraints from paleogeographic reconstructions. Int. J. Earth Sci. 90, 386-392.

Moore, G. F. and Sender, K. L., 1995. Fracture zone collision along the South Panama margin, in: Geologic and Tectonic Development of the Caribbean Plate Boundary. In: Mann, P. (ed), Southern Central America. Geol. Soc. Am. Spec. Pap.295, 201–212. Boulder, Colorado.

Morris, J.D. 1991. Applications of cosmogenic ^{10}Be to problems in the earth sciences. Annu. Rev. Earth Planet. Sci. Lett. 19, 313-350.

Müntener, O., Kelemen, P. B. and Grove, T. L., 2001a. The role of H_2O during crystallization of primitive arc magmas under uppermost mantle conditions and genesis of igneous pyroxenites: an experimental study. Contrib. Mineral. Petrol.141, 643–658.

Müntener, O., Kelemen, P. B. and Grove, T. L., 2001b. The role of H2O during crystallization of primitive arc magmas under uppermost mantle conditions and genesis of igneous pyroxenites: an experimental study. Contrib. Mineral. Petrol. 141, 643–658.

Mutter, C. Z. and Mutter, J. C., 1993. Variations in thickness of layer 3 dominate oceanic crustal structure. Earth. Planet. Sci. Lett. 117, 295–317

Patiño-Douce, A. E., 1999. What do experiments tell us about the relative contributions of crust and mantle to the origin of granitic magmas? In: Castro, A., Fernández, C., Vigneresse, J. L. (Eds.), Understanding Granites: Integrating New and Classical Techniques. Special Publications 168. Geological Society, London, pp. 55–75.

Patiño-Douce, A. E. and McCarthy, T. ., 1998. Melting of crustal rocks during continental collision and subduction. In: Hacker, B. R. and Liou, J. G. (Eds.), When Continents Collide: Geodynamics and Geochemistry of Ultrahigh-Pressure Rocks. Klewer Academic Publishers, pp. 27–55.

Patino, L. C., Carr, M. J. and Feigenson, M. D., 2000. Local and regional variations in Central American arc lavas controlled by variations in subducted sediment input. Contrib. Mineral. Petrol. 138, 265–283.

Peacock, S. M., Rushmer, T. and Thompson, A. B., 1994. Partial melting of subducting oceanic crust. EPSL 121, 227–244.

Pertermann, M. and Hirschmann, M., 2003. Anhydrous partial melting experiments on MORB-like Eclogite: Phase relations, Phase compositions and Mineral – Melt partitioning of Major Elements at 2-3 GPa. J. Petrology 44, 2173-2201.

Plank, T. and Langmuir C. H. 1993. Tracing trace elements from sediment input to volcanic output at subduction zones. Nature 362, 739-742.

Price, R. C., Gamble, J. A., Smith, I. E. M., Stewart, R. B., Eggins, S. and Wright, I. C., 2005. An integrated model for the temporal evolution of andesites and rhyolites and crustal development in New Zealand's North Island. J. Volcanol. Geotherm. Res. 140, 1-24.

Ramos, V. A., Kay, S. M. and Singer, S., 2004. Las adakitas de la Cordillera Patagonica: Nuevas Evidencias geoquímicas y geocronologicas. Rev. Asoc. Geol. Argentina 59, 693-706.

Rapp, R. P., Watson, E. B. and Miller, C. F. 1991. Partial melting of amphibolites /eclogite and the origin of the Archean trondhjemiites and tonalities. Precamb. Res. 51, 1-25.

Rapp, R. P., and Watson, E. B., 1995. Dehydration melting of metabasalt at 8–32 kbar: implications for continental growth and crust-mantle recycling. J. Petrol. 36, 891–931.

Rapp, R. P., Shimizu, N. and Norman, M. D., 2003. Growth of early continental crust by partial melting of eclogite. Nature 425, 605-609.

Rogers, R.D. 2003. Jurassic–Recent tectonic and stratigraphic history of the Chortis block of Honduras and Nicaragua (northern Central America). Ph.D.Thesis, University of Texas, Austin. Austin, Texas, pp.286.

Rose,W. I., Conway, F. M., Pullinger, C. R., Deino, A. and MacIntosh,W. C., 1999. An improved age framework for late Quaternary silicic eruptions in northern Central America. Bull. Volcanol. 61, 106–120.

Sallares V, Charvis P (2003) Seismic constraints on the Geodynamic evolution of the Galapagos province. Earth Planet. Sci. Lett. 214., 545–559.

Samsonov, A. V., Bogina, M. M., Bibikova, E. V., Petrova, A. Yu. and Shchipansky, A. A. 2005. The relationship between adakitic, calc-alkaline volcanic rocks and TTGs: implications for the tectonic setting of the Karelian greenstone belts, Baltic Shield. Lithos 79, 83-106.

Sass, J. H., Munroe, R. J. and Moses T. H., 1974. Heat flow from eastern Panama and Northwestern Colombia. Earth. Planet. Sci. Lett. 21, 134-142.

Sen, C. and Dunn, T., 1994. Dehydration melting of basaltic composition amphibolites at 1.5 and 2.0 GpA: implications for the origin of adakites. Contri. Min. Petrol. 117, 394-409.

Silver, P. G., Russo, R. M. and Lithgow-Bertelloni, C., 1998. Coupling of Southern American and African plate motion and plate deformation. Science 279, 60–63.

Sisson, T. W., Ratajeski, K., Hankins, W. B. and Glazner, A. F., 2005. Voluminous granitic magmas from common basaltic sources. Contrib. Mineral. Petrol. 148, 542–565.

Smith, I. E. M., Stewart, R. B. and Price, R. C., 2003. The petrology of a large intra-oceanic silicic eruption: the Sandy Bay Tephra, Kermadec Arc, Southwest Pacific. J. Volcanol. Geotherm. Res. 124, 173–194.

Stern, C. R.; Futa, K. and Muehlenbachs, K. 1984. Isotope and trace element data for orogenic andesites from the austral Andes, In: Harmon, R. S, and Barreiro, B. A.(eds), Andean magmatism Chemical and isotopic constraints. Cheshire, England, Shiva, pp. 31-46.

Stevenson, J. A., Daczko, N. R., Clarke, G. L., Pearson, N. and Klepeis, A., 2005. Direct observation of adakites melts generated in the lower continental crust, Fiordland, New Zeland. Terra Nova 17, 73-79.

Tamura, Y. and Tatsumi, Y., 2002. Remelting of an andesitic crust as a possible origin for rhyolitic magma in oceanic arcs: an example from the Izu-Bonin arc. J. Petrol. 43 (6), 1029–1047.

Tamura, Y., Yuhara, M., Ishii, T., Irino, N. and Shukuno, H., 2003. Andesites and dacites from Daisen Volcano, Japan: partial-to-total remelting of an andesite magma body. J. Petrol. 44, 2243–2260.

Tournon, J., Triboulet, C. and Azéma, J., 1989. Amphibolites from Panama: anticlockwise P-T paths from a pre-Upper Cretaceous metamorphic basement in Isthmian Central America. J. Metamorph. Geol. 7, 539-546.

van Andel, T., Heath, G. R., Malfait, B. T., Heinrichs, D. F. and Ewing, J., 1971. Tectonics of the Panama Basin, eastern equatorial Pacific. Geol. Soc. Am. Bull. 82, 1489-1508.

van der Hilst, R. and Mann, P., 1994. Tectonic implications of tomographic images of subducted lithosphere beneath northwestern South America. Geology 22, 451–454.

Vielzeuf, D., Holloway, J. R., 1988. Experimental determination of the fluid-absent melting reactions in the pelitic system. Contrib. Mineral. Petrol. 98, 257–276.

Villegas, A., 1997. Geodinámica de La Cordillera de Tilarán, Relacion entre la Volcanología y la Tectonica. Licenciatura en Geología Thesis, Universidad de Costa Rica. San Jose, 182 pp.

Villiger, S., Ulmer, P., Muntener, O. and Thompson, A. B., 2004. The liquid line of descent of anhydrous, mantle-derived, tholeiitic liquids by fractional and equilibrium crystallization—an experimental study at 1.0 GPa. J. Petrol. 45, 2369–2388.

Viray, E. L., 2003. Origin and Evolution of the Nicaraguan Silicic Ash- Flow Sheets. M.S. Thesis. Michigan State University, East Lansing, Michigan, pp 100.

Vogel, T. A., Patino, L. C., Alvarado, G. E. and Gans, P. B., 2004. Silicic ignimbrites within the Costa Rican volcanic front: evidence for the formation of continental crust. Earth Planet. Sci. Lett.226, 149–159.

Vogel, T. A., Patino, L. C., Alvarado, G. E. and Gans, P. B., 2004. Silicic ignimbrites within the Costa Rican volcanic front: evidence for the formation of continental crust. Earth Planet. Sci. Lett. 226, 149–159.

Vogel,T. A., Patino, L. C., Eaton, J. K., Valley, J. W., Rose, W. I., Alvarado, G. E. and Viray, E. L., 2006a. Origin of silicic magmas along the Central American volcanic front: Genetic relationship to mafic melts. J. Volcanol. Geotherm. Res. 156, 217-228.

Vogel, T. A., Flood, T. P., Patino, L. C., Wilmont, M. S., Maximo, R. P. R., Arpa, C. B., Arcilla, C. A. and Stimac, J. A., 2006b. Geochemistry of silicic magmas in the Macolod Corridor, SW Luzon magmas. Contrib. Mineral. Petrol. 151, 267-281.

Vogel, T. A., Patino, L. C., Alvarado, G. E. and Rose, W. I., 2007. Petrogenesis of ignimbrites, in: Bundschuh and Alvarado, G. E. (eds). Central America: Geology, Resources and Hazards. Taylor and Francis, Andover – Hants, United Kingdom, pp.1436.

Von Herzen, R. P. and Anderson, R. N., 1972. Implications of Heat Flow and Bottom Water Temperature in the Eastern Equatorial Pacific. Geophys. Journal Inter. 26, 427–458.

Wade, J. A., Plank, T., Stern, R. J., Tollstrup, D. L., Gill, J. B., O'Leary, J. C., Eiler, J. M., Moore, R. B., Wodhead, J. D., Trusdell, F., Fischer, T. P. and Hilton, D. R., 2005. The May 2003 eruption of Anatahan volcano, Mariana Islands: Geochemical evolution of a silicic island-arc volcano. J. of Volcanol. Geotherm. Res. 146, 139-170.

Westbrook, G. K., Hardy, N. C., and Heath, R. P., 1995.Structure and tectonics of the Panama-Nazca plate boundary, In: Mann, P. (ed), Geologic and Tectonic Development of the Caribbean Plate Boundary in Southern Central America. Geol. Soc. Am. Spec. Pap. 295, 91–110. Boulder, Colorado

White, A. J. R. and Chappell, B. W., 1983. Granitoid types and their distribution in the Lachlan Fold Belt, southeastern Australia. In: Roddick, J. A. (Ed.), Circum-Pacific Plutonic Terrains. Memoir 159. Geol. Soc. Am., Boulder, Colorado, pp. 21–34.

Williams, W. and McBirney, A., 1969. Volcanic History of Honduras. University of California Press, Berkeley, Los Angeles, pp. 101.

Xu, J.F., Shinjo, R., Defant, M. J., Wang, Q. and Rapp, R. P., 2002. Origin of Mesozoic adakitic intrusive rocks in the Ningzhen area of east China: partial melting of delaminated lower continental crust?. Geology 30, 1111-1114.

York, D., Hall, C. M., Yanase, Y., Hanes, J. A. and Kenyon, W. J., 1981. $^{40}Ar/^{39}Ar$ dating of terrestrial minerals with a continuous laser, Geophys. Res. Lett. 8, 1136-1138.